

# Handbook on Use of radio spectrum for meteorology: Weather, climate, water and related environmental applications

Edition of 2026







# HANDBOOK

## Use of radio spectrum for meteorology: weather, climate, water and related environmental applications

**Edition of 2026**

**Radiocommunication Bureau**



## NOTE

The designations employed in ITU and WMO publications and the presentation of material in this publication do not imply the expression of any opinion whatsoever on the part of ITU and WMO concerning the legal status of any country, territory, city or area, or of its authorities, or concerning the delimitation of its frontiers or boundaries.

Opinions expressed in ITU and WMO publications are those of the authors and do not necessarily reflect those of ITU and WMO. The mention of specific companies or products does not imply that they are endorsed or recommended by ITU and WMO in preference to others of a similar nature which are not mentioned or advertised.

Editorial correspondence and requests to publish, reproduce or translate this publication in part or in whole should be addressed to:

Chairperson, Publications Board  
World Meteorological Organization (WMO)  
7 bis, avenue de la Paix  
P.O. Box 2300  
CH-1211 Geneva 2, Switzerland

Tel.: +41 (0) 22 730 84 03  
Fax: +41 (0) 22 730 81 17  
E-mail: [publications@wmo.int](mailto:publications@wmo.int)

ITU

978-92-61-40681-3 (Electronic version)

978-92-61-42431-2 (paper version)

WMO

WMO-No. 1197

978-92-63-11197-5 (Electronic version)

© WMO-ITU 2026

The right of publication in print, electronic and any other form and in any language is reserved by ITU and WMO. No part of this publication may be reproduced, by any means whatsoever, without the prior written permission of ITU and WMO.

## FOREWORD

The Radiocommunication Study Group 7 for the Science Services was created through a structural reorganization in 1990 at the Düsseldorf CCIR Plenary Assembly.

Study Group 7 comprises four Working Parties (WP) that address technical issues related to specific disciplines under the umbrella of science services. Meteorology and related environmental activities fall within the remit of Working Party 7C (WP 7C). WP 7C carries out studies concerning the implementation and operation of meteorological passive and active sensors, from both ground-based and space-based platforms, as well as meteorological aids (mainly radiosondes and space weather sensors). As meteorology additionally depends on radiocommunications both to collect the data upon which its predictions are based, and to process and disseminate the resulting weather information and warnings to the public, this activity also concerns WP 7B. Finally, one can note that meteorological radars and wind-profiler radars are studied within WP 5B, under the general radiolocation service.

In the framework of achieving the UN Sustainable Development Goals (SDGs), a special role is assigned to Earth observation and meteorological systems. They provide both direct and indirect contributions to achieving the SDGs. Additionally, the data obtained by using radio frequencies are essential for monitoring the results of the adjusting actions taken. 30 of the 232 indicators developed to monitor the progress of these activities can only be assessed using data obtained from remote sensing satellites.

Meteorology is a crucial part of our everyday life and has many connections with our daily routines and activities. Reliable weather forecasts are key to our safety and our economies. To help save lives and reduce damage to property and infrastructure caused by storms, heavy precipitation, heat waves and tropical cyclones – as well as other hazards influenced by weather, such as floods or the dispersion of atmospheric or marine pollution – global citizens and decision-makers require timely warnings based on reliable weather forecasts.

Weather- and climate-related extremes are causing ever increasing amounts of economic losses. The importance of accurate and timely weather forecasts to support business continuity and protect economies increases in parallel. This is particularly true for the energy, transportation, construction, agriculture, tourism and utility sectors. Energy providers, for example, rely on weather forecasts to anticipate power demand and adapt their production during both hot and cold spells. With the development of renewable energy, production itself will increasingly depend on the weather. Likewise, forecasts of fog, snow, high winds, thunderstorms and weather-induced dispersion of ash particles are critical to aviation and air-traffic management, and by extension to the global economy.

The development of ITU-R Recommendations and preparations for World Radiocommunication Conferences (WRC) is the principal focus of the Study Group activities. There is an unmistakable need for the Study Group 7 experts to share this information not only with colleagues whose work depends on meteorological and related environmental data for improving the accuracy of weather and climate prediction, but also with policy-makers and spectrum regulators to understand the importance of using specific frequencies for meteorological and related environmental purposes and the ways to protect them so as to ensure the continuity of Earth system modelling and prediction capabilities with the highest possible degree of reliability.

Thus, it was decided to prepare and publish this Handbook, in collaboration with the Expert Team on Radio Frequency Coordination (ET-RFC) of the World Meteorological Organization (WMO), so that all users of meteorological and related environmental data could more completely understand meteorological systems. One primary purpose of this Handbook is to provide the reader with information about the use of radio systems and radio frequency (RF) bands by meteorologists and other scientists interested in environmental activities worldwide, and the importance of this use to public safety and the world economy.

Effective and prudent management of allocated frequency bands is paramount to maintaining and enhancing the quality and accuracy of weather and weather-related predictions. It is essential to understand for instance that if some of the frequency bands currently allocated for meteorological purposes were to be used by other radio systems that are incompatible with meteorological radio systems, then these bands could be rendered unusable for weather, climate and/or disaster prediction systems, thus making corresponding weather forecasts extremely difficult if not impossible with the required degree of reliability and accuracy.

As Chair of Study Group 7, it is my honour to present this Handbook to the community of users of meteorological and related environmental data, and to the frequency management community at large who will, I am sure, find it an important reference tool in their own work.

The update to this Handbook could not have been completed without the numerous contributors participating in Study Group 7 and WMO ET-RFC. To acknowledge their valuable contribution and leadership to this work, special thanks should be given to Natalia Donoho, Jesse Andries, Zoya Andreeva from WMO, David Franc (USA), Alec Casey (Canada), Eric Allaix (France), Kirsty McBeath (United Kingdom), Philippe Tristant (EUMETSAT) and Bruno Espinosa (Chair of WP 7C).

Additionally, special appreciation goes to the numerous contributors from around the world, and I hope not to have forgotten anybody:

NIE Jing, JIN Yuyan and LI Yingchong from China,

Sergey Uspensky and Anton Stepanov from the Russian Federation,

Edna Prado, Hui Shao, Daniel Gillies, Daniel Brewer, Gijs DeBoer, James Pinto and Tomasz Wojtaszek from the USA,

Dawn Harrison, Debbie O'Sullivan, David Jackson, David Edwards, Graeme Marlton, and Ben Pickering from the UK,

Mohammad Zomorodi from Australia,

Volker Lehmann, Marcus Pool and Dirk Brändlein from Germany,

Alexander Hafele and Maxime Hervo from Switzerland,

Annakaisa von Lerber, Juha Salmivaara, and Matti Lehmuskero from Finland,

Takahiro Mitome, Yasunori Iwana and Satoshi Hagiya from Japan,

Robin Fiory and Peter Leibiuk from Canada,

Flávio Archangelo and Joaquim Eduardo Rezende Costa from Brazil,

Nicole Vilmer and Olivier Traullé from France,

Roeland Van Malderen from the Netherlands,

Nico Cimini from Italy,

Katharina Andersen and Yan Soldo from ESA,

Bruce Ingleby from ECMWF,

and several colleagues from WMO supporting this activity.

Last but not least, our special gratitude is also due to Vadim Nozdrin of the Radiocommunication Bureau who has played an important role in the update of the content and publication of the Handbook.

Markus DREIS  
Chair, Radiocommunication Study Group 7

## TABLE OF CONTENTS

*Page*

FOREWORD.....	iii
INTRODUCTION.....	vii
CHAPTER 1 – WMO global infrastructure .....	1
1.1 Components of WMO global infrastructure.....	1
1.2 WMO Integrated Global Observing System (WIGOS).....	2
References .....	11
CHAPTER 2 – Meteorological satellite service (MetSat).....	13
2.1 Definition of the meteorological satellite service (MetSat) and its frequency allocations .....	13
2.2 MetSat systems using geostationary (GSO) satellites .....	16
2.3 MetSat systems using non-GSO satellites.....	19
2.4 Alternative data dissemination mechanisms .....	22
CHAPTER 3 – Meteorological aids service.....	25
3.1 Introduction.....	25
3.2 Examples of MetAids sensing systems .....	27
3.3 Factors influencing the characteristics of the MetAids systems .....	31
3.4 Characteristics of meteorological observations required from the MetAids service...	35
3.5 Variations in MetAids service operations .....	36
3.6 Future trends.....	38
References .....	38
CHAPTER 4 – Meteorological radars.....	41
4.1 Introduction.....	41
4.2 Weather radars.....	43
4.3 Wind profiler radars (WPRs) .....	80
4.4 Oceanographic High Frequency Radar .....	86
References .....	87
CHAPTER 5 – Passive and active spaceborne remote sensing for meteorological and related environmental activities .....	89
5.1 Introduction.....	89
5.2 Passive microwave radiometry sensing.....	91
5.3 Active sensors .....	112
CHAPTER 6 – Space weather.....	123
6.1 Definition of space weather and its associated radio communication service .....	123

6.2	Space weather observations .....	123
CHAPTER 7 – Other radiocommunication systems for meteorological and related environmental activities .....		131
7.1	Introduction .....	131
7.2	Data dissemination systems .....	131
7.3	Weather-sensing Uncrewed Aircraft Systems.....	132
7.4	Hydrological systems .....	132
7.5	Meteorological uses of Global Navigation Satellite Systems (GNSSs).....	134
7.6	Lightning detection systems.....	135
7.7	Ground-based microwave radiometers.....	138
7.8	Microwave Radio Attenuation systems.....	139
References .....		140
Annex – Acronyms and abbreviations.....		143
A.1	Acronyms and abbreviations commonly used in meteorology .....	143
A.2	Other acronyms and abbreviations used in this Handbook .....	150

## INTRODUCTION

Timely warning of natural and environmental disasters, accurate climate prediction and a detailed understanding, conservation and efficient management of scarce resources such as biomass, biosphere, mineral resources, water and energy are essential requirements for sustainable economic development. Information about weather, climate, water, environmental conditions and natural disasters is critically important for the global community. Monitoring activities provide essential information that is vital for weather forecasting and prediction, climate change science, environmental protection, sustainable economic development (including transport, energy, agriculture, urban development, natural resource management) and for safety of life, livelihoods and property. It is important to remember that this information is either based on measurements from systems using radio (electromagnetic) waves, or otherwise gathered, provided and distributed by radiocommunication systems. Radio systems are fundamental for monitoring the Earth's climate and supporting countries in mitigating and adapting to the effects of climate change, and in addressing its major challenges. Any system that relies on radio spectrum for its operation uses a limited, scarce natural resource. Ensuring the availability of radio frequency bands free from harmful interference is crucial for the development of all Earth observation systems.

The systems used to obtain and disseminate this information make use of a variety of radio technologies and require reliable access to radio frequencies throughout the radio spectrum, operating at centre frequencies ranging from a few kHz to several hundreds of GHz. These systems employ various types of technologies, including radiocommunication (e.g. radiosondes, satellites), active remote sensing (e.g. weather radars, wind profilers, precipitation radars, cloud profile radars) and passive remote sensing (e.g. microwave sounders, microwave radiometers, lightning detection). Space-based as well as surface-based equipment is being operated for these radiocommunication, active and passive sensing systems.

These radio-frequency applications are interconnected and collectively comprise a comprehensive global meteorological and related environmental monitoring system. The degradation of any of the radio components within this system, whether related to observation or data dissemination, can jeopardize the entire Earth system monitoring and prediction process.

It is also emphasised that systems using these frequencies play a crucial role in the detection, forecasting and warning of extreme weather, climate and water conditions worldwide. Given that these disasters account for more than 50% of all reported disasters, these systems are essential components of multi-hazard early warning systems that are crucial in mitigating disasters and emergencies.

The development of new, mass-market and added-value radio applications is putting increasing pressure on the frequency bands used for meteorological and related environmental applications. It presents the potential risk of limiting these applications in the future. At particular risk is satellite passive remote sensing, which involves the measurement of very low levels of naturally emitted radiation in a number of radio frequency bands. These bands are sensitive to multiple geophysical variables and must be used in combination to derive a number of different quantities. The radio frequencies required to do this are determined by fundamental physics and can therefore not be altered. Continuity of observations using these bands is also essential for monitoring and assessment of climate change.

Meteorological users of radio spectrum must remain vigilant and must proactively address the growing challenges of sharing spectrum with other radiocommunication services. The Nineteenth World Meteorological Congress (Cg-19, Geneva, June 2023) expressed "...its serious concern at the continuing threat to several radio-frequency bands allocated to the meteorological aids, meteorological-satellite, Earth-exploration satellite and radiolocation (weather and wind profiler radars) services posed by the development of other radiocommunication services". In recognition of the prime importance of the specific radiocommunication services required for meteorological and related environmental activities, Cg-19 adopted Resolution 31 that appeals to the International Telecommunication Union (ITU) and its Member Administrations:

- 1) To ensure the availability and absolute protection of the radio-frequency bands which, due to their special physical characteristics, are a unique natural resource for space-borne passive sensing of the atmosphere and the Earth's surface, and are of crucial importance for weather, water and climate research and operations;
- 2) To give due consideration to the WMO requirements for radio-frequency allocations and regulatory provisions for meteorological and related environmental operations and research;
- 3) To pay special attention to the WMO positions related to the World Radiocommunication Conference (WRC) agenda, in the light of appeals 1) and 2) above.

In this respect, the last WRCs made a number of important decisions to safeguard meteorological and related environmental operations, taking into account the growing demand for spectrum use from commercial services. This was the case at:

- WRC-15 that provided additional spectrum for the future development of space active remote sensing and high data rate telecommand links to communicate with Earth exploration satellites, as well as protection to passive observation bands potentially impacted by new allocations;
- WRC-19 that implemented protection mechanisms for meteorological radars and radiometers operating in the 5 GHz range, adequate regulations to ensure long-term operations of Data Collection Systems (DCS), and limitations of out-of-band emissions for terrestrial (including International Mobile Telecommunications) and satellite services in a number of frequency bands between 31 and 92 GHz adjacent to bands used for passive microwave measurements; and,
- WRC-23 that implemented further limitations for the protection of passive microwave sensor measurements at 18.7 GHz and 36.5 GHz, adopted new frequency allocations for passive microwave sensing for ice cloud measurements around 243 GHz, and provided the first level of recognition of space weather in the Radio Regulations through the definition of space weather, its service designation and a new Resolution outlining the importance of space weather applications.

To take into account these recent evolutions in the Radio Regulations, as well as evolutions in the radio technologies being employed, the Radiocommunication Working Party 7C (Remote Sensing Systems) of Radiocommunication Study Group 7 and the WMO Expert Team on Radio Frequency Coordination (ET-RFC) have prepared this revised Handbook. It is intended to serve as a guide to professional users of meteorological and related environmental data from radio-based systems, the public and governments relying on these systems, and the radiocommunications community, including regulators and the wireless telecommunications industry.

This Handbook presents the overall structure of the WMO global infrastructure and its observing components as well as an overview and discussion of each meteorological and related environmental system's technical and operational characteristics. The description of each meteorological system includes: the radio-frequency bands used, the criteria for predicting harmful interference from competing radiocommunication systems; and the potential impact of harmful interference on weather, climate, water, and related environmental data, forecasts and warnings. To assist in understanding this complex area, discussions have been divided into the following types of systems:

- 1 WMO global infrastructure
- 2 Meteorological satellite service systems
- 3 Meteorological aids service systems, mainly radiosondes
- 4 Ground-based meteorological radars, including weather radars and wind-profiler radars
- 5 Passive and active spaceborne remote sensing for meteorological and related environmental activities
- 6 Space weather sensor systems
- 7 Other radiocommunication systems for meteorological and related environmental activities.

To assist the reader, a brief compendium of acronyms and abbreviations along with a list of references is provided in the back matter of this Handbook.

## CHAPTER 1

### WMO global infrastructure

#### 1.1 Components of WMO global infrastructure

Weather, climate, water and related environmental phenomena are not limited by national boundaries. Near real-time, global exchange of information about these phenomena is essential to enable effective weather forecasting, climate prediction and water resource management, as well as many other related environmental services, for the benefit of the global society.

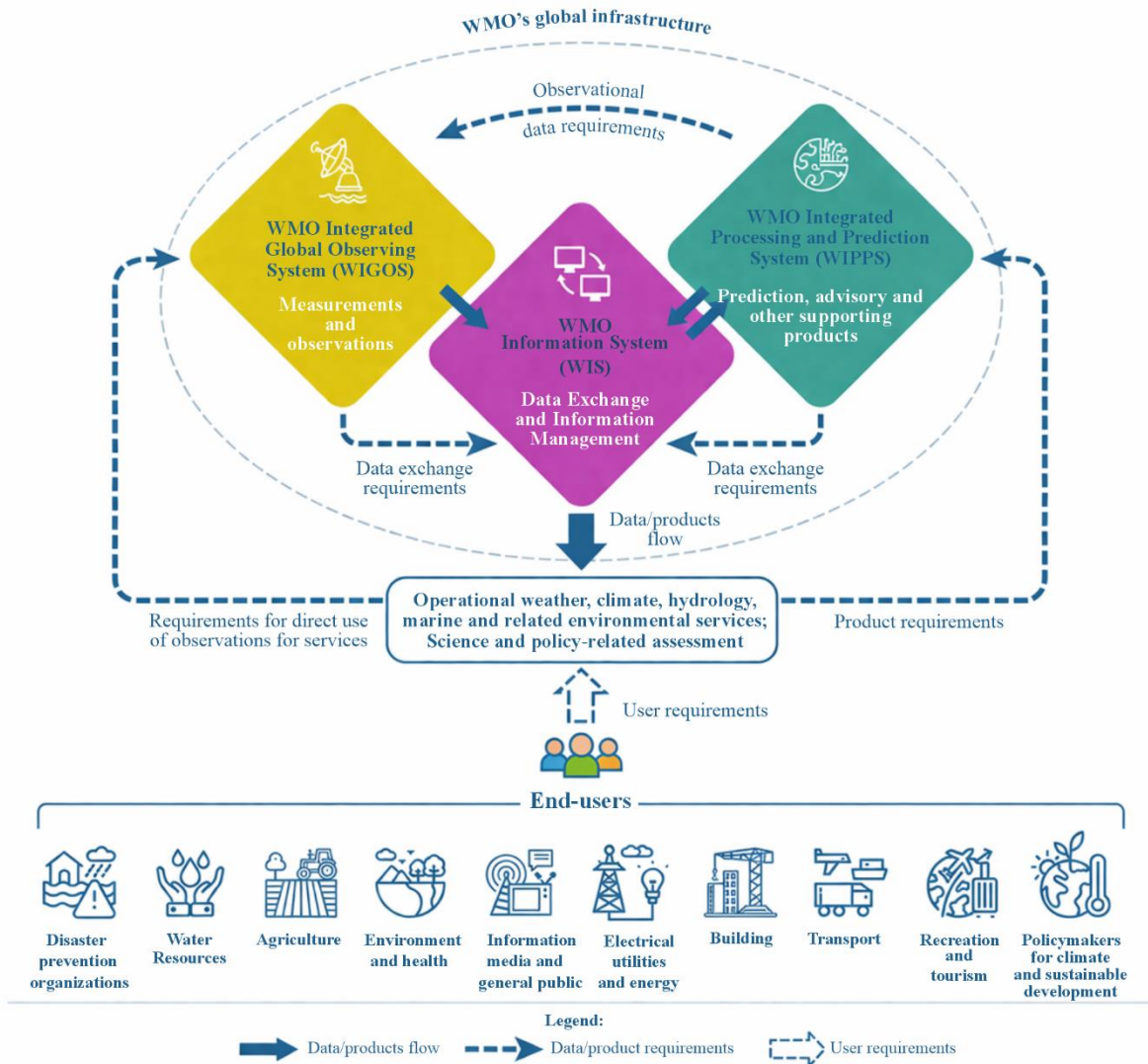
The WMO global infrastructure combines observing systems, telecommunication facilities, and data-processing and prediction centres – operated by the 193 Member States and Territories – that make meteorological and related environmental information available in support of services worldwide.

The WMO global infrastructure is composed of three integrated core system components (Fig. 1-1):

- The **WMO Integrated Global Observing System (WIGOS)** provides high-quality, standardized observations of weather, climate, water, and other environmental variables from all parts of the globe and from outer space. WIGOS consists of a multitude of individual surface- and space-based observing systems owned and operated by WMO Members and Partner Organizations worldwide.
- The **WMO Information System (WIS)** provides a coordinated network of systems for sharing authoritative data on weather, climate, water, and related environmental observations, products and warnings. The WIS provides data discovery capabilities for data produced under WIGOS and the WMO Integrated Processing and Prediction System (WIPPS).
- The **WMO Integrated Processing and Prediction System (WIPPS)**, formerly known as the Global Data-Processing and Forecasting System (GDPFS), is a worldwide network that coordinates Member capacities to prepare analyses and forecast products and make these available to all Members, enabling delivery of weather, climate, water and related environmental services. The WIPPS Centres support this network at the global, regional and national levels to ensure the provision of and access to WIPPS products.

FIGURE 1-1

### Components of WMO global infrastructure



Meteo-01-01

## 1.2 WMO Integrated Global Observing System (WIGOS)

WIGOS provides the global framework for all WMO observing systems and for WMO contributions to cosponsored observing systems in support of all WMO programmes and activities, in order to respond to user requirements. WIGOS encompasses the observing systems of the following Earth system domains: weather, climate, atmospheric composition, hydrology, cryosphere, ocean, and space weather [WMO-No. 1160].

The main components of WIGOS are:

- the observing component of World Weather Watch (WWW),
- the observing component of Global Atmosphere Watch (GAW),
- the observing component of Global Cryosphere Watch (GCW),
- the WMO Hydrological Observing System (WHOS), and
- the observing system for space weather.

In addition, WMO is working with partner organizations to complement these components of the WIGOS framework with climate monitoring and ocean observations via the Global Climate Observing System (GCOS) and the Global Ocean Observing System (GOOS), respectively.

Through the development of observing standards and recommendations, WIGOS supports the generation of quality-controlled products and information for effective weather, climate, hydrology, marine and related environmental services. As shown in Fig. 1-2, WIGOS is comprised of operational and research-funded surface-based and space-based subsystems, with physical observing infrastructure on land, at sea, in the air and in space.

The most obvious benefits of WIGOS are the safeguarding of life, livelihoods and property through the detection, forecasting, and early warning of severe weather events such as floods, droughts, heatwaves, tsunamis, local storms, tornadoes, hurricanes, or extra-tropical and tropical cyclones, and of space weather events such as solar flares and geomagnetic storms which can cause radio blackouts, degradation of Global Navigation Satellite Systems (GNSS) performance, widespread power grid failures, and other detrimental impacts.

A wide range of economic activities such as public health, disaster risk reduction, water resource management, food security, renewable energy, tourism, travel, insurance, and sustainable development, benefit enormously from the provision of accurate forecasts. Extended warning times for severe events enable civil authorities and first responders to take appropriate actions to protect their citizens.

FIGURE 1-2

**WMO Integrated Global Observing System (WIGOS)**



## 1.2.1 Weather observations

The WMO global infrastructure was originally developed as the World Weather Watch (WWW) to meet user requirements for weather monitoring and forecasting. The observing component of WWW provides the meteorological observations from all parts of the globe for the preparation of weather analyses, forecasts, advisories and warnings, and in support of the climate monitoring and related environmental activities carried out by WMO Members and partner organizations.

### 1.2.1.1 Surface land observations

The backbone of the surface-based sub-system consists of land-based stations that observe meteorological parameters such as atmospheric pressure, wind speed and direction, air temperature, and relative humidity at or near the Earth's surface. Data from these stations are exchanged globally in real time. A subset of these surface stations is also used for climate monitoring purposes via the Global Climate Observing System (GCOS) Surface Network.

### 1.2.1.2 Upper-air observations

Radiosondes attached to free rising balloons perform measurements of pressure, wind velocity, temperature and humidity from just above the ground to heights of up to or even above 30 km. This constitutes a global network of the upper-air stations. Over the oceans, radiosonde observations are collected from ships, primarily navigating the North Atlantic, equipped with automated shipboard upper-air sounding facilities. A subset of upper-air stations, specially fitted for monitoring the climate, comprises the GCOS Upper-air Network.

### 1.2.1.3 Weather and wind profiler radar observations

Weather radars have proven to be extremely valuable in providing data of high-resolution in both space and time over relatively large areas, especially in the lower layers of the atmosphere. These instruments are used for the real-time estimation and short-term forecasting of precipitation. They are also uniquely capable of observing the development of several severe weather phenomena, such as severe convective weather or tropical storms. Rainfall-related data products from radars can enable or enhance the detection and prediction of flash floods. These characteristics make weather radars essential systems to support the issuance of timely high-impact weather warnings.

In addition to their primary functions, operational weather radars can measure winds within precipitation, complementing other upper-air measurement technologies, such as radiosondes and wind profiler radars. Furthermore, the implementation of dual-polarization technology in weather radar systems has brought several benefits, including, but not limited to the improved detection of precipitation types, more accurate rainfall estimation, and improved overall quality of radar data. Weather radars have become a crucial component of modern national and regional observing networks.

Wind profiler radars provide continuous real-time profiles of wind direction and speed from heights near the surface up to the troposphere. These profiles complement other upper-air wind profiling methods, such as radiosondes, and are a valuable input to Numerical Weather Prediction (NWP) systems. As opposed to weather radars, these instruments can make useful measurements even in the absence of precipitation, by detecting echoes scattered from irregularities of the refractive index of air. This clear air sensing capability is a truly unique feature of this radar. In addition, wind profiler radars can also measure winds by detecting echoes from other targets such as precipitation.

### 1.2.1.4 Other ground-based remote sensing observations

Ground-based remote sensing observing systems, other than weather radars and wind profiler radars, typically provide data at high temporal and vertical resolution, which is an important advantage over conventional *in situ* observing and profiling methods. The following are some of the most used ground-based remote sensing instruments.

Ground-based microwave radiometers (MWR) are passive remote sensing instruments that measure thermal emissions from the atmosphere, which can then be processed further to profiles of atmospheric quantities such as temperature and humidity. These quantities can be used to derive common forecast indices on thunderstorm potential and other weather threats to support the work of operational meteorologists, or they can be assimilated directly into NWP models to improve their forecast quality.

Passive lightning detection systems (LDS) offer precise, real-time monitoring of lightning activity through a network of distributed ground-based sensors. They are able to locate thunderstorms or even individual lightning strikes, but also indirectly provide valuable information on other severe phenomena that are associated with thunderstorms, such as flash flooding or damaging winds. The detection accuracy, efficiency and range of LDSs depend on the type and number of sensors. Some networks are designed for local high-precision three-dimensional lightning detection, while long-range LDSs can cover continental-scale areas or detect lightning over oceans.

Light detection and ranging systems, commonly referred to as lidars, are active remote sensing instruments that use lasers to make observations based on scattering from atmospheric gas molecules and particles. There are several types of atmospheric lidars such as differential absorption lidars (DIALs), Raman lidars, and Doppler lidars, each with different characteristics and measurement capabilities. Lidars can retrieve information on a variety of atmospheric variables including atmospheric composition, clouds, water vapour, winds and temperature, which can be useful in a variety of applications, such as air quality monitoring, NWP and wind profiling.

In addition to ground-based remote sensing systems that use electromagnetic radiation explained above, some technologies employ acoustic waves for atmospheric profiling. Two key instruments in this field are sodars (Sound Detection and Ranging) and Radio Acoustic Sounding System (RASS). Sodar provides detailed measurements of wind profiles and the thermodynamic structure of the lowest atmosphere. RASS, on the other hand, extends these capabilities by also measuring quantitative temperature profiles. Both instruments are presently used mainly in research applications.

### **1.2.1.5 Aircraft meteorological observations**

Through arrangements with partner airlines, the International Air Transport Association (IATA) and the International Civil Aviation Organization (ICAO), aircraft-based meteorological observations are received from thousands of aircraft, providing reports of pressure, wind, temperature, humidity, turbulence and other parameters during flight. The Aircraft Meteorological Data Relay (AMDAR) system makes high-quality observations of air temperature and wind speed and direction at cruising level as well as at selected levels in ascent and descent. The amount of data from aircraft has increased dramatically during recent years providing more than half a million AMDAR meteorological observations per day, including from hundreds of airports globally. Providing great potential for measurements in places where there are little or no radiosonde data, these systems are making a major contribution of upper-air observations to the World Weather Watch.

In the future, WMO expects that another large source of aircraft-based observations will come from Uncrewed Aircraft Systems (UAS), made up of both small aircraft, such as drones, as well as a range of fixed-wing aircraft. UAS could support a potentially large range of applications in meteorological, hydrological and climate monitoring. WMO is supporting efforts towards understanding and advancing the use of UAS in their potential to measure weather parameters as a complementary observing system to traditional balloon-borne radiosondes.

### **1.2.1.6 Surface marine observations**

On the oceans, observations are obtained from the instruments on board satellites, ships, moored and drifting buoys and stationary platforms. Instruments employed on ships recruited under the WMO Voluntary Observing Ship Programme provide many of the same variables as those at surface land stations with the important inclusion of sea surface temperature, wave height and wave period. In addition, the operational Drifting Buoy Programme, comprising of about 1 200 drifting buoys, enables the observations of sea surface temperature, sea level pressure, surface currents and sea surface salinity, as well as the hourly transmission of these data through satellites.

### **1.2.1.7 Observations from meteorological satellites**

Space-based meteorological observations are performed within satellite programmes implemented by space agencies of WMO member countries and intergovernmental agencies operating meteorological and Earth Observation satellites. International coordination among satellite operators is achieved through the Coordination Group for Meteorological Satellites ([CGMS](#)).

The space-based backbone component of WIGOS includes constellations of Sun-synchronous low Earth orbit (LEO) satellites in three orbital planes and a ring of geostationary Earth orbit (GEO) satellites providing complete coverage outside the polar areas, complemented by satellites in other orbital planes and satellites in drifting and highly elliptical orbits.

Visible and infrared VIS/IR imaging from GEO enables very frequent sampling (at sub-hourly or minute rates), which is essential for monitoring rapidly evolving phenomena, such as tracking the movement and evolution of clouds, severe weather events, volcanic eruptions and forest fires. The requirement for non-polar frequent imaging from the geostationary satellites can be met with a minimum of five satellites providing complete Earth coverage. In an operational constellation, backup satellites are required to provide redundancy above this minimum.

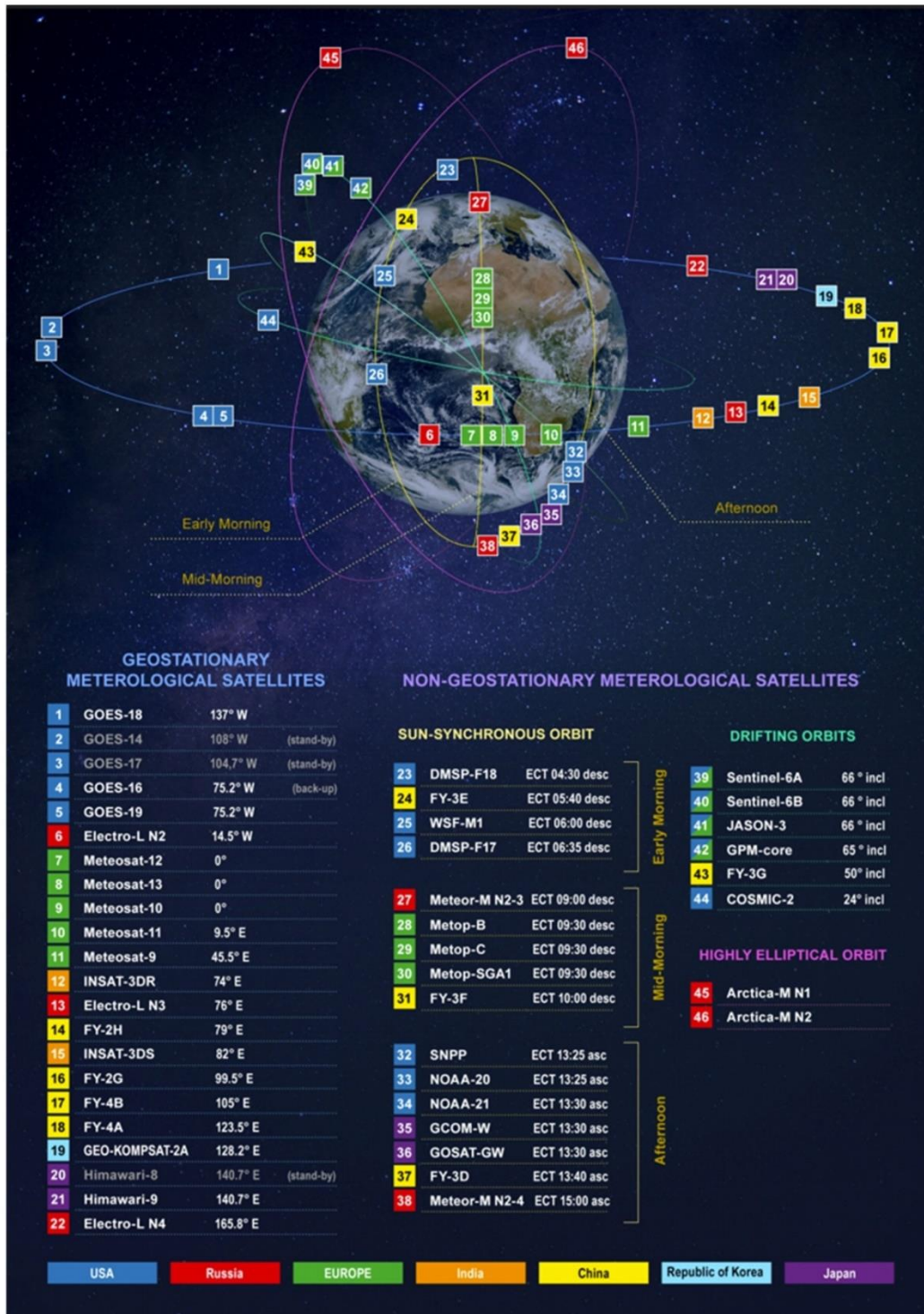
The Sun-synchronous orbit provides global coverage necessary for applications such as global NWP, polar meteorology, and climatology. For these applications, very frequent sampling is less critical than global coverage and high accuracy. Additional advantages of Sun-synchronous and other low Earth orbits are the capability to perform active sensing in the microwave (radar) and optical (lidar) ranges of the electromagnetic spectrum and limb measurements of the higher atmosphere.

Through improvements in NWP, increasingly sophisticated methods have been developed that allow to derive temperature and humidity information directly from satellite radiances. In the recent years, impressive progress has been made in weather and climate analysis and forecasts, including warnings for hazardous weather phenomena (heavy rain, storms, cyclones) that affect all populations and economies. This progress is largely to be attributed to the proliferation of space-borne observations and their assimilation in NWP models, which is significantly improving forecast skill and in turn increasing the lead time to respond to extreme weather events.

An overview of the currently operational meteorological satellites is shown in Fig. 1-3.

FIGURE 1-3

Constellation of the currently operational meteorological satellites of WIGOS (Status: March 2026)



Meteo-01-03

In order to ensure operational continuity of space-based meteorological observations the currently operational satellites are continuously being replaced by new satellites of the existing generation or by a new generation of meteorological satellites. In addition to assuring data continuity, new generations of meteorological satellites with increased observation capabilities provide users with new types of data. As a result, overall data

volumes are one or more orders of magnitude higher than those of the previous generation. Newly launched satellites are operated in parallel with aging satellites until they are gradually phased-out when reaching end of life. As the number of satellites in orbit continues to grow, so does the risk of space debris, particularly in Low Earth Orbit. This creates potential threats to the reliability of the space-based observing system. To address this, it is increasingly important to follow space sustainability guidelines and standards – including requirements for deorbiting older satellites at the end of their operational life.

A list of currently operational and planned meteorological and related environmental satellites and their parameters is available at the [WMO OSCAR/Space database](#).

The value of satellite observations for monitoring weather, climate and the Earth system in general has never been so high, whilst technical capabilities and the space industry as a whole are developing at a fast pace. Therefore, it is essential for satellite operators to adapt and optimize global observation architectures to meet operational user requirements and to address the evolving environment.

The development of small satellites is an evolution in the overall satellite industry that provides opportunities for greater and easier access to, and use of, space services by all countries due to the lower technical and capital barriers [ITU [Handbook on Small Satellites](#), 2023]. Correspondingly, constellations of smaller satellites continue to gain importance.

As a result, a hybrid satellite architecture, defined as a combination of reference platforms (LEO, GEO, etc.), small and other non-large satellites, has become an efficient approach to provide observations that are fundamental for meteorological and related environmental applications. The additional measurement capabilities also accelerate the development of these applications and services.

### 1.2.2 Atmospheric composition observations

Atmospheric composition observations are coordinated by the WMO's Global Atmosphere Watch ([GAW](#)). It is a WMO research programme that focuses on building a coordinated global understanding of atmospheric composition and its changes. It coordinates high-quality atmospheric composition observations (greenhouse gases, ozone, aerosol, selected reactive gases, total atmospheric deposition, ultraviolet radiation) across global to local scales to provide reliable scientific information for policymakers, support international conventions and contribute to improving our understanding of climate change and long-range transboundary air pollution.

The integrated observing system for atmospheric composition constitutes the backbone of the programme. This system includes ground-based and satellite observing components operated by Member countries and partner organizations. The ground-based observational network includes about 400 stations hosted by more than 100 countries, as well as stations operated by contributing networks. The network of stations is complemented by regular ship cruises and by airborne observations that help to characterize the upper troposphere and lower stratosphere, in particular with regards to ozone, solar radiation, aerosols and certain trace gases.

In recent years satellite programmes have produced important measurements of atmospheric compounds and related parameters that complement the GAW network measurements. When highly accurate local measurements from GAW ground-based stations are coupled with the near global coverage of satellite measurements, it results in a more complete picture of atmospheric composition and of the related processes on global scales, and provides complementary checks of instrument calibrations. Satellite observations of atmospheric composition are coordinated by the Committee on Earth Observation Satellites ([CEOS](#)) through the Atmospheric Composition Virtual Constellation ([AC-VC](#)), addressing issues of air pollution, greenhouse gases and stratospheric ozone.

### 1.2.3 Hydrological observations

The WMO's Hydrological Observing System ([WHOS](#)) is the framework for reliable hydrological data exchange and access at national, regional, and international levels for all hydrology data providers and users. It provides data and information exchange infrastructure to support Early Warning Systems (EWS) enabling data access, developing technical capabilities, and promoting data sharing policy.

WHOS provides for the measurement of basic hydrological elements from networks of hydrological and meteorological stations. These stations collect and – for the automatic ones – transmit in near real-time hydrological observations on the quantity and quality of both surface water and groundwater. Automatic

stations transmit data using mobile phone networks, VHF / UHF radio link or through meteorological or communication satellites. The transmission can be either at scheduled time slots, or triggered by particular events (e.g. exceeding a given water level threshold) on a dedicated emergency channel.

Over the last twenty years, the use of satellite altimetry data in hydrology has steadily increased for creating time series of stages, estimating discharges, etc. The precision of satellite altimetry measurements has also notably improved, making these data more usable for operational purposes, climate analysis and research. This evolution culminated in the December 2022 launch of the Surface Water and Ocean Topography (SWOT) mission dedicated to providing full coverage of the continental waters.

The near real time satellite derived rainfall estimation represents an essential input for water management purposes, in particular for flood warning systems, and can be integrated with local, ground-based observations for improving their quality.

Synthetic Aperture Radar (SAR)'s ability to collect data regardless of weather conditions, day or night, and cloud cover represents a clear advantage that allows this technology to find applications in various fields, such as disaster monitoring or environmental surveillance. SAR data are particularly well suited to flood mapping in support of disaster risk reduction.

Concerning water quality, the use of the spectral signature of water bodies, mainly in the visible and near infrared ranges, to estimate water quality variables is being tested and is demonstrating promising results for more operational use.

#### 1.2.4 Cryosphere observations

The WMO's Global Cryosphere Watch ([GCW](#)) is the crosscutting activity area focused on supporting WMO Members in sustainably enhancing their capabilities for observing and reporting on the changes in all components of the cryosphere, as well as predicting their changes and their impacts on weather, climate, water, environment and people.

The GCW surface observation network, called CryoNet, is comprised of core and contributing stations, as well as affiliated networks. As of 2023, there are more than 700 GCW stations registered in the WMO OSCAR/Surface database that are measuring one or more variables of a cryosphere component (snow, glaciers, sea ice, permafrost, etc.).

The observing technologies used for the measurement of cryosphere variables vary significantly from component to component of the cryosphere, with traditional and emerging methods being used. For example, new measuring systems based on GNSS or cosmic ray neutron/muon sensors are being tested for daily measurements of snow depth, the water equivalent of the snow cover (SWE), or both. The use of ground penetrating radar (GPR) to determine snow depth is becoming common practice on snow and glaciers. The surveying of glacier thickness is increasingly done by radio-echo sounding (RES), using equipment towed by vehicles, portable systems or air-borne instruments. Satellite borne radar sounders are also planned. Radar systems can also be used for investigating layering within glaciers and the snowpack, for studying the nature of the ice-bed interface, and for detecting subglacial and englacial water as well as liquid water content in snow.

Sea ice observations are made using manual methods and remote sensing techniques. There is a range of automated sensors that can be employed to measure or derive sea-ice thickness. This includes ground-penetrating radars, electro-magnetic sounding (often combined with laser-supported detection of the upper surface), sea-ice mass-balance stations, mechanical ice-thickness gauges or upward looking sonar units. The most efficient method to estimate sea ice extent, concentration, and stage of development is with the use of satellites using passive and active (e.g. SAR) microwave sensors, due to their ability to acquire data in all weather conditions and regardless of solar illumination conditions. Data from passive and active microwave sensors can be complemented by optical data acquired over cloud free areas. Electrical Resistivity Tomography (ERT) is commonly used to evidence the presence of ice and frozen bodies in ice-rich permafrost. In addition, rock glacier velocity is determined by either Terrestrial geodetic survey (TGS) or Synthetic Aperture Radar Interferometry (InSAR).

All these data allow for assessing globally the state of the cryosphere in the context of a changing climate and answering questions on freshwater resources in polar and mountain regions.

### 1.2.5 Space weather observations

Space weather encompasses the conditions and processes occurring in space, including on the sun, in the magnetosphere, ionosphere and thermosphere, which have the potential to affect the near-Earth environment. The physical variables that need to be monitored with respect to space weather phenomena include variables related to the solar origins of the perturbations (e.g. solar active regions, coronal mass ejections) as well as variables quantifying the perturbed Earth environment: the state of the ionosphere and magnetosphere, the ground-level magnetic fields and cosmic radiation.

Across those two categories, both *in situ* and remote sensing measurements are performed by both surface-based and space-based observing systems. Hence, also satellite based *in situ* measurements are involved.

Several different types of ground-based measurements are being performed in support of space weather services: optical solar observations, solar radio flux and radio spectrographic measurements, cosmic ray measurements by neutron monitors, surface magnetic field measurements, as well as measurements of the ionosphere through riometers, ionosondes, and GNSS receivers.

Space based instruments to monitor space weather include instruments on board satellites that are also used to monitor terrestrial weather. A number of geostationary satellites produce solar images in extreme ultraviolet (EUV), and measure EUV and X-ray flux as well as electron and proton fluxes.

In addition to this, measurements are performed from several LEO satellites, including solar imaging and flux measurements, auroral imaging, as well as radio occultation measurements to quantify ionospheric and thermospheric properties.

Finally, space-based measurements are also performed by spacecraft located further out in space. Most notably, upstream of Earth in the solar wind, around the L1 Lagrange point measuring solar wind plasma properties including magnetic field, as well as particle fluxes, and coronagraph images of the sun (images of an artificially eclipsed sun). Even further out are some spacecrafts orbiting the sun, providing a view of the solar surface that is not seen from Earth, side views on the propagation of ejecta travelling from the sun towards Earth, as well as *in situ* solar wind measurements.

### 1.2.6 Climate observations

Climate observations are coordinated by the Global Climate Observing System ([GCOS](#)). The GCOS is co-sponsored by the WMO, the Intergovernmental Oceanographic Commission of the United Nations Educational, Scientific and Cultural Organization (IOC-UNESCO), the United Nations Environment Programme (UNEP) and the International Science Council (ISC).

The GCOS is one of the key international coordination mechanisms for planning, developing and reviewing global observing systems for climate. It also plays a crucial role in defining observational requirements for climate applications. A set of variables identified by the GCOS, known as the Essential Climate Variables (ECVs), contribute to the characterisation of Earth's climate, providing a picture of climate change at a global scale.

Both satellite-based and surface-based observations are major contributors to global climate observations. The GCOS facilitates climate observations made by surface-based networks supported by the WMO, the Global Ocean Observing System ([GOOS](#)), space-based observations coordinated by CEOS and CGMS, as well as many other networks operated on land provided by partner organizations.

Long-term, accurate and stable observations are critical to understand climate change, and GCOS performs a vital role in ensuring that climate observations are globally coordinated for the timely delivery of information and for the establishment of best practices and methods to safeguard high data quality and calibration.

### 1.2.7 Ocean observations

Ocean observations are coordinated by the [GOOS](#). The GOOS is co-sponsored by WMO, IOC-UNESCO, UNEP and ISC. One of the primary objectives of GOOS is to facilitate the seamless integration of diverse observation platforms. These platforms encompass an extensive range, including but not limited to satellites, buoys, ship-based observations and autonomous vehicles. By leveraging technology across these platforms, the GOOS strives to capture a holistic view of the intricate processes and phenomena occurring in the world's oceans.

Satellites, equipped with advanced remote sensing instruments including active and passive microwave systems, play a pivotal role in monitoring large-scale ocean features. They provide a vantage point from space, allowing for the observation of broad oceanic patterns, such as sea surface temperature, ocean colour and sea level changes. These observations contribute significantly to our understanding of global climate systems and long-term trends.

Drifting buoys, strategically deployed across various oceanic regions, serve as sentinel outposts collecting real-time data on ocean conditions. These floating platforms are equipped with sensors that measure parameters, such as sea surface temperature, salinity and currents. The data retrieved from buoys contribute to the development of accurate models and forecasts, aiding in the prediction of events such as storms, tsunamis and climate variations.

Autonomous vehicles, including underwater gliders and profiling floats, delve into the depths of the ocean, providing invaluable insights into subsurface properties. These autonomous explorers traverse the ocean's depths, collecting data on temperature, salinity, and nutrient levels. Their ability to navigate vast expanses of the ocean allows scientists to obtain a three-dimensional perspective, enhancing our understanding of ocean stratification and circulation patterns.

In addition, there are several other Observations Coordination Group networks that provide long-term, global, high-quality, *in situ* ocean observations using various technologies. These networks track changes in global ocean conditions and variables such as ocean temperature, currents, waves, sea level, salinity, carbon and oxygen that are vital to characterizing changes in the global ocean environment.

## References

- [1] WMO-No. 1160 – Manual on the WMO Integrated Global Observing System, <https://library.wmo.int/records/item/55063-manual-on-the-wmo-integrated-global-observing-system-wmo-no-1160?offset=42>
- [2] The WMO Integrated Global Observing System (WIGOS) website, <https://community.wmo.int/en/activity-areas/WIGOS>
- [3] The Coordination Group for Meteorological Satellites (CGMS) website, <https://cgms-info.org/>
- [4] WMO OSCAR/Space database: <https://space.oscar.wmo.int/spacecapabilities>
- [5] ITU Handbook on Small Satellites, Edition of 2023, <https://www.itu.int/pub/R-HDB-65-2023>
- [6] The Global Atmosphere Watch Programme (GAW) website, <https://community.wmo.int/en/activity-areas/gaw>
- [7] The WMO Hydrological Observing System (WHOS) website, <https://community.wmo.int/en/activity-areas/wmo-hydrological-observing-system-whos>
- [8] The Committee on Earth Observation Satellites (CEOS) website, <https://ceos.org/>
- [9] The CEOS Atmospheric Composition Virtual Constellation website, <https://ceos.org/ourwork/virtual-constellations/acc/>
- [10] The Global Cryosphere Watch (GCW) website, <https://community.wmo.int/en/activity-areas/global-cryosphere-watch-gcw>
- [11] The Global Climate Observing System (GCOS) website, <https://gcos.wmo.int/>
- [12] The Global Ocean Observing System (GOOS) website, <https://goosoocean.org/>



## CHAPTER 2

**Meteorological satellite service (MetSat)****2.1 Definition of the meteorological satellite service (MetSat) and its frequency allocations**

The meteorological satellite service (MetSat) is defined in Radio Regulations (RR) No. **1.52** as “an *earth exploration-satellite service* for meteorological purposes”. It allows the radiocommunication operation between earth stations and one or more space stations, which may include links between space stations, with links to provide:

- information relating to the characteristics of the Earth and its natural phenomena, including data relating to the state of the environment, obtained from active or passive sensors on Earth satellites;
- information collected from airborne or Earth-based platforms;
- information distributed to earth stations;
- feeder links necessary for the operation of MetSat satellites and its applications.

This Chapter related to MetSat applications includes the following radiocommunication transmissions:

- transmissions of observation data from MetSat satellites to main reception stations;
- re-transmissions of pre-processed data to meteorological user stations through MetSat satellites;
- direct broadcast transmissions to meteorological user stations from MetSat satellites;
- alternative data dissemination to users (GEONETCast) via other satellite systems than MetSat;
- transmissions from data collection platforms to MetSat satellites.

Table 2-1 indicates the frequency bands that are allocated in the ITU Radio Regulations to the meteorological satellite (MetSat) service and the Earth exploration-satellite service (EESS). MetSat systems are entitled to also use the frequency bands allocated to EESS for data transmissions (see Note 1).

TABLE 2-1

**Frequency band allocations to MetSat and EESS in the ITU Radio Regulations  
for use by meteorological satellites for data transmissions**

<b>Available allocations for MetSat data transmissions</b>	
<b>space-to-Earth direction</b>	<b>Earth-to-space direction</b>
<b>137-138 MHz</b> (MetSat primary)	<b>401-403 MHz</b> (EESS and MetSat primary)
<b>400.15-401 MHz</b> (MetSat primary)	<b>2 025-2 110 MHz</b> (EESS primary) (Note 1) (and space-to-space direction)
<b>460-470 MHz</b> (EESS and MetSat secondary <sup>1</sup> )	<b>7 190-7 250 MHz</b> (EESS primary <sup>2, 3</sup> ) (Note 1)
<b>1 670-1 710 MHz</b> (MetSat primary)	<b>8 175-8 215 MHz</b> (MetSat primary)
<b>2 200-2 290 MHz</b> (EESS primary) (Note 1) (and space-to-space direction)	<b>28.5-30.0 GHz</b> (EESS secondary) (Note 1)

<sup>1</sup> By footnote RR No. **5.290**, MetSat service is allocated on a primary basis in some countries.

<sup>2</sup> By footnote RR No. **5.460A**, EESS service is limited to tracking, telemetry and command and shall not claim protection from the fixed and mobile services,

<sup>3</sup> By footnote RR No. **5.460B**, EESS service in the band 7 190-7 235 MHz shall not claim protection from existing and future stations of the space research service.

TABLE 2-1 (end)

Available allocations for MetSat data transmissions	
space-to-Earth direction	Earth-to-space direction
7 450-7 550 MHz (MetSat primary, limited to geostationary satellites only)	40.0-40.5 GHz (EESS primary) (Note 1)
7 750-7 900 MHz (MetSat primary, limited to non-geostationary satellites only)	
8 025-8 400 MHz (EESS primary) (Note 1)	
18.0-18.3 GHz (MetSat primary for space-to-Earth direction in Region 2, limited to geostationary satellites only)	
18.1-18.4 GHz (MetSat primary for space-to-Earth direction in Regions 1 and 3, limited to geostationary satellites only)	
25.5-27.0 GHz (EESS primary) (Note 1) (and space-to-space direction in 25.25-27.5 GHz)	
37.5-40.0 GHz (EESS secondary) (Note 1)	
65.0-66.0 GHz (EESS primary) (Note 1)	

NOTE 1 – Since the MetSat is a sub-class of the Earth exploration-satellite service (EESS), those allocations (for example: 8 025-8 400 MHz and 25.5-27.0 GHz) can also be used for the operation of MetSat satellites and their applications.

### 2.1.1 General concept of MetSat satellite systems

MetSat system commonly collect a variety of data with visible, near-infrared and infrared imagers as well as with passive and active sensing instruments using also microwave frequencies allocated to that purpose (see Chapter 5).

The raw data gathered by the instruments on-board geostationary meteorological satellites are permanently transmitted to a primary ground station of the operating agency, processed, and distributed to various national meteorological centres, to official archives, and other users. Raw data, for example, include images of the Earth taken at several wavelengths so as to provide a variety of measurement data. Processed data are either sent back to the meteorological satellite for re-transmission as part of a direct broadcast to user stations via low and/or high-rate digital signals or are directly distributed to users by using alternative means of data dissemination.

Different to geostationary MetSat satellites, where the satellite is permanently in visibility of its ground stations, the raw data acquired by the instruments on non-geostationary meteorological satellites have to be gathered and stored on-board the satellite until they can be transmitted to a primary ground station of the operating agency when the satellite passes over such a ground station. The raw instrument data are then processed by the operating agency and provided to the users by different data dissemination mechanisms. To improve the latency of the data, a subset of the data acquired by the instruments are “broadcasted” directly from the meteorological satellite and can be received by user stations when the satellite is in the visibility of such a user station which can be located anywhere. Such a service is called “direct read-out”.

To complement the gap in observations over the polar regions by the geostationary satellites, new highly elliptical orbit satellites were introduced, namely Arctica-M series. A set of two satellites working in turns provide geostationary-like coverage of the Arctic region. Raw data (images of the Earth taken in various visible and infrared bands) is transmitted to the primary ground station of the operating agency for further processing and distribution to users.

Meteorological satellites, geostationary and non-geostationary, also carry Data Collection Systems (DCS), namely Data Collection Platforms (DCPs) on geostationary orbit (GSO) satellites and systems such as Argos on non-geostationary orbit (non-GSO) satellites.

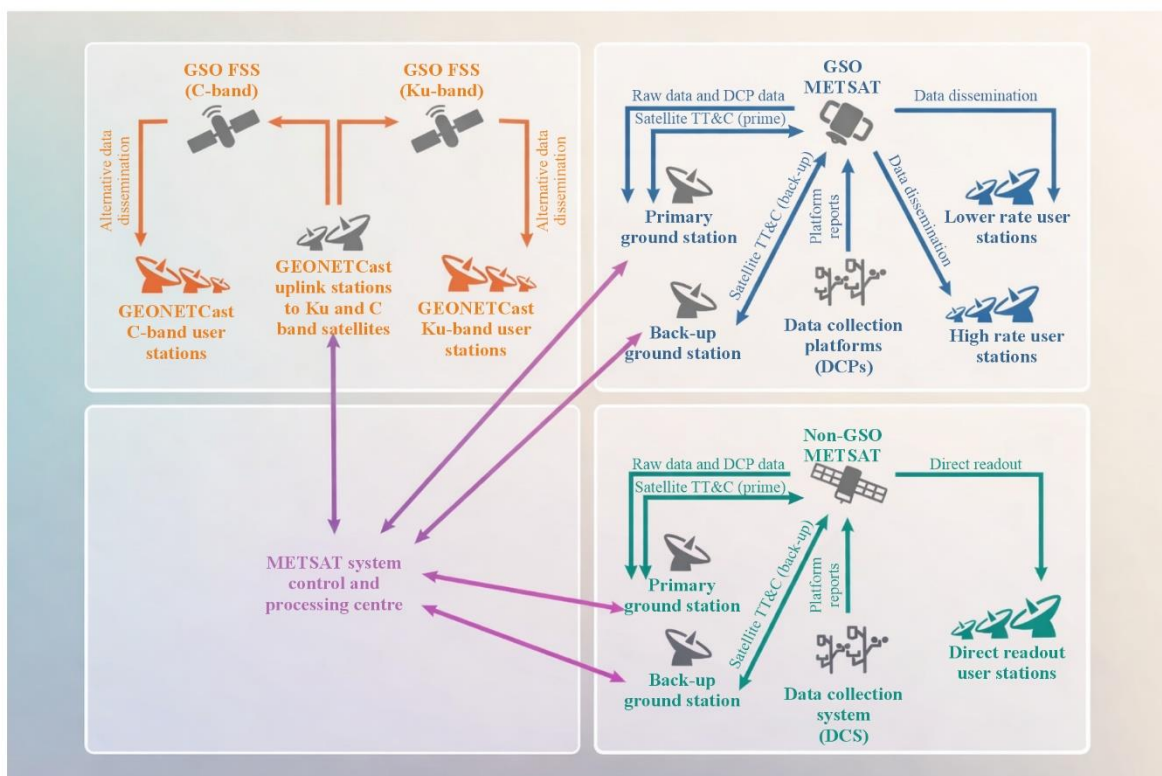
Data Collection Platforms (DCPs), typically located on ground, aircrafts, ships and floating buoys, transmit to geostationary meteorological satellites. The data collected by DCPs are on basic meteorological parameters such as surface temperature, wind velocity, rainfall rate, stream height, gases in the atmosphere, but also data for many other related purposes, such as detection of oceanic pollutants, forest fires, seismic alerting, tsunami warning, avalanche warning, water level monitoring and flood alerting, waterway management, water retention/allocation and for climate research. They may also transmit their current position, allowing movement to be determined. In addition to the operation of regional DCP channels, MetSat operators also contribute to the International Data Collection System (IDCS) through the operation of international channels. As an additional application, a dedicated number of IDCS channels can also be allocated for use by an emergency/disaster monitoring system.

Data collection platforms such as of the Argos system transmit to non-GSO MetSat satellites. When installed on buoys and floats, such platforms measure atmospheric pressure, wind speed and direction, sea surface currents and other sea parameters. Among other applications DCS systems on non-GSO satellites are also used to track animal movements as well as to monitor fishing fleets.

Figure 2-1 shows the general architecture of a MetSat system.

FIGURE 2-1

**General architecture of a MetSat system**



## 2.2 MetSat systems using geostationary (GSO) satellites

In the framework of the WMO Integrated Global Observing System (WIGOS), a number of meteorological satellites are operated at any point in time to ensure a full coverage observation of the Earth from the geostationary orbit (see Fig. 1-3). The continuous and long-term global coverage by observations from the geostationary orbit is ensured by scheduled future launches of meteorological satellites, replacing or further complementing existing satellite systems.

### 2.2.1 GSO MetSat raw image sensor data transmissions

Raw data obtained by the visible, near-infrared and infrared imagers and other sensors on board GSO meteorological satellites are transmitted to main operations Earth stations. The frequency band used for this downlink is determined by the bandwidth required to receive the amount of data generated by the instruments on-board of a GSO MetSat, ranging from using the frequency allocation to MetSat in the bands 1 670-1 698 MHz, 7 450-7 550 MHz, 8 025-8 400 MHz up to the band 25.5-27 GHz. This data is then processed on the ground, and the content is rebroadcasted in the 1 670-1 690 MHz band and/or distributed by other means of telecommunication, e.g. GEONETCast.

Figure 2-2 provides example images from imager instruments onboard GSO meteorological satellites.

FIGURE 2-2

#### Example Images from imager instruments onboard GSO meteorological satellites



Meteo-02-02

For the latest/next generation GSO MetSat systems currently under development and to be deployed in the timeframe 2024–2036, the data rates and the associated bandwidth requirements for the downlink of instrument data from these GSO MetSat systems will significantly increase (up to 1.2 Gbit/s). This has driven the use of higher frequencies such as the bands 7 450-7 550 MHz (Raw Data Transmission on the Electro-L and FY-4 series), 8 025-8 400 MHz (GOES-R and GeoXO), 18.0-18.3 GHz (Region 2), 18.1-18.4 GHz (Regions 1 and 3) (Himawari and FY-4 satellites), and in particular the band 25.5-27 GHz (Main Data Acquisition (MDA) on the Meteosat Third Generation (MTG) series and FY-4 satellites) will have to be used.

There is a limited number of Earth stations of this type around the world at one to three sites per satellite system with one antenna for each satellite of the operational fleet, which sums up to around 50 to 60 primary ground stations operated by the GSO MetSat operating agencies. They are equipped with antennas of approximately 6 m to 18 m diameter (depending on the frequency band used) and typically operate with a minimum elevation angle of 3 degrees.

### 2.2.2 GSO MetSat data dissemination

The following §§ 2.2.2.1 to 2.2.2.5 describe the direct dissemination functions of GSO MetSat systems operated in the framework of the WIGOS.

### 2.2.2.1 Stretched Visible Infrared Spin Scan Radiometer (S-VISSR)

The S-VISSR service is operated by the Chinese GSO MetSat system Feng-Yun-2 (FY-2) series of satellites.

Data observed by the VISSR sensors are transmitted to the main operations ground stations of this Chinese GSO MetSat system. On the ground, data are pre-processed in near real-time and retransmitted via the same satellite at a lower (stretched) data rate. These data are received by S-VISSR earth stations also called medium-scale data utilization stations (MDUSs). More than one hundred receiving stations of this type are known to be in operation. The main users are meteorological services and universities.

S-VISSR transmissions are performed in the sub-band 1 683-1 690 MHz with a centre frequency at 1 687.5 MHz. The data rate of the transmission is 660 kbit/s within a bandwidth of 2 MHz. The figure of merit of reception stations is 12 dB/K with antenna sizes of around 3m, and the minimum elevation angle of antennas is 5 degrees.

### 2.2.2.2 Geostationary Operational Environmental Satellites (GOES) Variable (GVAR)

As of September 2025, United States' geostationary operational environmental satellites (GOES) consist of the latest GOES-R series spacecraft (GOES-16, 17, 18, and 19) and the legacy GOES NOP spacecraft (GOES-13, 14, and 15) were retired by NOAA. The GOES-R Series GOES ReBroadcast (GRB) at 1 686.6 MHz replaces the legacy GOES Variable (GVAR) service, requiring a larger bandwidth to accommodate the much increased data rates on the order of 30 Mbit/s as opposed to GVAR with around 2 Mbit/s. The GVAR operated at 1 685.7 MHz requiring 4.22 MHz bandwidth, while GRB requires either 9.7 or 10.9 MHz to transmit the processed data and operates at 1 686.6 MHz. The GRB transmits the full set of level 1b products, including data from all GOES-R Series instruments, hemispherically (down to 5 degrees elevation) from the GOES-R equatorial locations of 75° W and 137° W. Just like GVAR, these broadcasts reach a wide range of receiving stations within the combined footprint of the GOES-R spacecraft. These include not only stations in North and South America, but also locations in New Zealand, France, Spain and Great Britain. The majority of these recipients are universities and government agencies involved with meteorological research or forecasting. Others include value-added providers supplying weather forecasts to commercial interests.

### 2.2.2.3 Weather Facsimile (WEFAX)

The remaining analogue Weather Facsimile (WEFAX) service still operational on some GSO MetSat satellites is in the process of being replaced by digital low-rate information transmission (LRIT) service on second-generation meteorological satellite systems. The WEFAX service consists of analogue transmissions to low-cost meteorological user stations within the reception area of meteorological satellites. The WEFAX service parameters were defined and agreed by the Co-ordination Group for Meteorological Satellites (CGMS), a forum for the exchange of technical information on geostationary and polar-orbiting meteorological satellite systems.

The WEFAX service on GOES-13, -14, and -15 (satellites meanwhile retired) at 1 691 MHz (586 kHz) was combined with the LRIT and the Emergency Managers Weather Information Network (EMWIN), operating at 1 692.7 MHz (27 kHz), into a single downlink known as HRIT/EMWIN, where the HRIT replaces LRIT. This combined service transmits at 1 694.1 MHz, with 1.21 MHz of bandwidth. The existing sensor data downlink at 1 676 MHz was moved to 8 220 MHz within the EESS X-band (8 025-8 400 MHz) to accommodate the greatly expanded data rates from the advanced sensors on-board the GOES-R spacecraft.

There are very few WEFAX reception stations that remain in operation at meteorological services as well as at other entities such as universities, environmental agencies, press agencies, schools and others.

The transmission of WEFAX services is in the sub-band 1. The remaining WEFAX services have a centre frequency of 1 691 MHz and a bandwidth between 0.03 MHz and 0.26 MHz. Typical WEFAX reception stations operate at elevation angles greater than 3 degrees and use antennas of 1.2 m diameter with a figure of merit ( $G/T$ ) of 2.5 dB/K. Content of WEFAX transmissions are sectors of satellite imagery, meteorological products in pictorial presentation, test images and administrative messages containing alphanumeric information in pictorial form.

#### 2.2.2.4 Low Rate Information Transmission (LRIT)

LRIT is a service that was initiated in 2003 on GOES geostationary meteorological satellites for transmission to low-cost user stations. This service was intended to replace the WEFAX service on other GSO MetSat satellites, serving a similar user community.

Transmissions of LRIT are performed in the sub-band 1 690-1 698 MHz with centre frequencies around 1 691 MHz. The bandwidth is up to 660 kHz. User station antennas have diameters between 0.6 m and 1.8 m and are operated with a minimum elevation angle of 3 degrees. The figure of merit for LRUS is 3-6 dB/K depending on the user station location. LRIT is operational on many MetSat systems, namely GOES, Meteosat second generation, GEO-KOMPSAT-2A, Himawari, Electro-L and FY-4 series satellites together with an Emergency Weather Alarm Information Broadcast (EWAIB).

#### 2.2.2.5 High Rate Information Transmission (HRIT)

HRIT service was introduced in January 2004 with the operation of the first satellite of the Meteosat second generation series satellites (Meteosat-8) and is operational on many MetSat systems, namely Himawari, GEO-KOMPSAT-2A, Electro-L and FY-4 series satellites. Also, the series of GOES satellites from GOES-R onwards operate an HRIT/EMWIN service.

The HRIT service is operated in the sub-bands 1 675-1 687 MHz, 1 684-1 690 MHz or 1 690-1 698 MHz. The antenna size for high-rate user station (HRUS) and MDUS is 4 m to 7 m diameter and the minimum elevation angle is 3 degrees (5 degrees for GOES) approximately. The figure of merit for the user stations is 12-14 dB/K depending on the user station location.

A new Direct Broadcast Global Specification (GEO HRIT/LRIT) has been published within 2013 by CGMS. This Direct Broadcast specification is applicable to existing and planned GEO systems, however not specifying user station characteristics. Work continues within CGMS to assess the need for further updating the GEO global specification in view of newly available and used standards on telecommunications and file formats.

### 2.2.3 GSO MetSat Data Collection Systems (DCS)

Data collection systems are operated on meteorological satellites for the collection of meteorological and other environmental data from remote DCPs. Transmissions from each DCP to a meteorological satellite are in the frequency band 401-403 MHz. DCPs are operated in time sequential mode. The transmission time slots are typically 1 min. Transmission rates are 100 bit/s. Higher data rate DCPs (300 bit/s and 1 200 bit/s) began operation in 2003 and have recently increased rapidly. Channel bandwidths of these high rate DCPs are 0.7510 kHz or 2.2510 kHz for 300 and 1 200 bit/s, respectively.

There are various types of DCP transmitters in operation generally ranging from 5 W, 10 W and 20 W output power with a directional antenna, or 40 W output power with an omnidirectional antenna. The resulting uplink equivalent isotropically radiated power (e.i.r.p.) is between 40-52 dBm. Data collection systems are currently operated on various geostationary meteorological satellite systems.

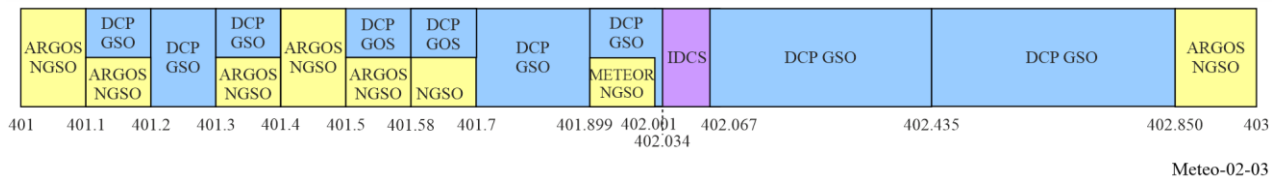
The DCPs reporting to geostationary MetSats use frequencies in the 401.1-402.85 MHz range, with 402.0355-402.0655 MHz for international use (11 channels (I12 to I22) of 3 kHz in bandwidth). By using narrow bands (as small as 0.75 kHz) and by shortening the reporting times to typically 10 s, it is possible to receive data from a large number of these platforms. For example, in the case of the GOES-R series satellites, in 2024 there were approximately 30 000 GOES high rate DCPs in operation, sending up to 1 000 000 messages per day, delivering more than 6 million observations into the WIGOS daily. User support for DCS remains steady, if not increasing. Future GSO MetSats are planned to include DCS, such as the GeoXO constellation launching in the 2030s – ensuring DCS support well into the 2050s.

#### 2.2.3.1 Basic general partitioning and sharing conditions for the band 401-403 MHz

The increased spectrum requirements of DCSs on both, geostationary and non-geostationary, MetSat and EESS systems require all operators to respect a basic general partitioning of the band 401-403 MHz for current and future DCSs (see Fig. 2-3) accompanied by sharing conditions as outlined in Recommendation ITU-R SA.2045.

FIGURE 2-3

**Basic general partitioning of the band 401-403 MHz for future long-term coordinated use of DCSs on geostationary and non-geostationary MetSat and EESS systems**



**2.3 MetSat systems using non-GSO satellites**

Beside the numerous GSO MetSat satellites, non-GSO MetSat systems, mostly sun-synchronous polar orbiting, but also highly elliptical orbit satellite systems, complement the satellite-based contribution to the WIGOS through global coverage measurement data from a variety of passive and active sensors observing in the visible, infrared and microwave spectral regions.

The continuous and long-term coverage of observations from the non-geostationary orbit will be ensured through the operation of current and future satellites operated by a number of national and regional meteorological organizations throughout the world (see Fig. 1-3).

Figure 2-4 provides example images from imager instruments onboard non-GSO MetSat systems taking global visible, near-infrared and infrared imagery of clouds, oceans and land surfaces. Examples of passive and active sensors observing in the microwave spectral region operated on non-GSO MetSat systems are provided in Chapter 5.

FIGURE 2-4

**Example images from imager instruments onboard non-GSO MetSat systems**



Meteo-02-04

**2.3.1 Non-GSO MetSat raw instrument data transmissions**

Raw data from the currently operational non-geostationary meteorological satellites, mostly polar-orbiting, a few non-sun-synchronous circular orbit with an inclination of 35, 50 or 66 degrees to the Equator, and highly elliptical orbiting satellites are transmitted in the frequency band 7 750-7 900 MHz or 8 025-8 400 MHz, depending on the bandwidth required, to dedicated main stations located mostly at high latitudes. The transmission takes place in bursts as each satellite overpasses its main station, with the transmitters switched off at other times. In case of highly elliptical satellites of Arctica-M series, the transmission is similar to the one of geostationary satellite and is performed every 30/15 minutes during the period of visibility of each of the satellites from the primary ground station.

### 2.3.1.1 Non-GSO MetSat raw instrument data transmissions using the band 25.5-27 GHz

Some future non-GSO MetSat systems (for example the EUMETSAT Polar System – Second Generation (EPS-SG) with its Metop-SG satellites and the satellites of the Joint Polar Satellite System (JPSS)) and future FY-5 satellites will need to use even higher frequency bands than those used by the currently operational satellites, i.e. the band 25.5-27 GHz, to be able to transmit the significantly increased data rates of up to 800 Mbit/s to its main ground stations. This link is called Stored Mission Data (SMD) downlink. Others will continue to use the frequency bands 7 750-7 900 MHz or 8 025-8 400 MHz (e.g. current JPSS, Suomi-NPP, Metop, FY-3, METEOR-M and Arctica-M).

### 2.3.2 Non-GSO MetSat data dissemination

Sections 2.3.2.1 and 2.3.2.2 describe the direct dissemination functions, called “direct read-out”, of non-GSO MetSat systems operated in the framework of the WIGOS. This direct read-out is to improve the latency of the data by transmitting a subset of the data acquired by the instruments directly from the meteorological satellite to user stations when the satellite is in the visibility of such a user station which can be located anywhere.

#### 2.3.2.1 Non-GSO MetSat data dissemination using the band 1 698-1 710 MHz

##### 2.3.2.1.1 Automatic Picture Transmission (APT)

The Automatic Picture Transmission (APT) service was introduced on some spacecraft already in the 1960s and became the most successful direct data dissemination system in the meteorological community. Thousands of such APT receiving stations are still in operation worldwide. APT stations are very low cost and are operated not only by meteorological services and universities but also by a large community of non-meteorological users.

APT stations typically consist of omnidirectional antennas and commercial-off-the-shelf (COTS) VHF receivers. Low-cost image processing systems are attached to this front-end, with low-priced software running on commonly available desktop computers. APT is operational on the NOAA satellites.

##### 2.3.2.1.2 Low Resolution Picture Transmission (LRPT)

The LRPT service was supposed to replace the APT application on most non-GSO MetSat systems. However, the only series of satellites of which the LRPT service was implemented and operational is METEOR-M. LRPT is based on digital transmission schemes and operates at 137.1 MHz and 137.9 MHz with a signal bandwidth of up to 150 kHz.

##### 2.3.2.1.3 High Resolution Picture Transmission (HRPT)

In the framework of the Coordination Group of Meteorological Satellites (CGMS) the revised version of Direct Broadcast Global Specification (LEO Direct Readout (HRPT/AHRPT)) was published in 2014 by CGMS. This Direct Broadcast specification is applicable to non-GSO MetSat systems using the band 1 698-1 710 MHz for data dissemination. The HRPT service provides high-resolution imagery to the meteorological community. HRPT transmitters are turned on continuously and can be received by any user station. HRPT data are essential to operations of meteorological services and are widely useful in other endeavours as well.

In the HRPT service like on the NOAA satellites (1 698/1 702.5/1 707 MHz) transmissions are performed in the frequency band 1 698-1 710 MHz with signal bandwidths between 2.7 MHz and 4.5 MHz. User stations are equipped with tracking parabolic antennas typically between 2.4 m and 3 m in diameter. The recommended minimum elevation angle for reception is 5 degrees, although some stations operate at elevation angles lower than this. The figure of merit for stations is 5 dB/K. There are other HRPT systems that operate at data rates that are about twice the rate of the original HRPT systems.

There is also an Advanced HRPT (AHRPT) application on some of the operational meteorological satellites, i.e. the series of METEOR-M (1 700/1 705 MHz), Metop (1 701.3/1 707 MHz) and FY-3 (1 701.3 MHz, 1 704.5 MHz or 1 706.7MHz) satellites. AHRPT transmissions use the same band as the other HRPT systems. The bandwidth ranges between 4.5 and 6.8 MHz. AHRPT reception stations receive with minimum elevation angles of 5 degrees. Antennas are parabolic with typical diameters between 2.4 m and 3 m. The  $G/T$  of AHRPT stations is around 6.5 dB/K.

### 2.3.2.2 Non-GSO MetSat data dissemination using the band 7 750-7 900 MHz

The trend for more and higher resolution data also requires using higher frequency bands for the direct dissemination of instrument data to user stations as the corresponding bandwidth requirement for such high-resolution data cannot be satisfied in the band 1 698-1 710 MHz. Thus, the next higher available frequency band allocated to MetSat in the space-to-Earth direction that has to be used is the band 7 750-7 900 MHz. In this band the bandwidth requirements of the new generation non-GSO MetSat systems, ranging from 30 to 150 MHz for the different downlinks (MPT (FY-3), High Resolution Data (HRD) (Suomi-NPP and JPSS) and Direct Data Broadcast (DDB) (Metop-SG)) can be satisfied.

The Medium-resolution Picture Transmission (MPT) provides a full set of data of the MERSI instrument measurements on-board the FY-3 series of satellites. The current FY-3 satellite data rate of the transmission is 45 Mbit/s within a bandwidth of 60 MHz centred at 7 780 or 7 820 MHz, or the data rate of the transmission is 77 Mbit/s within a bandwidth of 80 MHz centred at 7 790 or 7 860 MHz. In addition, on the FY-3 series a Delayed Picture Transmission (DPT) service is provided for dump data transmission at 8 212.5 MHz with a bandwidth of 375 MHz at a data rate of 455 Mbit/s. The HRD is a broadcast of a full resolution data set from Suomi-NPP and the series of JPSS satellites of up to the 15 Mbit/s data rate (30 MHz bandwidth) with its centre frequency at 7 812 MHz. The DDB on the Metop Second Generation (Metop-SG) series of satellites will broadcast at 7 825 MHz with a bandwidth of 150 MHz.

### 2.3.3 Non-GSO MetSat Data Collection Systems (DCSs)

Data collection systems on non-GSO MetSat satellites provide a variety of information used principally by governmental agencies but also by commercial entities.

Such data include a number of environmental parameters for oceans, rivers, lakes, land and atmosphere related to physical, chemical and biological processes. It also includes animal tracking data. However, use by commercial entities is limited. It comprises, for example, monitoring of oil pipeline conditions in order to protect the environment or maritime security. Some transmitters are also deployed to report emergencies and supply data such as for hazard/disaster recognition. Examples of DCSs operated from non-GSO meteorological satellites are Argos and Brazilian DCS. The third generation of Argos (Argos 3) is already operational on the series of Metop satellites, NOAA and a SARAL satellite.

These NOAA, Metop and SARAL satellites follow a polar orbit at 850 km altitude: they pass over the North and South poles at each revolution. The orbit planes turn around the poles axis at the same speed than the Earth around the Sun. Each satellite sees simultaneously and at all times all the beacons inside a circle of about 5 000 km in diameter. With the movement of the satellite, the ground track of this circle forms a band of 5 000 km wide which wrap around the Earth while passing at the North and South poles.

Currently, the Argos system operates in the 401.579-401.690 MHz band, though thousands of platforms (known as platform transmitter terminals), each requiring only few kHz of bandwidth. Taking advantage of the nature of the orbits of polar-orbiting satellites, it is possible to accommodate many Argos platforms. About 22 000 platforms are in operation. Each platform is characterized by an identification number which is unique and depends on its transmission electronics.

The transmission duration of each message is less than one second. The Argos-3 system generation introduces new data collection services offering high data rate (4 800 bit/s) and platform interrogation capability. Depending on the bit rate, the values of output power of platform range from  $-3$  dBW up to 7 dBW.

The platform known as PMT (Platform Messaging Transceiver) is interrogated by satellites using the 460-470 MHz band and is currently performed at 465.9 MHz.

For the fourth generation of the Argos system (Argos 4), it is expected that the system capacity and the bandwidth will have to be significantly increased using other frequency bands as shown in Fig. 2-3. In addition, the new Argos 4 system will implement a downlink within the 464.98775-466.98775 MHz frequency band and a spread spectrum multiple access will be implemented in order not to cause interference to terrestrial users.

The Brazilian DCS is based on SCD (25 degrees inclination orbit) and CBERS satellites using 401.605-401.665 MHz band for data collection platform reception. Due to the compatibility between the Brazilian DCS with the Argos system and complementary orbit satellites, data exchange between both systems has been implemented since 2001.

Data collection systems are also operated on highly elliptical orbit meteorological satellites of Arctica-M series for the collection of meteorological and other environmental data from remote DCPs. Transmissions from each DCP to Arctica-M satellite are in the frequency band 401-403 MHz.

## **2.4 Alternative data dissemination mechanisms**

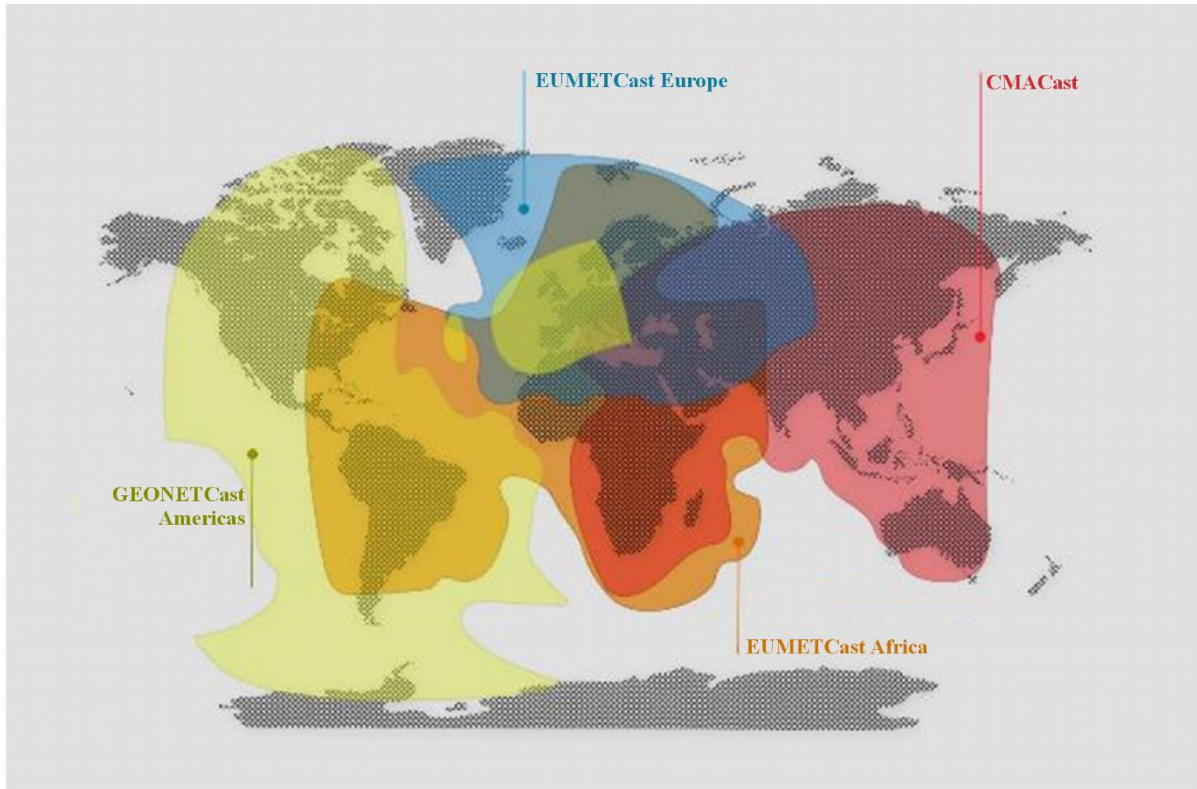
Beside the traditional dissemination mechanisms of GSO and non-GSO MetSat systems an additional dissemination system has been established, called GEONETCast (see Fig. 2-5), which is a major Global Earth Observation System of Systems (GEOSS) initiative, coordinated by the intergovernmental Group on Earth Observation (GEO), to develop a worldwide, operational, end-to-end Earth observation data collection and dissemination system, using existing global commercial telecommunications infrastructure in the C-band (3 800-4 200 MHz) and the Ku-band (10 700-11 700 MHz).

The GEONETCast concept is to use the multicast capability of a global network of communications satellites to globally disseminate weather, water and climate related information, including disaster warnings to meteorological agencies and user communities. In this context, the use of the C-Band satellites is particularly important in areas where propagation conditions (e.g. heavy rain in tropical and equatorial zones) make the use of any other telecommunication support impractical. To achieve and maintain this, several regional centres take on the responsibilities for establishing and maintaining a satellite-based regional dissemination system, based upon Digital Video Broadcast (DVB) technology, and provide complementary services to a common user community.

Current partners include the China Meteorological Administration (CMA), the European Organisation for the Exploitation of Meteorological Satellites (EUMETSAT), the National Oceanic and Atmospheric Administration (NOAA), as well as many third-party data providers.

The global coverage is provided through the integration of the CMACast system, covering the Asia Pacific region and part of Africa, the GEONETCast Americas component, covering the Americas and the EUMETCast system, covering Europe, Africa and part of the Americas.

FIGURE 2-5  
Global GEONETCast coverage



Meteo-02-05



## CHAPTER 3

### Meteorological aids service

#### 3.1 Introduction

The meteorological aids (MetAids) service is defined in No. **1.50** of the Radio Regulations (RR) as a radiocommunication service used for meteorological, including hydrological, observations and exploration. This Chapter only covers the upper-air *in situ* observation, other MetAids applications being covered in Chapters 6 and 7 of this Handbook.

In practice, MetAids service usually provides the link between an *in situ* sensing system for meteorological variables and a remote base station. The *in situ* sensing system may be carried, for instance, by a weather balloon. Alternatively, it may be falling through the atmosphere on a parachute after deployment from an aircraft. The mobile base station may be at a fixed location, or mounted on a mobile platform (for example, carried on ships, or research aircraft). The vast majority of such *in situ* sensing systems are radiosondes, most of which are launched regularly from fixed locations or mobile platforms, at least at 0000 and 1200 UTC, forming global WIGOS upper-air network (WMO-No. 1160).

The description of upper-air measurements is provided in Chapters 12 and 13 of the Guide to Instruments and Methods of Observation (WMO-No. 8), Volume I – Measurement of Meteorological Variables.

#### 3.1.1 Allocated RF bands

Table 3-1<sup>4</sup> indicates the frequency bands that are allocated in the ITU Radio Regulations (RR) to the MetAids service (other than those governed by country footnotes) for use by meteorological aids systems/applications.

TABLE 3-1

**Frequency band allocations to MetAids in the ITU Radio Regulations**

Frequency band
8.3-9 kHz
9-11.3 kHz
27.5-28 MHz*
400.15-401 MHz
401-402 MHz
402-403 MHz
403-406 MHz
1 668.4-1 670 MHz
1 670-1 675 MHz
1 675-1 690 MHz
1 690-1 700 MHz
35.2-36 GHz*

\* No information on the existing or planned usage of this frequency band was found in the ITU-R and WMO documentation.

<sup>4</sup> For current frequency allocation in these bands, the reader is referred to Article 5 of the RR.

There are also other primary services in these bands which place significant constraints on the systems operating under MetAids allocations. Co-channel sharing between other services and the MetAids service is rarely feasible because of the low power transmissions used by most MetAids systems for relatively long-range links. Hence, most band sharing relies on band segmentation. This may be organized internationally with other meteorological systems through the auspices of WMO, or at a national level with the non-meteorological systems.

Operational details of the radiosonde systems in use at each observing station, that exchanges data internationally, are/will be available in the OSCAR/Surface (<https://oscar.wmo.int/surface/>), the WMO repository of WIGOS metadata. The OSCAR/Surface is an online database which provides the detailed characteristics of measuring instruments. The WMO Members operating the stations are responsible for entering and maintaining those details.

Users of the MetAids service also include:

- environmental agencies
- disaster relief organizations
- universities and meteorological research groups
- defence services
- space launch operators.

Many of the non-WMO MetAids systems are usually operated independently from the routine operations of the national meteorological services and may not be registered in the OSCAR/Surface. Those systems are mounted on mobile platforms and may be deployed over a wide range of locations during operational use. The operation of those additional systems needs to be regulated in order to avoid any interference with the radiosondes operated by national meteorological services. This regulation is developed and implemented jointly by national radiocommunication authorities and national meteorological services.

In some countries, co-channel sharing between all the different groups of radiosonde operators is avoided by using a detailed channel plan. However, in many countries a pragmatic approach to spectrum use is still used. Before launching the radiosonde, the radiosonde system operator scans the available MetAids spectrum using the base station receiver. This identifies if there are any radiosondes already in use near the launch site. The frequency of the radiosonde to be launched is then selected (tuned as necessary before launch) so that it will function without detriment to the systems already in flight. The available MetAids spectrum for a national MetAids service is often limited to a sub-band of that allocated in the RR because of national sharing agreements with other radiocommunication services, as noted earlier.

Radiosonde systems operate in the WMO network in the 400.15-406 MHz and 1 668.4-1 700 MHz frequency bands. The reasons for the continued use of these two MetAids service bands is discussed in a later section, once the systems in use have been discussed in more detail.

### 3.1.2 Meteorological functions of the MetAids service

Accurate measurements of the vertical profiles of atmospheric temperature, pressure, relative humidity and wind speed and direction are crucial for operational meteorology. These measurements are essential input for numerical weather prediction models, for weather forecasting from very short range (nowcasting) up to longer (climate) predictions. They are further used for climate monitoring purposes. Short-term forecasts require temperature and relative humidity measurements with a vertical resolution of 100 m or better.

The MetAids service has been the main source of atmospheric measurements with high vertical resolution for many decades. In addition, these *in situ* measurements are essential for calibrating space-borne remote sensing, in particular passive sounders. Measurements of atmospheric constituents such as ozone, aerosol or radioactivity may also be included.

MetAids transmit data from *in situ* measurements of meteorological variables from locations above the surface to a base station consisting of a receiver and data processing system. From the base station, the data are transmitted to the meteorological communications networks for integration with data from other receiving stations. The MetAids systems are not usually recovered after use, so the cost of the transmitter and sensing package must be kept to a minimum, but without degrading the quality of the measurements.

MetAids systems currently deployed include:

Type	Description
Radiosondes	Instrument intended to be carried by a balloon through the atmosphere, equipped with devices to measure one or several meteorological variables (such as pressure, temperature, humidity), and provided with a radio transmitter for sending this information to the observing station.
Ozonesondes	Small, lightweight and compact balloon-borne instruments, developed for measuring the vertical distribution of atmospheric ozone up to an altitude of about 30-35 km.
Dropsondes	Dropped from high flying aircraft using a parachute, with the dropsondes usually transmitting back to a receiving station on the aircraft, from 15 minutes to about half an hour.
Tethersondes	Transmits back continuously from a tethered balloon usually within the atmospheric boundary layer.
Small pilot-less aircraft (remotely piloted vehicle (RPV) or uncrewed aerial system (UAS))	Carries a similar sensor package to the radiosonde to remote areas over the ocean and also transmits information back as a standard meteorological message.

Recently introduced, the Global Basic Observing Network (GBON) (for more information, see WMO-No. 1165, Chapter 11), together with an increased use of radiosondes for environmental and defence services as well as the increased requirement from national meteorological services for more *in situ* measurements over the ocean, is supposed to lead to the significant increase in the use of newer types of MetAids systems in the next decades to support these expanding requirements.

## 3.2 Examples of MetAids sensing systems

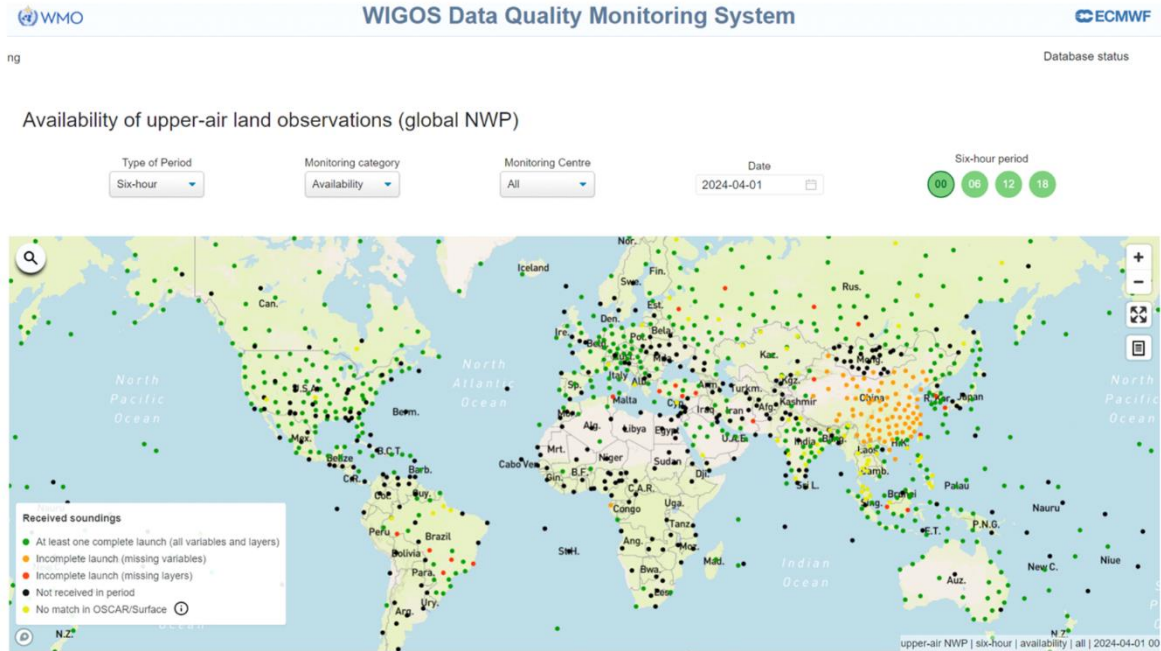
### 3.2.1 Radiosondes

Upper-air measurements of temperature, wind and relative humidity are three of the basic measurements used in the initialization of the analyses of numerical weather prediction (NWP) models for operational weather forecasting. Radiosondes provide most of the *in situ* temperature and relative humidity measurements over land, while radiosondes launched from remote islands or ships can provide limited but important coverage over the oceans.

Every day more than 1 500 radiosondes are launched in the WIGOS network (Fig. 3-1); of these radiosondes around 300 are for measurement at nominated Global Climate Observing System Upper-air Network (GUAN) sites. The information from each operational radiosonde is immediately used by national meteorological services to support local forecasting. This information is also required for numerical weather predictions for all parts of the world, and the goal is to circulate the completed message reports (in standardized meteorological code) to all meteorological services around the world within three hours. The messages are also archived and then used in a wide range of scientific research.

FIGURE 3-1

Availability of upper-air land observations as provided by the WIGOS Data Quality Monitoring System



Meteo-03-01

Usually, an operational radiosonde is carried by a weather balloon (Fig. 3-2) to heights up to 35 km where the balloon bursts. The height to which regular observations are performed varies with the application and geographical location and, for many countries, is limited by cost of balloons and lifting gas required. For these reasons, many observations worldwide are not made to heights greater than about 25 km. Forecasting on a global scale needs to take into account the movements of the air masses at the upper levels, but not in as much detail as the conditions closer to the surface. However, climate monitoring and associated scientific research require high resolution measurements from as high in the upper atmosphere as feasible.

FIGURE 3-2  
A radiosonde flight train



Meteo-03-02

The base station sites used to launch radiosondes are usually specially equipped so that the balloons can be launched in all weather conditions. The most critical sites are equipped with emergency power supplies and accommodation so that the measurements can continue even if the local infrastructure is affected by extreme weather or other circumstances such as an industrial accident.

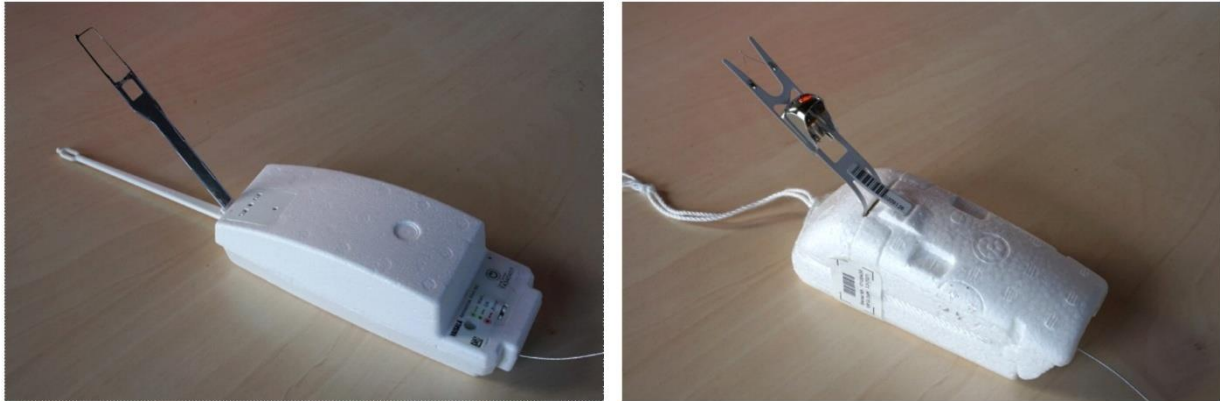
The balloons lifting the radiosondes are designed to provide optimum performance when ascending at about 300 m/min. They move with the upper atmospheric winds and on occasions may travel more than 250 km from the launch site during ascent. During descent, they may travel an additional 150 km. Descent data are considered to be of potential value as well. Radiosonde measurements are transmitted for up to three hours to a base station located at the balloon launch site. Any significant loss of reception early in an ascent (even for 10 s) is undesirable since this compromises the ability of the radiosonde to resolve the changes in temperature and relative humidity near the surface, required for local forecasting. Missing data for four or five minutes (even if only caused by faulty navigation signal reception for the wind measurements), or a termination before the target altitude, as defined by the operator who launched the radiosonde, often necessitates the launch of a second radiosonde to fulfil the operational requirements.

The transmission power is always low, because of the limitations imposed by the available batteries. Radiosondes typically use lithium or alkaline batteries that must function at the very low temperatures encountered during a flight, and must not endanger environment or public safety when falling to earth after the balloon bursts.

A typical radiosonde (see Fig. 3-3) contains several major components: a transmitter, battery, sensor pack, and usually a navigational aids NAVAID/GNSS (e.g. GPS) receiver. The transmitter transmits the data to the receiving station. The sensor pack contains the sensors that measure one or several of the atmospheric variables such as temperature, wind, relative humidity and pressure. In special cases, sensor packs can contain sensors for the measurement of ozone (ozonesondes). The sensor pack also encodes the sensor values sufficiently to transmit them to the ground station.

Radiosonde systems measure winds by tracking their balloon's motion through the atmosphere. Active tracking systems use primary (tracking of a reflector for radar signals suspended below the balloon) or secondary (tracking of a transponder integrated into a radiosonde) radar tracking. Passive tracking systems use NAVAID/GNSS receivers on the payload and transmit this data to the ground station, or radiotheodolite tracking of radiosonde signals.

FIGURE 3-3  
Radiosonde examples



Photos taken from Instruments and Observing Methods Report No. 143

Meteo-03-03

### 3.2.2 Dropsondes

Dropsondes have components similar to radiosondes but are designed to be dropped from aircraft to profile the atmosphere as they descend under a parachute (Fig. 3-4). All dropsondes are operated in the 401-406 MHz band and utilize NAVAID/GNSS for wind measurement. Operationally, at limited, targeted areas, dropsondes are deployed at a much higher density in space and time than radiosondes. They are primarily used in tracking and profiling tropical storms at sea. Several dropsondes may be placed in flight and tracked simultaneously. The high density of deployment necessitates the use of highly stable narrow-band transmitters, similar to those used in the denser parts of the radiosonde network. Dropsondes are also used for profiling weather phenomena or the basic atmospheric state in remote oceanic regions, and occasionally over land.

FIGURE 3-4

**A dropsonde**

Meteo-03-04

**3.3 Factors influencing the characteristics of the MetAids systems**

MetAids systems are comprised of several basic radiocommunication components. The ground portion of the system typically contains an antenna/receiver system and a signal processing system. Recommendation ITU-R RS.1165 – Technical characteristics and performance criteria for radiosonde systems in the meteorological aids service in the 403 MHz and 1 680 MHz bands, contains descriptions and technical parameters of the various types of systems used for MetAids operations.

**3.3.1 Ground-based receiver antenna system**

Radiosondes and dropsondes use a radio frequency link to transmit the data back to the antenna/receiver system located at the data processing location. Two frequency bands are used for this purpose (400.15-406 MHz and 1 668.4-1 700 MHz). For radiosondes, typically the antenna/receiver system is ground based, but in the case of dropsondes the antenna/receiver system is located on an aircraft. The particular antenna receiver system configuration varies based on the operating band and the maximum flight slant range expected. Omni-directional antennas and rosettes of Yagi antennas or corner reflectors are typically used for systems operated in the band 400.15-406 MHz (Fig. 3-5). Very high antenna gain is not needed by these types of antenna to maintain the RF link. Radio direction finding (RDF) is not used for measuring the winds in this band. The antenna gain of the antenna systems operated in the band 400.15-406 MHz range from 0 dBi to 10 dBi.

FIGURE 3-5

**Omni-directional antenna and directional systems (401-406 MHz)**

Photos taken from Instruments and Observing Methods Report No. 143

Meteo-03-05

Wind measurement is usually accomplished through GNSS, RDF or radar tracking in the 1 668.4-1 700 MHz band. Some countries still prefer using RDF to track a radiosonde as this allows the use of a radiosonde independently of the availability of NAVAID/GNSS systems – which may not be available during times of emergency. Therefore, tracking pedestals equipped with large parabolic antennas or phased array panels are used to avoid path loss (see Fig. 3-6). The antenna pedestal rotates the antenna in azimuth and elevation to track the MetAid movement. Antenna gains of 25-28 dBi are typical for antenna systems operated in the band 1 668.4-1 700 MHz.

FIGURE 3-6

**Tracking antenna systems (1 668.4-1 700 MHz)**

Meteo-03-06

**3.3.2 Ground-based processing system**

The receiver passes the baseband radiosonde signal to a signal processing system that decodes the analogue or digital radiosonde data and generates the required atmospheric measurement data. Some MetAids do not transmit the actual meteorological data (such as pressure, temperature, humidity, ozone, winds) to the receiving station but rather transmit the electronic characteristics of the sensors, NAVAID/GNSS data to minimize the cost of processing on the MetAid. The signal processing system on the ground then applies the capacitive and/or resistive sensor values and sensor calibration values, to a polynomial to calculate the meteorological variable. Other MetAids may perform most signal processing within the MetAids and transmit actual meteorological data directly. In this case the processing system on the ground may perform only a subset of the overall data processing.

### 3.3.3 Expendable sensing packages

The nature of the MetAids service operations places constraints on how they are manufactured. Most of the design constraints impact the radio frequency characteristics of MetAids expendables and hence the spectrum requirements of MetAids operations. The most significant constraint is the production cost of the devices. However, other constraints such as density, mass, operating environment and power efficiency are also major concerns to manufacturers and operators. The environmental impact of one-time-use sensing packages is also a significant consideration and is increasingly becoming a constraint in the selection of devices as NMHSs seek to improve the environmental sustainability of their operations and minimize unrecoverable waste.

Advancements in digital technology have provided opportunity to use cost effective integrated circuits to improve radiosonde performance. Historically, many of the improvements applied to radiosondes have been to improve measurement accuracy of the sensors and a reduction in the mass and size of the radiosondes. In recent years, operators have been forced to implement some improvements to the RF characteristics in order to increase network density. This resulted in that most world-leading manufacturers' radiosonde designs comply with quite stringent ETSI standards in respect to emission bandwidth and sideband radiation. Many basic radiosonde designs contain single stage transmitters. These designs are affected by changes in temperature, battery voltage, and capacitive loading of the antenna during handling. Use of commercially available application specific integrated circuits (ASICs) is now increasing as suitable devices that can be operated over the extreme temperature ranges.

The density of MetAids expendables must be limited for safety reasons. The mass of the MetAids expendables is also limited for both safety and operational reasons. While extremely unlikely, MetAids must be designed to ensure that a collision with an aircraft will not damage the aircraft and will not create a life-threatening situation. The density is primarily of concern if the device were to be ingested into the engine. The devices' mass is a concern since MetAids expendables drop back to the Earth's surface after a flight. A parachute is often used to control the rate of descent. However, an object with significant mass has the potential to cause damage. Most MetAids expendables now have a mass much less than 1 kg (without a balloon). Typically, radiosondes are housed in a foam, paperboard or plastic package that is lightweight and easily destructible. The circuit cards are small and contain a small number of components and the circuitry is designed for maximum power efficiency. The batteries that are necessary for operation of the sensing packages are becoming smaller and contribute to the reduction of the overall load, but they still present challenges with respect to environmental impact.

MetAids can be exposed to a variety of extreme conditions during flight. The temperature may range from 50 °C to -90 °C, humidity can range from very dry conditions to condensation, sublimation or precipitation. At higher altitudes, insufficient air for ventilation of the electronics and solar radiation can lead to overheating even at low temperatures. These extreme changes in conditions can have a dramatic effect on the performance and characteristics of all the device components including the transmitter. It was not uncommon for an older design radiosonde transmitter to drift 5 MHz or more due to extreme temperature changes and other effects such as icing of the antenna that causes capacitive loading. Due to limitations on the power consumption and the effect that generating heat can have on sensor performance, stringent temperature control of the electronics is not practical. In addition, it has been found that many of the commercially available transmitter integrated circuits used by the wireless telecommunications industry cannot operate at the extremely low temperature.

The power consumption of the MetAid electronics must be carefully managed in the design. Large batteries increase the environmental footprint of the sensing package, and increase the weight causing a potential safety hazard, and the additional weight increases operational costs by requiring larger balloons and larger amounts of gas for balloon inflation. Power efficiency is the primary reason that MetAids are designed to use as little transmitter output power as possible and still maintain a reliable telemetry link. Radiosonde transmitters typically produce 100-400 mW and the link budget at maximum range only has on the order of 0.5-2 dB of link margin. The commonly used single stage transmitter has been found to be very power efficient, while the more advanced transmitter designs have been found to consume 150-250% more power than the single stage transmitter. However, these single stage transmitters are vulnerable to the extreme temperature changes and capacitive loading of the antenna during handling resulting in large frequency drift. Modern digital transmitters are more spectral efficient compared to the old analogue transmitters.

### 3.4 Characteristics of meteorological observations required from the MetAids service

The characteristics of observations required from MetAids service operations are illustrated in this section with a few examples of radiosonde and ozonesonde measurements.

#### 3.4.1 Characteristics of radiosondes

Figure 3-7 shows an example radiosonde flight from Watnall on 2024/04/13 up to a maximum altitude of about 30 km. In this profile, the altitude and wind were derived from GPS, and the pressure was also derived from GPS altitude alongside temperature and relative humidity measurements. The use of GPS derived pressure is commonplace internationally.

In the left-hand panel of Fig. 3-7, the minimum temperature occurred at about 27 km. The relative humidity measurements trend towards 0% as the radiosonde approaches the tropopause at about 11 km.

In the right-hand pane of Fig. 3-7, the wind speed and direction are shown. There is a jet stream visible in the wind speed measurement, showing a maximum velocity of over 70 m/s at about 11 km. Wind velocity measurement accuracy is expected to be within  $\pm 0.15$  m/s at all altitudes.

FIGURE 3-7

#### Temperature, humidity and wind measurements by a radiosonde



Metco-03-07

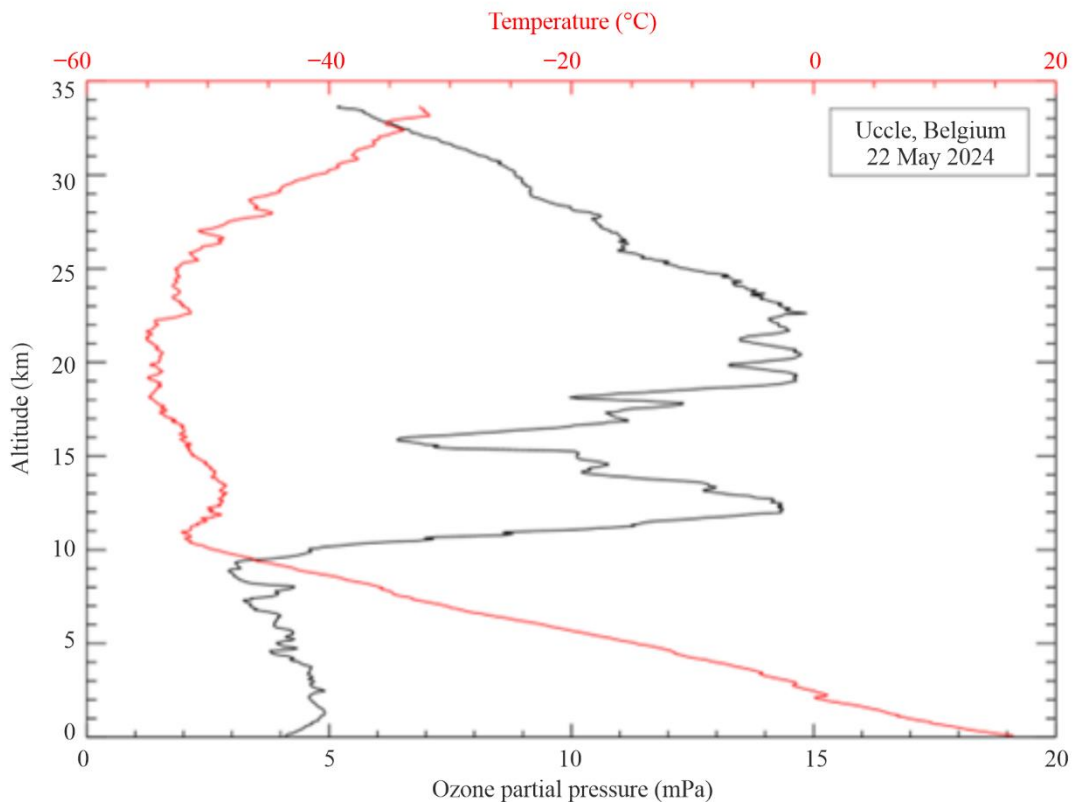
Upper wind measurements have a high value for air transportation and defence services. The results of a MetAids observation will usually be transformed into a special defence code at the base station and transmitted to the relevant operational units.

### 3.4.2 Characteristics of ozonesondes

At about 60 sites worldwide, ozonesondes are launched on a weather balloon, measuring the ozone concentrations via a chemical reaction from bubbling ambient O<sub>3</sub> into a two-chamber electrochemical cell containing a potassium iodide (KI) solution. The ozonesonde is coupled to a radiosonde that transmits O<sub>3</sub> partial pressure simultaneously with pressure, temperature, humidity (PTU) and GPS-derived wind data to a ground station. Figure 3-8 shows an example of the ozone concentration as a function of altitude (black line) from an ozonesonde launched at Uccle (50° N, 4° E), Belgium, together with the temperature profile from the coupled radiosonde (red line). Launch frequencies at the ozonesonde sites vary between once or twice a month up to three times a week (as is the case for Uccle), with weekly launches being the most prominent. Ozonesonde measurements are performed within the WMO Global Atmospheric Watch (GAW) programme to monitor the state of the ozone layer (maximum ozone concentrations between 20 and 25 km, see Fig. 3-8) and are stored in the WMO World Ozone and Ultraviolet Radiation Data Centre (WOUDC). Moreover, ozone in the troposphere (below 11 km in Fig. 3-8) is also an important greenhouse gas and boundary layer ozone has adverse effects on human health.

FIGURE 3-8

An example of the measurement of the vertical distribution of the ozone concentrations (black) in the atmosphere above Uccle (Belgium) by means of an ozonesonde, coupled to a radiosonde



Meteo-03-08

## 3.5 Variations in MetAids service operations

### 3.5.1 Variations in upper wind patterns and their impact on radiosonde operations

During the winter at high latitudes in the Northern Hemisphere, winds at heights above 16 km are not typically distributed symmetrically around the pole. Thus, very strong stratospheric winds are much more common over Europe than in North America. On the other hand, there are many countries where upper winds are consistently weak. These differences in upper wind conditions lead to significant variations in the operating conditions of relevant national radiosonde networks. In some countries, such as those in the tropics, radiosondes will always

remain at high elevations and short range; while in others, radiosondes must be tracked down to elevations lower than 5 degrees above the horizon, at ranges exceeding 200 km.

Where balloon elevations remain high (particularly if elevations remain higher than 15 degrees), some countries can still use lower-cost radiosondes even without a NAVAID/GNSS signal receiver and/or pressure sensor, to reduce the costs of the radiosonde measurement. Those radiosondes transmit at frequencies around 1 680 MHz and they can be tracked using a scanning directional antenna at the base station that is much smaller than the alternative antenna required for the radiosondes transmitting at frequencies near 403 MHz. The use of the radiosondes without a pressure sensor and without GNSS is discouraged because it can lead to significant height/pressure errors at upper levels if there is a large drift of the balloon (low radar elevation angles). In such cases, it is essential to use radiosondes that receive a GNSS signal to obtain reliable winds. The frequencies near 403 MHz are preferred for radiosonde operations with large horizontal drift and are able to provide good reception and accurate winds throughout the ascent.

### **3.5.2 Variations in network density**

WMO has defined and regularly reviews the minimum global and regional requirements of observing networks, including MetAids. According to the Global Basic Observing Network (GBON) requirements (WMO-No. 1160), the radiosonde measurements at upper-air land stations are performed with the required horizontal resolution of 500 km, and the recommended resolution of 200 km. At upper-air stations in the marine areas of WMO Members' jurisdictions, the required horizontal resolution is 1 000 km, while the recommended one is 500 km.

The spectrum requirements of the MetAids service vary on a country-by-country basis and must consider the entire user community, including defence, environmental, disaster relief organizations and space agencies. Despite the widespread use of more spectrum-efficient digital transmitters, some countries continue to operate radiosondes with analogue technology. Any estimate of spectrum needs must take into account the density of the network (higher network density requires greater spectrum efficiency), as well as the renewal of the existing radiosonde equipment that can still rely on analogue technology.

It is noted that there is a growing demand for fully automated balloon launch systems that can be supervised from a remote site, and many such systems are now in operation. These systems always use NAVAID/GNSS radiosondes operating in the 400.15-406 MHz band. As with crewed operations, if a radiosonde launch fails due to an early balloon failure, the radiosonde may continue to transmit. The failure can lead to the second radiosonde launch soon after. The automated launch system scans between 400.15 MHz and 406 MHz prior to each launch to ensure no other radiosonde is transmitting within the range at the selected frequency. In such situations, an alternative frequency must be available to obtain the operational measurement.

### **3.5.3 Use of the 401-406 MHz band**

Some countries in Europe operate very dense networks, using radiosondes with minimal drift and narrow-band emissions in this band. Some other countries operate broadband secondary radar systems where the ground station transmits a pulse to the radiosonde, and the radiosonde responds to the pulse and transmits the meteorological data. In both cases, nearly the full 400.15-406 MHz band is required for operations, given that the MetAids service must coordinate with the data collection platform transmissions of the EESS (Earth-to-space) and MetSat (Earth-to-space) services between 401 MHz and 403 MHz. China has developed the Round-trip Drifting Sounding System (RDSS), an innovative sounding system with three observation stages: ascending, drifting and descending. Specific channels in the 400.15-406 MHz band have been assigned for RDSS.

It has to be noted that in some countries there are only a limited number of launch stations. In such cases, resources may be available to procure transmitters that can make available parts of the band for other uses. Australia is an example where the full band is not required, and the administration uses a portion of the band for other radio communication services. WMO considers that the entire 400.15-406 MHz band is required for MetAids operations for the foreseeable future, being aware that standard radiosonde operations in the 400.15-401 MHz band may not be possible worldwide in the future due to co-channel sharing with satellite services.

### 3.5.4 Use of the 1 668.4-1 700 MHz band

The situation in the 1 668.4-1 700 MHz band is different from the 401-406 MHz band. This band is allocated to MetAids and the MetSat service on a co-primary basis. However, co-channel MetAids and MetSat operations are not compatible and significant band segmentation has already occurred. MetAids cause significant levels of interference to the MetSat ground stations. In discussing MetAids requirements in 1 668.4-1 700 MHz, it must be kept in mind that only a portion of the band is usually available. Most countries can conduct operations in the bandwidth of 7-8 MHz, while there are a number of countries where a bandwidth of more than 15 MHz is still required to support operations.

It is noted that radiosonde operations do not cover the entire 1 668.4-1 700 MHz frequency band but limited to the 1 668.4-1 690 MHz range. This usage is primarily in Europe, with a smaller number of systems also operating in Asia.

### 3.5.5 Requirements for retaining both bands

Each band provides unique characteristics required for different types of MetAids operations.

The 401-406 MHz band offers a lower propagation loss, providing an advantage in regions with high winds that result in long slant ranges between the base station and the radiosonde. The lower propagation loss also allows use of simpler, smaller receive antennas for tracking the flight. MetAids operations in this band use a form of radio navigation (GNSS) for measurement of winds since an RDF antenna would be prohibitively large. For either budgetary and/or national security reasons, some administrations use the band 1 668.4-1 700 MHz. This reduces the cost of the expendable devices and offer the possibility to operate MetAids systems independently of international NAVAID/GNSS systems.

Given the distinctive features of each frequency band and the current sharing conditions with other services, MetAids operations (meteorological, research, defence, and others) cannot rely solely on the availability of one band. Therefore, ensuring the availability of both frequency bands is deemed crucial for sustaining successful meteorological operations.

## 3.6 Future trends

While MetAids designs are typically very simple and use low-cost components, evolution has occurred and will continue to occur to improve the performance of the systems. The increasing requirement for additional frequency assignments in a given area to support meteorological and other environmental operations of different users has led to improvements in the RF technology and characteristics, through the replacement of analogue by digital transmitters.

In addition, implementation of GNSS on radiosondes for measuring winds and deriving pressures from GPS altitudes has already led to significant improvements in the spectrum efficiency of NAVAID/GNSS radiosondes. It also enhances the accuracy and resolution of upper wind and height measurements. The use of GNSS for pressure derivation enables the removal of dedicated pressure sensors, which can reduce the weight and cost of radiosondes. The availability of small low-cost GNSS receivers now allows that the GNSS signal is fully processed onboard the MetAids and that only wind and position data may be transmitted.

## References

- [1] WMO-No. 8 – Guide to Instruments and Methods of Observation , Volume I – Measurement of Meteorological Variables, [Guide to Instruments and Methods of Observation \(wmo.int\)](https://www.wmo.int/publications/meteorology/guide-to-instruments-and-methods-of-observation).
- [2] WMO-No. 1160 – Manual on the WMO Integrated Global Observing System, [Manual on the WMO Integrated Global Observing System](https://www.wmo.int/publications/meteorology/manual-on-the-wmo-integrated-global-observing-system).
- [3] OSCAR/Surface (<https://oscar.wmo.int/surface/>).
- [4] WMO-No. 1165 – Guide to the WMO Integrated Global Observing System, [Guide to the WMO Integrated Global Observing System](https://www.wmo.int/publications/meteorology/guide-to-the-wmo-integrated-global-observing-system).

- [5] Instruments and Observing Methods Report No. 143, Report of WMO's 2022 Upper-Air Instrument Intercomparison Campaign, [Report of WMO's 2022 Upper-Air Instrument Intercomparison Campaign](#).
- [6] Recommendation ITU-R RS.1165 – Technical characteristics and performance criteria for radiosonde systems in the meteorological aids service in the 403 MHz and 1 680 MHz bands.



## CHAPTER 4

### Meteorological radars

#### 4.1 Introduction

Ground-based meteorological radars operate under the radiolocation service and are used for operational meteorology, weather prediction, atmospheric research and aeronautical / maritime navigation. Most weather radars are in operation continuously 24 h/day and play a crucial role in the immediate meteorological and hydrological alert/warning processes. These radars represent the last line of defence against loss of life and property in flash flood or severe storms events and as such are among the best-known life savers in meteorology.

Meteorological radars are typically volume scanning, pencil beam radars, which detect and measure both hydrometeor intensities and their radial velocities. They are used to predict the formation of hurricanes, tornadoes and other severe weather events and to follow the course of storms on their destructive paths. Modern radars enable the tracking of large and small storms and provide precipitation rates data, which is used by forecasters in predicting the potential for flash floods. In addition, they provide relevant information on high winds and lightning potential. Meteorological radars are also a prime interest in aeronautical weather service in particular for detection of aircraft icing conditions and avoidance of severe weather for navigation. Modern radars digitize the return signal to facilitate creation of enhanced products via various algorithms. These data and products are typically archived for research and historical purposes.

This Chapter discusses operational ground-based radars deployed and near to be deployed in meteorology and their specificities compared to other radars.

#### 4.1.1 Meteorological radar types

The first and most common and widely recognised type of radars is the weather radar. These radars provide data within a volume which is centred on its own location. Familiar to many, the output of these radars is commonly shown in television weather forecasts. Table 4-1 provides the listing of frequency bands, which are commonly used for weather radar operations.

TABLE 4-1

**Main weather radars frequency bands**

<b>Frequency band (MHz)</b>	<b>Band name commonly used in meteorological community</b>
2 700-3 000 (mainly 2 700-2 900)	S-Band
5 250-5 725 (mainly 5 600-5 650)	C-Band
9 100-9 700 (mainly 9 300-9 500)	X-Band

Wind profiler radar (WPR) represent another important category of meteorological radar. These radars point vertically to provide wind velocity data within a roughly cone-shaped volume, which is directly above the radar. If properly equipped, e.g. with speaker units or a Radio Acoustic Sounding System (RASS), a WPR can also measure atmospheric virtual temperature as a function of height. The radio frequency bands used by the WPR are typically located around 50 MHz, 400 MHz, 1 000 MHz and 1 300 MHz (see details in § 4.3).

A third radar type used in meteorology and oceanography is Oceanographic High-Frequency (HF) Radar. These operate in the HF radio frequency band (3-30 MHz) and extract ocean surface information through the Bragg scattering phenomena. Oceanographic radars can be used in coastal areas to monitor ocean surface currents, waves and wind direction.

A fourth, less common type, is auxiliary radar which is used to track radiosondes in flight. The use of such radars is discussed in Chapter 3, which deals with radiosondes.

A fifth radar type used in meteorology are cloud radars. These radars operate normally around 35 GHz and 94 GHz because of higher sensitivity to smaller hydrometeors (for example fog) compared to S-, C- or X-Band radar systems. Cloud radars are used for studying microphysical properties of clouds and other particles within the sensitivity range of the radar system.

All radars operate by transmitting radio signals, which are reflected from a target such as vehicles, planes, raindrops or turbulence in the atmosphere. Despite emitting powerful signals, the return signal of radars is weak. This is because the radiated signal must traverse the path twice, once from the radar to the target and back to the radar, leading to atmospheric attenuation on both paths. In the case of meteorological radars, this weakness is even exacerbated since the meteorological targets (being either precipitation drops (rain, hail, snow, ...) or even in case of Doppler mode, dust, insects or solely atmospheric disturbances) are inherently not particularly efficient reflector. The amount of signal returned is related to target reflectivity and can vary depending on the size and nature of the target. To overcome these detection challenges, radar systems employ several key strategies: higher transmitter powers, large antennas exhibiting high gain beamwidth product, extremely sensitive receivers, and long signal integration times. To achieve successful detection, relatively “quiet” spectrum –absence of man-made electronic noise and interference– is therefore a critical requirement.

#### 4.1.2 Radar equation for Meteorological application

For conventional radars, on which a discrete target is detected by the radar, the simple radar equation suggests that returned power to the radar depends on the radar cross section (RCS) of a single target and is proportional to  $1/r^4$ , where “ $r$ ” is the distance between the radar and the target. However, this equation does not directly apply to meteorological radars, which are designed to detect a large volume of scatterers (typically precipitation particles) distributed throughout the radar’s beam volume of a pulse.

For the Meteorological radar applications, equation (4-1) describes the relationship between the returned power and the characteristics of the radar and the target. The equation can be expressed as follows:

$$\bar{P}_r = \frac{\pi^3 \cdot P_t \cdot G^2 \cdot \theta^2 \cdot c \cdot \tau \cdot |K|^2 \cdot L \cdot Z}{2^{10} \cdot \lambda^2 \cdot r^2 \cdot \ln 2} \quad (4-1)$$

where:

$\bar{P}_r$ : average return power (W)

$P_t$ : transmitter output power (W)

$G$ : antenna gain (dimensionless)

$\theta$ : antenna half power (3 dB) beamwidth (rad)

$c$ : speed of light (m/s)

$\tau$ : pulse width

$L$ : loss factors associated with propagation and receiver detection

$Z$ : effective radar reflectivity ( $m^3$ ).

$K$ : complex index of refraction (dimensionless)

$\lambda$ : radar wavelength (m)

$r$ : range to target.

Re-arranging terms results in an easy-to-understand formulation of the radar equation (4-2) which shows the different contributions to the received power in terms of constants, radar and target factors.

$$\bar{P}_r = \frac{\pi^3 \cdot c}{1024 \cdot \ln 2} \cdot \frac{P_t \cdot G^2 \cdot \theta^2 \cdot \tau \cdot L}{\lambda^2} \cdot |K|^2 \frac{Z}{r^2} \quad (4-2)$$

$\uparrow$                        $\uparrow$                        $\uparrow$   
 Constants      Radar factors      Target factors

Equation (4-2) can be applied to a distributed target when the following assumptions are satisfied:

- the target occupies the entire volume of the pulse
- the particles are spread throughout the contributing region
- the precipitation particles are homogeneous dielectric spheres with diameters small compared to the radar wavelength
- the size of the particles satisfies the Rayleigh Scattering condition
- the dielectric constant  $|K|^2$  and the size distribution of the scatterers are homogeneous in the volume  $V$  considered
- the antenna pattern can be approximated by a Gaussian shape
- the incident and back-scattered waves are linearly polarized
- the effects of multiple scattering are neglected.

A logarithmic form of the radar equation (4-2) [Doviak and Zrnica, 1984] is given in equation (4-3).

$$Z(Az, E1, R) \text{ (dBZ)} = 10 \log(P_r) + 20 \log(R) - 10 \log(L_p) + 10 \log(C) \quad (4-3)$$

This equation is the most useful in that it illustrates the need to have clearly identified various system parameters in order to make a calibrated reflectivity measurement. These parameters include:

- received power  $P_r$  (W),
- range  $R$  (m),
- azimuth and elevation angles (degrees),
- excess propagation loss  $L_p$  (dB), and
- so-called radar constant  $C$ .

The radar constant typically includes factors such as the antenna beam width, pulse width, receiver conversion gain and system losses.

As shown above, for meteorological radars, the radar equation is quite different since targets such as precipitations should fill the entire narrow radar beam, as assumed above. In this case the radar equation provides a received signal which is proportional to  $1/r^2$ . As a result, meteorological radars allow for larger detection ranges but this also means that they have a higher sensitivity to interference than a typical air traffic control type radar.

## 4.2 Weather radars

### 4.2.1 User requirements

Meteorologists use weather radar to detect, locate, and measure the amount of precipitation within or falling from clouds as well as to determine wind velocities and direction using the movement of the precipitation or atmospheric particles. The radars measure the intensity of precipitation over specific time periods as well as the motion of precipitation or atmospheric particles toward or away from the weather radar antenna. This allows meteorological events to detect rotational patterns in weather systems which is a critical factor in detecting severe weather events such as tornadoes or flash floods and ultimately improving early warning

systems. The main user requirement for the weather radar is to detect solid and liquid precipitation and estimate the rate of precipitation and the radial velocity<sup>5</sup>.

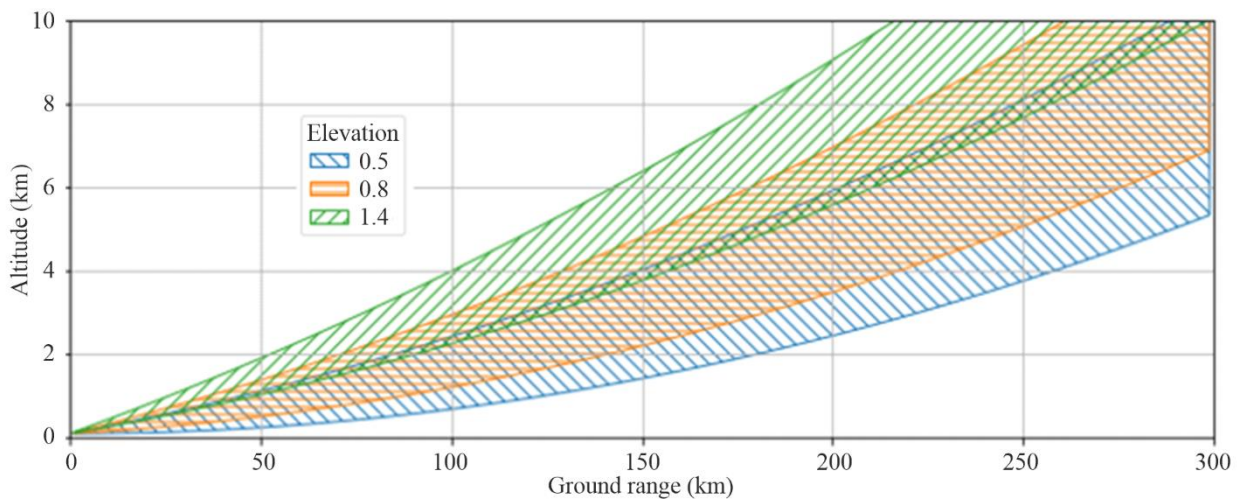
#### 4.2.2 Weather radar networks

The main limitation of a weather radar is the fact that the intensity of the echoes that are returned from a given meteorological event tend to decrease with increasing distance from the radar. This is not only due to free-space and other atmospheric attenuations but also to the fact that, as distance from the radar increases, the radar beam becomes higher above the ground (this is due to the Earth's curvature and the elevation angle of the beam) and also the beam broadens. (See Fig. 4-1 for first three scans of a radar with 3 dB beamwidth of 1 degree, at elevation angles of 0.5, 0.8 and 1.4 degrees. Note scans may have overlap areas as demonstrated in Fig. 4-1.)

This results in a decrease in the percentage of the meteorological event that is illuminated by the beam. While the upper portion of the event can still be seen by the radar, its lower parts may no longer be visible. Precipitation that is taking place at some distance away from the radar may remain undetected or may show up with a reduced intensity thereby limiting the quantitative operational range of the radar.

FIGURE 4-1

Three consecutive radar scans height versus range



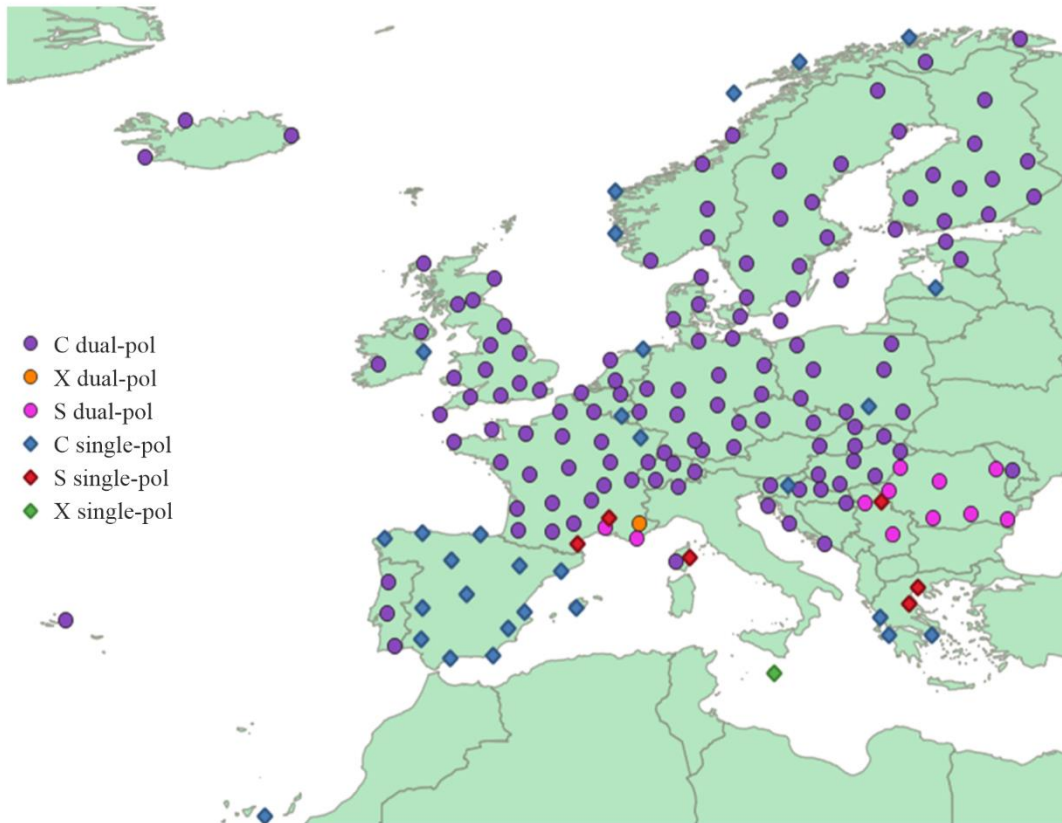
Meteo-04-01

To overcome this constraint, multiple radars are generally equally spaced into distributed networks. These networks operate 24 hours per day and cover, in general, large areas such as countries or even a portion of a continent in order to detect and follow the evolution of meteorological phenomena, therefore permitting early weather hazard warnings. One such network, comprising S-Band, C-Band and X-Band radars, as deployed in Western Europe, is given in Fig. 4-2.

<sup>5</sup> This is the velocity of the precipitation either toward or away from the radar (in a radial direction). No information about the strength of the precipitation is given. Precipitation moving toward the radar has negative velocity. Precipitation moving away from the radar has positive velocity. Precipitation moving perpendicular to the radar beam (in a circle around the radar) will have a radial velocity of zero.

FIGURE 4-2

**Example of a weather radar network  
(EUMETNET-OPERA update January 2025)**



Meteo-04-02

### 4.2.3 Operational aspects of reflectivity

Reflectivity is a radar term referring to the ability of a radar target to return energy. The reflectivity  $\eta$  of rain is related to the water relative permittivity  $\Sigma_r$ , the drop diameter  $D$ , and the wavelength  $\lambda$ . For raindrops contained within the volume  $V$  under consideration, the reflectivity can be expressed as equation (4-4).

$$\eta = \frac{\pi^5}{\lambda^4} |K|^2 \sum_j D_j^6 / V \quad \text{m}^{-1} \quad (4-4)$$

where  $|K|^2$  is 0.93 for liquid water and 0.18 for ice. Reflectivity is used to estimate precipitation intensity and rainfall rates and is a measure of the returned power.

For precipitation events where the raindrop size is known (or assumed), volume reflectivity can be related to the total liquid water volume per unit volume. The total volume of water in conjunction with the drop-size distribution and the corresponding terminal velocity of the drop facilitate the calculation of rainfall rate.

The radar reflectivity factor  $Z$  can be defined as:

$$Z = \frac{1}{V_e} \sum_i D_i^6 \quad (4-5)$$

where:

$Z$ : volume that is implied from the scatterer radar cross section of the total number of spheres in the volume

$D$ : water drop diameter  
 $V_e$ : effective drop volume.

The volume  $Z$  is related to the radar cross section per unit volume  $\eta$  by:

$$\eta = \frac{\pi^5}{\lambda^4} |K|^2 Z \quad (4-6)$$

where:

$Z$ : volume  
 $\eta$ : radar cross section per unit volume  
 $\lambda$ : incident wavelength  
 $|K|$ : complex index of refraction.

Since the diameter of raindrops within the scattering volume is not uniform, the raindrop distributions can be approximated by:

$$N(D) = N_0 \exp(-\Lambda D) \quad (4-7)$$

where:

$N(D)$ : number concentration of the diameter  
 $D$ : diameter  
 $\Lambda D$ : size interval  
 $N_0$  and  $\Lambda$ : constants for a given meteorological event.

When the raindrop size distribution is known, the summation  $\sum_i D_i^6$  over a unit volume is given by:

$$Z = \int_0^\infty D^6 N(D) \Lambda D \quad (4-8)$$

When the vertical airspeed is zero the rainfall rate,  $R$ , is given by:

$$R = \frac{\pi \rho}{6} \int_0^\infty D^3 v_t(D) N(D) \Lambda D \quad (4-9)$$

where:

$R$ : rainfall rate  
 $D^3$ : raindrop volume that is proportional to  $Z$   
 $v_t(D)$ : terminal velocity of a raindrop having a diameter  $D$   
 $\rho$ : density of water.

When  $N_0$  is constant, the implied  $Z$ - $R$  relationship can be described by equation (4-10):

$$Z = AR^b \quad (4-10)$$

Where  $Z$  is usually expressed as  $\text{dBZ} = 10 \log Z$  ( $\text{mm}^6/\text{m}^3$ ) and  $A$  and  $b$  are constants. ( $A$  is the scattering constant and  $b$  is the rate multiplier.) The most commonly used  $Z$ - $R$  relationship is the Marshall-Palmer where:  $Z = 200 \cdot R^{1.6}$   $Z$  and  $R$  are expressed in  $\text{mm}^6/\text{mm}^3$  and in  $\text{mm}/\text{h}$ , respectively. The  $Z$ - $R$  relationship is, however, not unique. Both  $A$  and  $b$  depend upon the drop size distribution (DSD) which varies with the type and intensity of rain.

## 4.2.4 Weather radars emission schemes, scanning strategies and operational modes

### 4.2.4.1 Emission schemes

To ensure volume scan processing, in so-called “scanning strategies” (typically in a range of 5-15 min), meteorological radars make use of a variety of different emission schemes at different elevations, using sets of different pulse width, PRFs and rotation speeds. There is not one ‘typical’ scheme, the schemes vary depending on a number of factors such as the radar capabilities and the radar environment for the required meteorological products. The schemes are hence tuned to best meet the requirements.

As an example, meteorological radars showed following large ranges of different emission scheme parameters:

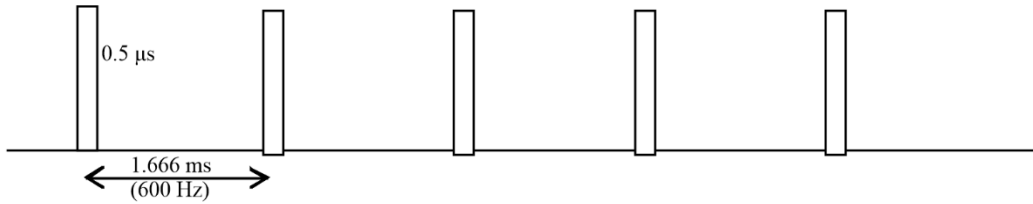
- Operational elevation ranging from  $0^\circ$  to  $90^\circ$   
  
Pulse width ranging from 0.5 to 3.3  $\mu\text{s}$  (for operational radars) for uncompressed pulses, typical in radars with traditional vacuum tube-based transmitters (magnetrons and klystrons). Some radars with solid-state transmitters use pulse compression with pulse width ranging from 30  $\mu\text{s}$  to 200  $\mu\text{s}$  (noting that use of pulse compression increases the 3 dB bandwidth up to 10 MHz)
- Pulse Repetition Frequency (PRF) ranging from 250 to 2 400 Hz (for operational radars). Some existing radars are capable of PRF up to 20 000 Hz
- Rotation speed ranging from 1 to 10 rpm
- Use on a given radar of different emission schemes mixing different pulse widths and PRFs, and in particular the use of a fixed, staggered or interleaved PRF (i.e. different PRF during a single scheme)
- Different transmitted pulse phase coding schemes for radars employing phase coherent transmitters (Klystrons or Solid State) such as constant phase, random phase, or specific codes like SZ8/64 designed to assist with second trip recovery.

Example of different emission schemes are provided in Fig. 4-3.

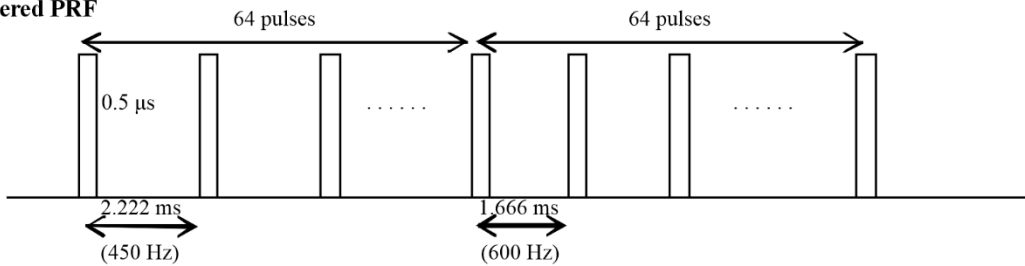
FIGURE 4-3

Some types of weather radar emission schemes

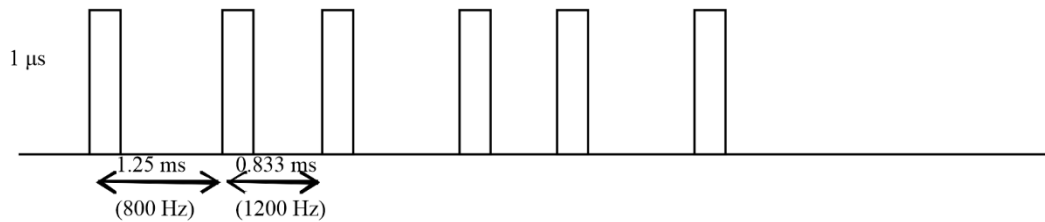
Fixed PRF



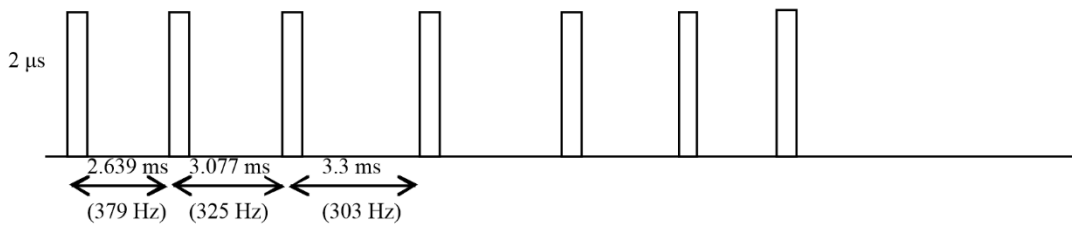
Staggered PRF



Double interleaved PRF (double PRT)



Triple interleaved PRF (triple PRT)



Meteo-04-03

These different emission schemes are used on a number of radars in their scanning strategy, during which, at different elevations and rotation speeds, one emission scheme is transmitted.

It has to be stressed that, from one radar to another, the PRF and pulse width values associated with these example schemes vary within the ranges defined above. In addition, for a given scheme, pulse widths can vary on a pulse-to-pulse basis.

Below is an example of such scanning strategy.

FIGURE 4-4

**Description of a weather radar scanning strategy**

**Typical scan strategy (total time around 15 min):**

- 1 round at elevation 0.8° with configuration 2 (2 rpm) (30 s)
- 1 round at elevation 10° for noise calibration (3 rpm) (20 s)
- 12 rounds at elevations 37, 29, 23, 21, 19, 17, 15, 13, 11, 9.5, 8.5 and 6.5° with configuration 3 (3.167 rpm) (19 s/turn) (3 min 47 s total)
- 1 round at elevation 0.8° with configuration 2 (2 rpm) (0.5 min)
- 2 rounds at elevations 6.5 and 5.5° with configuration 3 (3.167 rpm) (19 s/turn) (38 s total)
- 5 rounds at elevations 4.5, 3.5, 2.5, 1.5 and 0.5° with configuration 3 (3 rpm) (20 s/turn) (40 s total)
- 4 rounds at elevations 0.5, 1.5, 2.5 and 3.5° with configuration 1 (2 rpm) (2 min)
- 1 round at elevation 0.8° with configuration 2 (2 rpm) (30 s)
- 2 rounds at elevations 3.5 and 4.5° with configuration 1 (2 rpm) (60 s)
- 1 round at elevation 10.5° with configuration 3 (3 rpm) (20 s)
- 1 round at elevation 1.3° with configuration 2 (3 rpm) (20 s)
- 1 round at elevation 0.8° with configuration 2 (2 rpm) (30 s)
- 1 round at elevation 10° for noise calibration (3 rpm) (20 s)

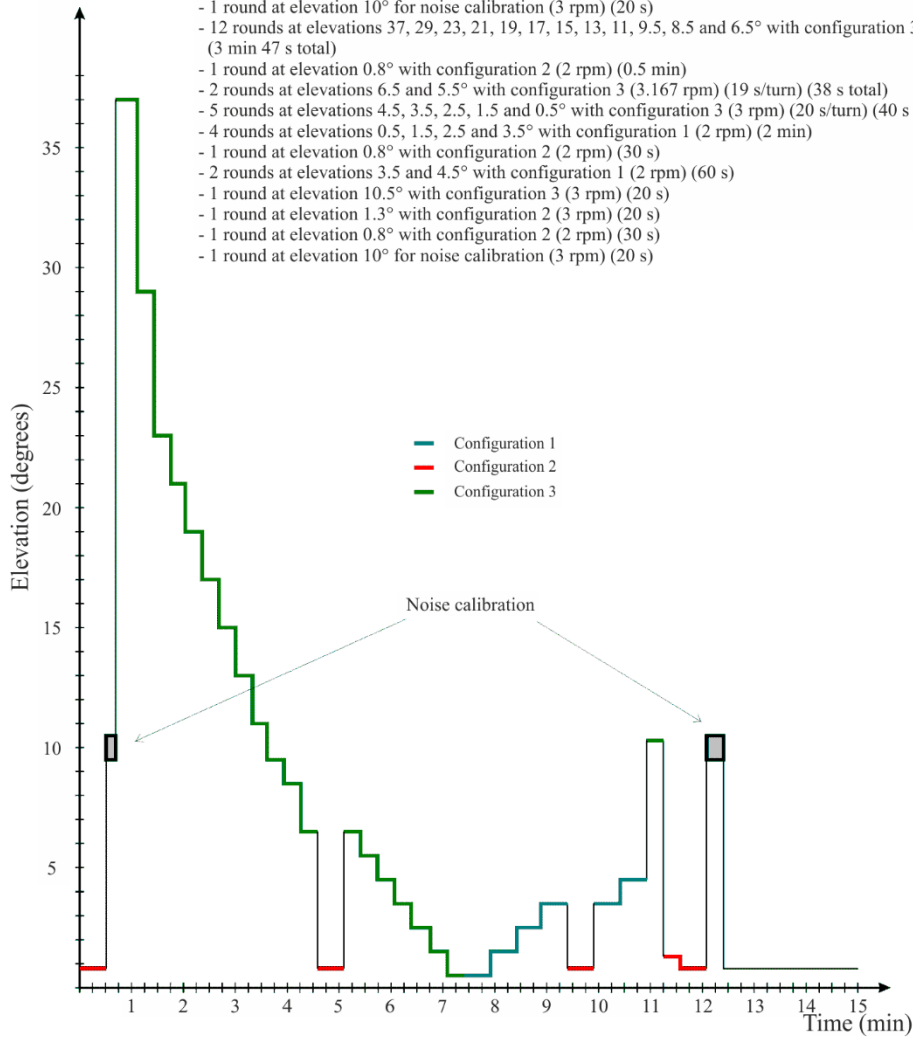
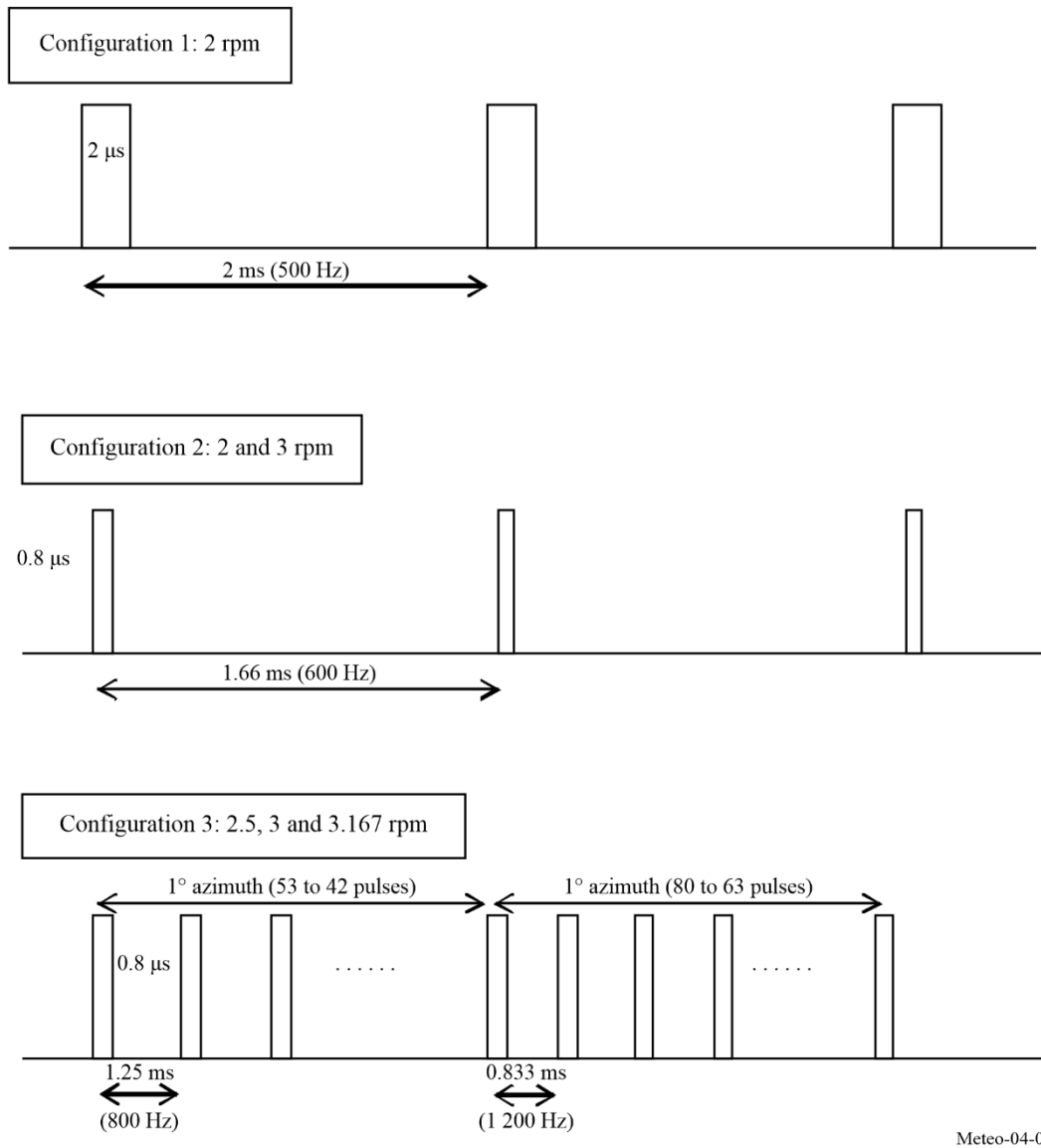


FIGURE 4-5

## Emission schemes associated with scanning strategy as in Fig. 4-4



#### 4.2.4.2 Noise calibration

Considering the weakness of the return signal to meteorological radars, the noise level has to be extracted from the signal in order to achieve the most accurate measurements and retrieve relevant meteorological products.

Noting  $N$ , the noise level and  $S$  the useful signal (i.e. meteorological signal return), meteorological radars perform the following process:

- 1 for each gate, the radar measures the return signal corresponding to the useful signal ( $S$ ) and the noise ( $N$ ), i.e.  $N + S$
- 2 To get the  $S$ , the radar extract from  $N + S$ , the noise level  $N$
- 3 Then, from the  $S$ , the radar is able to determine all meteorological products, such as the precipitation (dBz) or wind velocity by Doppler analysis.

In order to get the more precise meteorological products, the signal  $S$  has to be as accurate as possible which means that the noise calibration, also called “Zero check”, of the radar is a crucial issue.

“Zero check” is therefore performed on a regular basis, either during regular radar emissions (by estimation) or during specific measurement periods of time (see the example scanning strategy below) during which the noise is measured.

Noise calibration measurement is typically performed without radar transmission, which could in particular have an impact on the design of certain radio systems that aim at detecting radar signals to mitigate interference.

In all cases, interference received during the noise calibration will systematically corrupt all subsequent data collection until the next interference free calibration is performed. Such interference could lead to underestimated precipitation rates than the real situation, with obvious consequences on operational and alert processes.

#### 4.2.4.3 Operational modes for meteorological radar

Radars in some networks, e.g. NEXRAD in the USA, operate in two user selectable modes: Clear air mode and precipitation mode. The precipitation mode may be selected manually at any time during operation or can be automatically operated whenever the weather radar detects precipitation (based upon pre-determined values and area coverage of reflectivity). The radar may revert to clear air mode manually, or automatically if precipitation is not detected (based upon predetermined values of areal threshold coverage and time duration).

In general, meteorological radars take advantage of both modes.

##### 4.2.4.3.1 Clear air mode

Clear air mode provides meteorological radars the ability to detect early signs of precipitation activity.

There exist certain variables in low-level velocity and air density that allow for detection of potential precipitation. The radar utilizes a slow scan rate, coupled with a low PRF, to employ a high sensitivity capability. This high sensitivity is ideal for very subtle changes in atmospheric conditions at long ranges. The clear air mode is especially useful when there is little to no convective activity within the transmit range of the radar, and is ideally suited for detecting the signs of developing thunderstorms or other types of severe weather, and light snowfall.

Meteorological radar’s high sensitivity is due to the volume scan pattern within the clear air mode. By selecting a pattern in the clear air mode; the radar antenna is capable of dwelling for an extended period in any given volume of space and receives multiple returns, while allowing operation at a lower signal to noise ratio ( $S/N$ ). The configuration combines two key parameters, wide pulse width for increased energy transmission and a low PRF for extended listening time. Together, these features provide approximately 8 dB of additional echo power for a given dBz of reflectivity, significantly improving detection of weak atmospheric signals

##### 4.2.4.3.2 Precipitation mode

The precipitation mode performs a distinctly different purpose than the clear air mode. The scan rate for the precipitation mode is a function of the elevation angle. This dependence allows for the highest number of elevation angles possible in sampling the total radar volume. The precipitation mode takes advantage of multiple volume coverage patterns (VCPs) to implement different types of scan strategies (see example in § 4.2) with different elevation sampling. The precipitation mode specifically targets weather phenomena including convective storms (such as hail, severe thunderstorms, tornadoes), heavy precipitation events and large-scale synoptic systems.

#### 4.2.4.4 Fixed echo elimination

The so-called fixed echo includes several hidden fixed components; one that includes low frequency scattering, and a second that includes higher frequencies (e.g. due to vegetation ruffled by the wind). Echoes due to non-precipitation targets are known as clutter, and should be eliminated. Different ground clutter suppression methods are used in current weather radars:

- Doppler filtering uses a high pass filter to reduce low-velocity ground clutter. That process is efficient if the radial wind velocity is above the cut-off frequency of the Doppler filter.
- Statistical filtering exploits reflectivity variance differences to discriminate precipitation (high spatial/temporal variability) from ground clutter (statistically stable returns), since the variance of

rain is higher than the variance of ground clutter reflectivity. The statistical filtering process is efficient even when the rain radial velocity is null (tangential rain).

- The use of polarimetric radar for rain and ground clutter discrimination.

#### 4.2.5 Doppler radars

Doppler weather radars have been used since beginning of 1970's in atmospheric research to measure convection within thunderstorms and to detect gust fronts and are now widely used for operational weather radar systems. Unlike earlier radars, Doppler equipment is capable not only of determining the existence and position of reflective targets but also their radial velocity. This permits the measurement of wind speed, detection of tornadoes, and the measurement of a wind field using velocity azimuth display scanning.

Ground clutter suppression is an important capability. New developments in this area are focused on coherent transmitters such as klystrons (that are state-of-the-art nowadays), traveling wave tubes (TWTs) or Solid State. Conventional radar spectrum phase purity was limited by previous generation magnetron technology, but in modern magnetrons the phase purity is sufficient for effective clutter cancellation. However, the existing magnetrons can economically deliver high average power to increase the signal to noise ratio.

#### 4.2.6 Dual-polarization radars

Polarimetric or dual-polarization radars transmit pulses in both horizontal (h) and vertical (v) polarizations. This technology permits the identification of scatterers by remotely sensing their shapes and homogeneity. These radars provide significant improvements in rainfall estimation, precipitation classification, data quality and weather hazard detection over non-polarimetric systems.

Precipitation estimates now make use of the fact that falling raindrops tend to flatten (oblate spheroids), the flatness increasing with drop size in the horizontal direction. Combining reflectivity and dual-polarization fields, enables a better assessment of the coefficients  $A$  and  $b$  of the Z-R relationship in equation (4-10). Other algorithms, based on differential phase  $\varphi_h - \varphi_v$  and differential attenuation, are considered very promising for further improving accurate assessments of rainfall.

In addition to their shape, the hydrometeors are characterized by their frequency-dependent dielectric constants, a primary factor in computing scattering and attenuation cross sections. Dielectric properties of hydrometeors vary with radar frequency, where liquid water and ice differ significantly. Taking advantage of these characteristics, algorithms have been implemented to discriminate between rain and snow and to quantify liquid water and ice in clouds using differential attenuation measurements.

#### 4.2.7 Conventional meteorological radar base data products

A Doppler meteorological radar generates three categories of base data products from the signal returns: base reflectivity, mean radial velocity, and spectrum width. All higher-level products are generated from these three base products. The base product accuracy is often specified as a primary performance requirement for radar design. Without the required accuracy at this low level, as given in Table 4-2, the higher-level derived product accuracy cannot be achieved.

TABLE 4-2

**Representative met radar base data accuracy requirements**

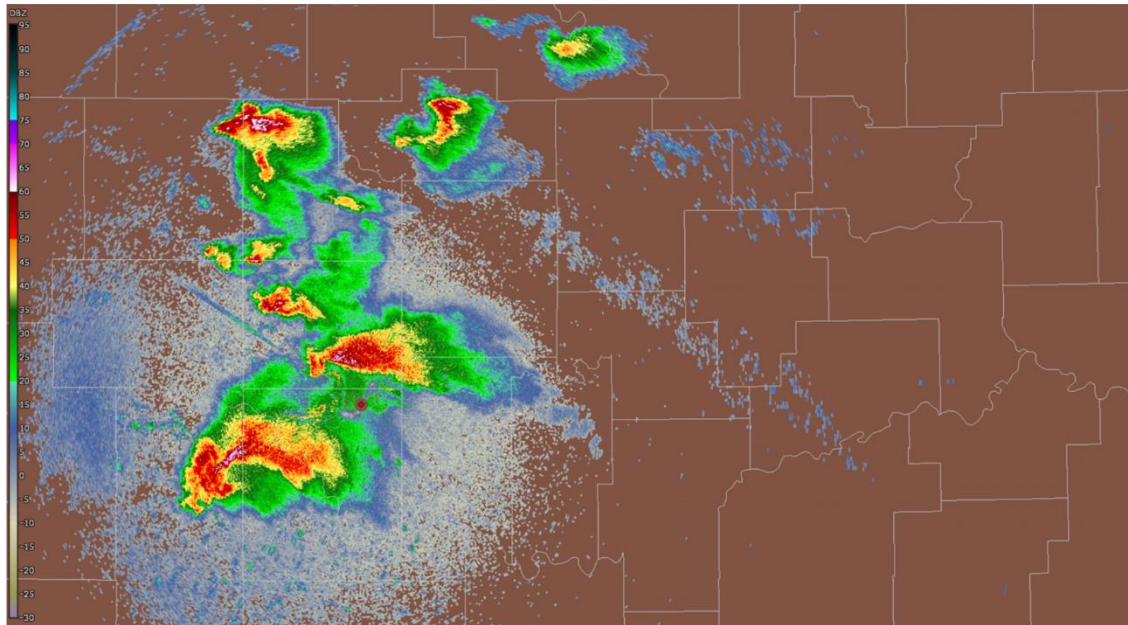
Base data product	Design accuracy requirement
Base reflectivity	< 1 dB
Mean radial velocity	< 1 m/s
Spectrum width	< 1 m/s

### 4.2.7.1 Base reflectivity

Base reflectivity is used in multiple weather radar applications, the most important of which is rainfall rate estimation. Base reflectivity is the intensity of the return pulses and is calculated from a linear average of return power. Any interference to the radar adds to the return pulse power and biases the reflectivity values. Reflectivity measurements can be compromised if the bias exceeds the base data accuracy requirements.

FIGURE 4-6

**Example of widespread supercells during a tornado outbreak as observed in KTLX reflectivity at 2023-04-20 00:10 UTC**



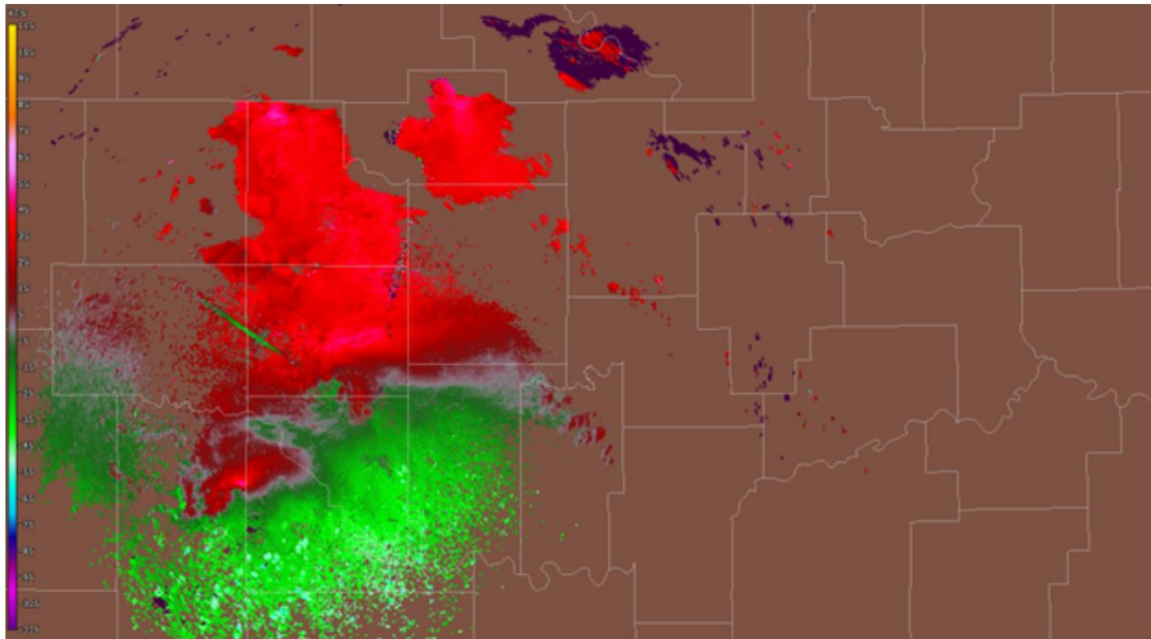
Meteo-04-06

### 4.2.7.2 Mean radial velocity

Mean radial velocity is also known as the mean Doppler velocity, and represents the reflectivity weighted average velocity of targets within a given volume sample. As the first moment of the Doppler spectral density, this base data product is typically derived from multiple successive pulses through analysis of the single-lag complex autocorrelation function. The complex covariance argument provides an estimate of the Doppler signal vector angular displacement between consecutive radar pulses. The Doppler vector angular velocity is equal to the displacement divided by the time interval between pulses. The complete Doppler spectrum characterizes the full distribution of radial velocities within the resolution volume, with each velocity component weighted by both the target reflectivity and the radar beam's weighting function.

FIGURE 4-7

**Example of widespread supercells during a tornado outbreak as observed in KTLX mean radial velocity at 2023-04-20 00:10 UTC**



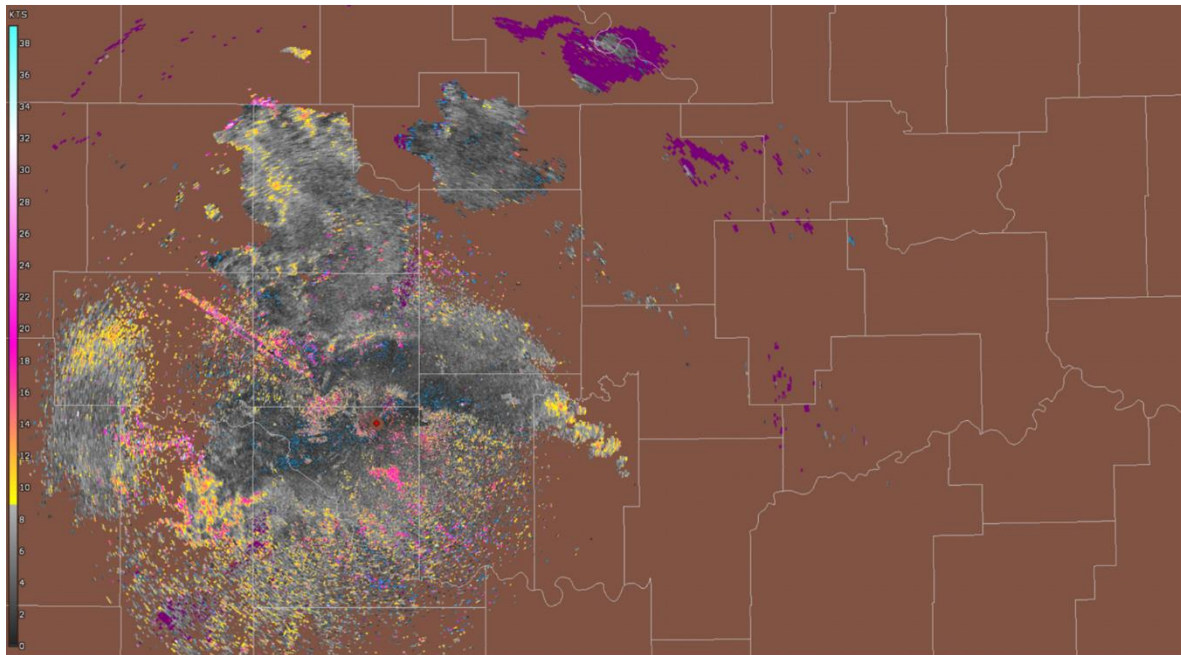
Meteo-04-07

### 4.2.7.3 Spectrum width

In meteorological radar systems, spectrum width is derived from the single lag correlation assuming a Gaussian spectral density. It is a measure of the dispersion of velocities within the radar sample volume and is the standard deviation of the velocity spectrum. Spectrum width depends on reflectivity and velocity gradients across the pulse volume and turbulence within the pulse volume [Doviak and Zrnic, 1984].

FIGURE 4-8

Example of widespread supercells during a tornado outbreak as observed in KTLX spectrum width at 2023-04-20 00:10 UTC



Meteo-04-08

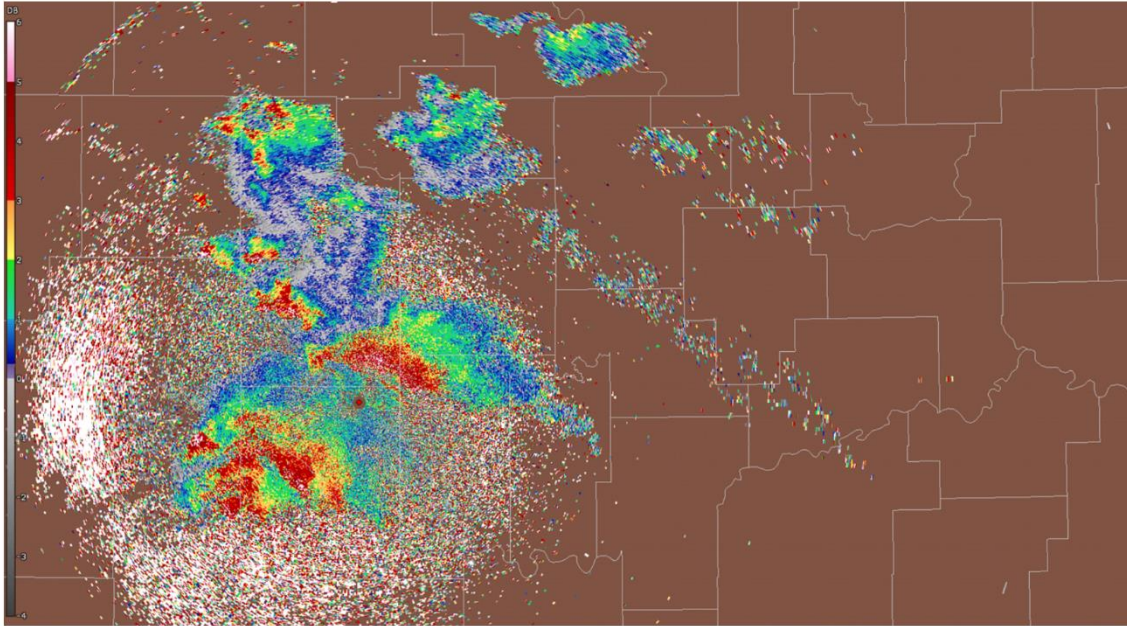
#### 4.2.7.4 Dual polarization meteorological radar products

##### 4.2.7.4.1 Differential reflectivity

Differential reflectivity is a fundamental polarimetric radar product defined as the ratio of the reflected horizontal and vertical power returns. Among other things, it is a good indicator of particle shape. In turn the shape is a good estimate of average particle size.

FIGURE 4-9

**Example of widespread supercells during a tornado outbreak as observed in KTLX differential reflectivity at 2023-04-20 00:10 UTC**



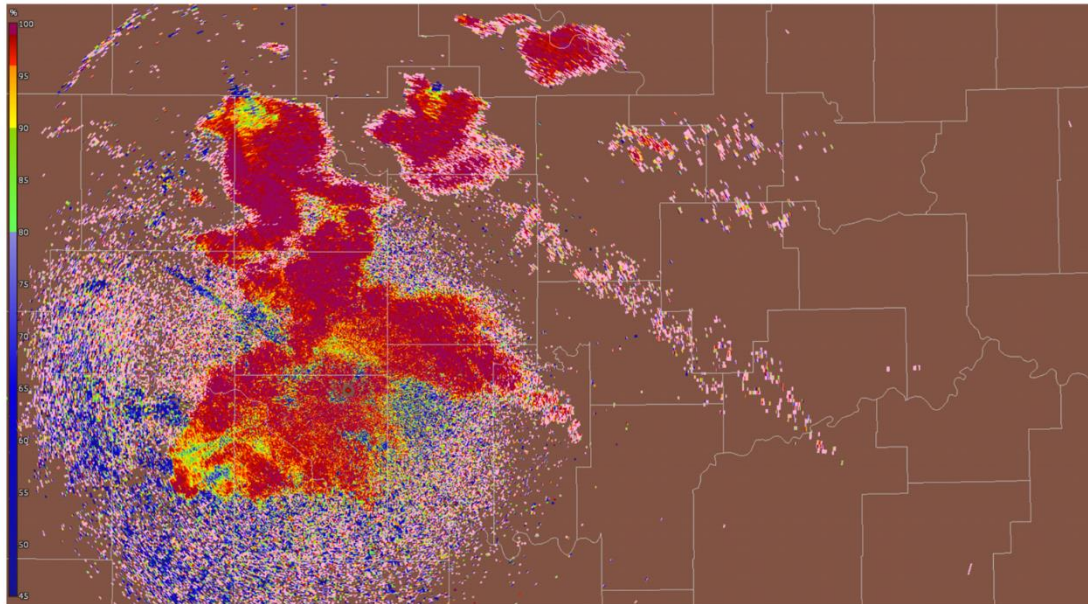
Meteo-04-09

#### 4.2.7.4.2 Correlation coefficient

Correlation coefficient is a polarimetric meteorological radar product and is a statistical correlation between horizontally (H) and vertically (V) polarized return signals. The Correlation coefficient describes the similarities in the backscatter characteristics of the horizontally and vertically polarized echoes. It is a good indicator of regions where there is a mixture of precipitation types, such as rain and snow.

FIGURE 4-10

**Example of widespread supercells during a tornado outbreak as observed in KTLX correlation coefficient at 2023-04-20 00:10 UTC**



Meteo-04-10

#### 4.2.7.4.3 Linear depolarization ratio

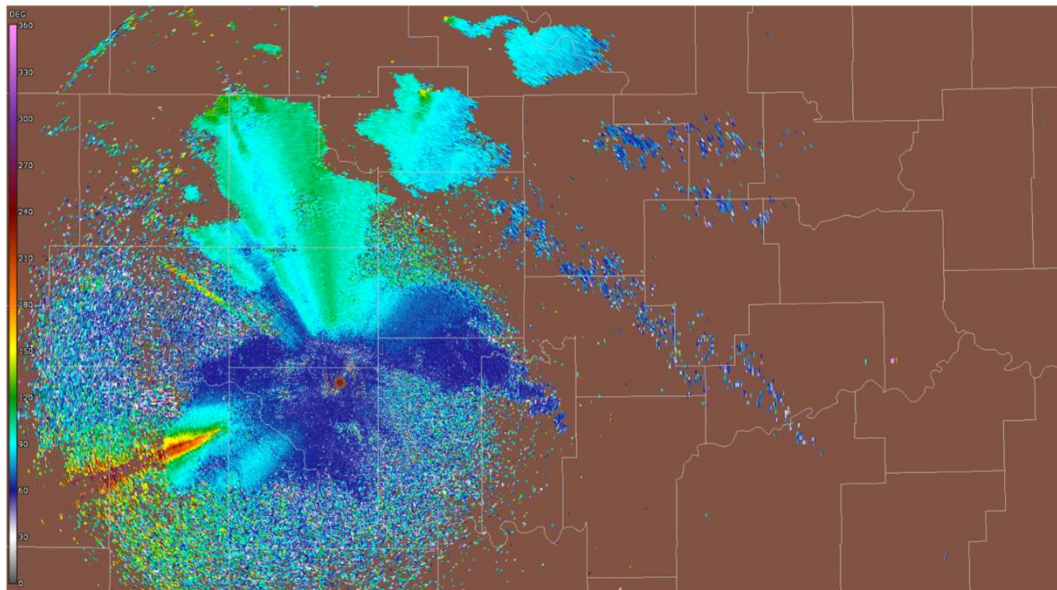
Another polarimetric radar product is linear depolarization ratio which is a ratio of Received power in orthogonal polarization (V from H transmit, or H from V transmit) and Received power in same polarization as transmit. Similar to correlation coefficient, it is a good indicator of regions where mixtures of precipitation types occur.

#### 4.2.7.4.4 Differential phase

The differential phase is a comparison of the returned phase difference between the horizontal and vertical pulses. This phase difference is caused by the difference in the number of wave cycles (or wavelengths) along the propagation path for horizontal and vertically polarized waves. It should not be confused with the Doppler frequency shift, which is caused by the motion of the cloud and precipitation particles. Unlike the differential reflectivity, correlation coefficient, and linear depolarization ratio, which are all dependent on reflected power, the differential phase is a “propagation effect”. It is also a very good estimator of rain rate and attenuation caused by rain. Specific differential phase (not shown), derived from differential phase, shows the rate at which the phase is shifting. This is especially useful for identifying regions of heavy rain.

FIGURE 4-11

**Example of widespread supercells during a tornado outbreak as observed in KTLX differential phase at 2023-04-20 00:10 UTC**



Meteo-04-11

#### 4.2.7.5 Derived data products

Using the base data products, the processor produces higher-level derived data products for the radar user. This document will not address the derived data products in detail as the products vary from radar to radar and the number of products is quite large. To ensure accuracy of the derived data products, the base data products need to be accurately maintained.

#### 4.2.8 Antenna pattern and antenna dynamics

##### 4.2.8.1 Antenna patterns

Meteorological radars typically use parabolic reflector antennas that produce a pencil beam antenna pattern. Antenna dynamics in the horizontal and vertical planes are considered to produce a volume scan. Example of such dynamics is described in § 4.2.4.1 above.

Three mathematical models for meteorological radar antenna patterns are currently used as given in Recommendations ITU-R F.699 (peak side lobes), ITU-R F.1245 (average side lobes) and ITU-R M.1652. Although representative of parabolic antennas, these Recommendations tend to slightly overestimate the beamwidth of a pencil beam antenna pattern.

It is noted that currently there are no defined radar antenna radiation pattern equations within ITU-R to represent such pencil beam antennas.

##### 4.2.8.2 Volume scan antenna movement

The horizontal and vertical coverage required for a volume scan to produce a horizontal sweep, is achieved by rotating the antenna in the horizontal plane at a constant elevation angle. The antenna elevation is modified by a pre-set amount after each horizontal sweep. The lowest elevation angle is typically in the range of  $-2^{\circ}$  to  $1^{\circ}$ , and the highest elevation is in the  $20^{\circ}$  to  $30^{\circ}$  range, though some applications can use elevations up to  $60^{\circ}$ . For a differential reflectivity calibration (Zdr) the antenna is usually pointing at  $90^{\circ}$  elevation and rotates at least  $360^{\circ}$ , known as bird bath scan. Rotation speed of the antenna varies depending on weather conditions and the product required at the time. The rotation speed as well as range of elevation, intermediate elevation steps, and

pulse repetition frequency, is adjusted for optimum performance. Slow antenna rotation provides a long per-radial dwell time for maximum sensitivity.

High antenna rotation speed allows the operator to generate a volume scan in a short period of time when it is desirable to cover the entire volume as quickly as possible. Variation of the elevation steps and rotation speed can result in volume scan acquisition times ranging from one minute up to 15 min. The long periods of time for a complete volume scan, compared to other radars that rotate at a constant elevation, is explained by the necessity to obtain a statistically significant sampling of results.

### 4.2.8.3 Other antenna movement strategies

Meteorological radars also use other antenna movement strategies for special applications and research.

Common strategies may include:

- Sector scans which acquire part of an elevation cut, or sector volume scans which perform a volume scan for a fraction of the 360° azimuth sweep at different elevations.
- Single pointing direction scans where the antenna is held at a constant azimuth and elevation to monitor a specific point in the atmosphere.
- RHI or “Range Height Indicator” scans where the antenna is held at a constant azimuth and swept in elevation instead to acquire detailed vertical information at a single bearing.
- Raster scans where a small rectangular patch bounded by fixed azimuth and elevations is scanned in a zig-zag pattern. This kind of scan is commonly used to observe the sun as part of solar calibration activities.

## 4.2.9 Present and future spectrum requirements

As for a number of radar applications, the choice of the frequency band (or wavelength  $\lambda$ ) mainly results from a trade-off between the range/reflectivity, which varies as  $\lambda^{-4}$ , the rain attenuation, meteorological variable accuracy, and cost. Attenuation in precipitation, which decreases as  $\lambda$  increases to become negligible at wavelengths in the decimetre range, is a dominant consideration. The Ka-band (around 35 GHz, 8.6 mm wavelength) is well suited for detecting small water drops, which occur in non-precipitating clouds. The S-band (2 700-3 000 MHz, 10 cm wavelength) may be chosen for detecting heavy rain at very long ranges (up to 300 km) in tropical and temperate climates.

### 4.2.9.1 Weather radar frequency bands

The three bands most commonly employed in meteorological radars are S-band (2 700-3 000 MHz), C-band (5 250-5 725 MHz), and X-band (9 100-9 700 MHz).

The S-band (2 700-3 000 MHz, 10 cm nominal wavelength) is the best choice overall in terms of quantitative accuracy and long-range performance. This is due to the low values of attenuation for both gaseous absorption and attenuation in precipitation (Fabry, 2015; Doviak, 1993). The longer wavelength also benefits mitigation of range – Doppler ambiguity issues (Doviak, 1978 and 1979). However, cost is a factor in the choice of S-band because the longer wavelength requires larger hardware components and a larger antenna for given requirements for beamwidth and gain.

The C-band (5 250-5 725 MHz, 5 cm wavelength) is generally employed in temperate climates, and in countries with reasonably small geographic areas requiring coverage. It can be a relevant compromise between the above-mentioned parameters, allowing rain detection at long ranges (up to 200 km) although its quantification would be in fact limited beyond 100 km, but offers the advantage of lower cost resulting from both lower power and smaller antenna size compared to lower-frequency radars having the same spatial resolution.

X-band (9 100-9 700 MHz, 3 cm wavelength) weather radars are more sensitive and can detect smaller particles but, since experiencing higher attenuation, are used for only very short-range weather observation (about 50 km). These radars are used for studies on cloud development because they can detect the tiny water particles and are also used to detect light precipitation such as snow. In addition, due to their small size, X-band weather radars are often used as mobile portable units. These radars are also used to detect wind variation in particular for aeronautical purposes (wind shear, vortex, ...).

### 4.2.9.2 Attenuation

Electromagnetic waves are attenuated by water vapour, gaseous absorption, clouds, and precipitation when propagating through the atmosphere (Fabry, 2015). By far the greatest attenuation is caused by precipitation, especially heavy rain. The propagation physics are such that the rate of attenuation (in dB per unit length) at C-band (5 cm) is about six to eight times that of S-band (10 cm) depending on rain rates [Bean and Dutton, 1966, Burrows and Attwood, 1949]. The attenuation problem for X-band is far worse, with attenuation rates of over 100 times those of S-band and over 15 times greater than C-band for rain rates of 6 mm/hr.

The severe impact of atmospheric attenuation at shorter wavelengths is well documented in the literature. Direct comparisons of performance between 5 and 10 cm radars were done by the National Severe Storms Laboratory in the 1980's and these tests demonstrated that use of 5 cm wavelengths in heavy rain could seriously impact severe storm forecasting and warning operations (Allen, 1981).

Attenuation correction presents significant technical challenges at shorter wavelengths due to stringent power measurement accuracy requirements (Hitschfeld, 1954). The reflectivity calibration accuracy requirements necessary for C and X-band to support attenuation correction algorithms exceed current requirements for the United States' Next Generation Radar (NEXRAD) program and are difficult to achieve in practice. The introduction of polarimetry to weather radars has changed the situation considerably because the differential phase provides estimates of the attenuation, which do not depend on the reflectivity calibration accuracy.

A somewhat related issue with attenuation drives the need for meteorological radars to employ linear polarization. At the start of the U.S. NEXRAD Weather Surveillance Radar – 1988 Doppler (WSR-88D) S-band radar deployment, the system featured elliptical polarization. This was done in order for efficient and cost-effective hardware design for the transmission and reception of the RF signal. However, system managers quickly discovered that depolarization in heavy rain severely impacted operations and the radar was modified to employ linear horizontal polarization (Sirmans, 1993). Because polarization is a factor in considering susceptibility to interference, the current ability to use linear polarization (horizontal and/or vertical), should be preserved.

### 4.2.9.3 Maximum unambiguous range and velocity estimates

The choice for frequency of meteorological radar also defines the performance characteristics of maximum measurable wind speed and maximum range. In pulsed radar, the time between pulses determines the maximum unambiguous range<sup>6</sup> of the radar. The reflection from a pulse must return to the receiver before the next pulse is transmitted, or the received pulse becomes ambiguous. In Doppler radar systems, the pulse repetition frequency (PRF) determines the maximum unambiguous range and velocity that the radar can measure (Doviak, 1979). In the design of the radar, the designer is limited by the unambiguous range-velocity product, a constant given by:

$$R_m \cdot V_m = c \frac{\lambda}{8} \quad (4-11)$$

where:

$R_m$ : radar unambiguous range (maximum range the radar can make a measurement)

$V_m$ : radar unambiguous velocity (maximum velocity the radar can measure)

$c$ : speed of light ( $3 \times 10^8$  m/s)

$\lambda$ : radar signal wavelength.

The wavelength of the signal, set by the radar frequency, is the only parameter at the discretion of the radar designer in order to maximize the maximum range and maximum velocity measurement of the radar. A reduction in wavelength requires a reduction in the effective range, effective velocity measurement capability, or a combination of both by the same magnitude as the increase in frequency. In order to limit ambiguity and

<sup>6</sup> The maximum unambiguous range is the longest range to which a transmitted pulse can travel and return to the radar before the next pulse is transmitted. In other words, the maximum unambiguous range is the maximum distance that radar energy can travel round trip between pulses and still produce reliable information.

improve the range-velocity product, modern weather radars, in particular in C-band, often make use of different emission schemes combining different PRFs (see § 4.2.4).

Values are given for different technologies: magnetrons, klystrons, and TWTs, the latter having the capability to deliver short emitted pulses characterized by wider emission spectra. Some magnetrons show a frequency shift of less than 1 MHz over a wide range of ambient temperatures. Pulse compression technique may require larger amount of spectrum.

Even at the longer wavelengths of S-band, it can be difficult to achieve acceptable radar performance over long ranges and large velocity spans. For example, the U.S. NEXRAD program employs numerous mitigation methods such as multiple scans at the same elevation using different PRFs and systematic phase coding. These issues become much more challenging at shorter wavelengths.

#### 4.2.9.4 Echo coherency

The limit on unambiguous velocity (Nyquist Frequency) is determined by the relationship between PRF and wavelength. The Nyquist co-interval (range of unambiguous velocities) is directly proportional to wavelength. The relevant equation is given by:

$$V_a = \frac{\lambda \cdot PRF}{4} \quad (4-12)$$

Thus, for a given PRF, the wavelength establishes the Nyquist co-interval, which in turn limits the accuracy of Doppler estimates in terms of the width of the spectrum. When the spectrum width becomes large relative to the Nyquist co-interval, the radar samples become incoherent between pulses and estimate accuracy decreases. Spectrum width can increase (spectral broadening) and become a large portion of the spectrum due to several factors including turbulence, shear, and fall speeds (Fabry, 2015, Section 5.2). If the spectrum width exceeds more than about  $(2\pi)^{-1}$  of the Nyquist co-interval, Doppler velocity estimate variance increases at an exponential rate (Doviak, 1978).

Because the effects of turbulence and shear increase as the radar sample volume increases, spectrum width is a function of radar effective beamwidth and range. The “coherency range” can be defined as the maximum range over which acceptable quality Doppler estimates can be obtained. For a given beamwidth, the longer wavelengths (such as 10 cm, S-band) are preferred.

#### 4.2.9.5 Resonance effects – quantitative intensity measurements

The effective backscatter cross section of spherical particles depends highly on the incident signal wavelength as well as the diameter of the sphere (Rheinstein, 1968). For accurate reflectivity estimates, which are a measure of the backscatter cross sections, the power returned must be a linear function of drop size. This dictates that the radar backscatter occurs in the Rayleigh region and the Mie region, which is very non-linear, should be avoided for normally expected rain drop diameters (Fabry, 2015). Resonance effects, in addition to attenuation, can have negative effects on polarimetric variable estimates (Zrnicek, 2000). As Zrnicek describes, at 5 cm wavelength, resonance occurs for drop sizes larger than about 5 mm and the polarimetric variable exhibits non-linear (non-monotonic) behaviour making accurate quantitative estimates impossible. Effects on correlation coefficient are quite obvious for C-band in particular for reflectivity values greater than 30 dBZ (Ryzhkov, 2005).

The uncertainty in the relationship between drop diameter and backscatter cross section in the Mie region can preclude acceptable reflectivity estimates for shorter wavelengths. At attenuating wavelengths, small errors in radar calibration constants cause large errors in the estimated rain rates (Hitschfeld, 1954).

#### 4.2.9.6 Conclusions

The choice of the frequency range for meteorological radars is linked with the coverage range required. If long coverage range is required or in geographical areas where heavy rains are typical, S-band permits higher quality estimates for intensity-based parameters and for Doppler estimates. In other geographical areas or at shorter ranges, C- and X-band radars are more adequate, respectively. Other major considerations are the inability to sufficiently mitigate range and velocity ambiguities due to the shorter unambiguous range necessitated by PRFs that are high enough to permit processing of accurate Doppler estimates. Other data accuracy impacts are due to resonance effects (Mie versus Rayleigh scattering) resulting in non-linear relations between the

return power (backscattered signal) and the drop size distributions of precipitation. This precludes accurate rain rate estimation and seriously degrades particle identification algorithms.

#### 4.2.10 Vulnerabilities of weather radars

A weather radar determines range to targets (weather) by measuring the time required for an emitted signal to travel from its transmitter to the target and return to the radar site. The travel time is a function of path length, and the accuracy with which it can be measured is critically dependent on the pulse rise- and fall-times, the sharper the transitions, the more precise the timing detection. The leading or trailing edge of a pulse is the marker by which arrival time of a returned pulse is measured, and the shorter it is, the greater the possible precision of the measurement.

The preservation of short pulse transition times requires phase linearity in the transmitter and receiver hardware over a wide bandwidth. The radar bandwidth is roughly proportional to the shorter of the two-pulse transition times, and attempts to reduce the bandwidth of the emitted signal (by additional filtering, etc.) below the necessary value degrade system accuracy. The radar bandwidth often surprises those not familiar with radar systems, the 3 dB bandwidth of weather radar can be between 5 and 10 MHz. Received interference within the radar's bandwidth also degrades performance.

It must also be reiterated that while most radiocommunication transmissions involve a single traversal of a path between antennas having known characteristics, a radar signal must cover the path twice with an intervening reflection from objects (raindrops, hailstones, wind-borne debris) not designed for that purpose. The resulting received signals are extremely weak.

Despite frequently using large transmitter powers and highly sensitive receivers, radars are extremely vulnerable to noise and interference.

##### 4.2.10.1 Types of possible interference

A weather radar's ability to accurately depict the current status of atmospheric conditions can be degraded by various forms of interference which can limit, or in the worst case nullify, the radars ability to detect the speed and direction of the wind at various altitudes, provide relevant quantification of rain rates and accumulation, locate and track hurricanes, typhoons, tornadoes, gales, and other storm-related phenomena. The exceptional sensitivity required for meteorological detection makes weather radars particularly vulnerable to interference, which can severely compromise their operational effectiveness. As such, it is important to identify the types of interference that can degrade the radar's operational capabilities.

Constant, time varying and pulse like intrusive signals are the primary types of interference that can be experienced by weather radars. Once these forms of interference have been identified, one can then establish the maximum interference level that meteorological radar systems can withstand before their forecasting capability is compromised.

Protection criteria levels for meteorological radars can be found in Recommendation ITU-R M.1849-1 as a maximum  $I/N = -10$  dB for constant interference.

##### 4.2.10.2 Impact of constant interference

###### 4.2.10.2.1 Geographical coverage

Constant interference can decrease the operational range of the radar resulting in limiting the geographical area of coverage due to the corresponding noise increase.

A protection criteria of  $I/N = -10$  dB corresponds to a noise or energy increase of 0.5 dB.

On the principle that radars are calibrated in order to coincide with the level of receiver noise (i.e. about  $-113$  dBm) with the 0 dBz reflectivity level at 100 km, a noise increase changes the nominal conditions of the radar, decreasing its operational range.

Current coverage of typical C-Band meteorological radars roughly extends up to 200 km. Table 4-3 summarizes the losses in range and coverage versus interference and noise increases.

TABLE 4-3  
Loss in range and coverage

Noise increase (dB)	Corresponding $I/N$ (dB)	Loss in coverage (km)	Loss in coverage (% relative to surface)
0.5	-10	11	11%
1	-6	22	21%
2	-2.3	42	38%
3	0	59	50%
4	1.8	75	61%
5	3.3	88	69%
6	4.7	100	75%
7	6	111	80%
8	7.3	121	84%
9	8.4	130	88%
10	9.5	137	90%

#### 4.2.10.2.2 Rain rate

Constant interference also creates an increase of the energy received by the radar that can impact the reflectivity measurement that is associated with various types of precipitation (e.g. rain, snow and hail). Table 4-4 summarizes the percentage increase for several precipitation events as interference (noise) increases.

Following the description in § 4.1.2, the precipitation rate corresponding to a certain reflectivity level (dB) is given by:

$$z = AR^B \quad (4-13)$$

where:

- Z : reflectivity
- A : scattering constant
- B : rate multiplier

and

$$Z = 10 \log Z \quad (\text{dBz})$$

where:

dBz: reflectivity (dB).

Rearranging terms and solving for  $R$  yields the following equation:

$$R_{(\text{mm/h})} = \left( \frac{10^{\left(\frac{\text{dBz}}{10}\right)}}{200} \right)^{\left(\frac{1}{1.6}\right)} \quad (4-14)$$

Assuming a constant energy increase,  $C$ , the resulting rain rate is:

$$R_{(\text{mm/h})} = \left( \frac{10^{\left(\frac{\text{dBz}+C}{10}\right)}}{200} \right)^{\left(\frac{1}{1.6}\right)} \quad (4-15)$$

The rain rate increase in percentage is then a constant that is given by:

$$p(R_{(\text{mm/h})}) = 100 \times \left( 10^{\left(\frac{C}{16}\right)} - 1 \right) \quad (4-16)$$

Table 4-4 lists typical scattering constants and rate multipliers for several types of precipitation<sup>7</sup>.

TABLE 4-4  
Scattering constants and rate multipliers for various precipitation events

Variables	Stratiform rain	Convection rain	Snow	Hail
Scattering constant (A)	200	500	2 000	2 000
Rate multiplier (B)	1.6	1.5	2	1.29

Table 4-5 summarizes the percentage rain increase for several precipitation events.

TABLE 4-5  
Precipitation rate increase

Noise increase (dB)	Corresponding <i>I/N</i> (dB)	Stratiform rain rate increase (%)	Convection rain rate increase (%)	Snow rate increase (%)	Hail rate increase (%)
0.5	-10	7.5	8.0	5.9	9.3
1	-6	15.5	16.6	12.2	19.5
2	-2.3	33.4	35.9	25.9	42.9
3	0	54.0	58.5	41.3	70.8
4	1.8	77.8	84.8	58.5	104.2
5	3.3	105.4	115.4	77.8	144.1
6	4.7	137.1	151.2	99.5	191.8
7	6	173.8	192.9	123.9	248.8
8	7.3	216.2	241.5	151.2	317
9	8.4	265.2	298.1	181.8	398.5
10	9.5	321.7	364.2	216.2	495.9

These calculations show that, irrespective of the rain value and precipitation type, the percentage of overestimation corresponding to a given constant energy increase is also constant, and hence cannot be neglected.

Also, considering the reflectivity calculation for a given range bin that are based on the average (dBz), over all estimates, and the related standard deviation, it is worth noting that an increase in interference would not modify the radars ability to detect rain cells (i.e. a measurement not considered as a rain cell will still not be considered as such) but would only have an impact on the rain rate.

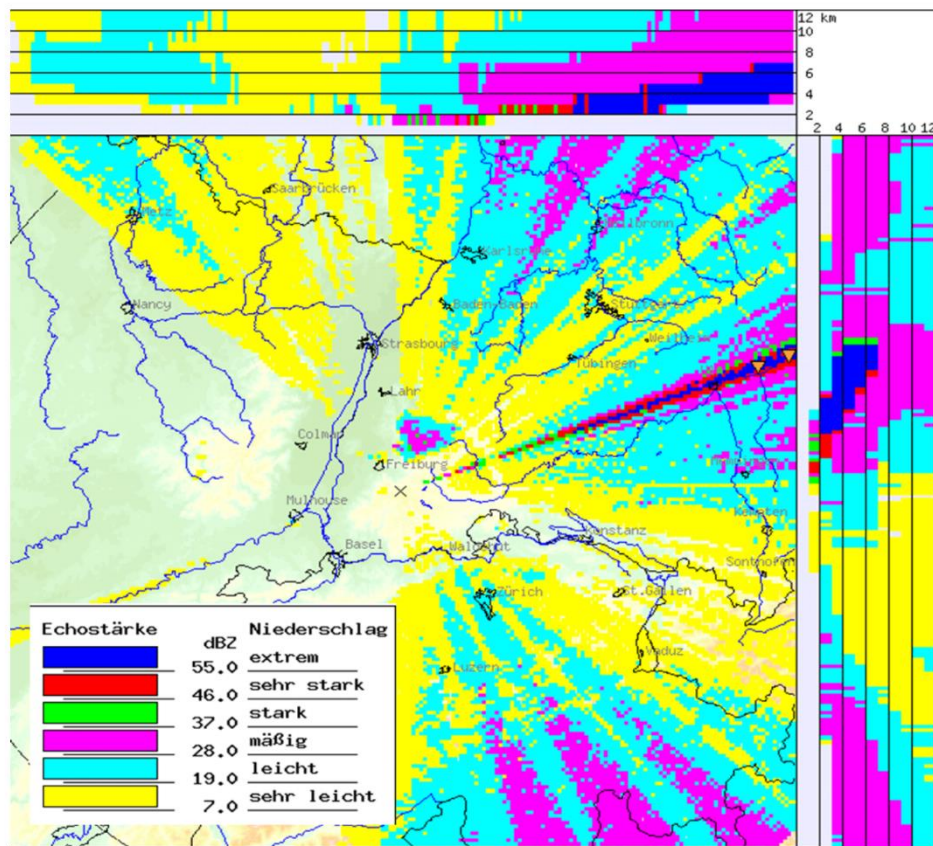
It is also interesting to note that either for the loss in coverage or the rain rate overestimation, the current agreed protection criteria of -10 dB *I/N* represents radar performance degradation in the range of 7 to 11%, comparable to performance degradation percentages generally agreed upon for all radiocommunication services.

<sup>7</sup> Stratiform rain, convection rain, snow and hail scattering constants and rate multipliers are derived from measurements.

An example of impact of a constant interference on a radar precipitation mode can be seen in Fig. 4-12. It is important to highlight that, although being a constant interference, the variation in impact is due to the rotation of the antenna, the maximum interference (in green on this picture) being produced in the azimuth of the interfering source.

FIGURE 4-12

#### Example of interference to precipitation mode of a weather radar



Meteo-04-12

#### 4.2.10.2.3 Wind measurement

In the case of Doppler measurements, a given constant interference affects wind velocity estimation differently, primarily through phase distortion of the desired signal. The impact depends critically on how the interfering signal's phase alters the composite signal phase used for Doppler processing.

This latter assumption is certainly not trivial to determine and will be signal and/or environmentally dependent. However, it is proposed to consider the different situations on a theoretical basis:

- *Case 1* – If the phase of the interfering signal detected by the radar is random, it means that the resulting vector would be statistically null; whatever would be its level. Hence, it would theoretically not have any impact on the wind measurements.
- *Case 2* – On the contrary, if the detected phase is not random and almost constant, it would result in a constant vector with a certain module and the impact on the wind measurement will depend on both the phase and module of such vector. However, the determination of such impact, even for a constant interference level is likely not to be easy and is hence not made at this point.

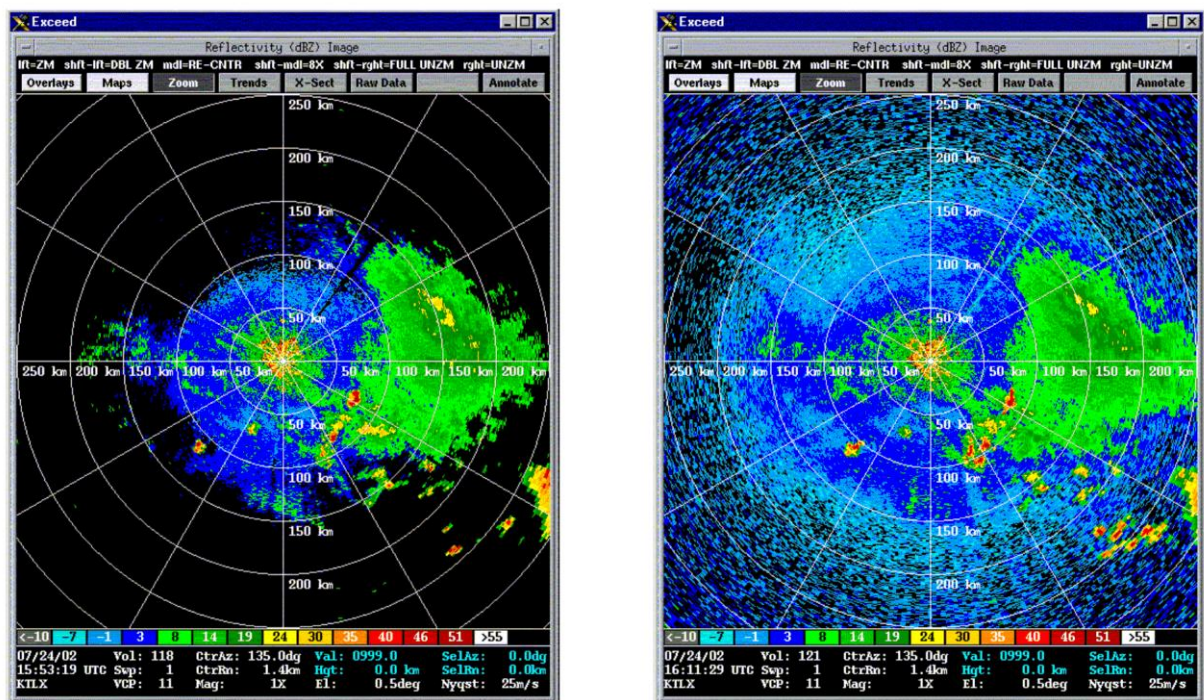
In addition, one can also assume that when the level of interference is much lower than the wanted signal, the phase of this latter is not modified whereas, on the contrary, if the interfering signal is much higher, then the phase detected by the radar will be the phase of the interfering signal. In this latter situation, the discussion on Cases 1 and 2 above will remain. In between these two situations, i.e. when the levels of both the interfering and wanted signals are consistent, it seems quite difficult to assess which of the signals will control the phase detection.

#### 4.2.10.3 Impact of persistent pulsed interference

Pulsed interference can have a significant impact on the reflectivity data and could result in a returned data that cannot reliably produce an image of targets in the atmosphere. An example of this can be seen in Fig. 4-13.

FIGURE 4-13

Comparison of interference free versus interference corrupted on precipitation mode of a weather radar



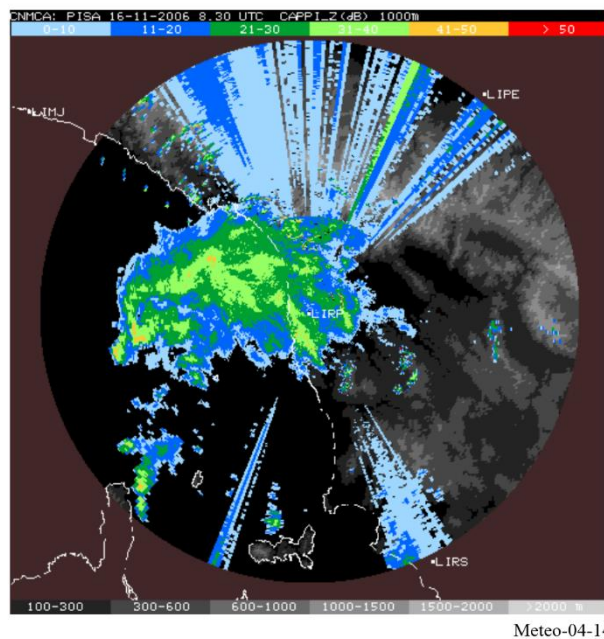
*Interference free*

*Interference corrupted*

Meteo-04-13

An additional example of interference to meteorological radar from a single indoor low power transmitter can be seen in Fig. 4-14. This interference appears as pencil-beam shaped artifacts in radar output products. Continuous reception of interfering signals with constant amplitude within and near the radar's operational bandwidth generates these artifacts. Their visual intensity depends on the distance between the interference source and radar location and the range correction factor applied by the radar based on received interference strength. (See details in § 4.2.10.5.)

FIGURE 4-14

**Interference to meteorological radar (precipitation mode)****4.2.10.4 Interference and coexistence between Meteorological radar and other radar systems**

Meteorological radars are typically protected against constant interference from systems of other services by ensuring a noise like interference-to-noise ratio ( $I/N$ ) of  $-10$  dB.

However, co-existence between two meteorological radars or between meteorological and non-meteorological radars could be less restrictive based on a case-by-case analysis. This is because the interference dynamics between two pulsed radar systems is fundamentally different from the sharing of radar frequencies with systems of other services. The following factors provides some examples of these differences:

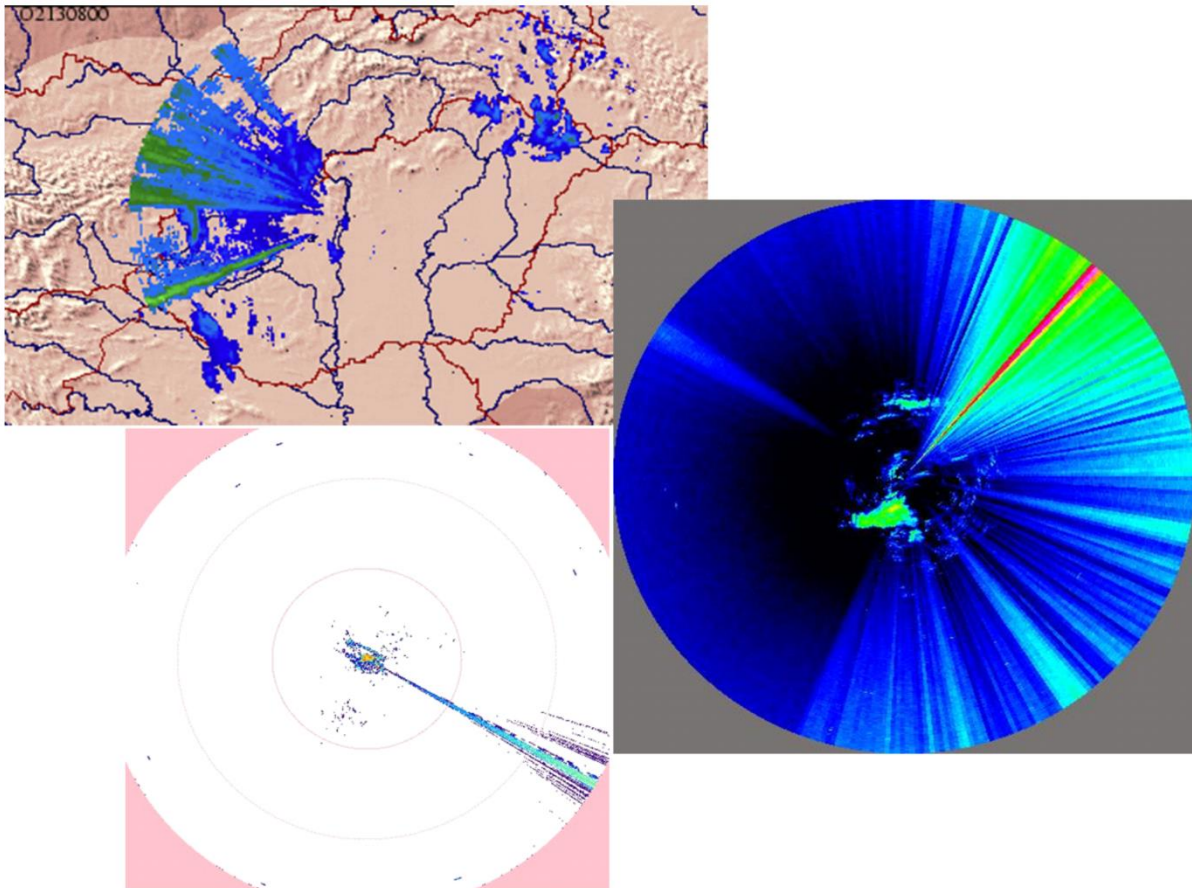
- **Asynchronous Nature of Interference:** The scanning strategy of one radar is not synchronized with the operation of another radar, minimizing the chance of continuous disruption.
- **Low Duty Cycle:** Radar systems typically emit signals intermittently in range 0.05-0.2%, which reduces the likelihood of continuous interference.
- **Low Probability of Main Beam Coupling:** The probability that the main beams of two radars will interfere with each other is low, especially when systems are properly aligned and spaced.
- **Robust Signal Processing:** Modern radar systems are equipped with advanced interference rejection (IR) circuits and signal processing capabilities that allow them to filter out unwanted signals.
- **Interference Suppression Techniques:** Techniques such as frequency hopping or the use of narrowband filters help suppress interference between radars.

**4.2.10.5 Interference to C-band radars from WAS/RLAN**

WRC-03 took the decision to authorise WAS/RLAN (e.g. WiFi) in the 5 150-5 350 MHz and 5 470-5 725 MHz band. The WRC-03 decision was associated with the requirement for WAS/RLAN of implementing Dynamic Frequency Selection (DFS) to detect and avoid radar frequencies.

Unfortunately, interference to weather radars started quite early, in 2006 in Europe, mainly in eastern countries, and has now been seen worldwide in most countries where C-Band radars are deployed in the 5.6 GHz band.

FIGURE 4-15

**Examples of WAS/RLAN interference to weather radar**

Meteo-04-15

It rapidly appeared that the specification of the DFS were not sufficiently addressing the specificities of Weather radars:

- Volume scanning over repeating strategy (typically 10 to 15 min).
- Operational elevation ranging from 0° to 90°.
- Pulse width ranging from 0.5 to 2.5  $\mu\text{s}$  (for operational radars).
- Pulse repetition frequency (PRF) ranging from 250 to 1 200 Hz (for operational radars).
- Fixed, staggered, interleaved PRF.
- Rotation speed ranging from 1 to 6 rpm.
- Noise calibration.

In Europe, the WAS/RLAN ETSI standard EN 301 893 was then modified to include new DFS specifications to address these specificities.

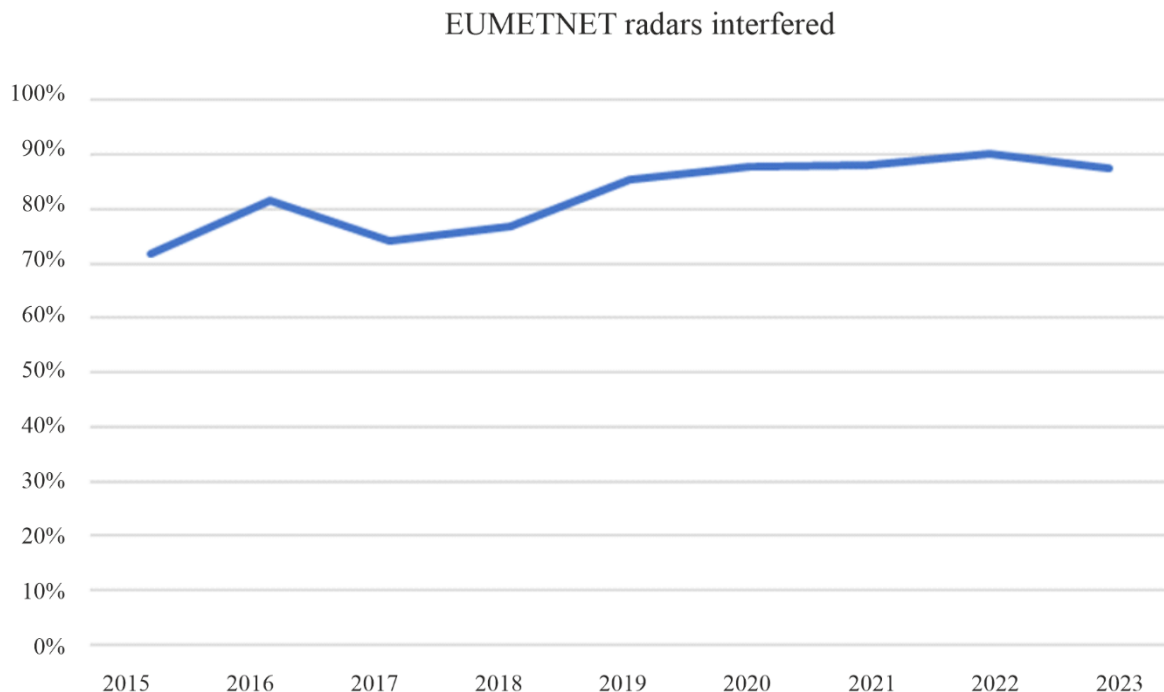
However, after a few years, interference cases started to dramatically increase. Further investigations showed that it was and is still now due to non-compliant WAS/RLAN:

- No DFS inside.
- DFS switched off.
- DFS specifications not fully implemented.

Since then, the meteorological community, in particular in Europe (through EUMETNET), has constantly been arguing with Regulators to find a definitive solution. Despite adoption of Reports, Action plans or “list of possible options that could help to alleviate the issue”, nothing has changed over years. Figure 4-16 depicts the percentage of weather radars in Europe that experienced interference, close to 90% yearly.

FIGURE 4-16

### Percentage of EUMETNET weather radars interfered



Meteo-04-16

In addition, the most recent market surveillance in Europe has shown that two-thirds of RLAN equipment on the European market are not compliant. Since 2015, EUMETNET undertakes a yearly questionnaire showing no improvement.

The situation is increasingly seen as a major threat to C-Band radars operation. A number of mitigations have been considered, among others:

- Exclude the use of 5 600-5 650 MHz band by WAS/RLAN equipment.
- Remove the use of 5 600-5 650 MHz band by fixed outdoor RLAN.
- Improve market surveillance.
- Highlight the band 5 350-5 470 MHz (no RLAN) as an alternative to 5.6 GHz.

Although listed in Reports in Europe (e.g. JRC report), most of the envisaged solutions have not been followed by any actions by regulators or have even been denied.

At current stage, only the alternative 5 365-5 470 MHz band is currently considered as a possible mitigation solution to the WAS/RLAN interference, from the meteorological community on its own expenses and efforts. However, before taking any action, it is essential to ensure that this frequency band is free from interference by conducting the necessary measurements.

#### 4.2.10.6 Use of the 5.4 GHz band for C-Band radars

The band 5 350-5 470 MHz is already used in some countries as their nominal frequency band for weather radars (e.g. Switzerland, China).

Before considering a wider usage, a technical analysis has been performed to verify the compatibility between a deployment of meteorological radars on this band and Earth Exploration Satellite Service (EESS) (active) sensors. This analysis led to the adoption of ECC Report 346 showing that “compatibility between weather radars and EESS (active) in the 5 365-5 470 MHz band can be ensured without the need for specific operational conditions for weather radars”, valid for a quite large deployment of weather radars (about 1/3 of existing radars).

It should be highlighted that some radio administrations in Europe are not favourable to such a move. This is fully respected but hence currently does not give any alternative to their meteorological service.

It should also be highlighted that the usage of the 5.4 GHz band could lead to additional constraints in particular with respect to the systems (on-board meteorological radars) operating under aeronautical radionavigation service as well as with respect of other radar deployment under the radiolocation service.

Also, ground-based weather radar will lose their regulatory status provided in the 5 600-5 650 MHz by footnote RR No. **5.450B** and will become a secondary status (see footnote RR No. **5.448D**).

Finally, another important issue relates to what has been recently raised by two eastern European countries about usage of the 5.4 GHz band by WAS/RLAN, although it is not authorised. This needs to be further confirmed to verify whether it could be the future situation in the most countries, since it obviously could jeopardise the potential use of the band 5 365-5 470 MHz that is currently the only real and long-term solution to solve the current interference situation at 5.6 GHz.

#### 4.2.10.7 Interference from wind farms

In recent years, increasingly larger wind turbines are being constructed and the number of typical generation facilities (or wind farm, including many wind turbines) is dramatically increasing. Wind turbines and farms, even at quite large distances present a high potential to degrade meteorological data over very large areas and do have a non-negligible impact on weather nowcasting and forecasts.

For accurate weather forecasting, weather radars are designed to look at a relatively narrow altitude band. Due to the sensitivity of the radars, wind turbines, if deployed with radio line of sight of a weather radar facility, can block the onward propagation of the radar signals, cause reflectivity clutter returns, and produce wake-turbulence-induced radar echoes. These interference mechanisms can result in false radar estimates of precipitation accumulation, false tornadic and mesocycle signatures, misidentification of thunderstorm features and incorrect storm cell identification. In addition, the interference mechanisms can result in degraded radar performance and negatively impact forecast and warning operations. There are three mechanisms through which the performance can be degraded: masking, clutter and backscatter.

##### 4.2.10.7.1 Masking

Any geographical feature or structure which lies between the radar and the target will cause a shadowing or masking effect. It is possible that, depending on their size, wind turbines may cause shadowing effects. Such effects may be expected to vary, depending upon the turbine dimensions, the type of transmitting radar and the aspect of the turbine relative to it (height, blade angle, rotation rate, and position relative to the radar of the turbine).

#### 4.2.10.7.2 Clutter

Radar returns may be received from any radar-reflective surface. In certain geographical areas, or under particular meteorological conditions, radar performance may be adversely affected by unwanted returns, which may mask those of interest. Such unwanted returns are known as radar clutter. For a weather forecaster, a wind turbine or turbines in the vicinity of weather radar can present operational problems.

Ground clutter signals exhibit large reflectivity, near-zero Doppler shift, small spectrum width, and are consistently localized. Compared to commonly occurring ground clutter (GC), interference caused by wind turbines is a much more difficult challenge. Direct reflections will be received from both the tower (stationary) and the blades (non-stationary). Like GC, the wind turbine clutter (WTC) signal should still have a significantly large reflectivity, with a possible modulation due to blade rotation causing a systematic variation in radar cross-section.

The Doppler shift will be affected by several factors, including the blade rotation speed and rotor orientation with respect to the radar beam. Doppler velocities should be maximum when the rotor is oriented 90 degrees from the radar line-of-sight and near zero when the rotor is facing either away or toward the radar. Since the resolution volume of the radar will likely encompass the entire wind turbine structure, it is expected that the spectrum width will be significantly enlarged. This is due to the blade rotation away and toward the radar. Multiple turbines within one resolution volume would only exacerbate this effect.

#### 4.2.10.7.3 Backscattered energy from turbulent eddies

In addition to WTC signals caused by reflections from the actual wind turbines, backscattered energy from turbulent eddies in the wake of the wind farm may be observed. It is expected that these echoes would exhibit characteristics similar to clear-air backscatter from discontinuities in the refractive index at the Bragg scale of the radar. These wake echoes would drift with the wind field and would likely have much lower reflectivity compared to the direct reflections from the turbines. Nevertheless, they could significantly enlarge the radar coverage area affected by WTC and thus exacerbate the problem.

#### 4.2.10.7.4 Examples of wind turbine clutter

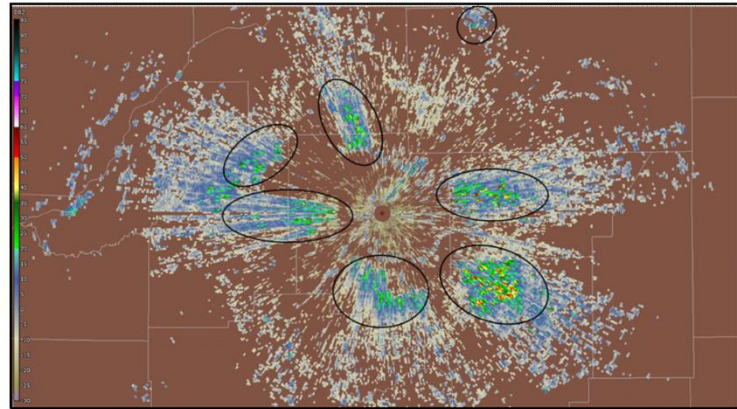
Two distinct examples of interference from Wind Farms<sup>8</sup> are provided in Fig. 4-17. As expected, the reflectivity shows large values near 45 dBz with sporadically large spectrum widths of over 10 m/s. The relatively small region of high reflectivity to the south-west of the radar is clearly visible and matches the location of a wind farm that is approximately 45 km from the weather radar location.

---

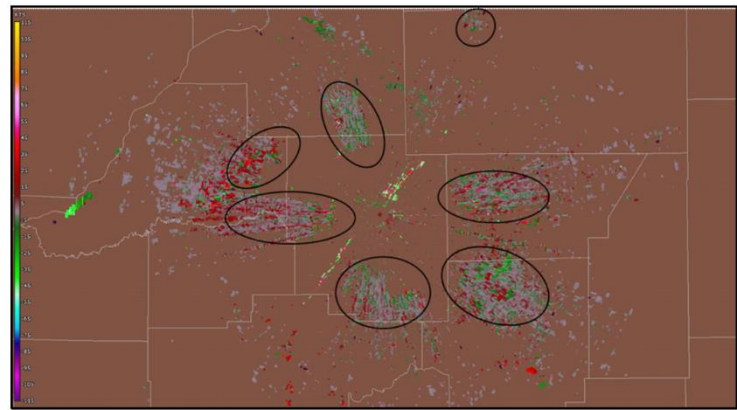
<sup>8</sup> Wind Farms are clusters of wind turbines that are used to generate power.

FIGURE 4-17

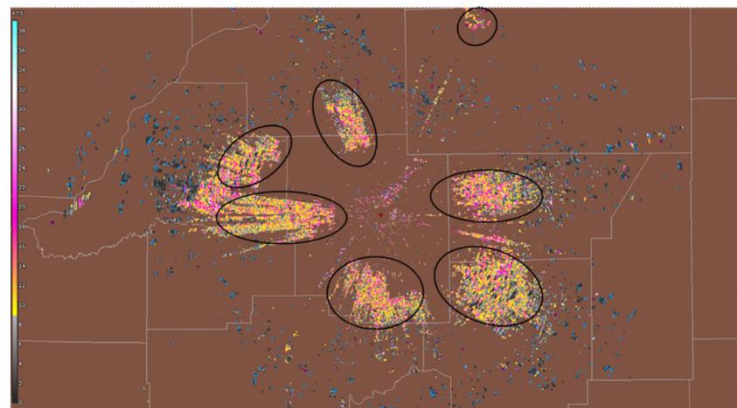
Examples of wind farm interference (circled) to weather radar under clear-sky conditions



Reflectivity (dBz)



Radial velocity (kts)



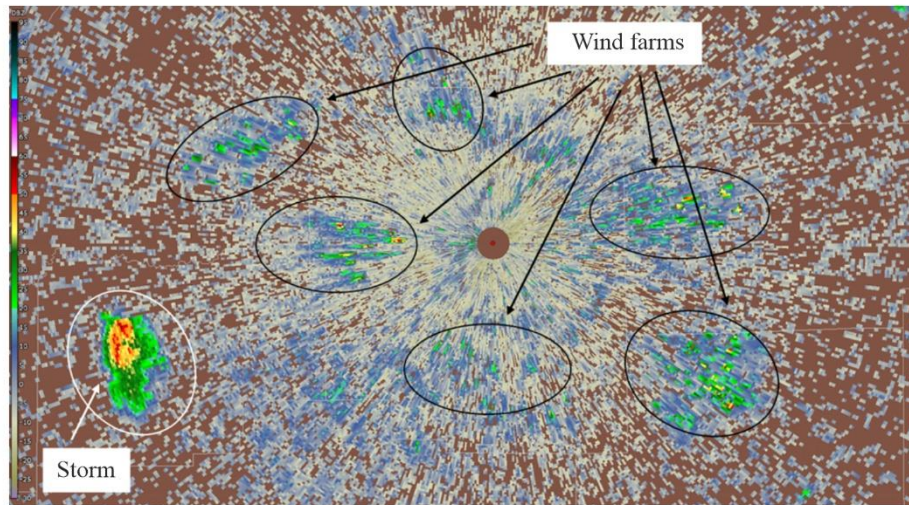
Spectrum width (kts)

Meteo-04-17

Figure 4-18 shows the same wind farm during a thunderstorm event.

FIGURE 4-18

**Example of interference from a wind farm and its impact upon reflectivity during an isolated thunderstorm incident**

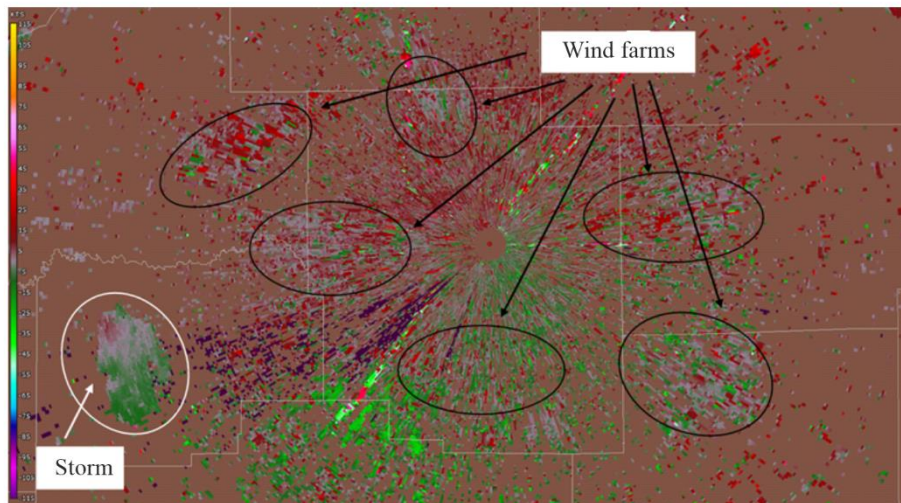


Reflectivity (dBz)

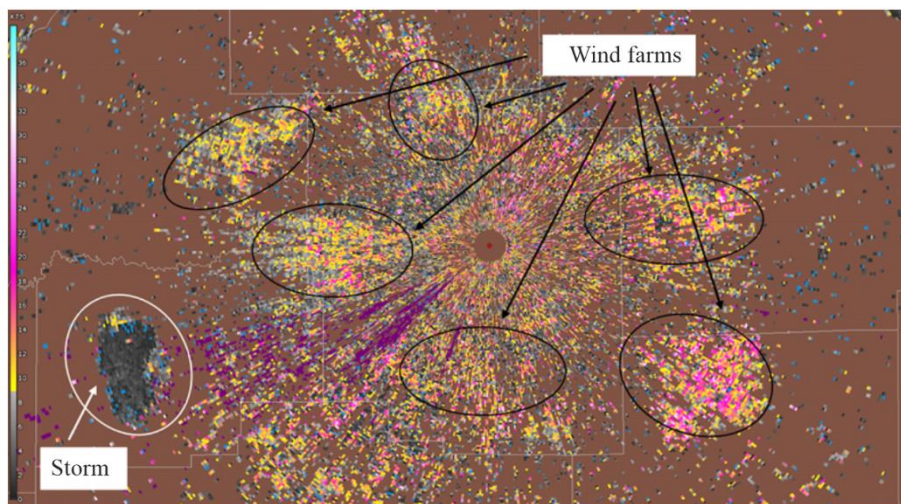
Meteo-04-18

Without prior knowledge, it would be extremely difficult to distinguish between the WTC and the thunderstorms. Since the blades rotate toward and away from the radar, one would expect a near-zero mean Doppler velocity. Of course, the large spectrum widths will reduce the accuracy of the Doppler velocity estimates as illustrated in Fig. 4-19 by small deviations from zero.

FIGURE 4-19

**Examples of Doppler velocity data estimates during a thunderstorm event**

Radial velocity (kts)



Spectrum width (kts)

Meteo-04-19

**4.2.10.7.5 Impact of WTC on meteorological radar operations and forecasting accuracy**

Field studies were conducted that illustrated the impact of WTC upon weather radars. These studies have shown that wind farms can have a significant effect upon meteorological radars and as such can degrade the accuracy of detecting severe weather events.

These analyses have clearly shown that the clutter produced by a wind turbine will be present over a large sector (several tens of degrees) compared to the direction of the wind turbine, even at quite large distances. Thus, the impact of the wind turbines on reflectivity operation of weather radars cannot be neglected.

In particular, the analyses have shown that the impact of one single wind turbine on weather radar Doppler mode is highly significant even at distances of several tens of kilometres. One can also stress that at distances lower than 10 km, all radar data will be erroneous at every azimuth, even at 180 degrees from the sector in which the wind farm resides.

Some form of WTC mitigation will be required in order to protect meteorological radars from harmful interference from wind turbine farms. Before any final conclusions can be made regarding processing methods to mitigate WTC, additional studies of WTC should be conducted in order to understand the full extent and

the impact of WTC on the meteorological radars. Once this has been defined, methods to mitigate WTC may need to be developed given the expected growth of wind-power based generation systems.

Pending the result of ongoing studies on mitigating WTC interference to meteorological radars, the current solution to avoid or limit impact of wind farms is to ensure separation distances between the two systems. For example, some European countries are currently considering the following recommendations:

- 1) that no wind turbine should be deployed at a range from radar antenna lower than:
  - 5 km for C-band radars
  - 10 km for S-band radars
- 2) that projects of wind farms should be submitted to an impact study when they concern ranges lower than:
  - 20 km for C-band radars
  - 30 km for S-band radars.

The continuous increase in the size of wind turbine structures has led to an expanding impact zone, which goes well beyond the limits previously proposed based on smaller turbine sizes. In Australia, for instance, there are a few examples of operational wind farms situated over 60 km away from a radar site over relatively flat area, with impacts observed on three to four scans of C-band radar. These impacts extend significantly with increased turbine size and altitude, especially in cases where the wind farm is located at higher elevations than the radar itself. For such scenarios, the impact zone can stretch beyond 100 km when using an S-band radar.

Offshore wind farms, in particular, are utilizing much larger turbine structures compared to onshore projects. Turbine tip heights in the range of 350 to 400 m have become standard for offshore turbines. Given that offshore sites lack the natural terrain features that can help mitigate radar interference (such as hills or mountains), the impact of offshore wind farms on weather radars – especially those located in coastal areas – could be substantial. These large turbine structures pose a considerable challenge to weather monitoring systems, potentially leading to significant radar clutter or even complete loss of radar data in certain zones, which could affect the effectiveness of weather forecasting and monitoring.

#### 4.2.11 Vulnerabilities of systems sharing spectrum with weather radars

As noted above, the transmitter power and antenna gain of weather radars are typically quite high to compensate for extended path lengths (typically around 100 dBW peak e.i.r.p.). These characteristics tend to extend the range over which a radar can interfere with systems on the same frequency (with due recognition given to the width of a radar channel). There have also been cases in which radar and fixed microwave links, which have coexisted for some time, become incompatible when the microwave system is upgraded from analogue to digital equipment with a greater vulnerability to pulsed interference.

#### 4.2.12 Future trends

##### 4.2.12.1 Hardware and algorithms improvements

Major hardware upgrades to various administrations' meteorological radar systems are in progress. Ongoing generation of upgrades includes implementation of polarimetric radar, which adds vertical polarization to the currently used horizontal radar waves. As of 2016, all NEXRAD radars in the United States of America and, as of 2024, almost all of OPERA radars in Europe have been upgraded to dual polarization. In Australia, nearly half of operational radars are upgraded to dual polarization by 2024.

Additional techniques to further improve the performance of meteorological radars are also under way. Foremost among these are various algorithms for resolving range/velocity ambiguities, increasing data acquisition speed, reducing the effects of artefacts, decreasing clutter and efficient processing of signals to provide meteorological estimates that are as accurate as possible. Other endeavours include combined use of weather and profiling radars. A modest effort is devoted to studies of lightning and its hazards, to determine whether its onset and termination might be predictable.

Advances in semiconductor technology (mainly in GaN transistors) have also enabled the use of solid-state power amplifiers in the radar transmitters, instead of traditionally used vacuum tubes (magnetrons, klystrons or TWT). Although having lower peak power, the long pulse widths and duty cycle available from solid-state

amplifiers enable preserving similar pulse energy and thus similar measurement sensitivity as with traditional tube-based transmitters.

Researchers have adapted phased array radar technology for use in weather surveillance applications. The phased array is expected to replace mechanically steered parabolic dish antennas with an electronically steered array antenna. This change will enable more flexible scanning strategies and more rapid updates of changing weather conditions. Early tests of the phased array radar system have proved promising. Phased array technology will increase fundamental understanding of storm evolution, in turn leading to improved computer models, more accurate forecasts and earlier warnings. In addition, this technology has the potential to increase the average lead-time for tornado warnings well beyond the current average of 13 minutes. System enhancements are more economically implemented via improvements to the receiver and signal processing subsystems. There is a possibility that the phased array upgrade (if implemented) will not reuse the existing transmitter, which will be replaced by distributed transmit/receive modules in the phased array. Possible implementation of phased array meteorological radar has been discussed in some regions.

#### 4.2.12.2 Solid state technology

Some weather radars using the solid-state transmitters (SSTX) are already reflected in Recommendation ITU-R M.1849-3 since some years in the 5 250-5 850 MHz frequency range.

##### *Characteristics of SSTX weather radars*

The transmitted peak power of solid state (SSTX) weather radar is between 4 to 8 kW. Which is lower than tube-based radar (several hundred kW in S-band and C-band); this lower peak power leads to a decreased sensitivity of the SSTX radar. To compensate for this impact and preserve the range resolution, pulse compression is used by extending the pulse width. The pulse width used by pulse compression can be up to 200  $\mu$ s (instead of 0.5 to 3.5  $\mu$ s for tube-based systems) to compensate average power. In an uncompressed pulse-modulated radar, the range resolution depends on the pulse duration. Pulse compression enables the utilization of longer pulses and lower-peak power transmitters without compromising range resolution. This is achieved using suitable frequency or phase modulation techniques.

The pulse compression ratio (PCR) can be defined as the ratio of the uncompressed transmission pulse width to the width of the compressed pulse, and calculated as product of the transmission pulse width and 3 dB bandwidth. Through pulse compression, a relatively long transmission pulse with a comparatively low peak power can achieve the same sensitivity and range resolution as predicted by the basic radar equation.

$$SNR = \frac{\pi^3 |K|^2}{2^{10} \ln(2) c} \cdot \frac{f^2}{r^2} \cdot \underbrace{G^2 \theta^2}_{\text{Antenna}} \cdot \underbrace{\tau P}_{\text{Transmit pulse energy}} \cdot \frac{1}{\underbrace{k_B T N_F B}_{\text{Receiver noise}}} \cdot Z \quad (4-17)$$

c:	speed of light	G:	antenna gain	N <sub>F</sub> :	noise figure
K  <sup>2</sup> :	0.93 (rain), 0.2 (ice)	θ:	Antenna beam width	T:	temperature
k <sub>B</sub> :	Boltzmann constant	τ:	pulse width	r:	range
SNR:	signal-to-noise ratio	P:	peak power	Z:	reflectivity
f:	Frequency	B:	3 dB bandwidth		

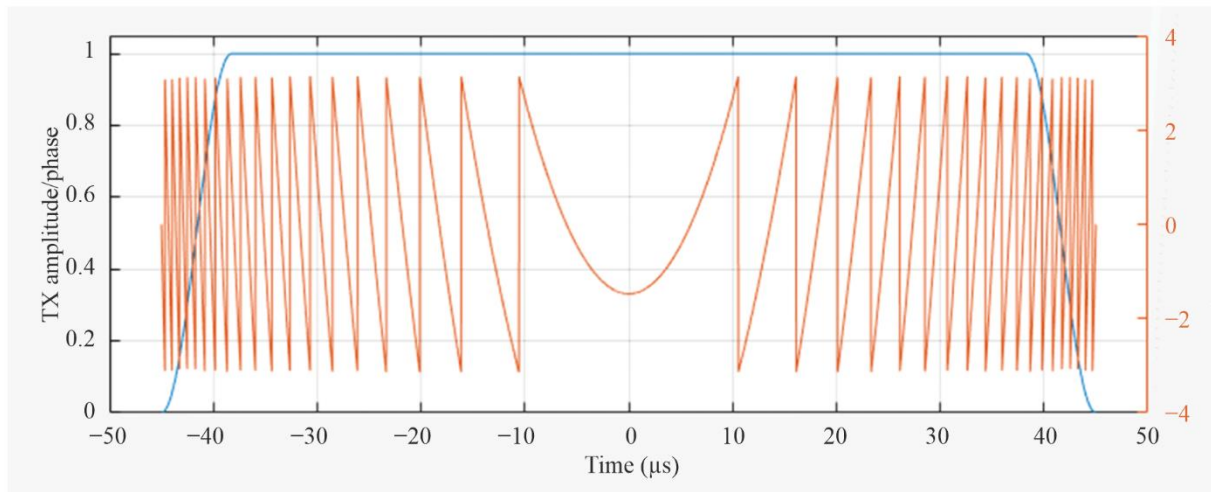
Pulse compression allows the independent adjustment of range resolution and range sensitivity. Range resolution is set inversely to the bandwidth  $B$  of the modulated transmitter signal. Range sensitivity is set proportional to the pulse energy  $\tau P$  and inversely proportional to the bandwidth  $B$ . This is attributed to pulse compression's ability to detect echo signals that have vanished in the noise before compression.

The implementation of pulse compression involves complex signal processing techniques. This complexity necessitates sophisticated hardware and software. Various modulation methods can be applied in pulse compression methods, including frequency modulated with linear (LFM) or non-linear frequency modulation (NLFM), time-dependent coded frequency modulation (e.g. Costas code) or phase modulated (PM). Usually,

the NLFM is used in weather radar applications. An example of a transmitter pulse with a pulse width of approximately 80  $\mu\text{s}$  is shown in Fig. 4-20.

FIGURE 4-20

**Time course of the nominal TX amplitude (blue) and phase (orange)**



Meteo-04-20

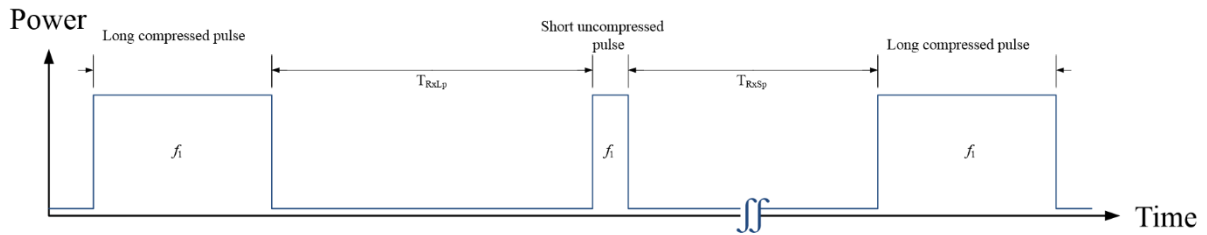
During the transmission of the long pulses, the radar receiver cannot receive data at the same time. This is due to the high power of the transmitter and the limited isolation between transmitter and receiver. Additionally, power is reflected from the antenna back into the receiver. To protect the receiver front end from damage caused by the high power, a transmit receive limiter (TR-limiter) blocks the incoming transmitter signal. This creates a so-called blind range where the receiver is blocked during the transmission of the long pulse. This makes the use of a short pulse (approximately 1  $\mu\text{s}$ ) necessary to cover the blind range. As one can see, SSTX weather radar still requires the transmission of a short pulse.

A SSTX needs to cover the blind range and the long range in order to have a complete picture of the precipitation situation. There are three methods for fulfilling this requirement.

### **Method 1: Dual Pulse Transmission on the same frequency**

The two pulses are transmitted with a pause between the long and short pulse as shown in Fig. 4-21. Both pulses have the same frequency, here  $f_1$ . The occupied frequency spectrum is limited to one “carrier”. The time  $\text{TRxLp}$  is needed to sample the echoes from the compressed pulse for the desired range. The disadvantage is a longer scanning time to capture a complete volume.

FIGURE 4-21

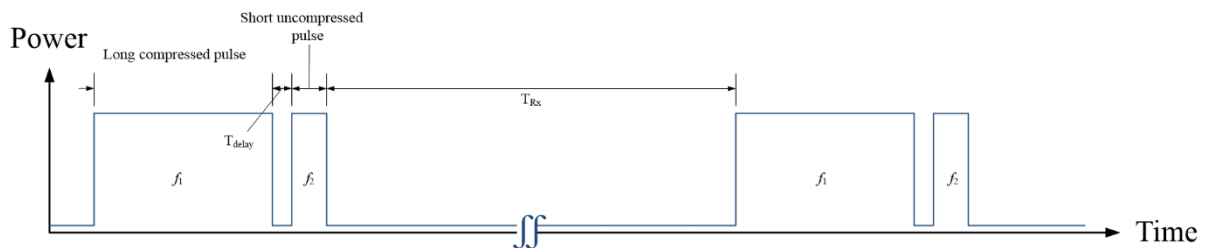
**Dual pulse transmission using a single frequency**

Meteo-04-21

**Method 2: Dual pulse transmission on two separate frequencies**

The two pulses are transmitted with a very short or no delay between the long and short pulse as shown in Fig. 4-22. Both pulses have different frequencies, here  $f_1$  and  $f_2$ . The advantage is a shorter scanning time to capture a complete volume compared with Method 1.

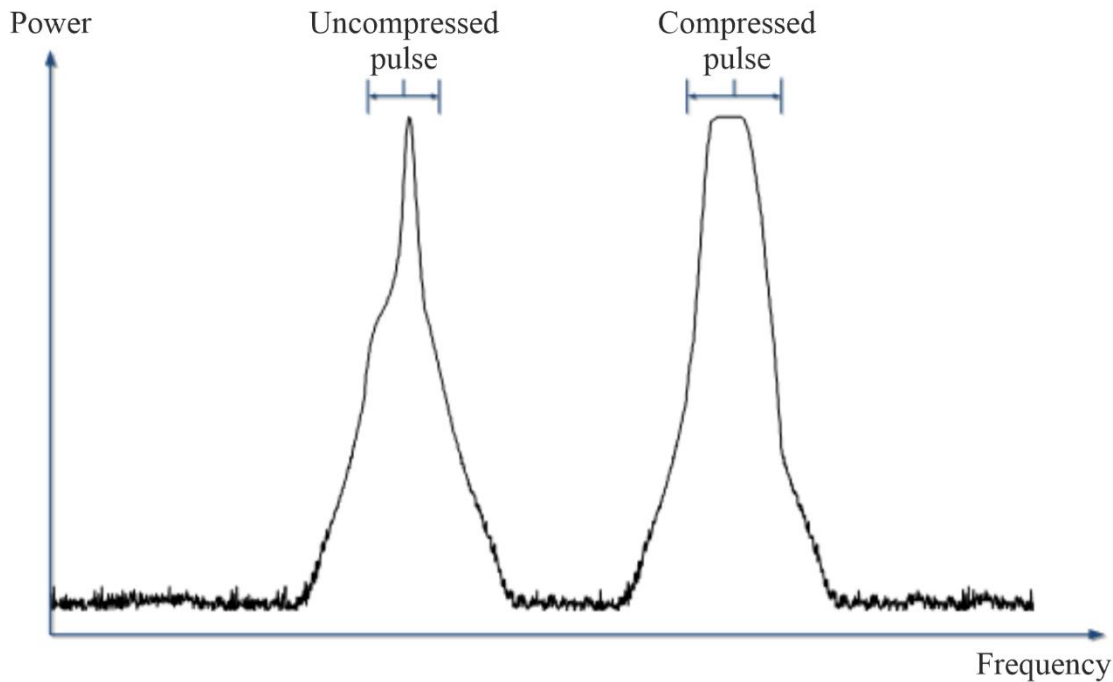
FIGURE 4-22

**Dual pulse transmission using two separate frequencies: Type A**

Meteo-04-22

As a disadvantage, a wider frequency spectrum is needed. The frequency separation is estimated to be between 3 and 6 MHz. An example of the occupied frequency spectrum can be seen in Fig. 4-23.

FIGURE 4-23

**Example of a frequency spectrum using PC on two frequencies: Type A**

Meteo-04-23

As a complete volume scan can be performed quicker by using two frequencies for the long and short pulse, it is assumed that this will be the preferred option for operational use.

**Method 3: Long pulse transmission**

It is possible to detect the blind range targets using a long pulse only, without any short pulse.

*SSTX weather radars deployment*

SSTX weather radars are already deployed in some countries, and interest in operating such systems is growing around the world. But due to the huge number of existing tube-based weather radar (more than 1 500) and their operational lifecycle of up to 20 years, even if the SSTX deployment will increase in the near future, both technologies will have to operate together during a long period transition.

It should be noted that a risk has been identified regarding the sharing with Radio Local Area Network (RLAN) devices in the 5 GHz band. Existing tube-based weather radars are already suffering significant interference from RLAN systems, despite the introduction of Dynamic Frequency Selection (DFS) to ensure that radars and RLAN devices could share the 5 GHz frequency band without any interference caused to the radar operation. Compared with tube transmitters, the SSTX power is much lower, leading to poorer detection performance in the RLAN device and possible decreased detection range of SSTX systems. Furthermore, there is some uncertainty on how RLAN devices will behave as the pulses transmitted by SSTX differ from the parameters of the radar test signals stored in the RLAN device. This question is of prime importance for weather radar using SSTX technology. This issue has been raised in ITU-R and study is ongoing in order to ensure the protection of the SSTX weather radar against RLAN interference in the future.

These future trends will need to be tracked and, as technologies evolve, will have an impact on any future interference mitigation strategies and protection criteria definitions.

### 4.3 Wind profiler radars (WPRs)

Wind Profiler Radars are used to obtain the vertical profiles of the wind by detecting the tiny fraction of emitted power backscattered from the atmosphere under all weather conditions, that is both in the clear as well as in the cloudy atmosphere. It needs to be stressed that no other remote sensing system for wind has this all-weather capability, which is due to the propagation properties of the rather long electromagnetic waves in the range spanning from VHF to L-band.

Figure 4-24 is a photograph of a typical fixed wind profiler radar installation.

FIGURE 4-24

**Photo of a 482 MHz wind profiler installation near Bayreuth, Germany**



Meteo-04-24

One of the major advantages of wind profilers to other wind measurement systems is their ability to continuously monitor the vertical profile of the horizontal wind field above the instrument site. In addition, they can also be used to detect precipitation, observe important features in the vertical velocity field (gravity waves and convective updrafts), assess the intensity of turbulence and measure atmospheric stability. They can also provide detailed information on the vertical profile of the atmospheric virtual temperature through the addition of a Radio Acoustic Sounding System (RASS)<sup>9</sup>.

#### 4.3.1 User requirements

Wind profiler radars are mainly used to measure the vertical wind profile at the instruments site in a 24/7 mode with a high temporal resolution. These data are important for numerical weather prediction and also for the calibration/validation of satellites (e.g. ESA Aeolus – ALADIN Doppler lidar). The main user requirement in

<sup>9</sup> RASS utilizes an acoustic source that is matched in frequency so that the wavelength of the acoustic wave is matched to half the wavelength of the radar transmitted electromagnetic wave (Bragg condition). RASS measures the speed of the acoustic wave which is dependent upon temperature. In this way RASS provides a remote measurement of the atmospheric virtual temperature.

an operational setting is a high accuracy, sufficient vertical resolution (commensurate with the typical vertical resolution of numerical weather prediction models) and a good altitude coverage.

The accuracy of the estimated wind is, among other things, depending on the availability of uncontaminated RF spectrum. As these radars are very sensitive to measure the weak returns from an optically clear atmosphere, any in-band interference is easily detrimental. While sophisticated signal processing can sometimes reduce such effects, software-based RF interference mitigation measures often lead to a reduction in altitude coverage because the sensitivity of the radar is inevitably being reduced.

The achievable altitude coverage is determined by the lowest intensity of the backscattered wave which can still be correctly analysed. The receiver signal therefore needs to have a minimal signal-to-noise ratio (SNR). The SNR depends on a number of factors which are contained in the so-called radar equation. A good way to examine the impact of user requirements upon wind profiler operating parameters and design is to consider the following simplified radar equation for clear-air scattering based on [Gossard and Strauch, 1983, their equation 12-3]:

$$SNR = \text{const} \frac{\bar{P}_t A_e \Delta z \lambda^{1/6} t_{obs}^{1/2} C_n^2}{T_{sys} z^2} \quad (4-18)$$

where:

- $\bar{P}_t$  : average transmitted power (W)
- $A_e$  : effective aperture (m<sup>2</sup>)
- $\Delta z$  : height resolution (m)
- $z$  : height (m)
- $\lambda$  : wavelength (m)
- $t_{obs}$  : observation (averaging) time (s)
- $T_{sys}$  : system noise temperature (K)
- $C_n^2$  : structure parameter of refractive index (m<sup>-2/3</sup>).

Clear-air scattering is typically generating signals with smaller SNR than scattering from precipitation particles and is therefore a more challenging situation because reliable all-weather operation requires an adequate SNR also when weak scattering conditions exist in the atmosphere. Typical situations are (wintertime) low humidity periods and cases of low turbulence, e.g. in the core of jet streams in the 10-15 km altitudes.

Equation (4-18) is only valid if the half-wavelength of the radar (the so-called Bragg wavelength) in the inertial sub-range of atmospheric turbulence lies within the inertial sub-range of fully developed turbulence, that is  $l_0 \leq \lambda/2 \leq L_0$ , where  $l_0$  denotes the inner scale (lower limit of this inertial sub-range) and  $L_0$  the outer scale of turbulence.

Indeed, the structure of atmospheric turbulence is physically limiting the usable wind profiler radar wavelength range to about 10-0.2 m (30 to 1 500 MHz). Turbulent structures of the refractive index field with size smaller than  $l_0$  are rapidly dissipated by viscosity to heat, leading to a viscous cut-off of the scattering process. For this reason, shorter wavelengths cannot be used for clear-air wind profiling due to the lack of refractive index fluctuations at scale of  $\lambda/2$ .

Furthermore, while the structure parameter of the refractive index is independent of frequency inside the relevant Bragg wavelength range bounded by the limits of the inertial sub-range, it has a strong dependence on height and varies over several orders of magnitude.

The remaining frequency dependence is mainly contained in the wavelength factor, with only the system noise temperature including a significant contribution from cosmic noise for wavelengths greater than about 1 m.

The SNR (according to equation (4-18)) can obviously be increased by using:

- large aperture antennas;
- high peak power and high pulse repetition frequency (PRF) to increase average power;
- use of pulse compression techniques;
- long wavelength;

- high receiver sensitivity and a low level of receiver noise;
- coarser height resolution (longer pulses); and
- longer averaging time.

However, such measures have always consequences for other performance parameters of the radar as well as for the cost of the instrument. Note in particular that increasing the PRF is only possible to the extent that range ambiguity problems (second trip echoes) are avoided. Since the range resolution is determined by the pulse width, there is furthermore a direct trade-off between range resolution and altitude coverage. For this reason, WPR are often operated in two modes: a low mode, using a short pulse for the best possible vertical resolution at the expense of vertical range; and a high mode, where a longer pulse with a coarser resolution is used to maximize height coverage.

### 4.3.2 Operational and frequency aspects

Large antenna aperture and high average emitted power are expensive. The cost of the antenna and power amplifier of a wind profiler radar often constitutes more than half the total cost of an installed system. Hence, technology developments in these areas are rather expensive options for improving performance.

In the case of antenna aperture, however, there is another factor to consider which establishes a minimum size. WPR operates by successively steering the main beam to different (at least three) independent directions. Earlier systems used two or four orthogonal azimuths at elevation angles of about 75° and sometimes to the vertical to acquire data. More recent antenna designs allow for much enhanced flexibility in beam steering. The antenna beamwidth must be narrow enough to delineate the multiple beam positions. 3 dB full-width beamwidths of 3° to 10° are usable and correspond to antenna gains of 36 dBi to 27 dBi, respectively. Gain determines the effective aperture through equation (4-19).

$$A_e = 10^{G/10} \lambda^2 / 4\pi \quad (4-19)$$

Because of interference and congestion in the radio-frequency spectrum and its consequent regulation, wind profiler radar frequencies cannot be freely chosen. Some demanding applications, such as the MU research radar in Japan and those at the Eastern and Western Space Launch Ranges in the USA, have resulted in the use of very large (about 10 000 m<sup>2</sup>), powerful (250 kW or more peak, 12.5 kW or more average), short pulse (1 μs) radars operating near 50 MHz. Researchers have also operated other profilers on a non-interference basis at frequencies between 40 and 70 MHz.

VHF wind profiler radars, for example in the range 46-68 MHz as per footnote RR No. **5.162A**, will provide wind profiles of up to 30 km height and as such are important component of Meteorological systems. Typical specifications of VHF wind profiler radars are:

- Maximum power of 10-80 kW and average power of less than 2 000 W.
- Antenna normally includes array of more than 100 elements that are grouped together differently for Tx and Rx mode with gain of 20-30 dBi.
- Normally vertically aligned but can rotate off-zenith of up to 20 degrees. The height resolution for VHF radars is in range 150-1 500 m depending on pulse duration as well as altitude of profile.
- Normal necessary bandwidth is 1 MHz.

Profilers operating in the range of 400-500 MHz have been designed to (see also Recommendation ITU-R M.1085):

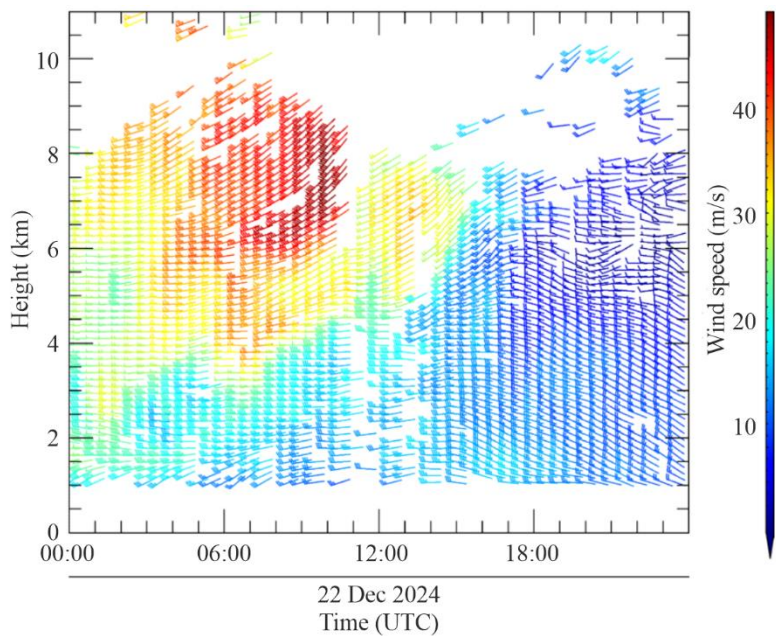
- measure wind profiles from about 0.5-16 km above the radar with vertical resolutions of 150-250 m at low altitudes and 300-1 000 m at high altitudes using antennas with typically 32-34 dBi gain;
- mean powers of about 500 W and 2 000 W when probing low and high altitudes, respectively;
- while operating with necessary bandwidths of less than 2 MHz.

Increasing the operational frequency of a wind profiler radar provides a higher degree of measurement resolution at the cost of lowering the overall height availability of the measurements. As such, profilers operating at 915 MHz and 1 270-1 375 MHz are typically regarded as boundary layer profilers, capable of measuring the wind profile in only the lowest few kilometres of the atmosphere. These perform with vertical resolution of about 100 m using antennas with gains below 30 dBi and mean powers of about 50 W while operating with necessary bandwidths of approximately 2.5 MHz.

As an example, a fixed installation 482 MHz profiling system produced the plots of wind velocity versus altitude shown in Figs 4-25 and 4-26. The orientation of each barb represents wind direction as a function of altitude (vertical axis) and time (horizontal axis), while its colour represents wind speed.

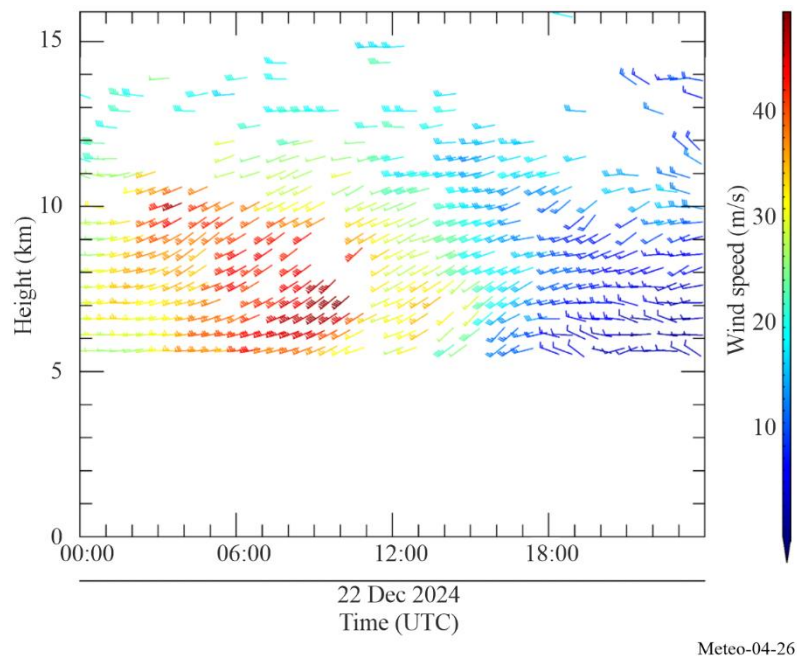
The plot in Fig. 4-25 shows data of the so-called low mode, using a short pulse width of 1 700 ns and a sampling range up to about 10.5 km. The data of the high-mode using a 4-bit 3 300 ns pulse (pulse compression using binary phase coding using complementary sequences) is given in Fig. 4-26. Note that the range sampling starts only at about 5 km height, but extends up to about 15 km.

FIGURE 4-25

**Wind velocity vs altitude – low mode (1 700 ns pulse)**

Meteo-04-25

FIGURE 4-26

**Wind velocity vs altitude – high mode (3 300 ns pulse, 4-bit phase-coded)****4.3.3 Present and future spectrum requirements**

Wind profiler radars are ground-based systems with antenna heights of 1 or 2 metres above ground and essentially vertically directed beams. Geographical separation and terrain shielding are effective protection against interference to and from other profilers. Hence, a network of wind profilers, say separated by at least 50 km over level terrain – less over more rugged or treed terrain – could operate on the same frequency. Under these rationales, profilers tend to be more easily compatible with ground-based services. However, co-existence of wind profiler radars with satellite systems could be difficult to achieve as the profiler radars are looking upward. In this scenario, sharing the same band could not be a practical solution.

It is generally agreed that for VHF wind profiler radars, a bandwidth of 0.5-1.5 MHz, for UHF system near 400 MHz a bandwidth of 2 to 3 MHz and bandwidth of 2.5 MHz for wind profiler radars near 1 000 MHz or 1 300 MHz are required. It can be assumed that provisions of Resolution **217 (Rev.WRC-23)**, as below, are sufficient to fulfil these requirements:

“... to urge administrations to implement wind profiler radars as radiolocation service systems in the following bands, having due regard to the potential for incompatibility with other services and assignments to stations in these services, thereby taking due account of the principle of geographical separation, in particular with regard to neighbouring countries, and keeping in mind the category of service of each of these services:

- 46-68 MHz in accordance with No. **5.162A**
- 440-450 MHz
- 470-494 MHz in accordance with No. **5.291A**
- 904-928 MHz in Region 2 only
- 1 270-1 295 MHz
- 1 300-1 375 MHz;”

“... that, in case compatibility between wind profiler radars and other radio applications operating in the band 440-450 MHz or 470-494 MHz cannot be achieved, the frequency bands 420-435 MHz or 438-440 MHz could be considered for use;”

#### 4.3.4 Sharing aspects of wind profilers

The bands for profiler use allocated by WRC-97 were carefully selected to minimize the likelihood of interference to and from other users of these bands. Before the identification of bands for wind profiler radars, an experimental network was developed in the band 400.15-406 MHz. Operational experience showed that operation of wind profiler radars in 400.15-406 MHz caused interference to COSPAS-SARSAT.

As a result, Resolution **217 (Rev.WRC-23)** identifies spectrum to be used for WPRs and specifically states that wind profiler radars should not be operated in the frequency band 400.15-406 MHz. The existence of this experimental network did provide considerable information on wind profiler radar compatibility with other services. The e.i.r.p. spectral density of these WPRs in the horizontal direction is about:

- –18 dB(W/kHz) at the centre frequency (449 MHz)
- –36 dB(W/kHz) 0.5 MHz away
- –55 dB(W/kHz) 1 MHz away
- –70 dB(W/kHz) 2 MHz away
- –79 dB(W/kHz) 4 MHz away.

These low values, when combined with low antenna heights and path losses proportional to  $1/r^4$  for propagation over the surface of the Earth, result in making geographical separation a very effective sharing tool.

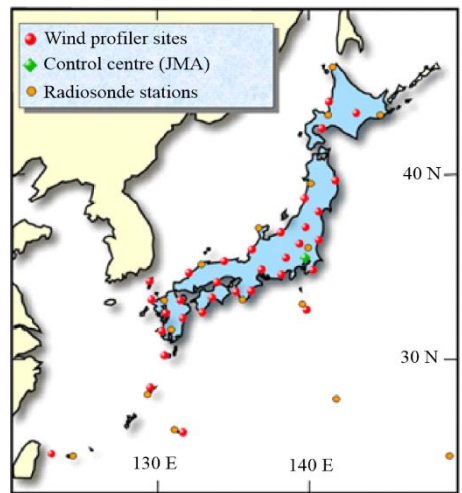
However, in the main beam, the e.i.r.p. spectral density is 57 dB greater and, as a consequence, airborne and satellite-based receivers are subjected to a much higher level of interference. Path losses proportional to  $1/r^2$  compound the problem. Subsequent efforts to alleviate the problem with WPR in the band 400.15-406 MHz showed that the modulation used by 404 MHz WPRs has a significant impact upon their sharing characteristics. Currently, the pulses are phase-coded to distinguish the two or three “chips” within each pulse so as to achieve pulse compression. Were no further coding done, the emitted spectrum would consist of lines separated by the PRF. However, one member of a 64-long pseudo-random phase code sequence was imposed on each pulse in succession so that the spectral lines appear at intervals of PRF/64 with line powers reduced by a factor of 64. In addition, the profiler transmitters were turned off under computer control whenever a COSPAS-SARSAT satellite appeared more than 41 degrees above the profiler’s horizon. (There being only a few of these satellites, these results in a negligible loss of profiler data.)

The phase coding applied to 404 MHz profiler emissions must be “undone” in the receiver. As a result, interference from other, non-WPR systems appears incoherent and noise-like to the profiler. Hence, the minimum detectable (profiler) signal is about –170 dBm, while interference is troublesome only at levels of –135 dBm or more.

As another example of sharing with WPR, the band 1 215-1 300 MHz was allocated to the radionavigation satellite service at WRC-2000. Since then, some technical studies were performed to assess compatibility between these RNSS systems and WPR’s operating in the 1 270-1 295 MHz band. Results of these studies can be found in ECC Report 90. This report concludes that RNSS systems could, under some conditions, interfere and degrade wind profiler operations, at least for three-beam WPRs. This report however lists a number of mitigation techniques (hardware or software) that could help overcome these difficulties. Some of these techniques include selection of antenna pointing, adding beams or implementing WPR frequencies at 1 274 or 1 294 MHz, at nulls of the RNSS modulations, this latter being likely the simpler one to apply.

The Japan Meteorological Agency (JMA) is operating a Wind Profiler Network and Data Acquisition System (WINDAS) network for the purpose of monitoring the development of and predicting severe weather events. The network consists of thirty-three 1.3 GHz wind profilers installed across Japan that communicate with a control centre which is located at the JMA headquarters in Tokyo (see Fig. 4-27).

FIGURE 4-27

**An example of a wind profiler radar network**

Meteo-04-27

The data is then distributed throughout the world, via the Global Telecommunication System and can also be found on the JMA website (<http://www.jma.go.jp/jma/indexe.html>). Furthermore, the data is combined with data from Doppler radars and commercial aircraft to provide a comprehensive “Upper-air wind analysis”.

#### 4.4 Oceanographic High Frequency Radar

In oceanography, High-Frequency (HF) Radar is a remote sensing technology employed for monitoring ocean surface currents, waves and wind direction. Operating in the HF radio frequency band (3-30 MHz), these radar systems extract ocean surface information through the Bragg scattering phenomena.

In this context, Bragg scattering describes the superposition of radio waves that are scattered from ocean surface waves where the ocean wavelength is half that of the radio wave. Oceanographic radars are coherent and can make use of the Doppler shift induced by the movement of the ocean surface to estimate the ocean surface velocity.

A variety of antenna types are currently used with oceanographic ocean observing radar systems. Some systems utilize either a 3-element Yagi antenna or phased-array system to sweep in the azimuthal direction using multiple sets of Yagi antenna for transmission, limiting the geography over which the oceanographic radar signal is propagated. The two main transmission techniques which are used in oceanographic radars are continuous wave (CW) pulses and linear Frequency-Modulated Continuous Wave (FMCW) chirps.

The radars are typically deployed in networks along coastlines, providing information in extended coastal zones up to 200 km from the shoreline. There are approximately 500 systems deployed globally. The systems are distributed within each of the three ITU Regions with the majority of systems along the coast of North America, Europe and Asia. It is anticipated that the number of systems will double within the next 20 years.

The ITU approved Resolution **612 (Rev.WRC-12)** at WRC-12, which provided detailed spectral space for oceanographic High Frequency radars. The frequency bands are delineated within each ITU Region and are shown in Table 4-6.

TABLE 4-6

**Frequency bands and total spectral widths allocated for oceanographic HF radars**

<b>Allocated frequency bands (kHz)</b>		
<b>ITU Region 1</b>	<b>ITU Region 2</b>	<b>ITU Region 3</b>
4 438-4 488		
5 250-5 275		
9 305-9 355	No allocation in this Region	9 305-9 355
13 450-13 550		
16 100-16 200		
24 450-24 600		
26 200-26 350		
39 000-39 500	No allocation in this Region	39 500-40 000
42 000-42 500	No allocation in this Region	No allocation in this Region

**References**

Springer Handbook of Atmospheric Measurements | SpringerLink – Chapter 31 (2021)

Cambridge University Press Atmospheric Radar (2016)

Radar for Meteorological and Atmospheric Observations | SpringerLink (2014)



## CHAPTER 5

### Passive and active spaceborne remote sensing for meteorological and related environmental activities

#### 5.1 Introduction

The existence of meteorological satellites is well known in most of the world and images produced by them are shown regularly on television, in the popular press and on the Internet. The public is nowadays used to seeing colour-augmented, map-registered images showing cloud cover, surface temperatures, snow cover and other weather phenomena, or, less frequent, images showing the distribution of wildfires and the resulting smoke clouds; volcanic ash; and the sea surface temperatures which have received wide public attention because of the *El Niño* phenomenon.

Many of these have in common the fact that they are generated primarily from data recorded using sensors in the visible and infrared regions. However, many of these products and other products are produced using a variety of microwave frequencies either in isolation or in conjunction with measurements at other frequencies.

It is therefore not widely known that spaceborne remote sensing of the Earth's surface and atmosphere, using radio frequencies, from VHF through microwaves and into the upper regions of the spectrum, has an essential and increasing importance in operational and research meteorology, in particular for mitigating the impact of weather and climate-related disasters, and in the scientific understanding, monitoring and prediction of climate change and its impacts.

The impressive progress made in the recent years in weather and climate analysis and forecasts, including warnings for dangerous weather phenomena (heavy rain, storms, cyclones) that affect all populations and economies, is to a great extent attributable to data from spaceborne observations and their assimilation in numerical models.

Remote sensing (passive and active) makes a major contribution to the performance of Numerical Weather Prediction (NWP), accounting for 50% (40% from passive sensors and another 10% from active sensors) of the improvement of forecast skills due to all observations ingested in real time models. Because of this high contribution to the improvement of forecast skills, a significant portion of the high socio-economic benefits of weather forecasting can be attributed to passive and active microwave sensors operated on meteorological and earth observation satellites.

There are two classes of spaceborne remote sensing widely employed, **passive** and **active**, that operate under the Earth exploration-satellite service (EESS) mostly on non-GSO satellites, though some planned systems of the EEES (passive) will operate in future geostationary orbit.

**Passive sensing** involves the use of pure receivers, with no transmitters involved. The radiation sought by these receivers occurs naturally, at very low power levels, and it contains essential information on the physical processes under investigation. Of interest are radiation peaks indicating the presence of specific chemicals, or the absence of radiation at certain frequencies indicating the absorption of the frequency signals by atmospheric gases. The strength or absence of signals at particular frequencies is used to determine whether specific gases (moisture and pollutants being obvious examples) are present and if so, in what quantity and at what location. A wide variety of environmental information can be sensed through passive sensors operating in frequency bands determined by the fixed physical properties (molecular radiation resonance or absorption) of the substance under examination and whose physical properties cannot be duplicated in other frequency bands. Signal strength at a given frequency may depend on several variables, making use of several frequencies necessary to match the multiple unknowns. The use of multiple frequencies is the primary technique used to measure various characteristics of the atmosphere and surface of the Earth.

**Active sensing** differs from passive sensing in that it involves both transmitters and receivers onboard a satellite. Normally the signal is transmitted and the reflected signal is received by the same satellite, though this is not always the case. The uses of active sensing include, but are not limited to, measuring the characteristics of the sea surface such as sea wave height and winds and determining the density of trees in the rain forest.

The issue of compatibility for both classes of remote sensing involves the same problems as those associated with other space services: mutual interference between the satellite receiver and other RF transmitting stations, either on the ground or in space. The resolution of these problems implies well-known techniques, typically related to coordination with other users on the basis of power limitations, antenna characteristics, and time and frequency sharing.

A form of vulnerability peculiar to passive remote sensing satellites, and particularly those having a large area measurement sample, derives from the fact that each measurement can be subjected to accumulated radiation from a multitude of emitters on the ground, both from in-band emitters and out-of-band emitters. Thus, while a single terrestrial emitter may not radiate enough power to cause errors in passive sensing measurements, a large number of these emitters may be harmful to the measurements being taken through the aggregation of those interfering signals. This aggregation of interference from multiple emitters is the basis for concerns regarding such things as high density mobile applications or broadband mobile (including International Mobile Telecommunications), high density fixed service (HDFS) emissions, ultra-wide band (UWB) applications, and short-range devices (SRD) or industrial, scientific and medical (ISM) devices. It is the spatial density of such emitters within a measurement area in combination with their individual characteristics which creates a potential problem. The situation tends to be more and more severe with the increased density of such terrestrial active devices and instances of harmful interference have already been reported.

Several geophysical parameters contribute, at varying levels, to the natural emissions of the specific parameter to be observed at a given frequency. Therefore, measurements at several frequencies in the microwave spectrum must be made simultaneously in order to isolate and to retrieve each individual contribution to the overall natural emissions, and to extract the required parameters from the given set of measurements. As a consequence, interference that impacts any of a number of “passive” frequency bands could thus have an impact on the overall measurement of a given atmospheric component obtained over a set of prescribed frequencies.

In the case of transmitter-receiver pairs, the nature and characteristics of the signal are known and it is relatively simple to determine whether the signal is being received correctly. The literature is full of useful techniques for dealing with error detection and correction in radiocommunication systems but these techniques are unfortunately of no use when the characteristics of the various received signals are unknown. This is precisely the case with passive remote sensing whose vulnerability to interference is unique because this vulnerability is caused by the non-deterministic nature of the natural signal that the passive sensor is designed to receive and the very low power level of natural radiation measured.

Even very low levels of interference received by a passive sensor may degrade its data and the biggest threat is perhaps that the interference will go undetected, that corrupted data will be mistaken for valid data and that the conclusions derived from the analysis of these corrupted data will be seriously flawed. In most cases, passive sensors are not able to discriminate between natural and man-made radiations and the resulting data errors can be neither detected nor corrected. Therefore, it appears that maintaining data integrity currently depends solely upon the prevention of interference and the use of regulatory limitations on interference and maximum emitter power on a global basis. One can note that a number of provisions in the Radio Regulations use such power limits to active service transmitters for the purpose of protecting passive sensors from in-band or out-of-band interference.

There has been considerable interest in recent years in the use of millimetre-wave cloud radars for research applications. The need for improved understanding of the role of clouds in our climate system has a very high priority in climate change research. Together with recent advancements in millimetre-wave radar technology this research need has been the driving force for development of millimetre-wave cloud profiling radars. Operating mainly near 36 GHz (Ka-band) and near 94 GHz (W-band), these radars now provide the necessary qualitative and quantitative information needed by climate researchers. Their sensitivity to small hydrometeors, high spatial resolution, minimal susceptibility to ground clutter, and their relatively small size makes the millimetre-wave radar an excellent tool for cloud research. They can be operated from fixed ground, mobile ground, airborne and space-based platforms.

## 5.2 Passive microwave radiometry sensing

Passive microwave radiometry is a tool of fundamental importance for Earth observation. Under the EESS, passive sensors operate that are designed to receive and measure natural emissions produced by the Earth's surface and its atmosphere. The frequency and the strength of these natural emissions characterize the type and the status of a number of important geophysical atmospheric and surface parameters (land, sea, and ice caps), which describe the status of the Earth/atmosphere/oceans system, and its mechanisms:

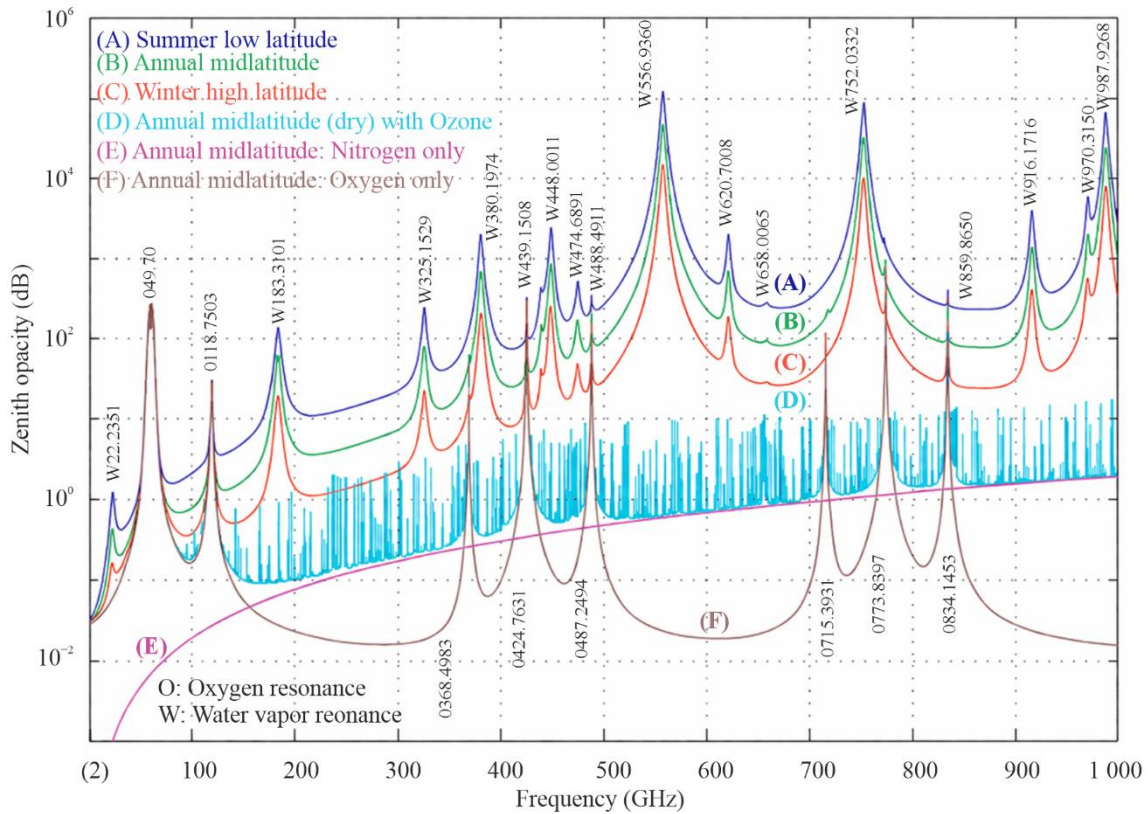
- Earth surface parameters such as soil moisture, sea surface temperature, ocean wind stress, ice extent and age, snow cover, rainfall over land; and
- three-dimensional atmospheric parameters (low, medium, and upper atmosphere) such as temperature profiles, water vapour content, and concentration profiles of radioactively and chemically important trace gases (e.g. ozone, nitrous oxide and chlorine).

Microwave techniques enable observation of the Earth's surface and its atmosphere from Earth orbit even in the presence of clouds, which are largely transparent at frequencies below 100 GHz. This all-weather capability has considerable interest for the Earth observation because more than 60% of the Earth's surface is usually covered with clouds. In addition to this all-weather capability, passive microwave measurements can also be taken at any time of day as they are not reliant on daylight. Passive microwave sensing is an important tool widely used for meteorological, climatological, and environmental monitoring and survey (operational and scientific applications), for which reliable repetitive global coverage is essential.

### 5.2.1 Spectrum requirements

Several geophysical parameters generally contribute, at varying levels, to natural emissions, which can be observed at a given frequency. Therefore, measurements at several frequencies in the microwave spectrum must be made simultaneously in order to isolate and to retrieve each individual contribution. The absorption characteristics of the atmosphere, as shown in Fig. 5-1, are characterized by absorption peaks due to the molecular resonance of atmospheric gases, and by the water vapour continuum which increases significantly with frequency. In Fig. 5-1, the zenith opacity indicates how transparent the atmosphere is to an electromagnetic wave at a specific frequency. Lower opacities indicate that a spaceborne sensor is able to image closer to the surface. Higher opacities indicate that measurements made from space will have a higher dependency on the atmospheric parameters that are causing the high opacity, which is typically oxygen or water vapor.

FIGURE 5-1

**Zenith opacity of the atmosphere due to water vapour and dry components**

Meteo-05-01

Similar charts for land and water surfaces are shown in Figs 5-2 and 5-3. These charts clearly show that each portion of the spectrum is unique in terms of sensitivity to various physical parameters. That is why passive measurements need to operate at specific frequencies in order to measure their target parameters.

The selection of the best-suited frequencies for passive microwave sensing depends heavily on the characteristics of the atmosphere:

- frequencies for observation of surface parameters are selected below 100 GHz, where atmospheric absorption is the weakest. One frequency per octave, on average, is necessary; and
- frequencies for observation of atmospheric parameters are very carefully selected mostly above 50 GHz within the absorption peaks of atmospheric gases.

The required frequencies, and bandwidths of interest below 1 000 GHz are listed in Table 5-1. Most frequency allocations above 100 GHz contain absorption lines of important atmospheric trace chemical compounds.

TABLE 5-1

## Frequency bands and bandwidths of scientific interest for satellite passive sensing below 1 000 GHz\*

Frequency band (GHz)	Bandwidth (MHz)	Main measurements
1.37-1.427	57	Soil moisture, salinity, ocean surface temperature, vegetation index
2.64-2.7	60	Ocean salinity, soil moisture, vegetation index
4.2-4.4	200	Ocean surface temperature
4.95-4.99	40	Ocean surface temperature
6.425-7.25 (RR 5.458)	350	Ocean surface temperature (no allocation)
10.6-10.7	100	Rain rate, snow water content, ice morphology, sea state, ocean wind speed
15.2-15.4	200	Water vapour, rain rate
18.6-18.8	200	Rain, sea state, ocean ice, water vapour, snow, ocean wind speed, soil emissivity and humidity
21.2-21.4	200	Water vapour, cloud liquid water
22.21-22.5	290	Water vapour, cloud liquid water
23.6-24	400	Water vapour, cloud liquid water, associated channel for atmospheric sounding
31.3-31.8	500	Sea ice, water vapour, oil spills, clouds, liquid water, surface temperature, reference window for 50-60 GHz range
36-37	1 000	Rain rate, snow, ocean ice, clouds
50.2-50.4	200	Reference window for atmospheric temperature profiling (surface temperature)
52.6-59.3	6 700 <sup>(1)</sup>	Atmospheric temperature profiling (O <sub>2</sub> absorption lines)
86-92	6 000	Clouds, oil spills, ice, snow, rain, reference window for temperature soundings near 118 GHz
100-102	2 000	N <sub>2</sub> O, NO
109.5-111.8	2 300	O <sub>3</sub>
114.25-122.25	8 000 <sup>(1)</sup>	Co, atmospheric temperature profiling (O <sub>2</sub> absorption line)
148.5-151.5	3 000	N <sub>2</sub> O, Earth surface temperature, cloud parameters, reference window for temperature soundings
164-167	3 000	N <sub>2</sub> O, cloud water and ice, rain, CO, ClO
174.8-191.8	17 000 <sup>(1)</sup>	N <sub>2</sub> O, Water vapour profiling, O <sub>3</sub>
200-209	9 000	N <sub>2</sub> O, ClO, water vapour, O <sub>3</sub>

TABLE 5-1 (end)

Frequency band (GHz)	Bandwidth (MHz)	Main measurements
226-231.5	5 500	Clouds, humidity, N <sub>2</sub> O (226.09 GHz), CO (230.54 GHz), O <sub>3</sub> (231.28 GHz), reference window
235-238	3 000	O <sub>3</sub>
239.2-242.2	3 000	Ice cloud particles
244.2-247.2	3 000	Ice cloud particles
250-252	2 000	N <sub>2</sub> O
275-286	11 000	N <sub>2</sub> O, ClO
296-306	10 000	Wing channel for temperature sounding, OXYGEN, HNO <sub>3</sub> , HOCl, N <sub>2</sub> O, O <sub>3</sub> , O <sub>17</sub> O
313-356	43 000	Water vapour profiling, cloud, Wing channel for temperature sounding HDO, ClO, HNO <sub>3</sub> , H <sub>2</sub> O, O <sub>3</sub> , HOCl, CH <sub>3</sub> Cl, O <sup>18</sup> O, CO, BrO, CH <sub>3</sub> CN, N <sub>2</sub> O, HCN
361-365	4 000	O <sub>3</sub>
369-392	23 000	Water vapour profiling, H <sub>2</sub> O
397-399	2 000	Water vapour profiling
409-411	2 000	Temperature sounding
416-434	18 000	Oxygen, temperature profiling, O <sub>2</sub>
439-467	28 000	Water vapour profiling, cloud, HNO <sub>3</sub> , H <sub>2</sub> O, O <sub>3</sub> , N <sub>2</sub> O, CO
497-502	5 000	Oxygen temperature profiling, wing channel for water vapour profiling, O <sub>2</sub> , O <sub>3</sub> , N <sub>2</sub> O, BrO
523-527	4 000	Wing channel for water vapour profiling
538-581	43 000	Water vapour profiling, ClO, H <sub>2</sub> O, O <sub>3</sub> , HNO <sub>3</sub>
611-630	19 000	Water vapour profiling, oxygen, H <sub>2</sub> O, ClO <sub>2</sub> , SO <sub>2</sub> , HNO <sub>3</sub> , BrO, CH <sub>3</sub> CN, (H <sup>37</sup> Cl), H <sub>2</sub> O <sub>2</sub> , HOCl, O <sub>3</sub> , HO <sub>2</sub> , H <sup>35</sup> Cl, CH <sub>3</sub> Cl, O <sup>18</sup> O
634-654	20 000	Wing channel for water vapour profiling, HOCl, H <sub>2</sub> <sup>18</sup> O, SO <sub>2</sub> , ClO, HO <sub>2</sub> , BrO, HNO <sub>3</sub> , O <sub>3</sub> , NO, N <sub>2</sub> O
657-692	35 000	Water vapour profiling, cloud, H <sub>2</sub> O, HO <sub>2</sub> , ClO, CH <sub>3</sub> Cl, CO
713-718	5 000	O <sub>2</sub>
729-733	4 000	HNO <sub>3</sub> , O <sup>18</sup> O
750-754	4 000	H <sub>2</sub> O
771-776	5 000	O <sub>2</sub>
823-846	23 000	O <sub>2</sub>
850-854	4 000	NO
857-862	5 000	H <sub>2</sub> O
866-882	16 000	Cloud, window
905-928	23 000	H <sub>2</sub> O
951-956	5 000	O <sub>2</sub> , NO, H <sub>2</sub> O
968-973	5 000	H <sub>2</sub> O
985-990	5 000	H <sub>2</sub> O

\* NOTE – For current information on passive sensor frequency allocations, the reader is referred to the Table of Frequency Allocations in Article 5 of the RR. For additional information on the preferred frequencies for passive sensing, the reader is referred to the most recent version of Recommendation ITU-R RS.515.

(1) This bandwidth is occupied by multiple channels.

## 5.2.2 Observation of Earth's surface features

For the measurement of surface parameters (e.g. water vapour, sea surface temperature, wind speed, rain rate), the radiometric “window” channels must be selected such that a regular sampling over the microwave spectrum from 1 GHz to 90 GHz is achieved (one frequency/octave, on average). In some cases, a highly accurate selection of frequencies is not required because natural emissions of surface parameters are not strongly frequency dependent. In general, several geophysical parameters contribute at varying levels to the natural emission, which can be observed at a given frequency. This is illustrated by Figs 5-2 and 5-3, which represent the sensitivity of natural microwave emissions to various geophysical parameters depending on frequency. Brightness temperature is a measure of the intensity of radiation thermally emitted by an object, given in units of temperature because there is a correlation between the intensity of the radiation emitted and the physical temperature of the radiating body.

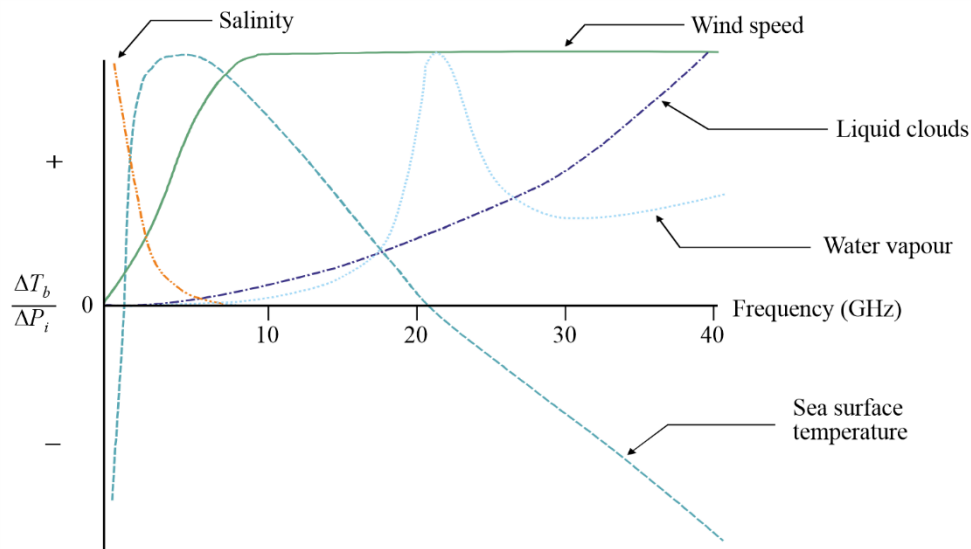
### 5.2.2.1 Observation over ocean surfaces

Remote sensing over ocean surfaces is used to measure many of the same parameters as are measured over land (e.g. water vapour, rain rate, wind speed) as well as parameters that provide information on the state of the ocean itself (e.g. sea surface temperature, ocean salinity, sea ice thickness).

Figure 5-2 shows the sensitivity of brightness temperature to geophysical parameters over ocean surfaces that:

- measurements at low frequency, typically around 1.4 GHz, give access to ocean salinity;
- measurements around 6 GHz offer the best sensitivity to sea surface temperature, but contain a small contribution due to salinity and wind speed which can be removed using measurements around 1.4 GHz and around 10 GHz;
- the 17-19 GHz region, where the signature of sea surface temperature and atmospheric water vapour is the smallest, is optimum for ocean surface emissivity, which is directly linked to the wind speed near the surface, or to the presence of sea ice. Ocean surface temperature also has some sensitivity to water vapour total content and to liquid clouds;
- total content of water vapour can be best measured around 24 GHz, while liquid clouds are obtained via measurements around 36 GHz; and
- for many applications, five frequencies (around 6 GHz, 10 GHz, 18 GHz, 24 GHz and 36 GHz) are necessary for determining the dominant ocean parameters.

FIGURE 5-2

**Sensitivity of brightness temperature to geophysical parameters over ocean surface**

Meteo-05-02

**5.2.2.2 Observation over land surfaces**

Remote sensing over land surfaces is somewhat more complex due to the high temporal and spatial variability of surface characteristics (from snow/ice covered areas to deserts and tropical rain forest). Moreover, the signal received by the passive sensor has been propagated through a number of different media: the soil, perhaps snow and/or ice, the vegetation layer, atmosphere and clouds, and occasionally rain or snow. The second factor to be taken into account is the fact that for each medium, several factors might have an influence on the emitted radiation. For instance, the soil will have a different brightness temperature depending on the actual soil temperature, soil moisture content, surface roughness, and soil texture. Similarly, the vegetation contribution will be related to the canopy temperature and structure through the opacity and single scattering albedo (i.e. the ratio of reflected to incident light). The ways that these factors affect the signal are frequency interdependent. Figure 5-3 depicts the normalized sensitivity as a function of frequency for several key parameters.

Figure 5-3 shows that over land and for an average temperate area, it is necessary to have access to:

- a low frequency to measure soil moisture (around 1 GHz);
- measurements around 5 GHz to 10 GHz to estimate vegetation biomass once the soil moisture contribution is known;
- two frequencies around the water vapour absorption peak (typically 18-19 GHz and 23-24 GHz) to assess the atmospheric contribution;
- a frequency around 37 GHz to assess cloud liquid water (with use of 18 GHz), and/or vegetation structure (with 10 GHz) surface roughness (with 1 GHz and 5 GHz or 10 GHz).

A frequency at 85 GHz or 90 GHz is useful for rainfall monitoring, but only when all the other contributing factors can be assessed with the lower frequencies.

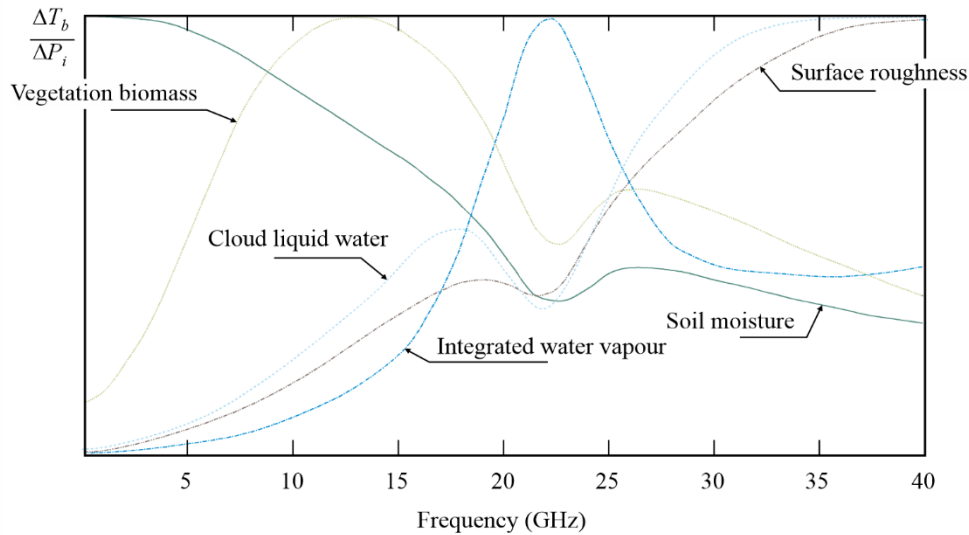
It has been shown through studies using the scanning multichannel microwave radiometer (SMMR) and the special sensor microwave/imager (SSM/I) that several other variables could be retrieved. These include surface temperature (less accurate than the infrared measurements but with all-weather capabilities) using a channel near 19 GHz when the surface and atmospheric contributions can be estimated.

Snow covered areas are important to monitor and here again the necessity for measurements over several frequencies is crucial. Actually, snow and ice must be distinguished as well as the snow freshness. The related

signal is linked to the structure of the snow layers and the crystal sizes. To retrieve such information, it has been shown that several frequencies are required, usually 19 GHz, 37 GHz and 85-90 GHz.

FIGURE 5-3

### Sensitivity of brightness temperature to geophysical parameters over land surfaces



Meteo-05-03

#### 5.2.2.3 Auxiliary parameters for other remote sensing instruments

Spaceborne radar altimeters are currently operated on a global basis above ocean and land surfaces, with important applications in oceanography and climatology (see § 5.2.3). In order to remove refraction effects due to atmosphere, the utilization of highly accurate altimetric data acquired, e.g. around 13.5 GHz, requires that they be complemented with a set of auxiliary passive measurements around 18.7 GHz, 24 GHz, and 31 or 36 GHz, and some high-frequency channels to get better measurements near coastlines.

To be able to separate the different contributions to the signals measured by a satellite, it is essential to have simultaneous access to measurements made at a minimum of five different frequencies.

#### 5.2.3 Performance parameters

Passive sensors are characterized by their radiometric sensitivity and their geometric resolution.

##### 5.2.3.1 Radiometric sensitivity

This parameter is generally expressed as the smallest temperature differential,  $\Delta T_e$  that the sensor is able to detect.  $\Delta T_e$  is given by:

$$\Delta T_e = \frac{\alpha T_s}{\sqrt{B\tau}} \quad \text{K} \quad (5-1)$$

where:

- $B$ : receiver bandwidth (Hz)
- $\tau$ : integration time (s)
- $\alpha$ : receiver system constant (depends on the configuration)
- $T_s$ : receiver system noise temperature (K).

##### 5.2.3.2 Radiometer threshold $\Delta P$

This is the smallest power change that the passive sensor is able to detect.  $\Delta P$  is given by:

$$\Delta P = k\Delta T_e B \quad W \quad (5-2)$$

where:

$$k = 1.38 \times 10^{-23} \text{ (J/K): Boltzmann's constant.}$$

$\Delta P$  above is computed using  $\Delta T_e$  and is used in determining the maximum allowable interference that a sensor can tolerate without degrading measurements. In the future,  $T_s$  will decrease as well as  $\Delta T_e$  (see equation (5-1)). Therefore, for the purpose of protecting passive sensor operations in the future,  $\Delta P$  must be computed using a reasonable foreseen  $\Delta T_e$  rather than the  $\Delta T_e$  of current technology. In the same manner, the integration time,  $\tau$ , will likely increase as remote sensing technology develops further (e.g. the so-called “push-broom” concept). Therefore, the integration time must also be chosen based on reasonable future expectations.

### 5.2.3.3 Geometric resolution

In the case of two-dimensional measurements of surface parameters, it is generally considered that the  $-3$  dB aperture of the antenna determines the transversal resolution. In the case of three-dimensional measurements of atmospheric parameters, the longitudinal resolution along the antenna axis must also be considered. This longitudinal resolution is a complex function of the frequency-dependent characteristics of the atmosphere and the noise and bandwidth performance of the receiver.

### 5.2.3.4 Integration time

Radiometric receivers sense the noise-like thermal emissions collected by the antenna and the thermal noise of the receiver. By integrating the received signal, the random noise fluctuations can be reduced, and accurate estimates can be made of the sum of the receiver noise and external thermal emission noise power. The integration time is simply the amount of time it takes the receiver to integrate the received signal. The integration time is also an important parameter for passive remote sensing, which results from a complex trade-off taking into account in particular the desired geometric resolution, the scanning configuration of the sensor, and its velocity with respect to the scene observed.

## 5.2.4 Typical operating conditions of passive sensors

Passive spaceborne sensors are deployed essentially on two complementary types of satellite systems: low earth-orbiting satellites and geostationary satellites.

### 5.2.4.1 Low Earth-orbiting satellites

Systems based on satellites in low, sun-synchronous (i.e. an orbit where the satellite passes over any given point of the Earth's surface at the same local solar time), polar orbits are used to acquire high-resolution environmental data on a global scale. The nature of such orbits limits the repeat rate of measurements. A maximum of two global coverages at 12-hour intervals are obtained daily, with a single satellite. Over the polar region, repeat observations could reach 14 times per day. This is because the low-Earth orbit satellites circle the Earth 14 times a day and the orbit paths converge over the polar regions. Passive radiometers operating at frequencies below 100 GHz are currently flown only on low-orbiting satellites. This is essentially due to the difficulty of obtaining adequate geometric resolution at relatively low frequencies from higher orbits; however, this may change in the future.

### 5.2.4.2 Geostationary satellites

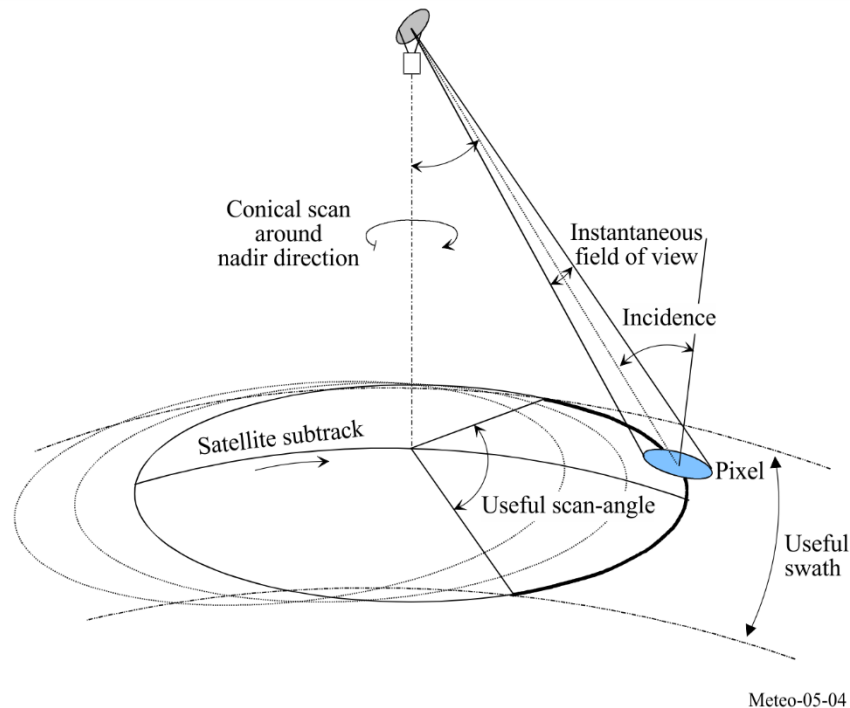
Systems involving satellites in geostationary orbit are used to gather low to medium resolution data on a regional scale. The repeat rate of measurements is limited only by hardware technology.

## 5.2.5 Observation geometries

### 5.2.5.1 Conical scan

Most passive microwave sensors designed for imaging the Earth's surface features use a conical scan configuration (see Fig. 5-4) centred on the nadir (i.e. the point directly below the satellite) direction, because it is important, for the interpretation of surface measurements, to maintain a constant ground incidence angle along the entire scan lines. The geometry of conically scanned instruments is described in Fig. 5-4.

FIGURE 5-4

**Typical geometry of conically scanned microwave radiometers**

The following are typical geometric characteristics (for 803 km altitude):

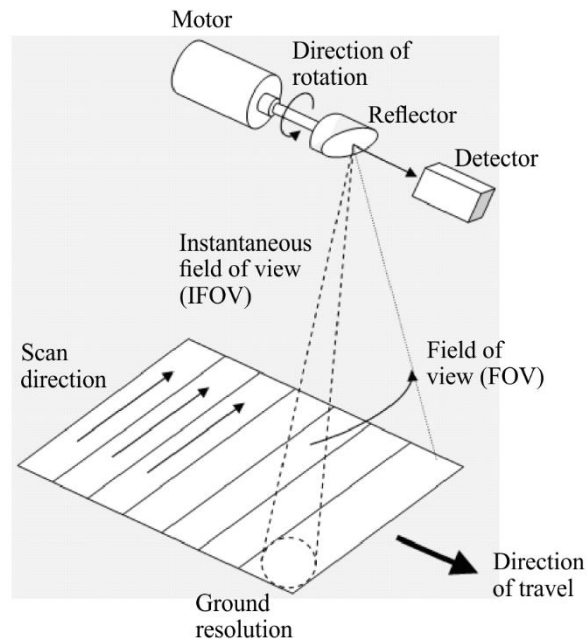
- ground incidence angle around 55 degrees;
- half-cone angle 46.7 degrees with reference to the nadir direction;
- swath width: 1 600 km (limited by the scanning configuration), enabling two complete coverage's to be achieved daily by one instrument, at medium and high latitudes;
- pixel size varies with frequency and antenna size, typically from 50 km at 6.9 GHz to 5 km at 89 GHz (based on 2 m effective antenna diameter); and
- scanning period and antenna feed arrangement are chosen in order to ensure full coverage and optimal integration time (and therefore radiometric resolution) at all measured frequencies, at the expense of hardware complexity.

### 5.2.5.2 Cross-track scan

Another common geometry for microwave radiometers is cross-track scanning. Sensors with this geometry make measurements along a direction that is perpendicular to the motion of the satellite. This is usually achieved with a rotating reflector onboard the satellite, as shown in Fig. 5-5.

Cross-track scanning allows microwave radiometers to make measurements over a wide swath while also making measurements in the nadir direction, where atmospheric path effects are minimal.

FIGURE 5-5

**Typical geometry of cross-track scanning microwave radiometers**

RS.1861-03

With this geometry, the field of view (FOV) of the sensor will have variable size on the ground depending on the look angle, i.e. the angle between the sub-satellite point and the direction of the peak antenna gain. The FOV will have its minimal size when the sensor is oriented towards the sub-satellite point.

During part of the rotation, the sensor will be pointing away from Earth. Measurements done during that portion of the rotation are used for calibration, i.e. they are used to point the sensor towards space (which is the reference cold load) and to a warm calibration load onboard the spacecraft.

Typical characteristics of a cross-track sensor are (for 830 km altitude):

- off-nadir pointing angles ranging from -50 to +50 degrees (i.e. from one side of the spacecraft to the other)
- swath width: 2 300 km
- scan period: 2-8 s
- pixel size varies along the scan as well as with frequency and antenna size.

### 5.2.5.3 Push-broom

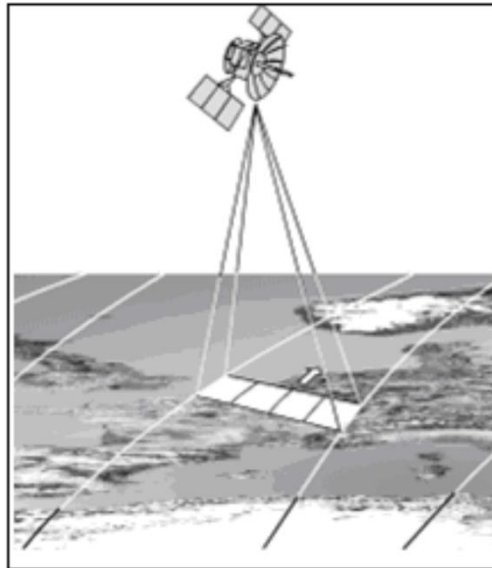
Non-scanning nadir looking instruments may also be used to provide auxiliary data for particular applications, given the removal of atmospheric effects from radar-altimeter measurements. In order to ease their accommodation on board satellites, interferometric techniques are being developed, essentially to improve spatial resolution at low frequencies. Such sensors will use fixed arrays of small antennas instead of large scanning antennas.

A “push-broom” (along track) sensor is a type of sensor system that consists of a line of sensors arranged approximately perpendicular to the flight direction of the spacecraft as illustrated in Fig. 5-6. Different areas of the surface are detected as the spacecraft flies forward. The push-broom radiometer is a purely static instrument with no moving parts. The major feature of the push-broom radiometer is that all of the pixels in a scan line are acquired simultaneously and not sequentially as with mechanically scanned sensors, enabling this type of sensor to significantly increase the achievable radiometric resolution; however, the absence of a scanning mechanism makes it more difficult to image over large swaths with fine geometric resolution.

Push-broom sensors can be used for a variety of applications including measurements of temperature profiles of the atmosphere, soil moisture and ocean salinity.

FIGURE 5-6

### Typical geometry of push-broom passive microwave radiometers



Meteo-05-06

The types of measurements for EESS (passive) applications are provided in Recommendation ITU-R RS.1861.

### 5.2.6 Performance and interference criteria

The performance and interference criteria for spaceborne passive sensors operating in the EESS are contained in Recommendation ITU-R RS.2017.

### 5.2.7 Three-dimensional measurement of atmospheric parameters

The electromagnetic spectrum contains many frequency bands where, due to molecular resonances, absorption mechanisms by certain atmospheric gases are taking place (see Fig. 5-1). Frequencies at which such phenomena occur characterize the gas (e.g. O<sub>2</sub>, O<sub>3</sub>, H<sub>2</sub>O, ClO). The absorption coefficient depends on the nature of the gas, on its concentration, and on its temperature. Combination of passive measurements around these frequencies can be performed from spaceborne platforms to retrieve temperature, water vapor, and/or concentration profiles of absorbing gas. Of particular significance to passive remote sensors operating below 200 GHz are the oxygen resonance frequencies between 50 GHz and 70 GHz, at 118.75 GHz, and the water vapour resonance frequency at 183.31 GHz.

Absorbing gas at wavelength  $\lambda$  radiates energy (at the same frequency) at a level that is proportional to its temperature  $T$  and to its absorption ratio  $\alpha = f(\lambda)$ . This is governed by the relationship given in equation (5-3):

$$l = \alpha \cdot L \quad (5-3)$$

where:

$l$ : spectral brightness of the gas at temperature  $T$

$L = 2 \cdot k \cdot T/\lambda^2$ : spectral brightness of the black body at  $T$  (W/(m<sup>2</sup> · sr · Hz))

$k = 1.38 \times 10^{-23}$ : Boltzman's constant (J/K)

$\alpha$ : characterizes the gas (O<sub>2</sub>, CO<sub>2</sub>, H<sub>2</sub>O, O<sub>3</sub>, etc.).

Two atmospheric gases, CO<sub>2</sub> and O<sub>2</sub>, play a predominant role in passive sensing for meteorology because their concentration and pressure in the atmosphere (two parameters which determine the absorption ratio  $\alpha$ ) are almost constant and known all around the globe. It is therefore possible to retrieve atmospheric temperature profiles from radiometric measurements at various frequencies in the appropriate absorption bands (typically in the infrared region around 15  $\mu\text{m}$  for CO<sub>2</sub>, and in the microwave region around 60 GHz and 118.75 GHz for O<sub>2</sub>).

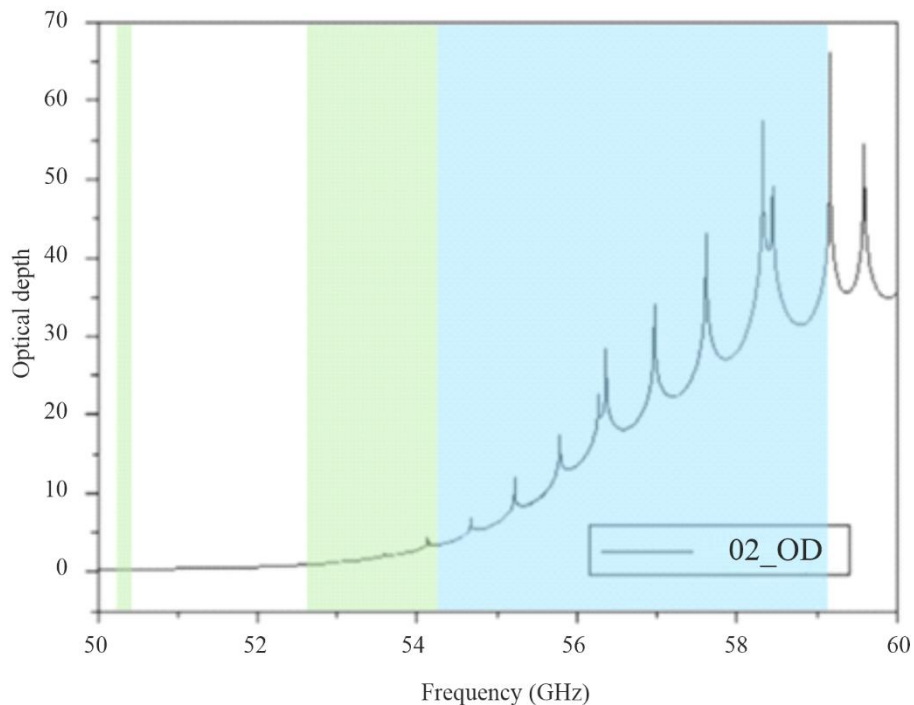
Radiometric measurements in the specific absorption bands of other radioactively and chemically important atmospheric gases of variable and unknown concentration (H<sub>2</sub>O, O<sub>3</sub>, CH<sub>4</sub>, ClO, etc.) are also collected. But in this case, the knowledge of atmospheric temperature profiles is mandatory in order to retrieve the unknown vertical concentration profiles of these gases.

### 5.2.7.1 Passive microwave atmospheric vertical sounders

Atmospheric sounding is a measurement of vertical distribution of physical properties of a column of the atmosphere such as pressure, temperature, wind speed, wind direction, liquid water content, ozone concentration, pollution, and other properties. Vertical atmospheric sounders (i.e. instruments that take atmospheric sounding measurements) are nadir-looking sensors, which are used essentially to retrieve vertical atmospheric temperature and humidity profiles. They use frequency channels carefully selected within the absorption spectra of atmospheric O<sub>2</sub> and H<sub>2</sub>O. Detailed absorption spectra in the vicinity of their main resonance frequencies below 200 GHz are shown in Figs 5-7 to 5-9. Note the very important variability of the water vapour absorption spectrum around 183 GHz, depending on climatic zone and on local weather conditions.

FIGURE 5-7

#### O<sub>2</sub> optical depth between 50 and 60 GHz (multiple absorption lines)

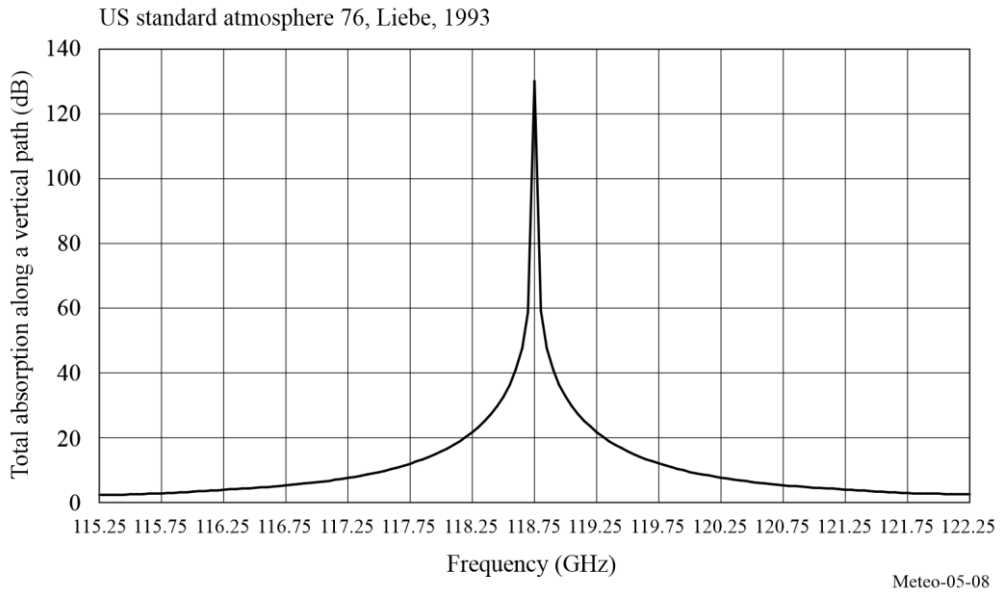


Meteo-05-07

NOTE – Figure 5-7 also depicts the position and the EESS allocations and their status between 50 and 60 GHz (50.2-50.4 GHz (exclusive), 52.6-54.25 GHz (exclusive) and 54.25-59.3 GHz (shared)).

FIGURE 5-8

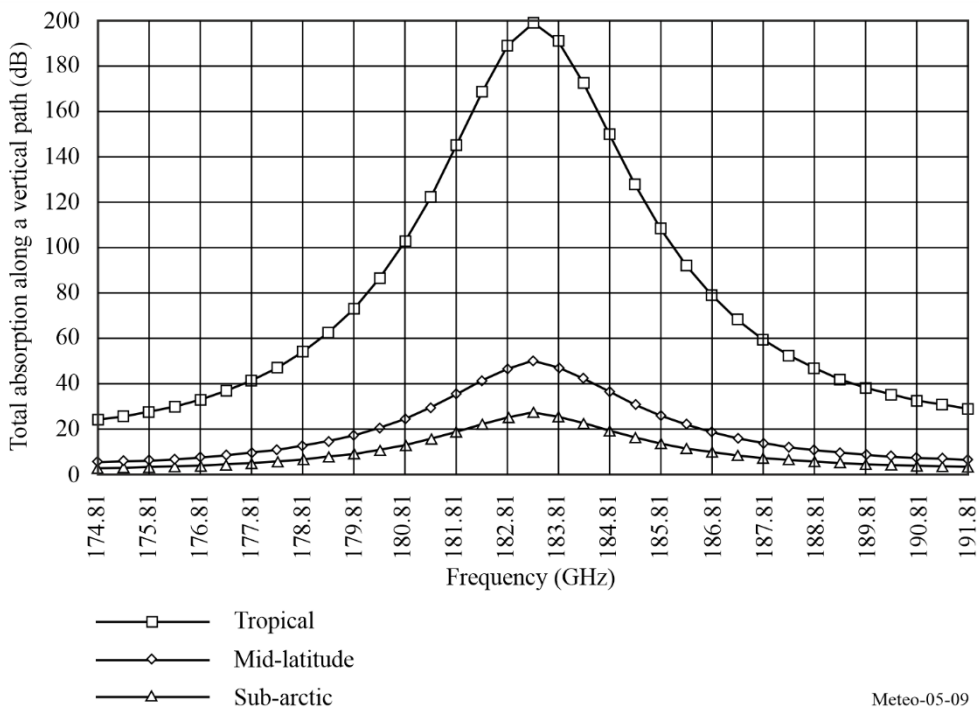
**O<sub>2</sub> absorption spectrum along a vertical path around 118.75 GHz  
(one unique absorption line)**



NOTE – The EESS (passive) has allocations at 114.25-116 GHz (exclusive) and at 116-122.25 GHz (shared).

FIGURE 5-9

**Water vapour absorption spectrum along a vertical path around 183.31 GHz**



NOTE – The EESS (passive) has allocations at: 174.8-182 GHz (shared), 182-185 GHz (exclusive), 185-190 GHz (shared) and at 190-191.8 GHz (exclusive).

### 5.2.7.2 Mechanism of vertical atmospheric sounding

In the case of vertical atmospheric sounding from space, the radiometer measures at various frequencies (infrared (IR) or microwave) the total contribution of the atmosphere from the surface to the top.

Each layer (characterized by its altitude) radiates energy proportionally to its local temperature and absorption ratio. The upward energy from the surface and lower layers (in the direction of the radiometer) is partly absorbed by the upper layers.

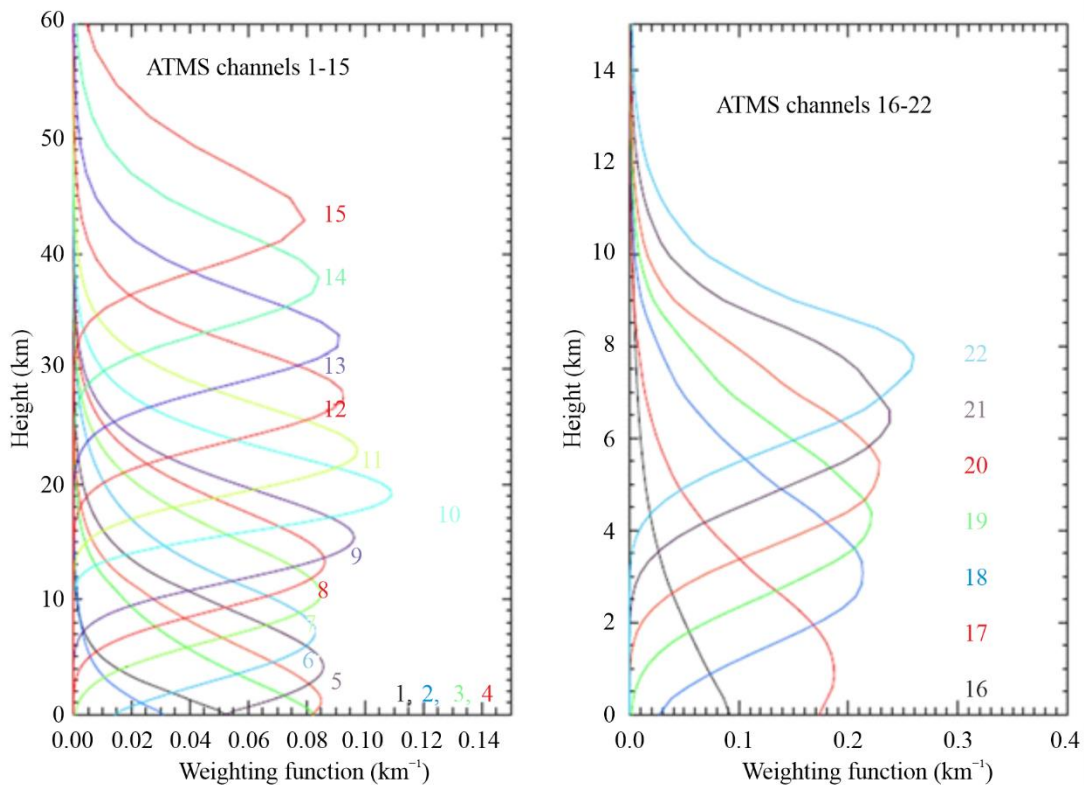
Integration of the radiative transfer equation along the path from Earth's surface to the satellite reflects this mechanism, and results in a weighting function which describes the relative contribution of each atmospheric layer, depending on its altitude, and represents also the longitudinal (vertical) resolution of the sensor.

The peak of the weighting function may occur at any altitude, and depends on the absorption ratio at the frequency considered. At a frequency where the absorption is low, the peak is near the earth's surface. At a frequency where the absorption is high, the peak is near the top of the atmosphere. A sounder incorporates several frequency channels (see Fig. 5-10 for example). They are extremely carefully selected within the absorption band, covering a wide range of absorption levels in order to obtain the best atmospheric samples from the surface up to stratospheric altitudes.

Typical weighting functions for a microwave temperature sounder operating in the 60 GHz band are shown in Fig. 5-10.

FIGURE 5-10

#### Typical weighting functions for a microwave temperature sounder operating near 60 GHz



In addition, the particular importance of Channels 1 (23.8 GHz), 2 (31.5 GHz), and 15 (90 GHz) (not shown in Fig. 5-10 above) is to be highlighted. These are auxiliary channels, which play a predominant role in the retrieval process of measurements performed in the O<sub>2</sub> absorption spectrum. As such, they must have similar geometric and radiometric performances and must receive similar protection against interference.

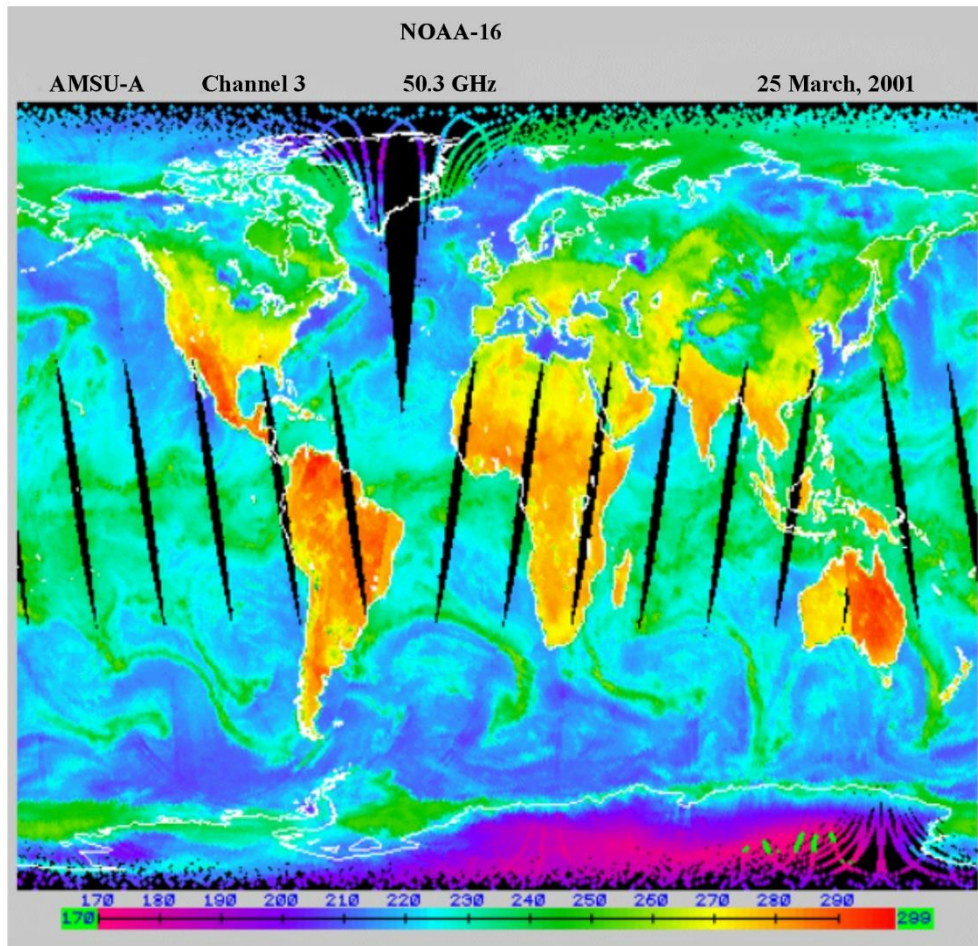
- Channel 1 is close to a H<sub>2</sub>O absorption peak. It is used to retrieve the total water vapour content along the line of sight, and to determine the corrections, which are necessary in the other channels.
- Channel 2 has the lowest cumulated effects due to oxygen and water vapour. It is the optimum window channel to see the Earth's surface, and is the reference for the other channels.
- Channel 15 can detect atmospheric liquid water and is used to decontaminate the measurements performed in the other channels from the effects of precipitation.

### **5.2.7.3 Utilization of vertical atmospheric sounding**

The vertical temperature and humidity profiles are essentially used as inputs to the NWP models, which need to be initialized at least every 6 h. Global NWP (worldwide) models are used to produce a 5-to-10-day weather forecast with a geographical resolution of around 10 km. Also, in increasing numbers, there are regional/local models for a fine mesh prediction (few km) on a short-range basis (6 to 48 h). Figure 5-11 shows the global composite of temperature (K) measurements from the AMSU-A passive microwave sensor, containing measurements produced in a time period of about 12 h. The observations include emission and reflection from the surface plus emission from oxygen mostly in the first 5 km above the surface (see Fig. 5-10).

FIGURE 5-11

## Global composite of temperature (K) measurements from AMSU-A

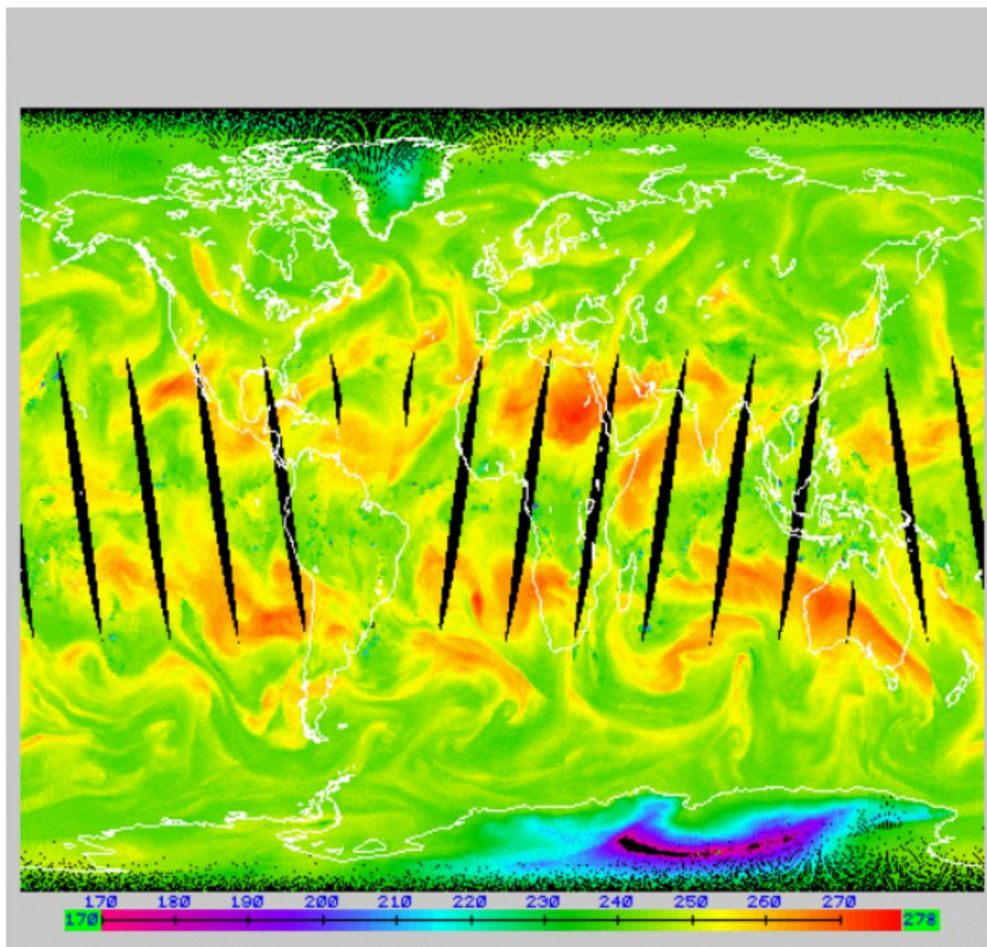


Meteo-05-11

Figure 5-12 shows the global composite of temperature (K) measurements from AMSU-B. It contains measurements produced in a time period of about 12 h. AMSU-B is a radiometer operated together with AMSU-A to improve the sensing of tropospheric water vapour. At 183 GHz, the radiometer observes high temperature (orange/red colouring) in the tropics and midlatitudes when the upper parts of the troposphere are dry and the sensor observes nearer the surface, and low brightness temperatures (green) where humidity is high and the radiation originates from higher levels.

The NWP models use partial differential Navier-Stokes equations. Because they simulate highly unstable atmospheric mechanisms, they are extremely sensitive to the quality of the initial three-dimensional profiling. This problem has been described by Lorenz and is now clearly explained by the “chaos theory”. To run NWP models, the most powerful super computers are needed.

FIGURE 5-12

**Global composite of temperature (K) measurements from AMSU-B**

Meteo-05-12

In order to increase the effectiveness of NWP, the models need to be initialised at least every six hours on a worldwide basis and at a resolution of 50 km for global NWP and 10 km for regional/local NWP. In the future, it will be necessary to get information to allow initialization of the NWP models approximately every three hours.

The microwave sounder observations also play a vital role in monitoring long-term climate change. The Microwave Sounding Unit (MSU), AMSU-A, and Advanced Technology Microwave Sounder (ATMS) provided continuous atmospheric temperature observations with similar channel frequencies from 1978 to the present. Scientists have merged observations from the three generations of microwave sounders to construct long-term climate data records of channel-based atmospheric layer temperatures from the lower-troposphere to the upper stratosphere. With their unique feature of global coverage, the climate data records are broadly used for climate change assessment during the satellite era. The climate data records provided quantitative estimates of global warming rate in the troposphere and global cooling rate in the stratosphere. As these microwave sounder observations become longer, the climate data records are becoming an essential dataset for investigating global climate change and for validating climate model simulations. This is a critical step for building confidence in climate model simulations to use them for predictions of future climate change.

#### **5.2.7.4 Characteristics of nadir-looking passive sensors operating in the 60 GHz range**

Most passive microwave sensors designed for measuring tropospheric/stratospheric parameters, are nadir-looking instruments. They use a cross-track mechanical (current) or push-broom (future) scanning configuration in a plane normal to the satellite velocity containing the nadir direction. This configuration

provides optimum field-of-view (FOV) and optimum average quality of data. Typical characteristics of temperature sounders working around 60 GHz and operated on board low Earth orbiting satellites are given in Table 5-2.

TABLE 5-2

**Typical characteristics of microwave vertical sounders in the 60 GHz frequency range**

Characteristic	Mechanical scanning (current)	Push-broom scanning (future)
Channel bandwidth (MHz)	400	15
Integration time (s)	0.2	2.45
Antenna diameter (cm)	15	45
3 dB points IFOV (degrees)	3.3	1.1
Cross-track FOV (degrees)	±50	±50
Antenna gain (dBi)	36	45
Far lobes gain (dBi)	-10	-10
Beam efficiency (%)	> 95	> 95
Radiometric resolution (K)	0.3	0.1
Swath-width (km)	2 300	2 300
Nadir pixel size (km)	49	16
Number of pixels/line	30	90

### 5.2.7.5 Passive microwave limb sounders

Microwave limb sounders (MLSs), which observe the atmosphere in directions tangential to the atmospheric layers, are used to study low to upper atmosphere regions, where the intense photochemistry activities may have a heavy impact on the Earth's climate. Major features of tangential limb emission measurements are the following:

- the longest path is used, which maximizes signals from low-concentration atmospheric minor constituents, and renders possible soundings at high altitudes;
- the vertical resolution is determined by the radiative transfer through the atmosphere and by the vertical field of view of the antenna. A typical example is shown in Fig. 5-13;
- the horizontal resolution normal to the line of sight is determined principally by the horizontal field of view of the antenna and the smearing due to the satellite motion;
- the horizontal resolution along the line of sight is principally determined by the radiative transfer through the atmosphere;
- the space background is optimum for calibration of emission measurements; and
- limb measurements are extremely vulnerable to interference caused by inter-satellite links.

Microwave limb sounders were first launched in 1991, and perform the following functions:

- scan the atmosphere vertically in the 15-120 km altitude range, in two side-looking orthogonal directions;
- typical vertical resolution for profile measurements (weighting functions width at half value) is about 3 to 6 km, as shown on Fig. 5-13;
- typical horizontal resolution is 30 km across and 300 km along the direction of observation;
- complete profiles are obtained in less than 50 s; and
- observes thermal limb emission in five microwave spectral regions (see Table 5-3).

FIGURE 5-13

Microwave limb sounding vertical weighting functions (based on a 1.6 m antenna at a 600 km altitude)

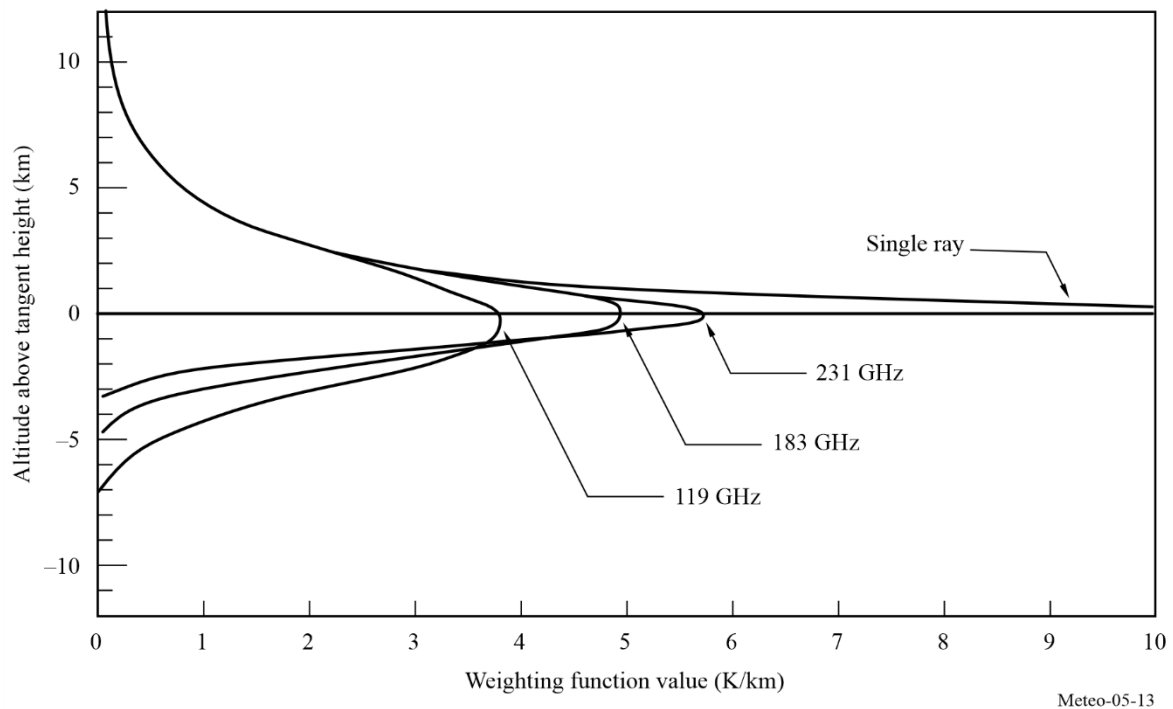


TABLE 5-3

Example measurement objectives of typical microwave limb sounders and spectral regions

Geophysical parameter	Spectral region (GHz)	Altitude (km)	Root mean square noise (interval time)
Atmospheric pressure	50-60	3 070	1% (2 s)
Wind velocity	119	70 110	2-10 m/s (10 s)
Temperature		20 100	0.53 K (2 s)
O <sub>2</sub>		80 120	$3 \times 10^{-3}$ v/v (2 s)
Magnetic field		80 110	0.3-1 m Gauss (10 s)
H <sub>2</sub> O		183	1 590
ClO	205	2 040	$2 \times 10^{-10}$ v/v (10 s)
O <sub>3</sub>		1 590	$1 \times 10^{-8}$ v/v (2 s)
H <sub>2</sub> O <sub>2</sub>		2 050	$9 \times 10^{-10}$ v/v (10 s)
O <sub>3</sub>	231	1 590	$1 \times 10^{-8}$ v/v (2 s)
CO		15 100	$1 \times 10^{-7}$ v/v (10 s)

The new generation of microwave limb sounders measure lower stratospheric temperature and concentrations of H<sub>2</sub>O, O<sub>3</sub>, ClO, BrO, HCl, OH, HO<sub>2</sub>, HNO<sub>3</sub>, HCN, and N<sub>2</sub>O, for their effects on, and diagnoses of, ozone depletion, transformations of greenhouse gases, and radiative forcing of climate change. MLS also measures upper tropospheric H<sub>2</sub>O, O<sub>3</sub>, CO, and HCN for their effects on radiative forcing of climate change and for diagnoses of exchange between the troposphere and stratosphere.

Microwave limb sounders observe the details of ozone chemistry by measuring many radicals, reservoirs and source gases in chemical cycles that destroy ozone. This set of measurements will provide stringent tests on

understanding of global stratospheric chemistry, will help explain observed trends in ozone, and can provide early warnings of any changes in the chemistry of this region.

The original microwave limb sounders demonstrated the capability of measuring upper tropospheric water vapour profiles. This knowledge is essential for understanding climate variability and global warming but which previously has been extremely difficult to observe reliably on a global scale.

Future microwave limb sounders may observe additional atmospheric chemistry components and species at other frequencies.

#### 5.2.7.6 Vulnerability to interference of passive microwave sounders

Passive sensors integrate all natural (wanted) and man-made (unwanted) emissions. They cannot, in general, differentiate between these two types of signals because the atmosphere is a highly unstable medium with rapidly changing characteristics, both spatially and temporally. A particular problem for passive sensors is the presence of large numbers of low power emitters within the sensor's measurement area. Among such low power emitters are UWB devices, industrial, scientific and medical (ISM) applications and short-range devices (SRD). The situation tends to be more and more critical with the increased density of such terrestrial active devices and instances of harmful interference have already been reported.

The passive sensor measurements are therefore extremely vulnerable to interference, even at very low power levels, which may have very serious detrimental consequences:

- It has been demonstrated that as few as 0.1% of contaminated satellite data samples could be sufficient to generate unacceptable errors in numerical weather prediction forecasts, thus destroying confidence in these unique all weather passive measurements.
- The systematic deletion of data where interference is likely to occur (should it be detectable) may cause vital indications of rapidly developing potentially dangerous storms may to be missed and render impossible the realization of new developing weather systems.
- If interference is at a low enough power level that it is not detected, which is more than likely, corrupted data will be mistaken for valid data and the conclusions derived from the analysis incorporating these corrupted data will be seriously flawed.
- For climatological studies and particularly for “global change” monitoring, interference may lead to misinterpretation of climate signals.

Recommendation ITU-R RS.2017 provides the required radiometric performance and the permissible interference level under which the required performance can be met.

#### 5.2.8 Cold sky calibration

In order to calibrate their measurements, EESS (passive) instruments need known hot and cold targets. The hot load is typically included within the instrument itself. For the cold load, the instrument takes measurements of outer space, i.e. pointing towards portions of the sky that do not include the Earth (or other near celestial bodies such as the Sun or the Moon).

The way measurements of outer space are made depends on the type of EESS (passive) sensor:

- Push-broom sensors are rotated so that the whole satellite points towards outer space;
- Cross-track scanning sensors have a portion of the scan dedicated to views of the cold sky, typically near 90 degrees off-nadir angle;
- Conical scanning sensors take cold calibration measurements by either rotating the entire satellite so that a portion of the scan is pointed away from Earth, or by using a different reflector during part of the conical scan;
- Nadir-pointing sensors have sometimes a different feedhorn pointing at outer space for the cold sky calibration measurements; in other cases, the entire satellite is rotated to point at outer space.

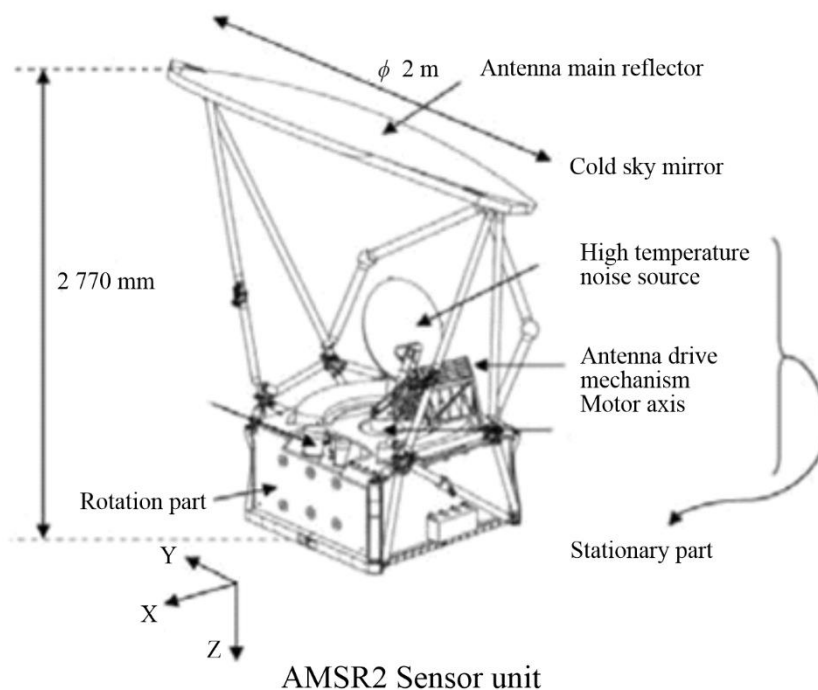
As an example, the text below describes in some detail the cold sky calibration and the high-temperature calibration for the AMSR2's instrument onboard the GCOM-W satellite.

AMSR2 consists of a sensor unit (see Fig. 5-14) — essentially a rotating scanner — and a fixed control unit as well as a momentum wheel system carried by the satellite mission chassis. During one rotation, the sensor collects surface observation data over a  $\pm 75^\circ$  (the performance guarantee range is  $\pm 61^\circ$ ) degree range centred on the flight direction and calibrator data (from a high-temperature noise source and a cold sky mirror) at all other angles.

AMSR2 collects low-temperature and high-temperature calibration data each 1.5-second scanning cycle that is used to correct receiver gain fluctuations.

The high-temperature noise source is a microwave absorber (called high-temperature noise source, HTS) which is temperature-controlled to about 300 K, and the cold sky mirror (CSM) is a reflector oriented toward deep space (approximately 2.7 K). The data obtained from these two measurements are used for two-point calibration purposes. The scanning rotational speed must be kept constant to collect in sequence low-temperature calibration data, surface observation data, and high-temperature calibration data at the correct rotational angles.

FIGURE 5-14

**Exterior schematic of AMSR2**

Meteo-05-14

However, the brightness temperature measured during the cold sky views rises above the nominal temperature of 2.7 K due to the effect of receiving radiation other than deep space background radiation. There are many error factors affecting the low-temperature calibration brightness temperature: Earth radiation, moon radiation, radio frequency interference from stationary satellites, solar contamination, radiation from the satellite structure itself, and Earth radiation projecting on the main reflector. The largest of these are Earth radiation, moon radiation, radio frequency interference and solar effects.

Also, the high-temperature calibration brightness temperature may contain errors, due to HTS non-uniformities or discrepancies with the platinum sensor measurement temperature.

These errors are corrected in the processing sequence for calculating radiometric data.

- 1) Identifying and averaging equal gain/offset points

Identify the range in which low-temperature and high-temperature correction data have been obtained at the same auto gain control (AGC) level (gain and offset) and average the calibration data obtained at equal gain levels. Data obtained at differing gains and offsets are not averaged.

2) Correct the high-temperature noise source/cold sky mirror

The following corrections are made to the high-temperature noise source's temperature and the cold sky mirror's count value.

- a) Correct the high-temperature noise source's temperature (using a correction algorithm).
  - b) Correct the cold sky mirror's temperature (eliminate the effects of the moon, Earth emissions, RFI, and sunlight).
- 3) Calculating the antenna temperature conversion coefficients at all frequencies

The first-order calibration equation coefficients ( $A$ ,  $B$ ) are calculated in order to convert the observation count value ( $C_{obs}$ ) to an antenna temperature ( $T_A$ )

$$T_A = A \times C_{obs} + B \quad (5-4)$$

It should be noted that, while this process can correct for the known error sources (e.g. the position and intensity of the Sun are well-known), it cannot correct for the impact of interference, which is dynamic and unknown in general.

## 5.3 Active sensors

### 5.3.1 Introduction

The purpose of this section is to describe the radio spectrum frequency needs of the spaceborne active sensors, and in particular, those sensors used in the monitoring of meteorological phenomena. The intent is to present the unique types of sensors and their characteristics which determine their individual frequency needs; to present performance and interference criteria necessary for compatibility studies with other services in the frequency bands of interest and to present the status of current compatibility studies of spaceborne active sensors and other services, along with any issues or concerns.

There are six key active spaceborne sensor types addressed in this Handbook:

*Type 1: Synthetic aperture radars (SAR)* – Sensors looking to one side of the nadir track, collecting a phase and time history of the coherent radar echo from which typically can be produced a radar image of the Earth's surface.

*Type 2: Altimeters* – Sensors looking at nadir, measuring the precise time between a transmit event and receive event, to extract the precise altitude of the Earth's ocean surface, including coastal and inland waters.

*Type 3: Scatterometers* – Sensors looking at various aspects to the sides of the nadir track, using the measurement of the return echo power variation with aspect angle to determine the wind direction and speed on the Earth's ocean surface, including coastal and inland waters. Backscatter is also used to look at all land surfaces, providing Earth's surface conditions such as soil moisture and rain over land.

*Type 4: Precipitation radars* – Sensors scanning perpendicular to nadir track, measuring the radar echo from rainfall, to determine the rainfall rate over the Earth's surface and three-dimensional structure of rainfall.

*Type 5: Cloud profile radars* – Sensors looking at nadir, measuring the radar echo return from clouds, to determine the cloud reflectivity profile over the Earth's surface.

*Type 6: Radar sounders* – Sensors looking at nadir employing lower centre frequencies for ground-penetrating radar (GPR) applications, which measure the radar return from the Earth's surface and subsurface to identify and characterize underground features such as aquifers and ice sheets.

The characteristics of the six key types of active spaceborne sensors are summarized in Table 5-4.

TABLE 5-4

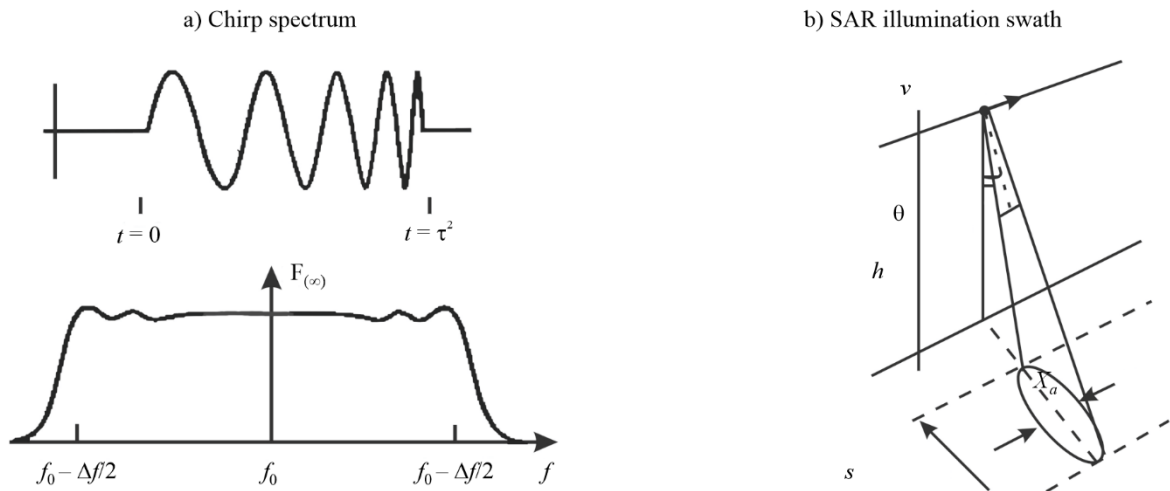
## Active spaceborne sensor characteristics

Sensor types						
Characteristics	SARs	Altimeters	Scatterometers	Precipitation radars	Cloud profile radars	Radar sounders
Viewing geometry	Side-looking at 10°-55° off nadir	Nadir-looking Multi incidence looking	– Three/six fan beams in azimuth – One or more conically scanning beams	Scanning across-track around Nadir-	Nadir-looking	Nadir-looking
Footprint/dynamics	– Fixed to one side – ScanSAR – Spotlight	Fixed at nadir Multi incidence looking	– Fixed in azimuth – Multiple conically scanning beams	Scanning across nadir track	Fixed at nadir	Fixed at nadir
Antenna beam	Fan beam	Pencil beam	– Fan beams – Pencil beams	Pencil beam	Pencil beam	Wide beam
Radiated peak power (W)	1 500-8 000	20	100-5 000	600	1 000-1 500	100
Waveform	Linear FM pulses	Linear FM pulses	Interrupted CW or short pulses (ocean) or linear FM pulses (land)	Short pulses	Short pulses	Linear Fm pulses
Bandwidth	20-1 200 MHz	320/500 MHz	5-80 kHz (ocean) or 1-4 MHz (land)	14 MHz	300 kHz	10 MHz
Duty factor (%)	1-30	46	31 (ocean) or 10 (land)	0.9	1-14	10.2
Service area	Land/coastal/ocean	Ocean/ice/coastal/ Inland water	Ocean/ice/land/coastal	Land/ocean	Land/ocean	Ice sheets/deserts
Typical frequency bands	1.3 GHz, 5 GHz, 9 GHz and 36 GHz	5 GHz, 13 GHz and 36 GHz	1.3 GHz, 5 GHz and 13 GHz	36 GHz and 78 GHz	94 GHz, 138 GHz and 238 GHz	45 MHz

### 5.3.2 Synthetic aperture radars (SARs)

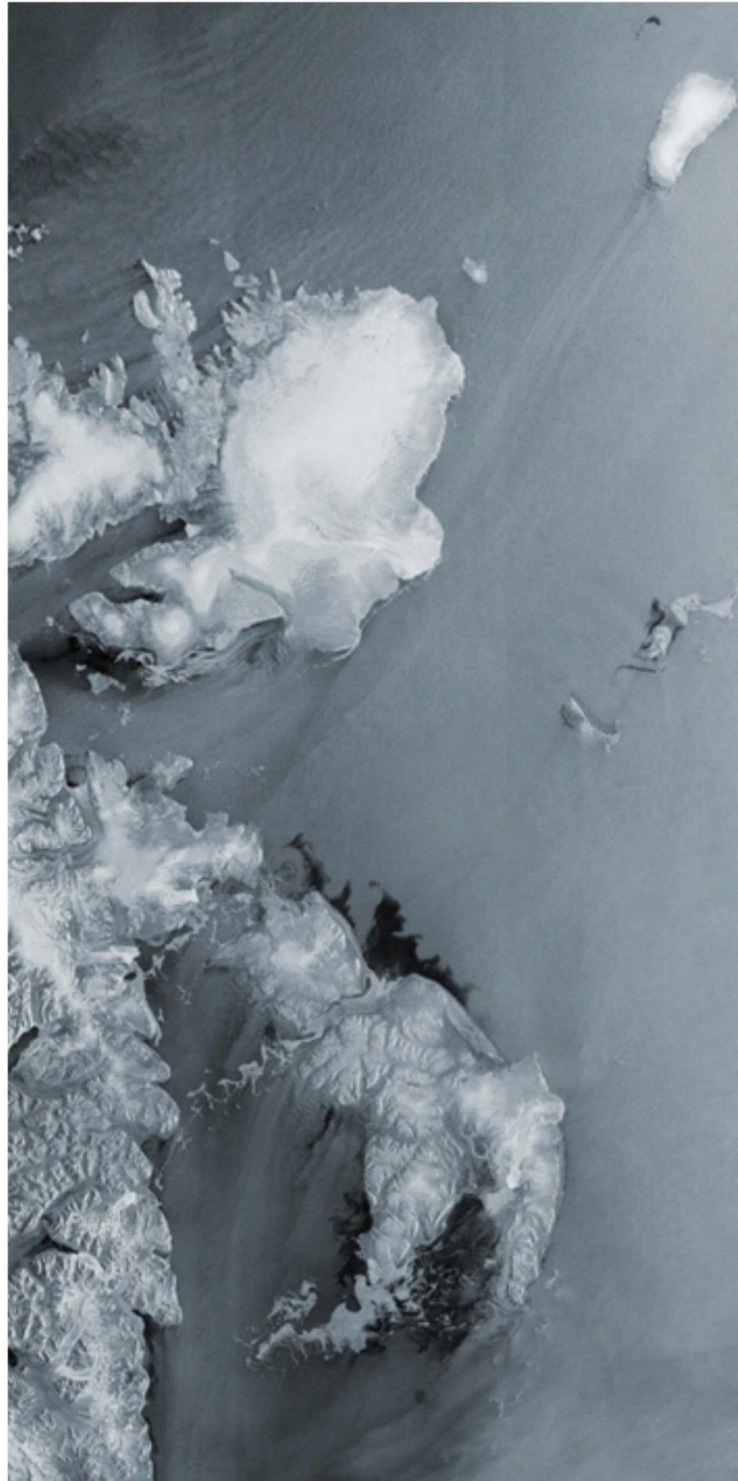
SARs provide radar images of the Earth's surface. The choice of RF centre frequency depends on the Earth's surface interaction with the EM field. The RF bandwidth affects the resolution of the image. In Fig. 5-15 a), the chirp pulse is shown, and the corresponding RF bandwidth is shown below. The range resolution is equal to  $c/2/(BW \sin \theta)$ , where  $c$  is the velocity of light,  $BW$  is the RF bandwidth, and  $\theta$  is the incidence angle. To obtain 1 m range resolution at 30° incidence angle, for instance, the RF bandwidth should be 300 MHz. Many SARs illuminate the swath off to one side of the velocity vector as shown in Fig. 5-15 b). Any interference sources within the illuminated swath area will be returned to the SAR receiver and degrade the image pixel quality. The allowable image pixel quality degradation determines the allowable interference level. Figure 5-16 shows a SAR image taken of the Dead Sea between Israel and Jordan.

FIGURE 5-15

**Chirp spectrum and SAR illumination swath**

Meteo-05-15

FIGURE 5-16  
SAR image of Svalbard, Norway



Meteo-05-16

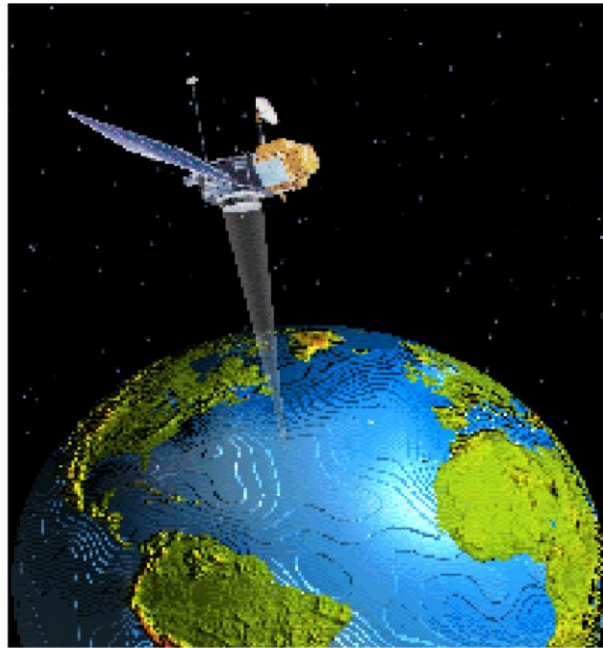
### 5.3.3 Altimeters

Altimeters provide measurements of the altitude of the Earth's surface, and are typically used over the ocean. Figures 5-17 and 5-18 are an illustration of a satellite altimeter and its typical measurement accuracy. The choice of RF centre frequency depends on the ocean surface interaction with the EM field. Dual frequency operation allows ionospheric delay compensation. For instance, the use of frequencies around 13.6 GHz and

5.3 GHz illustrates one possible dual frequency arrangement. The wide RF bandwidth affects the height measurement accuracy. The time difference accuracy  $\Delta t$  is inversely proportional to BW, where BW is the RF bandwidth. The allowable height accuracy degradation determines the allowable interference level. Some satellite altimeters have measured ocean topography to an accuracy of better than 2 cm. The allowable performance degradation prescribed by Recommendation ITU-R RS.1166 is 4%.

Altimeters are often accompanied by a supporting radiometer pointing in the same direction as the altimeter. This is done to have simultaneous measurements of the atmospheric water vapor, which extends the time necessary for the altimeter signal to reach the surface and return to the satellite.

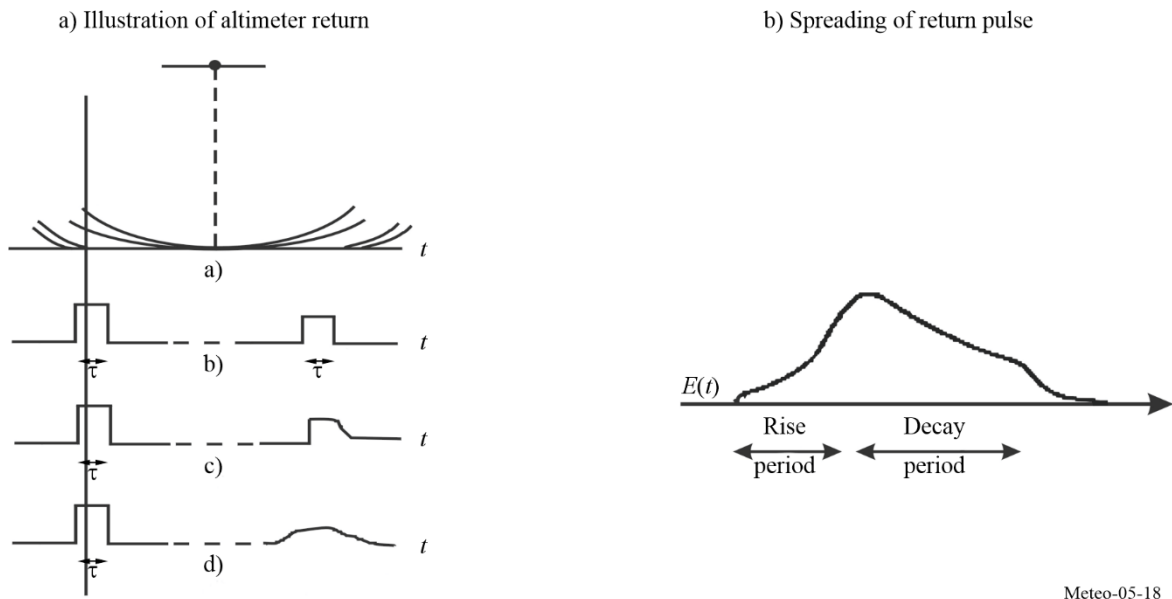
FIGURE 5-17

**Microwave satellite altimeter**

Meteo-05-17

FIGURE 5-18

**Illustration of altimeter return and spreading of return pulse**

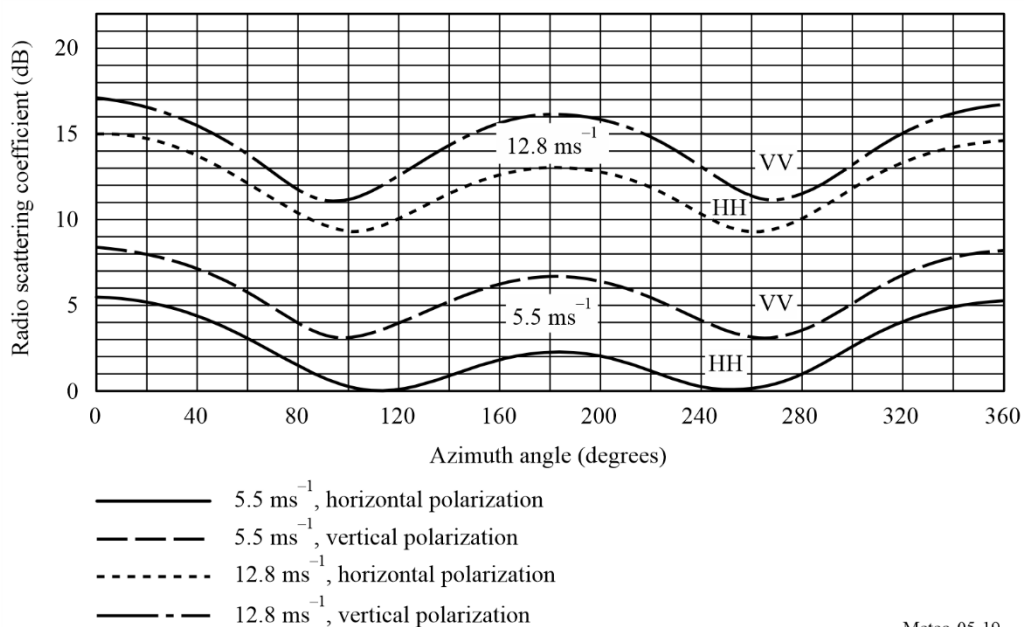


**5.3.4 Scatterometers**

Scatterometers mainly provide measurements of the wind direction and speed over the Earth’s ocean surface and sea ice extent and characteristics. The choice of RF centre frequency depends on the ocean surface interaction with the EM field and its variation over aspect angle. Figure 5-19 shows the variation of backscatter level with aspect angle relative to the wind velocity vector direction.

FIGURE 5-19

**Variation of backscatter with aspect angle**



As shown in Fig. 5-20, a typical scatterometer illuminates the Earth's surface at several different fixed aspect angles. In Fig. 5-21 a scatterometer scanning pencil beam illuminates scans at two different look angles from nadir, and scans 360 degrees about nadir in azimuth. The narrow RF signal bandwidth provides the needed measurement cell resolution.

FIGURE 5-20

**Scatterometer fixed footprint**

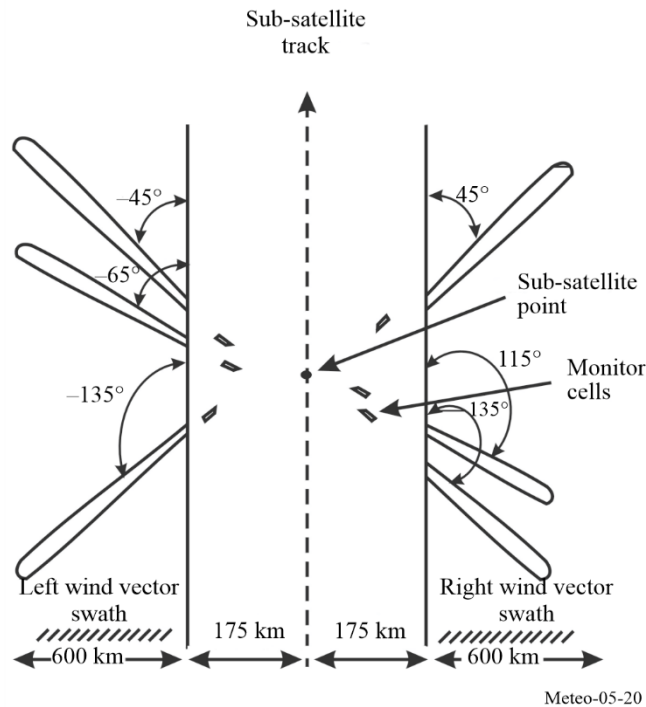
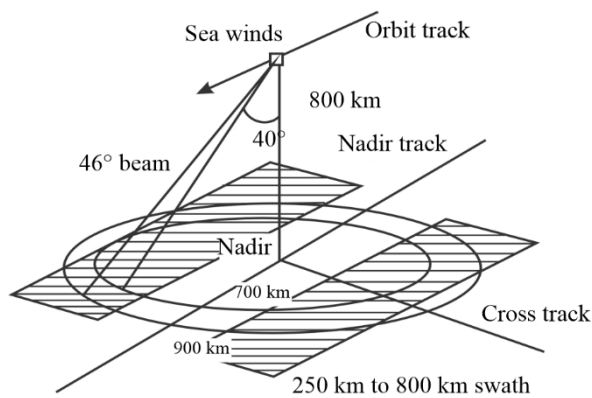


FIGURE 5-21

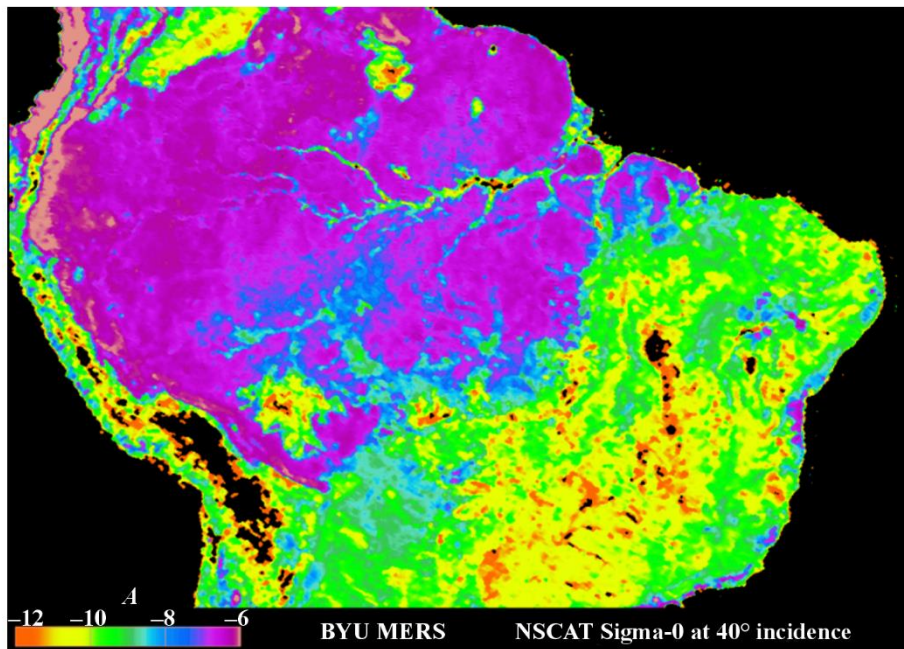
**Scatterometer pencil beam scan**



The scatterometer's primary function is to study winds over the oceans, but scientists have devised a way of studying changes in the instrument's radar backscatter to also look at all land surfaces, providing Earth's surface conditions such as soil moisture and rain over land. Figure 5-22 shows an example radar image taken from the NSCAT scatterometer of the Amazon rainforest in South America. The scatterometer's radar was sensitive to conditions on the Earth's surface, such as the type and density of vegetation.

FIGURE 5-22

NSCAT scatterometer radar image of the Amazon rainforest in South America



Meteo-05-22

### 5.3.5 Precipitation radars

Precipitation radars provide measurements of the precipitation rate over the Earth's surface, typically concentrating on rainfall in the tropics.

The choice of RF centre frequency depends on the precipitation interaction with the EM field. The backscatter cross section of a spherical hydrometeor is:

$$\sigma_b = \pi^5 |K_W|^2 D^6 / \lambda^4 = \pi^5 |K_W|^2 Z / \lambda^4 \quad (5-5)$$

where:

$|K_W|^2$ : related to the refractive index of the drop's water

$D$ : diameter of the drop (m)

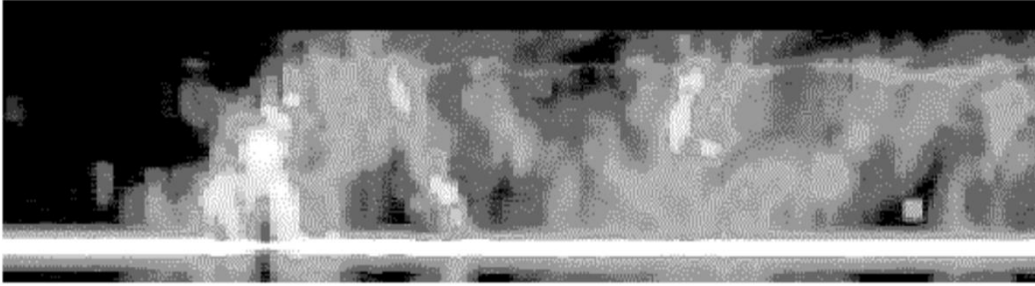
$\lambda$ : wavelength of the radar (m)

$Z$ : radar reflectivity factor.

The backscatter increases as the fourth power of the RF frequency.

Figure 5-23 shows an example of a vertical cross section of radar reflectivity factor. The narrow RF signal pulse-width provides the needed measurement range resolution. One example precipitation radar uses a pulse width of 1.6  $\mu$ s, though the value may vary with other systems. The allowable minimum precipitation reflectivity degradation determines the allowable interference level.

FIGURE 5-23

**Synthesized reflectivity from precipitation reflectivity measurements**

Meteo-05-23

**5.3.6 Cloud profile radars**

Cloud profile radars provide a three-dimensional profile of cloud reflectivity over the Earth's surface. Figure 5-24 shows a representative backscatter reflectivity versus altitude.

The choice of RF centre frequency depends on the ocean surface interaction with the EM field and its variation over aspect angle.

Equation (5-6) gives the expression for calculation of the return power level of the clouds.

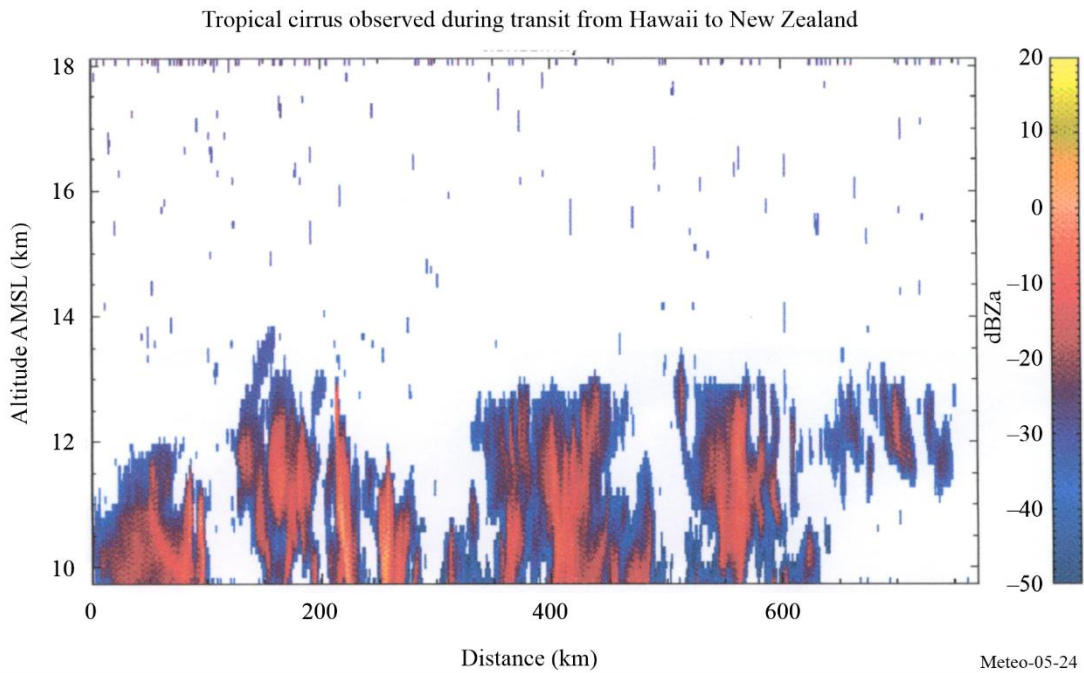
$$\tilde{P} = \frac{\pi^5 10^{-17} P_r G^2 t \theta_r^2 |K_W|^2 Z_r}{6.75 \times 2^{14} (\ln 2) r_0^2 \lambda^2 l^2 l_r} \quad \text{mW} \quad (5-6)$$

where:

- $\tilde{P}$ : return power level of the clouds (mW)
- $P_r$ : radar transmit power (W)
- $G$ : antenna gain (numeric)
- $t$ : pulse width ( $\mu\text{s}$ )
- $\theta_r$ : 3 dB antenna beamwidth (degrees)
- $K_W$ : dielectric factor of the cloud water content
- $Z_r$ : cloud reflectivity factor ( $\text{mm}^6/\text{m}^3$ )
- $r_0$ : range distance (km)
- $\lambda$ : radar wavelength (cm)
- $l$ : signal loss due to atmospheric absorption
- $l_r$ : radar system loss.

As illustrated by this equation, the return power decreases with the square of the wavelength. Since frequency is inversely proportional to wavelength, the return power increases with the square of the RF frequency. In the case of small particles (Rayleigh regime), the return power increases as the frequency to the power of four since the ratio depends on the relative particle size with respect to the wavelength. The cloud profile radar antennas have very low sidelobes so as to isolate the cloud return from the higher surface return illuminated by the sidelobes.

FIGURE 5-24  
**Example of cirrus cloud reflectivity**

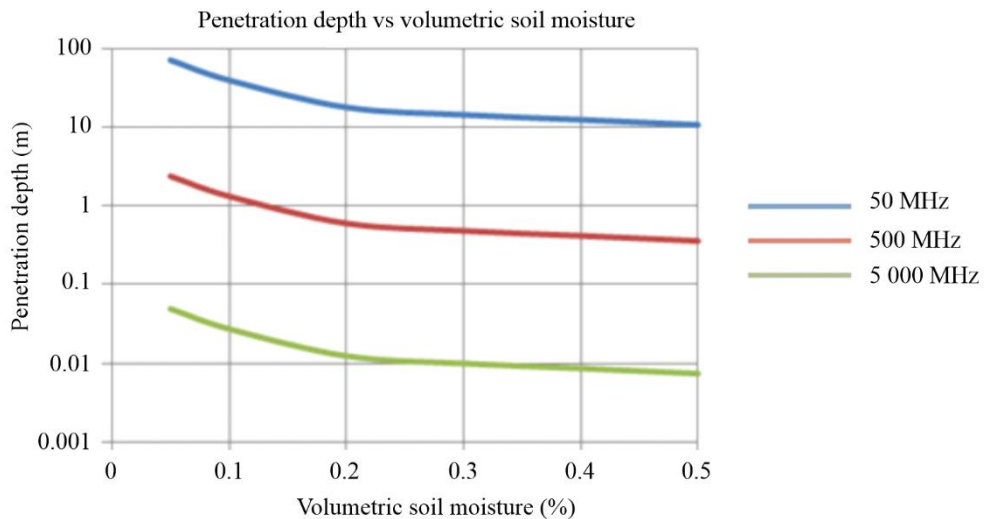


### 5.3.7 Radar sounders

Radar sounders are ground-penetrating radar (GPR) systems that employ lower centre frequencies when compared with other active sensor types, in order to penetrate the surface of the Earth. This can be used to provide radar maps of subsurface scattering layers to locate and characterize underground water and ice deposits.

The penetration depth that can be reached by radar sounders depends on the soil moisture and on the frequency, as shown in Fig. 5-25.

FIGURE 5-25  
**Surface penetration depth**



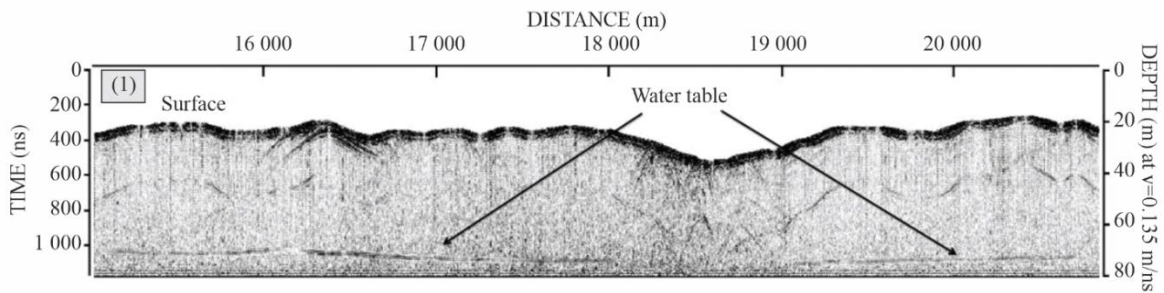
Given that penetration depth increases with the wavelength, radar sounders need to operate at low frequencies. And given that dry environments are needed, these radars could operate only in dry ice sheets or in desertic areas.

Specifically, the frequency range of 40-50 MHz, targeted for use by radar sounders, represents a trade-off between penetration depth and resolution, and it can be used to provide detailed mapping of the spatial distribution of shallow aquifers (on the order to 10-100 m in depth) in arid regions, as well as to perform basal interface topography and determine ice-sheet thickness (on the order of 5 km).

Figure 5-26 shows a two-dimensional profile of horizontal distance versus time or depth, called a radargram, taken from an airborne very high frequency (VHF) radar campaign over an aquifer in Kuwait in 2011. This Figure highlights variations in the depth of the water table from 49 to 52 m.

FIGURE 5-26

**Radargram taken from airborne VHF radar campaign over aquifer in Kuwait in 2011**



Meteo 05-26

**5.3.8 Sensor interference and performance criteria**

The criteria for performance and allowable interference are provided in Recommendation ITU-R RS.1166 for the various types of active spaceborne sensors. The recommendation is periodically revised to reflect regulatory modifications, such as a new EESS (active) allocation, and changes in the sensor state-of-the-art that would affect existing criteria for performance and allowable interference.

**5.3.9 Power flux-density (pfd) levels**

The characteristics of the various types of active spaceborne sensors as shown in Table 5-4 indicate that the transmitted peak power and therefore the power levels received at the Earth’s surface will vary significantly in level. Table 5-5 shows the active sensor power flux-density levels at the Earth’s surface for some typical sensor configurations.

TABLE 5-5

**Typical pfd levels at Earth’s surface**

Parameter	Sensor type					
	SAR	Altimeter	Scatterometer	Precipitation radars	Cloud profile radars	Sounders
Radiated power (W)	1 500	20	100	578	630	100
Antenna gain (dB)	36.4	43.3	34	47.7	63.4	10
Range (km)	695	1344	1 145	350	400	400
pfd (dB(W/m <sup>2</sup> ))	-59.67	-77.25	-78.17	-46.55	-31.64	-93.03

## CHAPTER 6

### Space weather

#### 6.1 Definition of space weather and its associated radio communication service

WRC-23 approved the following definition for space weather:

*space weather*: natural phenomena, mainly originating from solar activity and occurring beyond the major portion of the Earth's atmosphere, that impact Earth's environment and human activities;

Article **29B.1** of the Radio Regulation defines the radio service related to space weather observations: "Space weather sensors may operate under the meteorological aids service in the subset MetAids (space weather) allocations."

#### 6.2 Space weather observations

##### 6.2.1 Phenomena observed

A variety of physical phenomena are associated with space weather as shown in Fig. 6-1. These include geomagnetic storms and sub-storms, energization of the Van Allen radiation belts, auroras, ionospheric disturbances, scintillation of satellite-to-ground radio signals, long-range radar signals, and geomagnetically induced currents at Earth's surface. Coronal mass ejections and their associated shock waves, solar energetic particles, high speed solar wind streams, and solar flares are important drivers of space weather phenomena.

FIGURE 6-1

#### Space weather phenomena



Steele Hill/NASA

## 6.2.2 The requirement for space weather observations

Space weather observations are required:

- to monitor and forecast the occurrence and probability of space weather disturbances (including monitoring those aspects of solar activity pertinent to the above-mentioned disturbances induced by space weather);
- to drive hazard alerts when disturbance thresholds are crossed;
- to guide the design of both space-based systems (i.e. satellites and astronaut safety procedures) and ground-based systems (i.e. electric power grid protection and air traffic management);
- to allow for safe and secure operations of energy infrastructures, transport systems and communication infrastructures, including also the Global Navigation Satellite System (GNSS) and critical infrastructures, with potential effects on human safety and welfare;
- to provide input data to develop and validate numerical models of space weather conditions;
- to conduct research that will enhance our understanding of the Sun and solar activity on Earth's extended atmosphere; and
- to provide the constant monitoring, nowcasting and predictions required by mobile services, including International Mobile Telecommunications (IMT).

## 6.2.3 Space weather sensor systems using radio spectrum

Operational space weather products and services are delivered by a diverse set of organizations around the globe, in some cases unified into global networks. The products and services which support space weather observations needs can be organized into four broad categories: Solar and Interplanetary (solar wind), Energetic Particles, Geomagnetic, and Ionospheric.

Across these categories, observations are obtained from a combination of ground-based and space-based instruments. Measurements of energetic particles and the geomagnetic field are generally performed *in situ*: in space, in the atmosphere and at ground level. Their detection methods do not make any direct use of radio signals, so these types of observations will not be considered further in this chapter.

The remaining remote sensing instruments that make use of radio wave emissions and radio wave propagation to perform their measurements include both passive (receive only) and active (emit and receive) systems.

Many of the receive-only sensor systems make use of signals of opportunity (either man-made such as GNSS signals, or of natural origin such as cosmic radio sources). The active (emit and receive) sensor systems are employed to probe the state of the ionosphere by the propagation of radio signals.

### 6.2.3.1 Solar observations

Solar radio emissions are observed with ground-based radio frequency spectrographs, imagers and single-frequency solar radio flux monitors. Radio observations are provided by:

- 1) single antennas that observe the full Sun at selected frequencies,
- 2) spectrographs that observe the full Sun over an extended frequency range, and
- 3) imagers, or radio heliographs, based on the technique of aperture synthesis (interferometry) that provide two-dimensional maps of solar activity.

Solar radio observatories are deployed worldwide and provide 24-hours, 7-days a week coverage of solar radio emissions.

#### 6.2.3.1.1 Solar flux

Microwave emission from the Sun is observed at various frequencies to study different energetic solar processes and their influence on the Earth's thermosphere (solar extreme ultraviolet (EUV) emission, solar activity in the less energetic part of the UV spectrum, such as solar plages, faculae and hot coronal loops). These various observations are necessary to receive a reliable and stable assessment of the characteristics of the thermosphere including, for example, its density or ionization.

### 6.2.3.1.2 Solar spectrograph

Solar radio spectrographs typically sweep through a range of frequencies ranging from a few tens of MHz to a few GHz. They are particularly useful for observing solar radio bursts that are indicators of flares, Coronal Mass Ejections and other solar phenomena, and can be used as indications of the speed of shocks and emergent plasma in the solar wind. They are required with a stated cadence of 0.1 to 60 seconds (though a cadence of as long as 60 seconds is not particularly useful for radio bursts) and a delay of availability of 1 to about 30 minutes.

### 6.2.3.1.3 Heliograph

Solar radio heliographs use aperture synthesis techniques to rapidly map solar radio fluxes in two dimensions. Most solar radio heliographs also cover many frequencies simultaneously.

## 6.2.3.2 Heliospheric observations

Heliospheric observations aim to understand the solar atmosphere and solar activity, from the generation and emergence of the Sun's magnetic field to the creation of the solar wind and the acceleration of solar energetic particles.

### 6.2.3.2.1 Interplanetary scintillations (IPS)

IPS refers to variations in the intensity of radio waves from a distant, compact, radio source observed as they propagate through disturbed plasma density in the solar wind, particularly near the Sun. The amount of disturbance in the solar wind (or the solar wind density itself) can be estimated from the amplitude of the scintillation. Solar wind speed can be derived from the scintillation spectrum of the IPS obtained from a single IPS station, or from the time lags between two IPS patterns obtained from separated multiple IPS stations. Most observation systems that exploit IPS operate at single frequencies.

## 6.2.3.3 Ionospheric observations

Ionospheric observations aim to understand ionospheric variability, which is coupled to solar activity, the Earth's magnetosphere and neutral atmosphere. These observations are necessary to anticipate the impact on modern technologies.

### 6.2.3.3.1 Ionosondes

An ionosonde transmits a sweep of radio signals (pulsed or continuous wave (CW-chirp)) into the ionosphere. Echoes are returned where the radio frequency equals the local plasma frequency, which is proportional to the square root of the electron density. The peak frequency returned from each ionospheric layer is therefore a direct measure of the electron concentration. In contrast, the height of each layer is estimated from the time of flight of the radio signal assuming propagation through free space. Since the plasma frequency (electron density) is altitude dependent and also time-dependent with geophysical conditions, ionosondes must span a significant frequency range (e.g.  $\sim 0.5$  to 15 MHz). Altitude coverage is limited by the peak ionospheric cut-off frequency. Higher frequencies beyond the local plasma frequency can be used for oblique sounding up to 30 MHz. Modern research ionosondes can also be used to measure additional variables, most notably plasma velocities and the spectrum of gravity waves.

### 6.2.3.3.2 Incoherent Scatter Radars

Incoherent scatter radar (ISR) is a radar technique for the precise measurement of the thermal ionospheric plasma. The technique observes very weak scatter from thermal plasma ion-acoustic and Langmuir mode resonant oscillations. Primary measurements include electron density, electron temperature, ion temperature and ionospheric drifts. A wide range of derived products are possible under certain conditions including electric fields, neutral winds and ion compositions. Measurements are spatially resolved and can be made above and below the ionospheric peak. While the height of ionospheric layers can be determined very accurately with ISRs, cross-calibration with ionosondes or the use of specific features in the ISR spectra are required to calibrate the electron concentration since the electron concentration is inferred from the total returned power. Estimates of the horizontal distribution of ionization can be obtained by moving the radar dish or by altering the phase of an antenna array. Vector velocities can be calculated by combining data from different antennas or from different beam directions.

The radars switch between multiple beams after each transmitted pulse, and each beam is visited many times during a typical integration period of 15 to 60 s. Data from multiple beams provide volumetric images of the ionospheric electron density, electron temperature, ion temperature, and line-of-sight velocity. The line-of-sight velocities from multiple beams can be combined to produce estimates of the vector electric field's E-region neutral winds.

ISRs transmit powerful VHF or UHF radio pulses into the ionosphere. Typical HF/VHF/UHF/L-band centre frequencies are used with up to 30 MHz bandwidth on receive and typically up to 1 MHz bandwidth on transmit for existing systems. Up to 10 MHz transmit bandwidth is planned for future systems. Significant power is required with most systems being multi-megawatt class with antennas between 25 and 300 m in size. High power is needed due to the very weak radar cross-section of thermal ionospheric plasma. Older systems are typically single antenna (parabolic reflector) based, while more modern systems have phased array radar antenna designs.

#### **6.2.3.3.3 Coherent Scatter Radars**

These radar systems measure coherent scatter from ionospheric irregularities due to plasma instabilities, waves and structures. In this way, the returned power and line-of-sight velocity can be determined. Vector velocities can be calculated by combining data from two or more radar stations. Coherent scatter radars have often been deployed as transportable systems which can be moved to allow for the study of different regions of the ionosphere. Typically, dedicated systems are developed at 30, 50 or 144 MHz with bandwidths in the 1 MHz range.

#### **6.2.3.3.4 Other radars**

HF Doppler system radar consists of a CW radio transmitter and several receivers, which are highly frequency stable combined with a recording device. The CW signals are typically transmitted at frequencies between 3 and 10 MHz. When a radio wave is reflected from the ionosphere, a movement of the reflection point will produce a change in signal phase path and hence a Doppler shift proportional to the time rate of change of the path. HF Doppler measurements can be used to study ionospheric disturbances such as atmospheric gravity waves, travelling ionospheric disturbance ionospheric sporadic E and spread F layer occurrences, as well as magnetic pulsation ultra-low frequency waves such as Pi2 pulsations. Understanding travelling ionospheric disturbances and atmospheric gravity wave characteristics are important in space weather monitoring since the propagation of ionospheric scintillations caused by these phenomena allows short-time forecasting of the impacts of space weather on radiocommunications and GNSS reliant applications.

Mesosphere/lower thermosphere dynamics radars provide measurements of the mesosphere regions through partial reflection observations, often augmented with Faraday rotation. The mesosphere is a crucial atmospheric layer and is especially observed through the application of meteor radars and medium frequency radars. These radar measurements of the mesosphere/lower thermosphere have widely been used to detect mean winds and tides, and to get insight into the seasonal, interannual, and long-term behaviour of the mesosphere/lower thermosphere circulation including long-term trends.

#### **6.2.3.3.5 Ionospheric tomography**

Ionospheric tomography is a technique for analysing electron density in two or three dimensions. The method is based on ground-based measurements of LEO satellite dual-frequency signals of 150 MHz and 400 MHz. Dual-frequency radio receivers measure the phase difference of signals transmitted by the satellites. Several receivers are required for a tomographic analysis. Depending on the algorithm in use, electron density measurements from other instruments (e.g. from GNSS receivers) can also be used.

#### **6.2.3.3.6 Radio telescopes**

Radio telescopes can be used to observe the Sun and the solar wind, but also the ionosphere. Wide-bandwidth observations can identify ionospheric scintillation, leading to improved monitoring of the mid-latitude ionosphere.

### 6.2.3.3.7 Riometer

Ground-based measurements of radio signals from known sources above the atmosphere (usually cosmic radio sources) can be used to map absorption in the lower ionosphere using relative ionospheric opacity metres, or riometers. The three most common types of radio wave absorption are:

- 1) auroral absorption caused by precipitating electrons;
- 2) polar cap absorption associated with >10 MeV protons in the near-earth environment; and
- 3) X-ray induced absorption causing sudden cosmic noise absorption resulting from solar X-ray bursts that generate an anomalous level of electrons in the D-region (typically 60-100 km altitude).

Ground based riometers measure the power of the background cosmic radio noise, which is absorbed in the ionospheric D region. The D-region absorption is a function of the degree of ionization (electron density) present. To obtain the amount of absorption due to excess ionization, the riometer signal voltage of any given day is compared to the so-called Quiet-Day Curve (QDC), which is determined during selected days when there are no geomagnetic disturbances (i.e. geomagnetically quiet), the solar proton flux is at background levels, and there are no solar X-ray bursts.

A riometer is a type of CW radio receiver with receive sensitivity at the noise temperature of the background sky and is designed to measure the absorption of radio waves that traverse the ionosphere. Typically, a twin-dipole antenna is orientated to the zenith resulting in a beam that has a diameter of ~100 km at the 90 km atmospheric altitude. For most of the time, the received RF level is dominated by radio emissions of galactic origin and has a regular variation in sidereal time that can be characterized with a QDC. Absorption of radio waves by the ionosphere reduces the voltage level of the riometer to less than that of the QDC.

Multiple riometers can give some general background information for the near-Earth environment and the extent of the atmospheric absorption region.

There are three categories of riometers:

- broad-beam riometers have a single antenna and operate at 20.5, 30, 38.2 and 51.4 MHz;
- imaging riometers have multiple narrow beams, usually employing phased array antennas, to achieve higher temporal and spatial resolution. They typically use the same frequencies as those for broad-beam riometers;
- spectral riometers measure cosmic radio noise at multiple frequencies, ranging typically between 20 and 60 MHz.

There are approximately 50 riometer sites around the world, and most of these are located at high latitudes.

### 6.2.3.3.8 Global Navigation Satellite System (GNSS)

The total electron content (TEC) along a given propagation path can be measured by tracking the time delay and phase shift of GNSS radio signals by space-borne or ground-based receivers. As the navigation satellites move relative to the receiver, the TEC along the many available propagation paths is used to determine regional and global distributions of the ionospheric electron density. Corresponding GNSS receivers used for space weather observations measure amplitude, pseudo range, and phase at two or more radio frequencies at either 1 or 30 s time resolution.

Based on large global station networks and station distribution, it is possible to determine dedicated ionospheric maps by assuming all electrons are located within a thin layer at a specific height of 350 or 450 km.

Additionally, ionospheric scintillation is typically measured using GNSS observations but applying an enhanced sampling rate (typically 50-100 Hz). Ultra-low noise scintillation indices can be generated from GNSS amplitude and phase data. The scintillations are related to the occurrence of small-scale structures in the ionosphere, which are closely related to space weather phenomena.

Space-based radio occultation (RO) data obtained from low-Earth orbit (LEO) satellites equipped with GNSS receivers can also be used to provide high-resolution information about the vertical ionospheric structure including global information on disturbances such as sporadic E-Layers or Equatorial Plasma Bubbles. These observations are particularly important over ocean areas where observations from ground-based networks are not possible. Measurements from space-based GNSS-RO receivers provide one of the only ways of obtaining

global vertical profiles of electron density. In addition, dual-frequency carrier phase observations taken by the roof antenna(s) of satellites equipped with a GNSS receiver for positioning purposes provide information on the integrated electron content of the ionosphere and plasmasphere above the satellite's orbit height.

### 6.2.3.3.9 Very low frequency (VLF)

One of the few techniques that can probe the ionospheric D-region uses VLF electromagnetic radiation trapped between the lower ionosphere (approximately 85 km) and the Earth; these signals can be received thousands of kilometres from the source. The nature of the received radio waves is determined by propagation inside the Earth-ionosphere waveguide, with variability largely coming from changes in the electron density profiles at and below the lower ionosphere (the D-region). During solar flares, these D-region electron densities are driven, in large part, by soft (1-10 keV) X-rays from the flare itself. Hence, these observed anomalies produce an indirect observation of the nature of the solar flare.

## 6.2.4 Categorization of the RF-based sensors in regard to support of current space weather products

Based on studies conducted in WMO and ITU-R, in particular Report ITU-R RS.2456, which provides information on the characteristics of specific instrument types, a non-exhaustive categorization of space weather sensor systems using radio spectrum based on the application of current space weather observational products has been established as follows:

- Systems and frequencies used in operational space weather applications (for real time monitoring, near real time initialisation of forecast models).
- Systems and frequencies transitioning from research to operations.
- Research systems currently not used operationally (e.g. data not available in near real time, gaps in data provision).

Tables 6-1 to 6-3 include a brief summary of space weather radio frequency instruments and their categorization. The frequencies presented in the Handbook are for informational purposes only and do not represent nor suggest any regulatory provision.

TABLE 6-1

### Category 1 – Systems in operational use

Instrument type	Frequency (MHz)	Bandwidth	Location (country/region)
Solar Radio Flux monitoring	245, 410, 610, 8 800, 15 400	Varies	Australia, Italy, USA
	2 695	Varies	Australia, Italy, USA Belgium
	1 415, 4 995	Varies	Australia, Italy, USA Canada, Belgium, China
	2 200, 2 300, 2 730, 3 350, 4 542, 4 500, 5 000, 8 000, 9 000, 9 081	10 MHz	China
	2 800	Varies	Canada, Belgium, China, Korea (Republic of), Poland
	1 000	Varies	Japan, Belgium, Poland

TABLE 6-1 (end)

Instrument type	Frequency (MHz)	Bandwidth	Location (country/region)
Spectrograph	30-3 000	2 970 kHz	Korea (Republic of)
	20-650	1 000 kHz	Greece
	70-9 000	8 930 kHz	Japan
	232-258, 389-431, 500-18 000	18 000 kHz	Korea (Republic of)
	10-80	70 kHz	France
	20-80	60 000 kHz	Belgium
	45-450	400 MHz (98 kHz freq. resolution)	
	275-1 495	1 220 MHz	
	45.0-870.0	0.08, 0.30, 2.40 MHz	Global
	140-1 000	860 MHz	France
	25-180	Not available	Australia, Italy, USA
	35 300-36 300 37 300-38 300	500, 1 000 MHz	Finland
	15-15 000 15 000-40 000	Varies	China
Radio Heliograph	150-450	0.7 MHz	France
Interplanetary Scintillation (IPS)	327	10 MHz	Japan
	10-90; 110-190; 170-230; 210-250	80 MHz	Europe (LOFAR) Finland (KAIRA)
	139.65	Not available	Mexico
Ionosonde	0.5-33.0	42 kHz, 50 kHz, 60 kHz	Global
Ionospheric Tomography	150	6.0 MHz	Finland, Norway, Sweden
	400	8.0 MHz	
Riometers	20.5, 30, 32.4, 38.2, 51.4	15, 30, 100, 250 kHz	Canada, Iceland, Argentina, Australia, USA, South Africa, Northern Europe, Greenland, China, Antarctica, Russian Federation, Brazil
	20-60	200, 250 kHz	Finland
RNSS ionospheric monitoring	GPS (L1, L2, L5) BeiDou (B1, B2, B3) GLONASS (L1, L2) Galileo (E1, E5, E6)		Global

TABLE 6-2

## Category 2 – Systems in transition from research to operational use

Instrument type	Frequency (MHz)	Bandwidth	Location (country/region)
Interplanetary Scintillation	10-85	80 MHz	France
	50-350	300 MHz	Australia
Incoherent Scatter Radar	1-20	Variable	Italy, Argentina
	427-453	25 MHz	Northern Europe, North America, Japan
Coherent Scatter Radar	40.8	18.1-404 kHz	Republic of Korea
	0.3-26	10 kHz	Global
Mesosphere/lower thermosphere dynamics radar (meteor radar)	33.2	18.1 kHz	Republic of Korea
	3.17	40 kHz	Germany
	2	200 kHz	China
	35.24	10 MHz	
	39	1 MHz	
3.18	40 kHz	Norway	
Additional instrument types for opportunistic observations:			
VLF receivers	0.01-0.5	50 kHz, various	Global

TABLE 6-3

## Category 3 – Research systems

Instrument type	Location (country/region)
Solar radio telescope	Russian Federation
	Finland (MRO-14 and MRO-1.8)
Radio heliograph	Finland, Japan, USA, Russian Federation, India
Spectrograph	India, Russian Federation, Ukraine, Czech Republic, Switzerland
HF spectrograph	France (Decameter Array), Japan
Ionospheric	Norway (Tromso), USA (Alaska, Puerto Rico), Russian Fed. (Vasilsurks), Germany
Ionosondes	Germany
Coherent scatter radar	Norway (MAARSY)

## CHAPTER 7

### Other radiocommunication systems for meteorological and related environmental activities

#### 7.1 Introduction

As discussed in Chapter 1, weather, climate, hydrological, marine and related environmental services need to collect observations from many remote sites, on land, over the sea, in the air and in space. Thus, the WMO global infrastructure is dependent on many other radiocommunication services in addition to the MetSat, MetAids, radiolocation and EESS services described in previous Chapters. This Chapter describes some of these additional systems which rely on radio frequency for their operation.

Sections 7.2 to 7.4 provide information about systems used to share data from *in situ* measurement systems and the dissemination of forecast data. Sections 7.5 to 7.8 describe observation systems which rely on access to radio spectrum in order to measure specific environmental characteristics such as the location and timing of lightning strikes. Some of these systems make use of signals of opportunity generated by other radio spectrum applications to make measurements of atmospheric characteristics.

The increase in NWP model resolution has increased demand for *in situ* measurements of environmental parameters, many of which can now be delivered using automated systems. Wireless communications technology can enable these systems to operate and share data from remote sites, in some cases these links can also enable remote control and maintenance, reducing the need for human intervention and making it easier to maintain remote stations. As technology has continued to evolve, these systems now make use of various radiocommunication services to share data between remote sites and data processing hubs.

It is also essential to ensure that meteorological information and warnings are disseminated to end users with minimal delay, whether in densely populated urban areas or in remote sparsely populated regions. In addition, weather, climate, hydrology, marine and related environmental services are supplied to support maritime and aviation operations worldwide, enabling safe operations of these very weather-sensitive sectors. The dissemination systems for meteorological products make use of a wide range of radiocommunication services to support a diverse range of end users.

#### 7.2 Data dissemination systems

As noted in § 7.1, demand for more *in situ* measurements to support advances in weather forecasting has driven a growth in the use of automatic measurement systems, which require reliable communication links to share data and enable remote command and control. Technical characteristics, including operating frequencies, of these systems vary widely and almost any of the meteorological RF bands may be used; operators may also make use of commercially available communications links (e.g. mobile internet). Selection is frequently made based on the necessary bandwidth, which in turn is determined by the type and quantity of information to be carried.

Dissemination of forecasts is of equal importance to the collection and archiving of weather data. Making these predictions available to the public is a prerequisite to saving lives in order for people to take the steps necessary to protect their lives and property. The United Nations Early Warnings for All (EW4ALL) initiative aims to ensure universal protection from hazardous weather, water, or climate events through life-saving early warning systems. It is built on four pillars to deliver effective and inclusive multi-hazard early warning systems. The third pillar, [\*Warning Dissemination and Communication\*](#), led by the ITU, focuses on last-mile connectivity to ensure that warnings reach people at risk in time to take action.

A number of specialized radio systems have been developed over the years by which forecasts and other meteorological data are distributed. Among the simplest of these is voice broadcasting. Typically using VHF radio, these systems require minimal equipment to be used by the general public. These systems serve to warn the public of threatened storms, floods, extreme temperatures and other natural and human-caused hazards. Enhancements may be provided such as brief data transmissions accessible to deaf persons using special equipment. These systems may also be designed to provide continuous data distribution, or to remain silent

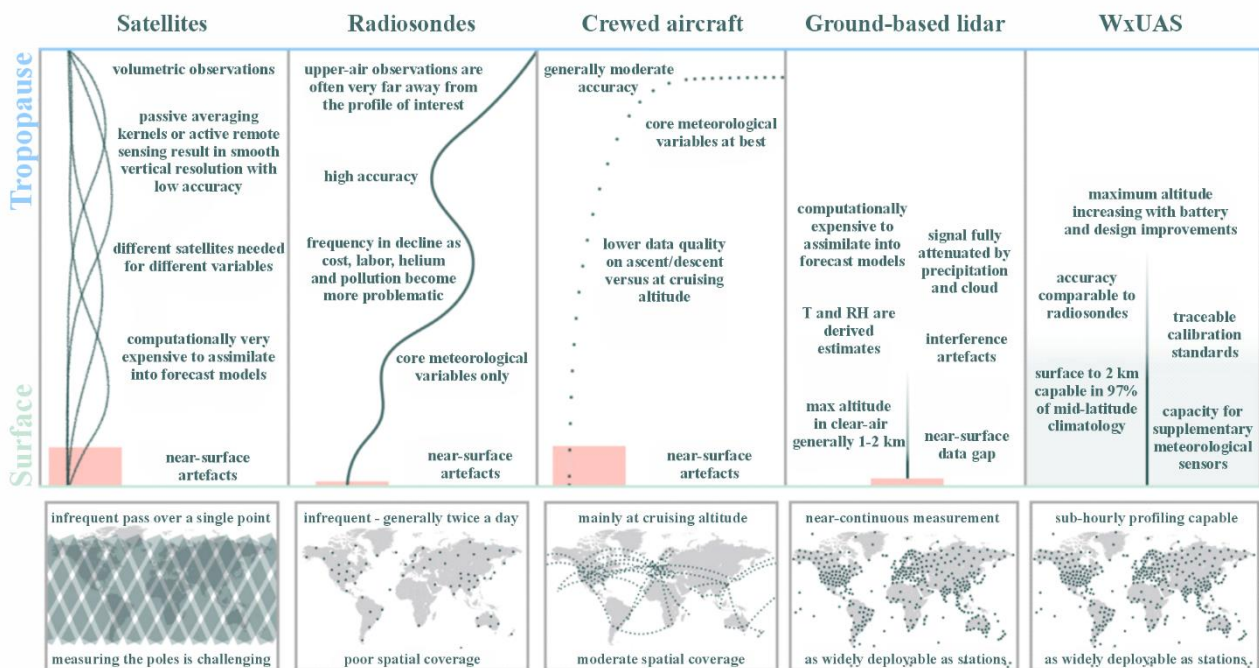
until triggered by an alert tone signifying a special event such as foul weather or other imminent hazards. Dissemination systems may be found in the fixed and mobile services, including maritime mobile service. Other dissemination systems operate via radio and television broadcasts (terrestrial and satellite) and on MetSat downlinks (details of which are provided in Chapter 2).

### 7.3 Weather-sensing Uncrewed Aircraft Systems

Weather-sensing Uncrewed Aircraft Systems (Wx-UAS) are becoming increasingly important for meteorological and Earth observations operations. Within many current observing networks, the boundary layer and lower atmosphere are not sampled at time and space scales needed to improve mesoscale analyses Wx-UAS have created novel opportunities for partially filling this observational gap (see Fig. 7-1).

FIGURE 7-1

Diagram comparing the horizontal and vertical coverage of five measurement systems, noting the gaps in near-surface measurements



Meteo 07-01

Wx-UAS are used for applications that include routine vertical profiles of the boundary layer, release of dropsondes over ocean areas where radiosonde data has historically been missing, flights into tropical cyclones for *in situ* data collection, and aerial reconnaissance of areas impacted by severe weather or drought conditions. The use of Wx-UAS for meteorological operations can improve Numerical Weather Prediction as well as enhancing forecasting of hurricane landfall areas, extend lead times provided to the public and allow for increased understanding of climate conditions.

Wx-UAS operations for meteorological purposes often use unlicensed spectrum for command and control of the aircraft, though some systems do use licensed frequencies. In addition to the command and control of the Wx-UAS, spectrum is needed for payload data transmission.

### 7.4 Hydrological systems

Floods are a natural phenomenon occurring in much of the world, and systems that can aid in predicting their occurrence, location and magnitude have saved many lives and a significant amount of property. Advance

knowledge permits the implementation of appropriate mitigation measures, such as evacuation of vulnerable populations, the construction of levees and dams, and the relocation of valuable property where possible.

As a complement to meteorological radar networks (see Chapter 4) and other *in situ* observations that are an essential tool in observing the hydrological processes, specific hydrological systems are also used to measure precipitation, stream height and the depth and extent of snow pack, all of which are parameters required in the prediction and early warning of flooding. These parameters are also useful in estimating the availability of water resources.

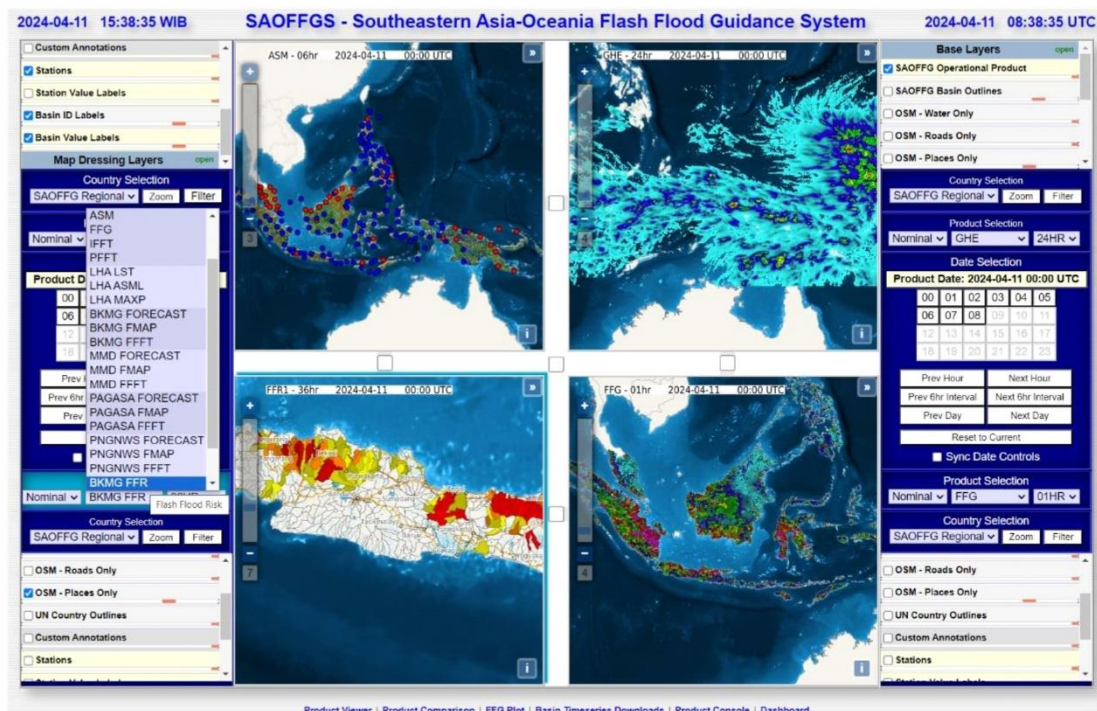
Communities with persistent flood problems and those vulnerable to great losses when flooding does occur are continually seeking ways to minimize flood related losses; and at the same time maintain a viable use of the floodplain where often major agricultural and industrial activities are located, together with human settlement. Automated hydrological observation systems are an attractive solution because of their low cost of operation and because they can complement and enhance the operation of other flood management methods such as reservoir floodgate operation, flood insurance, or floodplain zoning.

An automated hydrological observation system consists of event-reporting meteorological and hydrological sensors measuring the relevant parameters, radiocommunications equipment, and computer software and hardware. In its simplest form, coded signals are transmitted via the radiocommunication equipment, usually using the VHF or UHF bands under the fixed or mobile services, to a base station, often through repeater sites. The base station collects these coded signals and processes them into meaningful hydrometeorological information that can be displayed or tied to an alarm system and may notify emergency managers when the predetermined criteria are exceeded.

An example can be found in the Flash Flood Guidance System with global coverage (FFGS/WGC). By integrating remote-sensed precipitation data (such as radar and satellite-based rainfall estimates) alongside soil saturation information, hydrological and NWP models, it empowers national operational forecasters and disaster management agencies with real-time guidance products. These resources are essential for developing flash flood warnings in more than 70 countries worldwide (see Fig. 7-2).

FIGURE 7-2

### Example of FFGS MapServer interface



## 7.5 Meteorological uses of Global Navigation Satellite Systems (GNSSs)

Signals of all global GNSS systems are exploited for meteorological applications as described in this section. These measurements are opportunistic in nature, as National Meteorological and Hydrological Services rely on signals from systems designed to support radionavigation rather than environmental monitoring; this includes multiple systems operated by various satellite agencies:

- US Global Positioning System (GPS): with signals transmitted at 1 575.42 MHz (designated L1), 1 227.6 MHz (L2) and 1 176.45 MHz (L5);
- European Galileo system: with frequencies of 1 575.42 MHz (denoted E1), 1 176.45, 1 191.795 and 1 207.14 MHz (E5) and 1 278.75 MHz (E6);
- China’s BeiDou Navigation Satellite System (BDS): with frequencies of 1 575.42 MHz (B1), 1 176.45 MHz (B2) and 1 268.53 MHz (B3);
- Russian GLONASS system: with frequencies centred around 1 601.72 MHz (L1) and 1 245.78 MHz (L2);
- Some regional GNSS systems like the Japanese QZSS, transmitting signals at GPS frequencies.

### 7.5.1 Accurate location and timing of meteorological observing platforms

*Location of mobile meteorological observing platforms* such as radiosondes carried by weather balloons, dropsondes falling on parachutes (see Chapter 3), unmanned aircraft carrying meteorological sensors (see § 7), or marine meteorological systems such as ocean buoys.

*Precise and accurate time synchronization between remote observing sites*, as required for instance by lightning detection systems (see § 7.6).

### 7.5.2 Atmospheric and surface measurements

*Measurement of total water vapour in the atmosphere* can be derived from the phase delay in the GNSS signals received by ground-based receivers (“GNSS ground-based observations”) (M. Bevis, et al., 1992, Bonafoni et al., 2019). The computation of total water vapour requires accurate knowledge of the positions of the various GNSS satellites as well as the receiver, along with estimates of clock errors of both transmitters and receivers. Phase delays introduced in signal transmission through the ionosphere are identified from the differences in the phase delays between two GNSS frequencies and are corrected accordingly. If the surface pressure and temperature are also known, the phase delay caused by the signal propagation through the atmosphere can be further separated into a dry and a wet part, eventually allowing an estimate of the total water vapour along the path to the satellite. The GNSS sensor at the surface receives signals from many directions in a short period of time but can be mapped to the total water vapour in the vertical.

*Measurement of temperature and humidity profiles* can be derived from space-based or airborne occultation measurements of the GNSS signals, known as Radio Occultation (RO). An RO receiver on an independent satellite, aircraft or balloon receives signals from the GNSS constellation passing through the atmosphere in a limb-sounding geometry. The amount of bending experienced by the GNSS signals due to their refraction of the GPS signals by the neutral atmosphere and ionosphere (“bending angle”) is measured at a range of heights above the Earth’s surface. This allows the refractivity of the air to be derived as a function of height. Two GNSS frequencies are exploited to remove the ionosphere’s influence on the received signals, and, therefore, an ionosphere correction is performed before the neutral atmospheric retrievals. At upper levels in the neutral atmosphere, humidity can be omitted, and the refractivity of air can be assumed to be directly dependent on temperature. At levels closer to the surface, temperature and humidity influence the refractivity and need to be separated using, e.g. variational retrievals. In NWP applications, bending angle or refractivity observations can be used directly without retrieving temperature and humidity. The measurement of meteorological variables derived from this technique exhibits a high vertical resolution in the order of a few hundred metres, with about 200-300 km horizontal resolution along the line of sight and 1.5-2 km across. As with the total water vapour measurement, this technique requires precise knowledge of both satellites’ position and clock errors (Anthes (2011), Yue et al., (2014), Bonafoni et al., (2019), and Ho et al., (2020)).

*Measurement of the presence of hydrometeors:* In an evolution of ordinary RO (Polarimetric RO, or GNSS-PRO), the observation of the horizontal and vertical polarisation components of GNSS signals separately allows for the detection of hydrometeors, in addition to the traditional RO measurement. Such measurements have demonstrated sensitivity to large water droplets related to strong precipitation and ice particles in clouds (F. Turk et al., (2024)).

*Measurement of ionosphere and electron density:* The utilization of GNSS signals for ionospheric measurements and Space Weather monitoring is described in detail in Chapter 6 (§ 6.2.3.3.8).

*Measurement of ocean surface wind speed, soil moisture, sea ice characteristics and snow depths:* (1) GNSS signals reflected from the Earth's surface (GNSS Reflectometry, or GNSS-R) and observed from space carry information on ocean surface wind speeds (though not directions), soil moisture, sea ice characteristics and snow depth when observed in a nadir-viewing geometry and are based on the amplitude or signal to noise ratio measurements, typically taken at a single frequency only; (2) Grazing GNSS-R observations at very low elevation angles and under calm surface conditions additionally allow altimetric retrievals of the sea surface and sea ice properties through carrier phase measurements. (3) Airborne; and (4) ground-based GNSS receivers can observe soil moisture, snow, and ice characteristics using the reflected signals from the surface using the GNSS-R technique (Rodriguez-Alvarez (2023)).

## 7.6 Lightning detection systems

Remote sensing of lightning activity is an important tool used by operational meteorologists as accurate and timely information about lightning has clear links to public safety considerations on land, sea and air. User requirements are evolving in conjunction with advancements in the use of weather radar and meteorological satellite products.

The reliable operation of these systems is directly linked to considerations of public safety, as provision of an effective forecast service impacts the efficiency of commercial and defence activities. The safety of engineers working on power lines and personnel handling explosive devices are examples of activities that benefit from effective lightning forecasts.

The detection of lightning is a passive activity involving the use of radio receivers to detect the electromagnetic emission from lightning (spheric). Data from individual detection sites may be distributed by a range of communications technologies including fixed links, mobile networks, internet, etc (as described in § 7.2).

In current operational systems, the position of the lightning flash is either determined by measuring the direction of arrival of the associated spheric (triangulation); the time of arrival (TOA) of the spheric; or a combination of both.

If using triangulation, measurements are required at three or more widely spaced sensing sites. However, for TOA based systems the minimum number of sites used is 4 or more. In practice more than the minimum number of sites are used in order to improve the reliability of the reported locations. TOA systems usually provide more accurate locations than direction-finding systems when observing at ranges over several hundred kilometres. This is due to the direction of reception of skywaves sensed at the site, which usually differs slightly from the actual direction of the discharge and will vary according to the state of the surface layers near the sensing site. TOA systems usually rely heavily on GNSS signals (as noted in § 7.5.1) to achieve the necessary time synchronization at the various sensing sites. All systems rely on cost effective, reliable communications from the remote sites to the central processor.

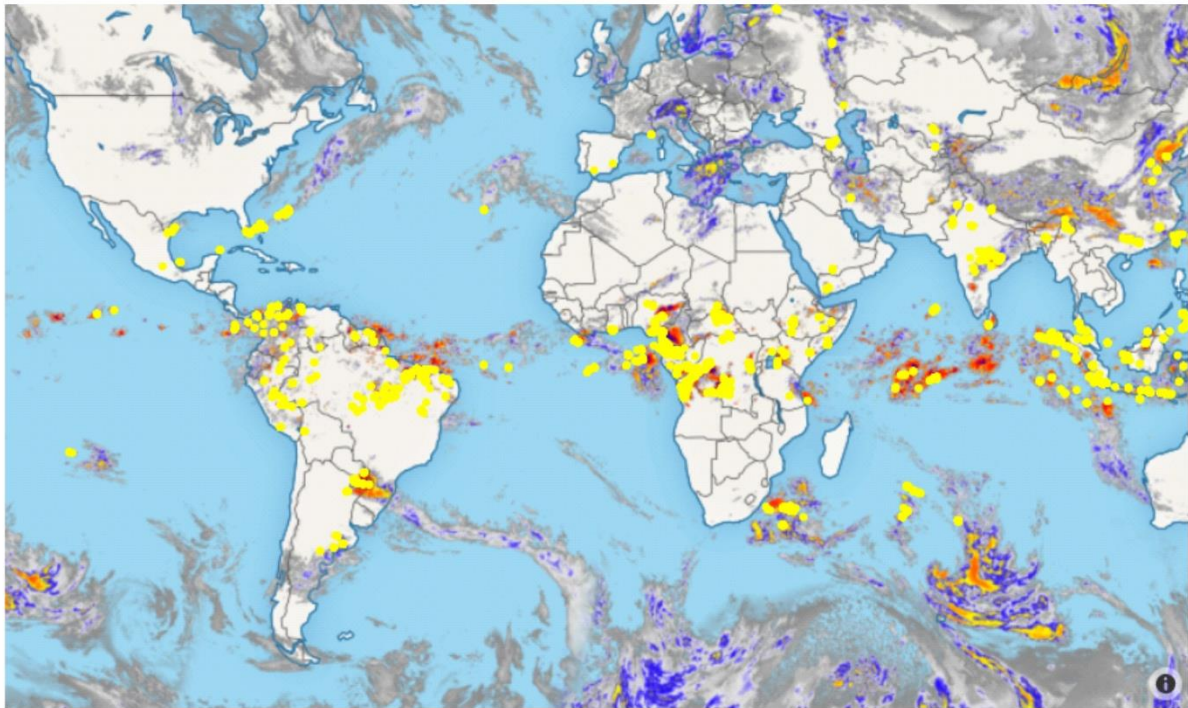
The radio frequency used to locate lightning activity varies according to the area of monitoring required and the specific purpose of the system.

Very long-range locations at distances of several thousand kilometres are achieved operationally by observing frequencies in the VLF centred around 10 kHz (8-11.3 kHz), such as the World Wide Lightning Location Network (WWLLN), Global Lightning Dataset (GLD360) (see Fig. 7-3), the Global Lightning Detection Network (LINETglobal), or the Lightning Electromagnetic Emission Location using Arrival time differencing (LEELA). For these systems the spherics are received at stations with typical spacings of several thousand km apart. The spherics are recorded at the sensor sites and the timed samples are immediately transmitted to a central control station where the locations of the lightning discharges are computed from the differences in arrival times at the sites. Low levels of interference can sometimes be countered by using an adjustable notch

filter at the affected sensor sites, but widespread and higher levels of interference are extremely detrimental to the operation of the system.

FIGURE 7-3

**Two minutes of global lightning detection data measured by the GLD360 for long range lightning detection network superimposed on satellite data showing cloud and precipitation**



Meteo 07-03

For example, in the LEELA system (operated by the UK Met Office), 11 receivers sited across Europe with spacing of up to 2 000 km, continuously stream timestamped VLF data to a central processor. LEELA's central processor then extracts the lightning waveforms from the incoming data streams, groups them based on waveform correlation and then uses the arrival time difference between the waveforms to compute the location of a lightning strike using multilateration. The LEELA waveform extraction algorithms allow the lightning waveform and background noise to be decomposed allowing interference to be mitigated automatically.

Taking into account the importance of such long-range lightning detection and the need for a global recognition, a specific allocation to the Meteorological Aids service, limited to passive sensors, was made at WRC-12 in the band 8.3-11.3 kHz. As lightning detection uses passive (receive-only) sensors, lightning detection systems can also operate in different frequency bands on a non-protection basis.

The most widely used operational systems cover a more limited area in detail. In this case, the spherics are observed at higher frequencies centred around 200 kHz (the wideband receivers used are most sensitive in the middle of their range of 1 kHz to 350 kHz), and the sensing sites are usually spaced between 100 km and 400 km apart, depending on whether the emphasis is on cloud-to-ground or cloud-to-cloud flashes. At these higher frequencies, a discharge from the cloud-to-ground can be identified by a pronounced rise in amplitude defining a leading edge to the spheric. The arrival of this leading edge can be accurately timed. The times from the network sites are transmitted to a central processor and used to compute the positions of the discharges. In some cases, the network arrival time differences are operated in conjunction with magnetic direction-finding systems installed in earlier years. An overview of the technology and systems is available in the WMO No. 8 Guide to Instruments and Methods of Observation Volume III – Observing Systems in Chapter 6.

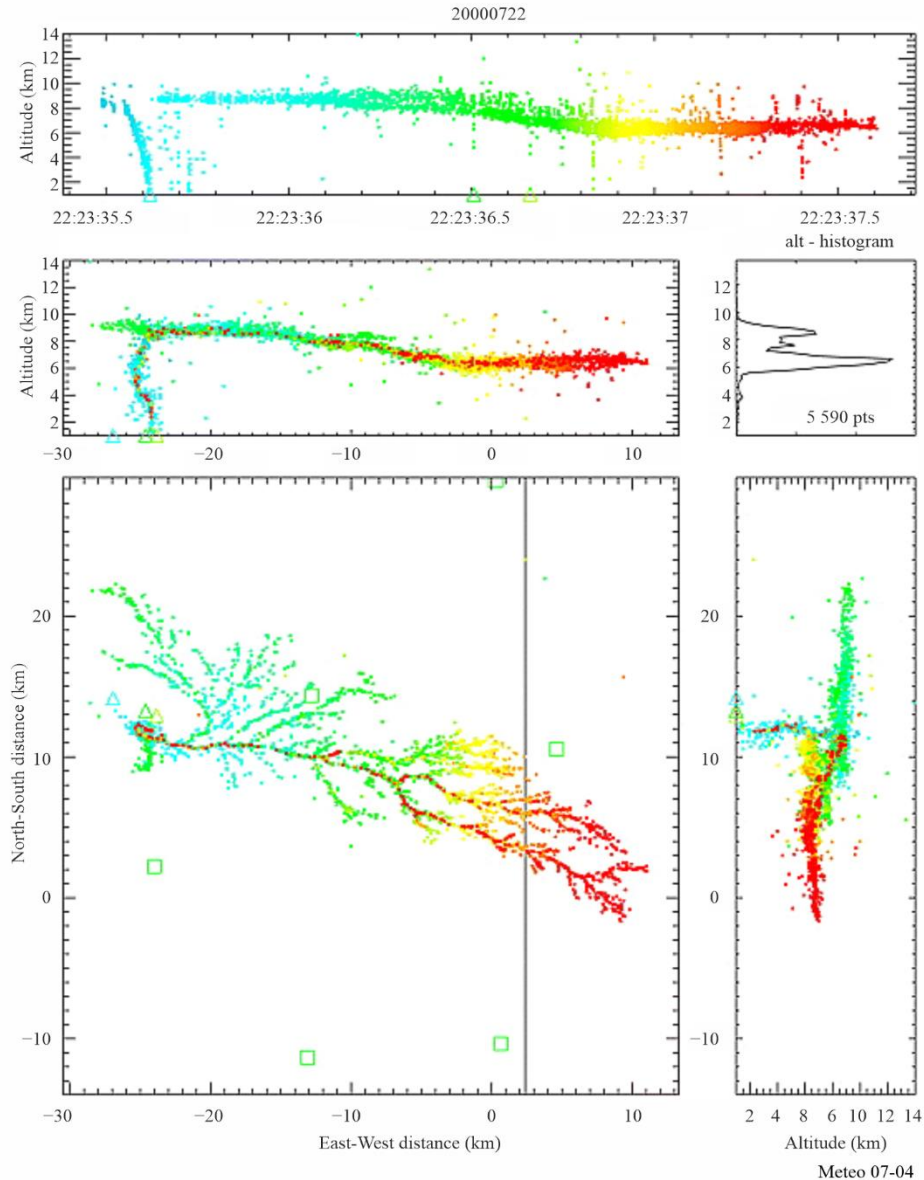
In addition, to map the complete lightning channels there are lightning mapping array (LMA) systems which observe at very much higher frequencies (VHF band 60-66 MHz), an example is the New Mexico Tech LMA (Thomas et al., 2004). Figure 7-4 shows an example of a lightning discharge observed by the New Mexico Tech LMA that illustrates the spatial resolution that the system is able to obtain. The flash was a negative polarity cloud-to-ground discharge that occurred over the northern part of the network and was accurately located by the measurements. The discharge propagated over a large horizontal distance (40 km) through its parent storm; in the process the breakdown channels developed a fine dendritic structure that was well resolved by the mapping system. More than 5,000 sources were located during the 2 s duration of the flash.

For such detailed detection, the storms must remain within line-of-sight if all the activity is to be observed. This requires that the ground sensors be located in a short baseline configuration – the sensors need to be 30 km apart, and about 50 m from the ground to fulfil the radar horizon criteria. In practice, however, some operational systems observing cloud-to-cloud activity are operated with the ground sensors further apart, relying on the cloud-to-ground systems at lower frequencies to fill in the details of the discharges at lower levels.

The different panels of Fig. 7-4 show the evolution of the flash in height-time (top), plan view (bottom left), and in east–west (middle left) and north–south (bottom right) vertical projections. The histogram panel (middle right) shows a histogram of the source heights. The triangles indicate negative ground strike times and locations from the National Lightning Detection Network (NLDN). The squares in the plan view indicate the location of measurement stations, and the vertical line denotes the Colorado-Kansas state border.

FIGURE 7-4

**Radiation sources for a negative polarity cloud-to-ground discharge observed by the New Mexico Tech LMA that illustrates the spatial resolution that the LMA system can obtain**



## 7.7 Ground-based microwave radiometers

Vertical atmospheric sounding using passive remote sensing from satellites is described in detail in Chapter 5 (§ 5.1). Meteorologists making detailed local forecasts or scientists investigating the planetary boundary layer have requirements for atmospheric sounding with higher vertical resolution near the ground than can be provided by satellite-based systems.

One method of providing this information is to use upward-looking passive remote sensing, with a radiometer mounted at the Earth's surface. These radiometers use a selection of channels to produce a measurement of temperature structure in the following two oxygen bands: 22 GHz – 32 GHz and 50 GHz – 58 GHz. They are described in the Report ITU-R RS.2489 and reflected in Table 7-1 below. Measurement of water vapour and clouds also benefits from additional observations around 90 GHz and in the lower wings of the water vapour absorption band at 183 GHz. Passive ozone (in particular at 142 GHz) also benefits from a significant number of ground-based radiometry sites.

Although the channels for ground based remote sensing of temperature and humidity are in a similar region to passive satellite remote sensing frequency bands, they are generally using wider bands including bands shared with other services. In some frequency bands, in particular those covered by RR No. **5.340** or allocated to Radioastronomy service, ground-based radiometers benefit from the same protection as satellite remote sensing; but in other bands ground-based radiometers are not protected on an international basis.

TABLE 7-1  
Frequency bands used by ground-based passive radiometers

Channel centre frequency (GHz)	Channel centre frequency (GHz)
22.24	
23.04	
23.84	RR No. <b>5.340</b> applies (23.6-24 GHz)
25.44	
26.24	
27.84	
31.4	RR No. <b>5.340</b> applies (31.3-31.5 GHz)
51.26	
52.28	
53.86	RR No. <b>5.340</b> applies (52.6-54.25 GHz)
54.94	Primary EESS (passive) allocation (54.25-59.3 GHz)
56.66	
57.3	
58.0	

The number of ground-based radiometers in operation globally is still relatively small (a few hundred), but larger numbers are expected to be deployed in the near future. A pragmatic method of sharing may have to be developed where radiometers are deliberately sited to avoid interference from the other services.

## 7.8 Microwave Radio Attenuation systems

Various techniques are being explored to estimate rainfall using the attenuation of signals from Commercial Microwave Links (CML) such as mobile network backhaul or satellite data transmissions. While slightly different approaches are required when considering ground-based mobile networks or satellite links, both techniques rely on transmissions between 5 GHz and 40 GHz. Unlike GNSS measurements (described in § 7.5), CML measurements rely on gaining access to third-party data with sufficient temporal resolution and timeliness – which can prove challenging when the data owners may not have an interest in environmental measurement.

These techniques measure changes in signal strength caused by rainfall in the transmission path. Attenuation of signals in this range are susceptible to attenuation ( $k$  in dB/km) related to the rain rate ( $R$  in mm/h) according to the following equation:

$$k = aR^b$$

Where  $a$  and  $b$  depend on the transmission's frequency and polarisation. The value of  $a$  increases with frequency. That is, high frequencies experience stronger attenuation for the same amount of rain. The value of  $b$  is close to 1, in particular around 30 GHz, making the relationship linear, or almost linear.

Measurements rely on the removal other sources of signal variation such as transmission adjustments, antenna wetting, scintillation and solar blinding – which can be of comparable magnitude to rain fade – to determine an accurate baseline from which to quantify the rain fade along the transmission path. Signals may also be

attenuated to the point of dropping out completely during periods of intense rainfall – arguably when rainfall measurements are most important.

Data from CML could provide a useful additional source of rainfall measurements over land areas with high numbers of commercial microwave links. Helping to fill gaps in data from rain gauges and weather radar networks, which may prove especially valuable in countries without existing rainfall measurement networks. While research is ongoing, CML measurements have yet to be adopted operationally by many national meteorological services.

## References

### WMO TEXTS

- WMO-No. 8 – Guide to Instruments and Methods of Observation Volume III – Observing Systems: Guide to Instruments and Methods of Observation <https://library.wmo.int/records/item/68661-guide-to-instruments-and-methods-of-observation?offset=3>
- WMO-No. 1318 – Global Demonstration Campaign for Evaluating the Use of Uncrewed Aircraft Systems in Operational Meteorology: White Paper [2023], <https://library.wmo.int/records/item/66308-global-demonstration-campaign-for-evaluating-the-use-of-uncrewed-aircraft-systems-in-operational-meteorology-white-paper>

### ITU-R TEXTS

- Recommendation ITU-R M.1874-1 – *Technical and operational characteristics of oceanographic radars operating in sub-bands within the frequency range 3-50 MHz.*
- Report ITU-R M.2321 – *Guidelines for the use of spectrum by oceanographic radars in the frequency range 3 to 50 MHz.*
- Report ITU-R RS.2489 – *Technical and operational characteristics of ground-based passive sensors operating in the 51-58 GHz frequency range.*

### BIBLIOGRAPHY

- ALLEN, R. H, BURESS, D. W. and DONALDSON, R. J. [1981] *Attenuation Problems Associated with a 5 cm Radar*, Bulletin of the American Meteorological Society, 62, No. 6, June 1981.
- ANTHES, R.A. [2011], *Exploring Earth's atmosphere with radio occultation data: contributions to weather, climate and space weather*, Atmos. Meas. Tech., 4(1077-1103), doi: <https://doi.org/10.5194/amt-4-1077-2011>
- BÄRFUSS, K. B., SCHMITHÜSEN, H., AND LAMPERT, A.: *Drone-based meteorological observations up to the tropopause – a concept study*, Atmos. Meas. Tech., 16, 3739–3765, <https://doi.org/10.5194/amt-16-3739-2023>, 2023.
- BEAN, B. R. and DUTTON, E. J. [1966] *Radio Meteorology*, National Bureau of Standards Monograph 92, US Government Printing Office, Washington DC, United States.
- BEVIS, M., S. BUSINGER, T. A. HERRING, C. ROCKEN, R. A. ANTHES, AND R. H. WARE [1992], *GPS meteorology: Remote sensing of atmospheric water vapor using the global positioning system*, J. Geophys. Res., 97(D14), 15787–15801, doi: <https://doi.org/10.1029/92JD01517>
- BONAFONI, S., BIONDIB, R., BRENOTC, H., ANTHES, R. [2019], *Radio occultation and ground-based GNSS products for observing, understanding and predicting extreme events: A review*, Atmospheric Research, 230(104624) doi: <https://doi.org/10.1016/j.atmosres.2019.104624>

- BURROWS, C. R. and ATWOOD, S. S. [1949] *Radio Wave Propagation, Consolidated Summary Technical Report of the Committee on Propagation of the National Defense Research Committee*, Academic Press, New York, United States.
- CHWALA C, KUNSTMANN H. [2019], *Commercial microwave link networks for rainfall observation: Assessment of the current status and future challenges*. WIREs Water. 6:e1337. <https://doi.org/10.1002/wat2.1337>
- DOVIAK, R. J. and ZRNIC, D. S. [1984] *Doppler radar and weather observations*. Academic Press, Inc., San Diego, United States of America.
- DOVIAK, R. J. and ZRNIC, D. S. [1993] *Doppler radar and weather observations, 2<sup>nd</sup> Ed.* Academic Press, Inc., San Diego, United States of America.
- DOVIAK, R. J., ZRNIC, D. and SIRMANS, D. [November 1979] *Doppler Weather Radar. Proc. IEEE*, Vol. 67, 11.
- DOVIAK, R. J., SIRMANS, D., ZRNIC, D., AND WALKER, G. B. [1978] *Considerations for Pulse-Doppler Radar Observations of Severe Thunderstorms*, Journal of Applied Meteorology, 17 No. 2, February 1978, American Meteorological Society.
- FABRY, F. [2015] *Radar Meteorology – Principles and Practice*, Cambridge University Press, University Printing House, Cambridge United Kingdom.
- GIANNETTI, F, AND RUGGERO R. [2021]. *Opportunistic Rain Rate Estimation from Measurements of Satellite Downlink Attenuation: A Survey*, Sensors 21, no. 17: 5872. <https://doi.org/10.3390/s21175872>
- GOSSARD, E. E. and STRAUCH, R. G. [1983] *Radar Observation of Clear Air and Clouds*. Elsevier, New York, United States of America, 280 pages.
- HITSCHFELD, W. and BORDAN, J. [1954] *Errors Inherent in the Radar Measurement of Rainfall at Attenuating Wavelengths*, Journal of Meteorology, 11, February 1954, American Meteorological Society.
- HO, S.-P., ANTHES, R.A., AO, C.O., HEALY, S., HORANYI, A., HUNT, D., MANNUCCI, A.J., PEDATELLA, N., RANDEL, W.J., SIMMONS, A., STEINER, A., XIE, F., YUE, X., ZENG Z. [2019], *The COSMIC-FORMOSAT-3 radio occultation mission after 12 years: accomplishments, remaining challenges, and potential impacts of COSMIC-2*, Bull. Am. Meteorol. Soc., 100, p. 2019, DOI: <https://doi.org/10.1175/BAMS-D-18-0290.1>
- JAKOWSKI, N., & HOQUE, M. M. [2019]. *Estimation of spatial gradients and temporal variations of the total electron content using ground-based GNSS measurements*, Space Weather, 17, 339–356. <https://doi.org/10.1029/2018SW002119>
- LEE, A. C. L. [1986] *An experimental study of the remote location of lightning flashes using a VLF arrival time difference technique*. Quarterly J. R. Meteorological Society.
- LEE, A.C.L. [1986b] *An operational system for the remote location of lightning flashes using a VLF arrival time difference technique*. Journal of Atmospheric and Oceanic Technology, 3(4), 630–642.
- LENNON, C. and MAIER, L. [1991] *Lightning mapping system. Proc. of International Aerospace and Ground Conference on Lightning and Static Electricity*, Cocoa Beach, FL., United States of America. NASA Conf. Pub. 3106, Vol. II, p. 89-1, 89-10.
- MCLAUGHLIN, D. J., CHANDRASEKAR, V., DROEGEMEIER, K., FRASIER, S., KUROSE, J., JUNYENT, F., PHILIPS, B., CRUZ-POL, S. and COLOM, J. [January 2005] *Distributed Collaborative Adaptive Sensing (DCAS) for Improved Detection, Understanding, and Prediction of Atmospheric Hazards. Ninth Symposium on Integrated Observing and Assimilation Systems for the Atmosphere, Oceans, and Land Surface (IOAS-AOLS)*, American Meteor. Society.
- RHEINSTEIN, J. [1968] *Backscatter from Spheres: A Short Pulse View*, IEEE Transactions on Antennas and Propagation, AP16, No. 1, January 1968.

- RODRIGUEZ-ALVAREZ, N.; MUNOZ-MARTIN, J.F.; MORRIS, M., [2023] *Latest Advances in the Global Navigation Satellite System—Reflectometry (GNSS-R) Field*, *Remote Sens.*, 15, 2157. <https://doi.org/10.3390/rs15082157><https://doi.org/10.3390/rs15082157>
- SEEMALA, GOPI KRISHNA, [2023], Chapter 4 - *Estimation of ionospheric total electron content (TEC) from GNSS observations*, Editor(s): Abhay Kumar Singh, Shani Tiwari, In *Earth Observation, Atmospheric Remote Sensing*, Elsevier, Pages 63-84, ISBN 9780323992626
- RYZHKOV, A. and ZRNIC, D. [2005], *Radar Polarimetry at S, C, and X Bands Comparative Analysis and Operational Implications*, 32nd Conference on Radar Meteorology, American Meteorological Society.
- SIRMANS, D, *WSR-88D Antenna Polarization Change*, Titan Corporation, report to the WSR-88D Operational Support Facility, January 15, 1993, available from the WSR-88D Radar Operations Center.
- THOMAS, R. J., P. R. KREHBIEL, W. RISON, S. J. HUNYADY, W. P. WINN, T. HAMLIN, and J. HARLIN [2004], *Accuracy of the Lightning Mapping Array*, *J. Geophys. Res.*, 109, D14207, doi: <https://doi.org/10.1029/2004JD004549>
- TURK, F. J., and Coauthors, [2024], *Advances in the Use of Global Navigation Satellite System Polarimetric Radio Occultation Measurements for NWP and Weather Applications*. *Bull. Amer. Meteor. Soc.*, 105, E905–E914, <https://doi.org/10.1175/BAMS-D-24-0050.1>
- YU.V. YASYUKEVICH, A.A. MYLNIKOVA, A.S. POLYAKOVA, [2015], *Estimating the total electron content absolute value from the GPS/GLONASS data*, *Results in Physics*, 5 (32-33), ISSN 2211-3797, <https://doi.org/10.1016/j.rinp.2014.12.006>
- YUE, X., W. S. SCHREINER, N. PEDATELLA, R. A. ANTHES, A. J. MANNUCCI, P. R. STRAUS, AND J.-Y. LIU (2014), *Space Weather Observations by GNSS Radio Occultation: From FORMOSAT-3/COSMIC to FORMOSAT-7/COSMIC-2*, *Space Weather*, 12, 616–621, doi: <https://doi.org/10.1002/2014SW001133>
- ZRNIC, D. S., KENNAN, T., CAREY, L. D and MAY, P. [2000] *Sensitivity Analysis of Polarimetric Variables at a 5-cm Wavelength in Rain*, *Journal of Applied Meteorology*, **39**, September 2000.

## Annex

### Acronyms and abbreviations

#### A.1 Acronyms and abbreviations commonly used in meteorology

<b>A</b>		ATSR	Along-Track Scanning Radiometer
A/D	Analogue-to-digital	AVCS	Advanced Video Camera System
AAAS	American Association for the Advancement of Science	AVHRR	Advanced Very High Resolution Radiometer
AARS	Automated Aircraft Reporting System	AWIPS	Advanced Weather Information Processing System
ABSN	Antarctic Basic Synoptic Network	<b>B</b>	
ACARS	Aircraft Communications Addressing and Reporting System	BCD	Binary Coded Decimal
ACCAD	Advisory Committee on Climate Applications and Data	BER	Bit Error Rate
ACMAD	African Centre of Meteorological Applications for Development	BPS	bits per second
ADAS	Airborne Data Acquisition System	BPSK	Binary Phase Shift Keying
ADC	Analogue-to-Digital Converter	BR	ITU Radiocommunication Bureau
ADEOS	Advanced Earth Observation Satellite (Japan)	BW	Bandwidth
ADP	Automatic Data Processing	<b>C</b>	
ADPE	Automatic Data Processing Equipment	$C/N_0$	Carrier-to-noise density ratio
AFC	Automatic Frequency Control	C&DH	Command and Data Handling
AFOS	Automatic Forecasting and Observing System	CaeM	Commission for Aeronautical Meteorology
AGC	Automatic Gain Control	CAgM	Commission for Agricultural Meteorology
AGRHYMET	Regional Training Centre for Agrometeorology and Operational Hydrology and its Applications	CAS	Commission for Atmospheric Sciences
AIRS	Advanced Infrared Sounder (NASA instrument)	CBS	Commission for Basic Systems
ALC	Automatic Level Control	CCD	Charge Coupled Device
AM	Amplitude Modulation	CCIR	International Radio Consultative Committee (see ITU-R)
AMDAR	Aircraft Meteorological Data Relay	CCI	Commission for Climatology
AMI	American Meteorological Society	CCRS	Canada Centre for Remote Sensing
AMSR	Advanced Meteorological Temperature Sounder	CCSDS	Consultative Committee for Space Data Systems
ANSI	American National Standards Institute	CDA	Command and Data Acquisition
AOPC	Atmospheric Observation Panel for Climate	CDAS	Command and Data Acquisition Station
AOS	Acquisition of Signal	CEOS	Commission on Earth Observation Satellites
APT	Automatic Picture Transmission	CERES	Cloud and Earth's Radiative Energy System
ARGOS	Data collection and location system on NOAA series satellites	CGMS	Co-ordination Group for Meteorological Satellites
ASCII	American Standard Code for Information Interchange	CHy	Commission for Hydrology (WMO)
ASIC	Application Specific Integrated Circuit	CIESIN	Consortium for International Earth Science Information Networks
ATMS	Advanced Technology Microwave Sounder (NPOESS/NASA)	CIMO	Commission for Instruments and Methods of Observation
ATOVS	Advanced TIROS Operational Vertical Sounder	CIMSS	Cooperative Institute for Meteorological Satellite Studies
		CLICOM	Climate Computing
		CLINO	Climatological Normals
		CLIPS	Climate Information and Prediction Services

<b>C (cont.)</b>		DAS	Direct Access System
CLIVAR	Climate Variability and Predictability	dB	Decibel
CMA	China Meteorological Administration	DB	Direct Broadcast
CMD	Command	DBMS	Database Management System
CMIS	Conical-scanning Microwave Imager/Sounder (NPOESS instrument)	DCPLS	Data Collection Platform Location System
CMM	Commission for Marine Meteorology	DCP	Data Collection Platform
CNES	Centre National d'Etudes Spatiales	DCPI	Data Collection Platform Interrogation
CNIE	Comisión Nacional de Investigaciones Espaciales	DCPR	Data Collection Platform Reception
COADS	Comprehensive Ocean-Atmosphere Data Set	DCR	Differential Correlation Radiometer
CONUS	Continental United States	DCS	Data Collection System
COP	Conference of the Parties	DEMUX	De-Multiplexer
COPUOS	Committee on the Peaceful Uses of Outer Space	DIFAX	Digital Facsimile
CORSSAC	Civil Operational Remote Sensing Satellite Advisory Committee	DIR	Daytime Infrared
COSPAS	A Russian satellite-borne search and rescue system. See SARSAT	DLI	Down-Link Interface (DM/PM)
CPCSA	Climate Program Coordination and Support Activities	DLM	Down-Link Monitor
CPR	Cloud Physics Radiometer, or Cardio-pulmonary Resuscitation	DLR	German Space Agency (Deutsche Zentrum für Luft- und Raumfahrt)
CPU	Central Processing Unit	DMSP	Defense Meteorological Satellite Program
CRC	Cyclic Redundancy Check/Cyclic Redundancy Code	DN	Descending Node
CrIS	Cross-track Infrared Sounder (NPOESS instrument)	DOMSAT	Domestic (Communications) Satellite
CrMIS	Cross-track Microwave Imager-Sounder (NPOESS instrument)	DPT	Digital Picture Terminal
CRT	Cathode Ray Tube	DR	Direct Readout
CSA	Canadian Space Agency	DRGS	Direct Readout Ground Stations
CS&C	Communications Switching and control (CDA portion of GMACS System)	DS	Dwell Sounding or Sounding (GOES-4/7 VAS operating node)
CSIRO	Commonwealth Scientific and Industrial Research Organization	DSARS	DAMUS Satellite Archive and Retrieval System
CSIS	Centralised Storm Information System	DSB	Direct Sounder Beacon
CSM	Climate System Monitoring	DSB	Direct Sounder Broadcasts
CSMA/CD	Carrier Sensing Multiple Access with Collision Detection	DSN	Deep Space Network
CSTR	Council for Scientific and Technical Research	DUS	Data Utilisation System
CTCS	CDA Telemetry and Command System (CDA portion of GIMTACS System)	<b>E</b>	
CW	Continuous Wave	EBR	Electron Beam Recorder
CZCS	Coastal Zone Colour Scanner	EC/AGE	Executive Council Advisory Group on the Exchange of Meteorological and Electronics Calibration
<b>D</b>		ECMWF	European Centre for Medium-range Weather Forecasts
D/A	Digital-to-analogue	EDC	EROS Data Center
DAAC	Distributed Active Archive Center	EDIMS	Environmental Data & Information Management Systems
DADS	Data Archive and Distribution System	EES	Earth Exploration Satellite
DAPS	DCS Automated Processing System	EESS	Earth Exploration-Satellite Service
DAS	Data Acquisition System	EIRP	Equivalent Isotropically Radiated Power
DAS	Data Base Administration System	EIRPSD	Equivalent Isotropically Radiated Power Spectral Density
		ELT	Emergency Locator Transmitter
		ELV	Expendable Launch Vehicle
		EMC	Electromagnetic Compatibility
		EMI	Electromagnetic Interference
		ENSO	<i>El Niño</i> /Southern Oscillation
		ENVISAT	Environmental Satellite
		EOS	Earth Observation Satellites
		EPIRB	Emergency Position-Indicating Radio Beacon

**E (cont.)**

EPOCS	Equatorial Pacific Ocean Climate Studies
EPS	Energetic Particle Sensor
ERB	Earth Radiation Budget
ERBE	Earth Radiation Budget Experiment
ERL	Environmental Research Laboratory
EROS	Earth Resources Observing Satellite
ERS	ESA Remote Sensing Satellite
ESA	European Space Agency
ESD	Electrostatic Discharge
ESMR	Electronically Scanning Microwave Radiometer
ETA	Estimated Time of Arrival
ETM	Engineering Test Model
ETM	Enhanced Thematic Mapper
ETS	Engineering Test Satellite
EUMETSAT	European Organization for the Exploitation of Meteorological Satellites
EUV	Extreme Ultraviolet
<b>F</b>	
FAX	Facsimile
FC	False Colour
FCC	False Colour Composite
FCC	Federal Communications Commission
FDM	Frequency Division Multiplexing
FFT	Fast Fourier Transform
FIFO	First-In-First-Out
FM	Frequency Modulation
FOV	Field of view
fps	Frames Per Second
FSK	Frequency Shift Keying
FSS	Fixed-Satellite Service
FSS	Flight Scheduling Software System
<b>G</b>	
GAC	Global Area Coverage
GAME	GEWEX Asian Monsoon Experiment
GARP	Global Atmospheric Research Program
GARS	GOES Archive and Retrieval System
GAW	Global Atmosphere Watch
GCIP	GEWEX Continental-scale International Project
GCM	General Circulation Model
GCOS	Global Climate Observing System
GDTA	Groupement pour le Développement de la Télédétection Aérospatiale
GEO	Geostationary Earth Orbit
GEWEX	Global Energy and Water Cycle Experiment
GHz	Gigahertz
GIMGSP	GOES I-M Ground System Project
GIMTACS	GOES I/M Telemetry and Command System
GIS	Geographical Information Systems

GMACS	GOES Monitoring and Control system (current GIMTACS)
GMDSS	Global Maritime Distress and Safety System
GMS	Geostationary Meteorological Satellite
GMT	Greenwich Mean Time
GNSS	Global Navigation Satellites Systems
GOES	Geostationary Operational Environmental Satellite
GOMS	Geostationary Operational Meteorological Satellite
GOOS	Global Ocean Observing System
GOS	Global Observing System
GOSSP	Global Observing Systems Space Panel
GPCP	Global Precipitation Climatology Project
GPS	Global Positioning System
GPSOS	GPS Occultation Sensor
GRC	Glenn Research Center formerly the Lewis Research Center (LeRC)
GRS	Ground Receiving Station
GRT	GOES Real-time (database)
GSFC	Goddard Space Flight Center
GSN	GCOS Surface Network
GSTDN	Ground Spaceflight Tracking and Data Network
<i>G/T</i>	Antenna Gain to System Noise Temperature Ratio (dB/K)
GTOS	Global Terrestrial Observing System
GTS	Global Telecommunications System
GUAN	GCOS Upper-air Network
GVAR	GOES VARIable
GWC	Global Weather Center
<b>H</b>	
H1/3	Significant wave height
HEPAD	High Energy Proton and Alpha Detector
HiRID	High Resolution Imager Data
HIRS	High-resolution Infrared Sounder (TIROS instrument)
HOMS	Hydrological Operational Multipurpose System
HRD	Hurricane Research Day
HRD (10)	Hurricane Research Day – GOES-East scans every 10 minutes at selected times.
HRIS	High Resolution Infrared Sounder, or High Resolution Interferometric Sounder
HRPT	High Resolution Picture Transmission
HRSD (S)	Hurricane Rapid Scan Day (Stereo) GOES-East and West scan every 7 1/2
Hz	Hertz formerly cycles per second

<b>I</b>		<b>J</b>	
I/O	Input/Output	JDIMP	Joint GCOS/GOOS/GTOS Data Management and Information Panel
I/S	Imager and Sounder	JERS	Japanese Earth Resources Satellite
IAHS	International Association of Hydrological Sciences	JIC	Joint Ice Center
IAMAS	International Association of Meteorology and Atmospheric Sciences	JMA	Japan Meteorological Agency
IASI	Infrared Atmospheric Sounding Interferometer	JPL	Jet Propulsion Laboratory
ICES	International Council for the Exploration of the Sea	JSC	Joint Scientific Committee Johnson Space Center
ICSAR	International Committee for Search and Rescue	JSTC	Joint Scientific and Technical Committee
ICSU	International Council of Scientific Unions	<b>K</b>	
IEEE	Institute of Electrical and Electronics Engineers	K	Kelvin
IF	Intermediate Frequency	kbit	kilobit(s)
IFOV	Instantaneous Field of View	kB	kilobyte(s)
IFRB	International Frequency Registration Board (see BR)	kbit/s	kilobits per second
IGBP	International Geosphere-Biosphere Programme	keV	Thousand Electron Volts
IGF	Image Generation Facility	kHz	kilohertz
IGFOV	Instantaneous Geometric Field of View	KSC	Kennedy Space Center
IGOSS	Integrated Global Ocean Services System	KSPS	kilo samples per second
IHP	International Hydrological Programme	<b>L</b>	
INDOEX	Indian Ocean Experiment	LANDSAT	U.S. earth remote sensing satellite
INPE	Instituto de Pesquisas Espaciales	LANDSAT-TM	Landsat Thematic Mapper instrument
INR	Image Navigation and Registration	LaRC	Langley Research Center
INR	Interference to Noise Ratio	LAT/LON	Latitude/Longitude
INSAT	Indian Satellite	LE	Landmark Extraction
IOC	Intergovernmental Oceanographic Commission	LEO	Low Earth Orbit
IODE	International Oceanographic Data and Information Exchange	LEOP	Launch and Early Orbit Phase
IPCC	Intergovernmental Panel on Climate Change	LeRC	see GRC
IPD	IF Presence Detector (CDA)	LGSOWG	LANDSAT Ground Station Operations Working Group
IR	Infrared	LHCP	Left-Hand Circular Polarisation
IRIG	Inter-Range Instrumentation Group	LIDAR	Light Detection and Ranging
IRIS	Infrared Interferometer Spectrometer	LMT	Local Mean Time
IRS	Indian Remote Sensing Satellite	LOS	Loss of Signal
IRU	Inertial Reference Unit	LPA	Low Power Amplifier
ISETAP	Intergovernmental Science Engineering & Technology Advisory Panel	lpi	lines per inch
ISO	International Organization for Standardization	lpm	lines per minute
ITOS	Improved TIROS Operational System	LRIT	Low Rate Information Transmission
ITPR	Inferred Temperature Profile Radiometer	LRPT	Low Resolution Picture Transmission
ITU	International Telecommunication Union	LUT	Look-up Table, or Local User Terminal
ITU-R	ITU Radiocommunication Sector (former CCIR and IFRB)	LW	Long Wave
		LWIR	Long Wave Infra-Red
		<b>M</b>	
		mb	Millibars
		Mbit/s	Megabits per second
		MB/s	Megabytes per second
		MCC	Mission Control Center
		MCDW	Monthly Climatic Data for the World
		MCS	Moisture Channel Support
		MDHS	Meteorological Data Handling System
		MDUS	Medium-scale Data Utilisation Stations
		MEO	Medium Earth Orbit

**M (cont.)**

MEPED	Medium Energy Proton and Electron Detector	NOAA	National Oceanic and Atmospheric Administration
MetAids	Meteorological Aids	NOAA	Polar METSAT
METEOSAT	European Geostationary Meteorological Satellite	NOS	National Ocean Survey
METOP	European Polar-orbiting Meteorological Satellite	NPOESS	National Polar-Orbiting Operational Environmental Satellite System
MetSat	Meteorological Satellite	NRCT	National Research Council of Thailand
MeV	Million Electron Volts	NROSS	Navy Remote Ocean Sensing System
MeV/n	Million Electron Volts Per Nucleon	NRSA	National Remote Sensing Agency
MHS	Microwave Humidity Sounder	NRZ	Non-Return to Zero
MHz	Megahertz	NRZ-L	Non-Return to Zero Level
MLS	Microwave Limb Sounder	NSSFC	National Severe Storms Forecast Center
MODEM	Modulator/Demodulator	NSSL	National Severe Storms Laboratory
MODIS	Moderate Resolution Imaging Spectroradiometer (NASA instrument)	nT	Nano Tesla
MOPITT	Measurement of Pollution in the Troposphere (NASA)	NWP	Numerical Weather Prediction
MOS	Marine Observation Satellite (Japan)	NWS	National Weather Service
MPERSS	Marine Pollution Emergency Response Support System	<b>O</b>	
mr	Milliradians	O&M	Operations and Maintenance
MSFC	Marshall Space Flight Center	OAD	Orbit and Attitude Determination
MSI	Multi-spectral Imaging	OAR	Office of Oceanic and Atmospheric Research
MSS	Mobile-Satellite Service	OCTS	Ocean Colour Temperature Sensor
MSS	Multi-spectral Scanner	OHP	Operational Hydrology Programme
MSU	Microwave Sounding Unit	OMI	Ozone Measuring Instrument
MTBF	Mean Time Between Failures	OMPS	Ozone Mapping and Profiler Suite (NPOESS)
MTF	Modulation Transfer Function	OOPC	Ocean Observations Panel for Climate
MUX	Multiplexer	OQPSK	Offset QPSK
MW	Momentum Wheel Medium wave Microwave Megawatt	<b>P</b>	
<b>N</b>		P/SEC	Pulses per second
N/S	North/South	P-P	Peak to Peak
NASA	National Aeronautics and Space Administration	PA	Power Amplifier
NASCOM	NASA Communications Network	PAM	Pulse Amplitude Modulation
NASDA	National Space Development Agency	PCM	Pulse Code Modulation
NCDC	National Climatic Data Center	PDL	Processor Data Load
NE-delta-N	Noise Equivalent Change in Radiance	PDR	Processed Data Relay (GVAR RF link)
NE-delta-T	Noise Equivalent Change in Temperature	PE	Primitive Equation
NERC	National Environmental Research Council	PEP	Peak Envelope Power
NESDIS	National Environmental Satellite Data and Information Service	PEP	Polynomial Error Protection (NASA)
NF	Noise Figure	PFD	Power Flux-Density
NHC	National Hurricane Center	Pixels	Picture Elements
NHS	National Hydrological Service	PKM	Perigee Kick Motor
NIR	Night Infrared, or Near Infrared	PLL	Phase Locked Loop
NMC	National Meteorological Center	PM	Phase Modulation
NMS	National Meteorological or Hydrometeorological Service	PN	Pseudonoise
NNODS	NOAA/NOSS Ocean Data System	POES	Polar-orbiting Operational Environmental Satellite
		PPM	Parts per million
		PPS	Pulses per second
		PR	Precipitation Radar
		PRF	Pulse Repetition Frequency
		PROFS	Program for Regional Observing and Forecasting Service
		PROMET	Working Group on the Provision of Meteorological Information

<b>P (cont.)</b>		SCSMEX	South China Sea Monsoon Experiment
PSK	Phase Shift Keying	SDUS	Small-scale Data Utilisation Station
PWM	Pulse-width Modulation	SeaWiFS	Sea-viewing Wide Field-of-view Sensor
<b>Q</b>		SEC	Second
QC	Quality Control	SEM	Space Environment Monitor
QPSK	Quadrature PSK	SEU	Single Event Upset
<b>R</b>		SGLS	Space Ground Link System
R	Rayleigh	SIGWX	Significant Weather
RA	Radar Altimeter	SIR	Shuttle Imaging Radar
R/Y	Roll/Yaw	SIRS	Satellite Infrared Spectrometer
R&D	Research and Development	SIT	CEOS Strategic Implementation Team
RBSN	Regional Basic Synoptic Network	SLAR	Side-looking Airborne Radar
RCS	Reaction Control System	SN	Space Network
RF	Radio Frequency	SNR	Signal-to-Noise Ratio
RFI	Radio Frequency Interference	SOCC	Spacecraft Operations Control Center
RGB	Red/Green/Blue	SOES	Subcommittee on Operational Environmental Satellites
RH	Relative Humidity	SOLAS	International Convention for the Safety of Life at Sea
RHCP	Right-Hand Circular Polarisation	SPM	Solar Proton Monitor
RMDCN	Regional Meteorological Data Communication Network	SPOT	Satellite Probatoire d'Observation de la Terre
RMS	Root Mean Square	SQPSK	Staggered QPSK
RPM	Revolutions Per Minute	SPREP	South Pacific Regional Environment Programme
RSS	Root Sum of the Squares	SR	Scanning Radiometer
RSU	Remote Sensing Unit	sr	Steradian
RT	Real Time	SR-IR	Scanning Radiometer-Infrared Channel
RW	Reaction Wheel	SR-VIS	Scanning Radiometer-Visible Channel
RWA	Reaction Wheel Assembly	SSA	WWW System Support Activities
<b>S</b>		SSM/I	Special Sensor Microwave/Imager
S/C	Spacecraft	SST	Sea Surface Temperature
S/N	Signal-to-noise ratio	SSU	Stratospheric Sounding Unit
S/N <sub>0</sub>	Signal-to-noise density ratio	STA	Science and Technology Agency
S-VAS	Stretched Visible Infrared Spin Scan Radiometer Atmospheric Sounder	STC	Scientific and Technical Committee
S-VISSR	Stretched Visible Infrared Spin Scan Radiometer	Ster	Steradian
SAD	Sounder/Auxiliary Data	STS	Space Transportation System
SAGE	Stratospheric Aerosol and Gas Experiment	SW	Short wave
SAR	Synthetic Aperture Radar, or Search and Rescue	SWIR	Switch
SARSAT	Search And Rescue Satellite-Aided Tracking; see COSPAS	SXI	Short Wave Infrared
SATCOM	Satellite Communications	SXT	Solar X-ray Imager
SBUV	Solar Backscatter Ultraviolet		Solar X-ray Telescope (Solar-A mission)
SC/N <sub>0</sub>	Subcarrier-to-noise density ratio	<b>T</b>	
SC/OMS	Subcommittee on Operational Meteorological Satellites	T/P	Topex/Poseidon
SC/OES	Subcommittee on Operational Environmental Satellites	T/V	Thermal Vacuum
SCHOTI	Standing Conference of Heads of Training Institutions of National Meteorological Services		
SCIAMACHY	Scanning Imaging Absorption Spectrometer for Atmospheric Cartography		
SCO	Subcarrier Oscillator		

**T (cont.)**

T&C	Telemetry and Command
TBUS	A 4-letter designator for Ephemeris data message
TDM	Time Division Multiplexing
TDRS	Tracking and Data Relay Satellite
TDRSS	Tracking and Data Relay Satellite System
TED	Total Energy Detector, or Turtle Excluder Device
TEMS	Terrestrial Ecosystem Monitoring System
TES	Tropospheric Emission Spectrometer
TIP	TIROS Information Processor
TIR	Thermal Infrared
TIROS	Television Infra-Red Observational Satellite
TLM	Telemetry
TM	Thematic Mapper
TMI	TRMM Microwave Imager
TMR	Topex Microwave Radiometer
TO	Transfer Orbit
TOGA	Tropical Ocean and Global Atmosphere
TOPC	Terrestrial Observation Panel for Climate
TOMS	Total Ozone Mapping Spectrometer
TOS	TIROS Operational System
TOVS	TIROS Operational Vertical Sounder
TRMM	Tropical Rainfall Measurement Mission
TRUCE	Tropical Urban Climate Experiment
TT&C	Tracking Telemetry
TV	Thermal Vacuum, or Television
TVM	Transparent VAS Mode

**U**

UHF	Ultra-High Frequency
UNEP	United Nations Environment Programme
μrad	Microradian
μs	Microsecond
UTC	Universal Time Coordinated
UV	Ultraviolet

**V**

VAS	VISSR Atmospheric Sounder
VCP	Voluntary Cooperation Programme
VDB	VISSR Data Base
VDUC	VAS Data Utilisation Center
VHF	Very High Frequency
VIIRS	Visible Infrared Imager/Radiometer Suite (NPOESS instrument)
VIP	VAS Image Processor (with P/DU current SPS)
VIRGS	VISSR Image Registration and Gridding System
VISSR	Visible & Infrared Spin Scan Radiometer

VOS	Voluntary Observing Ship
VREC	Very High Resolution Radiometer Data Recorder
VSWR	Voltage Standing Wave Ratio
VTPR	Vertical Temperature Profile Radiometer

**W**

WAFc	World Area Forecast Centre
WCASP	World Climate Applications and Services Programme
WCDA	Wallops Command and Data Acquisition (Station)
WCDMP	World Climate Data and Monitoring Programme
WCFP	World Climate Data Programme
WCP	World Climate Programme
WCRP	World Climate Research Programme
WDC	World Data Centre
WEFAX	Weather Facsimile
WHYCOS	World Hydrological Cycle Observing System
WMO	World Meteorological Organization
WRC	World Radiocommunication Conference
WSFO	Weather Service Forecast office
WSFO-Tap	WSFO ground communications link relaying GOES data

WWRP	World Weather Research Programme
WWW	World Weather Watch
WX	Weather

**X**

XBt	Expendable Bathythermograph
XRI	X-Ray Imager
XRS	(Solar) X-Ray Sensor

**Y**

yr	Year
----	------

**Z**

Z	Common abbreviation for Greenwich Meridian Time or Universal Time
---	---

**A.2 Other acronyms and abbreviations used in this Handbook**

CML	Commercial microwave links
DFS	Dynamic frequency selection
ERT	Electrical resistivity tomography
ET-RFC	Expert Team on Radio Frequency Coordination
GCOS	Global climate observing system
GRB	GOES ReBroadcast
GSO	Geostationary orbit
HRIT	High-rate information transmission
IPS	Interplanetary scintillations
JPSS	Joint polar satellite system
LDS	Lightning detection systems
LMA	Lightning mapping array
non-GSO	Non-geostationary orbit
RASS	Radio acoustic sounding system
RLAN	Radio local area network
SMMR	Scanning multichannel microwave radiometer
TWTs	Traveling wave tubes
UAS	Uncrewed aircraft systems
UWB	Ultra-wide band
VLF	Very low frequency
WHOS	WMO's Hydrological Observing System
WIGOS	WMO Integrated Global Observing System
WIPPS	WMO Integrated Processing and Prediction System
WIS	WMO Information System
WPR	Wind profiler radar
Wx-UAS	Weather-sensing uncrewed aircraft systems

---



International  
Telecommunication  
Union

Place des Nations  
CH-1211 Geneva 20  
Switzerland

ISBN 978-92-61-40681-3



9 789261 406813

Published in Switzerland  
Geneva, 2026  
Photo credits: Adobe Stock